On Holographic Methods in Cosmology

Till Heckelbacher

München 2022

On Holographic Methods in Cosmology

Till Heckelbacher

Dissertation
der Fakultät für Physik
der Ludwig-Maximilians-Universität
München

vorgelegt von
Till Heckelbacher
aus Moosburg an der Isar

München, den 06. Mai 2022

"If there is something comforting - religious, if you want - about paranoia,
there is still also anti-paranoia, where nothing is connected to anything,
a condition not many of us can bear for long."

- Thomas Pynchon, *Gravity's Rainbow*

Erstgutachter: Prof. Dr. Ivo Sachs
Zweitgutachter: Prof. Dr. Pierre Vanhove
Tag der mündlichen Prüfung: 24. Juni 2022

Contents

Zusammenfassung

Diese Arbeit beschäftigt sich mit kosmologischen Korrelationsfunktionen einer Quantenfeldtheorie in der asymptotischen Zukunft eines beschleunigt expandierenden Universums. Insbesondere berechnen wir Quantenkorrekturen der Vierpunktsfunktion eines konform gekoppelten, skalaren Feldes mit quartischem Wechselwirkungsterm bis zur ersten Schleifenordnung in einer vierdimensionalen de Sitter Raumzeit (dS).

Diese können wir in konformen Blocks einer dualen Theorie entwickeln und deren konforme Daten bis zur zweiten perturbativen Ordung berechnen. Wir finden geschlossene Ausdrücke für alle anomalen Dimensionen. Da diese einigen nicht-trivialen, konformen Konsistenzbedingungen gehorchen, zeigen wir in erster Schleifenordung, dass kosmologische Korrelationsfunktionen in der asymptotischen Zukunft des dS holographisch durch eine euklidische, konforme Feldtheorie bestimmt sind.

Als Zwischenschritt berechnen wir Quantenkorrekturen der selben Theorie im euklidischen Anti-de Sitter Raum (EAdS), welche wir wiederum in konformen Blocks der dualen Theorie am Rand entwickeln und geschlossene Ausdrücke für alle anomalen Dimensionen extrahieren.

Im Zuge dieser Rechnung entwickeln wir ein Methode die involvierten Integrale auf äquivalente Ausdrücke in einer flachen Raumzeit abzubilden, welche wir mit Hilfe von etablierten Techniken aus der Berechnung von Feynmanintegralen analytisch auswerten. Dazu konstruieren wir ein adaptiertes dimensionelles Regularisierungschema für gekrümmte Raumzeiten. Wir zeigen, dass bis zur betrachteten Ordung alle kosmologischen Korrelationsfunktionen durch multiple Polylogarithmen gegeben sind, wohingegen die Integrale im EAdS auch elliptische Polylogarithmen enthalten.

Abstract

In this thesis we consider cosmological correlation functions of a quantum field theory in the asymptotic future of a Universe with an accelerated expansion. In particular, we calculate quantum corrections to the four point function of a conformally coupled scalar field with a quartic interaction term up to one loop order in a four dimensional de Sitter space-time (dS).

This can be expanded in terms of conformal blocks of a dual theory and we determine the conformal data up to the second order in perturbation theory. We find closed expressions for all anomalous dimensions. Since they obey some non-trivial conformal consistency conditions, we show, up to first loop order, that cosmological correlation functions in the asymptotic future of dS are holographically determined by a euclidean, conformal field theory.

In an intermediate step we calculate quantum corrections of the same theory in euclidean Anti-de Sitter space (EAdS) which we expand in terms of conformal blocks as well and find closed expressions for all anomalous dimensions.

To perform these computations we develope a method to map the involved integrals to equivalent expressions in flat space, which we evaluate analytically, using established techniques from the calculation of Feynman integrals. For that, we construct an adapted dimensional regularisation scheme for curved space-times. We show that, up to the considered order, all conformal correlation functions can be expressed in terms of multiple polylogarithms while the integrals in EAdS contain elliptic polylogarithms as well.

Chapter 1

Introduction

1.1 Cosmology and holography

Understanding the large scale structure of the Universe, its history, evolution and origin has been the desire of humanity for as long as it existed. As in ancient times the technical and observational tools to make scientific statements about the Universe were very limited or simply not available, cosmological theories usually consisted of some postulates which reflected the religious and philosophical mainstream of the society it originated from. To some extend one can argue that this is still more or less the case with the big difference being that through the development of experiments and scientific and mathematical methods we can put our cosmological models on a much more solid ground. Certain observational facts are indisputable and the influence of the ideological superstructure of society is left to the philosophical interpretation of the ontological consequences of the theory.

Modern, scientific cosmology in the above sense, i.e. a dynamical model for the entire Universe, based on observations and mathematical predictions only began in the early twentieth century with a work by Einstein [1], proposing a static universe with a positive cosmological constant. Shortly after, de Sitter developed a different space-time model [2], given by a static, empty space with a positive cosmological constant as well. Later it was realized, that de Sitter only considered a special static patch and that his model actually describes an exponentially expanding universe in both time directions which will be a major topic of this thesis. It was finally Friedmann [3, 4] who found the most general solutions to the Einstein equations compatible with the cosmological principle, postulating spatial homogeneity and isotropy on large scales. Friedmann's model led Lemaître [5] and later Hubble [6] to develop the Hubble-Lemaître law which introduces a proportionality constant that connects the recession velocity of an object to its distance and could explain the already discovered red shift of distant galaxies.

With the discovery of the cosmic microwave background (CMB) by Penzias and Wilson [7] the cosmological principle was finally put on a solid experimental basis to be taken serious as more than just a postulate. The following understanding of the evolution of the Universe got widely accepted as the standard model of cosmology. The Universe on very large scales (> 100 Mpc) has the geometry of a Friedmann space-time with a flat spatial profile. A Big Bang initializes a phase of decelerating expansion whose evolution is determined by the dominant content of the Universe, which at first is given by radiation, then dust and, due to the discovery of accelerated expansion [8], dark energy or a positive cosmological constant.

To overcome some observational and conceptual problems of this picture, a prequel to the Big Bang was introduced, which replaces the initial singularity in the decelerating Friedmann model with a stage of accelerated expansion, called inflation. This idea was first formulated by Starobinsky [9] and Guth [10] and further developed by Linde [11], Albrecht and Steinhardt [12]. Geometrically inflation corresponds to de Sitter's solution of Einstein's equations, with a slightly broken symmetry to allow a graceful exit into a decelerating Friedmann universe. A major breakthrough for inflation was the discovery by Mukhanov and Chibisov [13] that the spectrum of inhomogeneities of the temperature of the CMB and matter density distribution in the Universe can be traced back to quantum fluctuations originating from inflation. Their theory is based on the idea that Planck sized fluctuations are stretched out by the accelerated expansion and get frozen as soon as their wavelength exceeds the size of the cosmological horizon. This makes their evolution independent from the poorly understood phase of reheating and the very early universe. Their spectrum is predicted to be almost scale invariant and Gaussian. The scale dependence parametrizes the deviation of the inflationary Universe from an exact de Sitter geometry (dS). These stretched out fluctuations are the seeds of inhomogeneities in the gravitational potential.

The discovery of the quantum origin of structure in the Universe has far reaching consequences. First and foremost it is a big step in cosmology itself since the form of the density fluctuations can be derived from first principles, while previously they had to be postulated as initial conditions. Furthermore, it turns the earliest universe into a gigantic particle collider which can be used to test theories beyond the standard model of particle physics, since the relevant energies involved during this time are about $\sim 10^{14}$ GeV, which is beyond anything ever accessible in an experiment on earth. New, heavy excitations should produce very weak non-Gaussianities in the spectrum of primordial fluctuations and even though these have not been detected so far, making theoretical predictions about their structure has recently been an active field of research (see e.g. [14–17]).

For this approach to work it is crucial to understand how to formulate quantum field theory (QFT) in an inflationary background and to specify what the observables are which we would like to calculate. Experimentally we can directly access the CMB and the density fluctuations in the distribution of galaxies in the Universe, which are a result of the inhomogeneities in the gravitational potential. Therefore the observables are given by correlation functions at the end of inflation. As a simplification of the problem we will, however, consider an exact dS space-time.

From the point of view of the dS itself, which we refer to as the bulk, these observables lie on the space-like surface at future infinity. Note, that no observer in the bulk will ever be able to measure these correlation functions. But since we assume that inflation ends at some point and the Universe enters a phase of decelerated expansion, we can consider ourselves as sitting behind future infinity, having access to the section of the future boundary surface of de Sitter which lies in our past lightcone.

We therefore see a euclidean correlation function which should have the time evolution from the bulk encoded in its structure. This means that the cosmological correlation function is of holographic nature with the bulk time as an emergent direction. It is tempting to compare the cosmological situation to a different space-time, where holography is a well established concept, which is Anti-de Sitter space-time (AdS).

Even though AdS is an unrealistic model for any actual physical scenario, it serves as a useful playground to test potential theories of quantum gravity and quantum field theory in curved space-time due to its well understood realization of holography. It is related to dS by a change in the sign of the cosmological constant. Consequently the physical behavior and geodesics in AdS are quite different. Instead of experiencing an accelerated expansion, as in dS, everything is reflected back from spatial infinity into the bulk, even light rays, which is one of the main reasons why AdS should not be considered for any realistic scenario. This phenomenon is connected to the fact that AdS is not globally hyperbolic [18] and we have to impose extra conditions on the spatial boundary to have a well defined Cauchy problem.

The structure of AdS, however, makes a formulation of holography much more straightforward than in other space-time models. The AdS/CFT correspondence states that any quantum field theory and even quantum gravity in the bulk of AdS can be formulated as a conformal field theory (CFT) living on the boundary at spatial infinity and there exists a precise dictionary between boundary and bulk degrees of freedom [19–22]. Intuitively this can be motivated by the fact that the AdS symmetry group acts on the boundary as the conformal group.

One of the major reasons why holography in AdS is generally accepted as a well established concept, is the fact that the AdS/CFT correspondence can be derived from string theory, with a concrete conjecture first proposed by Maldacena [19]. This has not been achieved yet for other space-times.

A technical reason that makes AdS more attractive for testing holography is the fact that it is a static space-time, meaning that there exists a time translation invariant vacuum state, which makes a well defined formulation of perturbative quantum field theory much easier than in a non-static Universe. The technique of visualizing perturbative QFT calculations through Feynman diagrams can be applied straightforwardly in AdS [21,22] which now graphically depict the boundary correlation functions in terms of bulk propagators and vertices. At tree-level this method is quite effective and results were obtained quite early after its introduction [23].

But going beyond tree-level is still very hard since no Fourier transformation in all space-time directions exists and the calculation has to be performed in position space. There have been many interesting attempts of getting around this problem. A very successful method is to make use of the conformal structure on the boundary and apply the conformal bootstrap to extract information about the bulk theory. This approach has been followed for example in [24–47]. Another recent advance is to develop new techniques to perform the calculation in the bulk itself, for example by using unitarity based methods [48–52], a differential representation of the propagator [53,54] or direct integration [55–57].

Although the study of perturbative quantum field theory in AdS is mathematically interesting in itself and can even be turned on its head by using bulk theories to calculate correlators of a CFT, in this thesis we are mainly motivated by computing cosmological correlators in dS. Ideally we would like to carry over some results and methods from AdS calculations. This is less straightforward as one might think. At first sight AdS and dS seem to look geometrically very similar, in fact they can be related by an analytic continuation. There are, however, some properties of dS that make the interpretation of QFT quantities more complicated.

In contrast to AdS, dS is not a static space-time which means that if we quantize a field theory on space-like slices there is no global vacuum state defined on every slice. Correlation functions in dS have to be calculated using time-dependent non-equilibrium techniques like the Schwinger-Keldysh formalism [58,59] and cannot be obtained from

AdS by a simple analytic continuation. Naive Wick rotation of an AdS correlation function to dS transforms it into a matrix element between an in and out vacuum (see e.g. [60]). It is important to stress that there is no scenario in which these two vacua are the same state since the boundary conditions, which have to be imposed in AdS, get rotated into conditions at future infinity of dS that are in contradiction with unitary time evolution.

It turns out that the objects obtained by Wick rotation from AdS still have an interesting interpretation in dS as the coefficients in the semiclassical expansion of the wave function of the Universe in the Schrödinger picture of QFT. This idea goes back to a work by Hartle and Hawking [61] and was further developed in [62–64]. The Wick rotation performed on the partition function in EAdS naturally selects the Bunch-Davies vacuum [65–67] as the initial state, which is the unique vacuum that provides the correct analytic structure of the propagator in the flat space limit [68], and returns its wave function as the amplitude with respect to a field configuration in the future.

The dS/CFT correspondence, as first formulated in [69], states that the Bunch-Davies wave function can be interpreted as the generating functional of a euclidean CFT at future infinity whose correlation functions are calculated by functional derivation with respect to the boundary values of the bulk field. This idea was further developed in [14] and led to new approaches to compute the wave function and relate it to a CFT at the future infinity surface of dS [62–64, 70–79]. Although there exists an explicit model that conjectures the correspondence between higher spin gravity in four dimensional dS and a CFT of anticommuting scalar fields at future infinity [80], the dS/CFT correspondence stands on much weaker feet than its sister in AdS since no construction based on string theory along the lines of [19] has been found so far.

The wave function, however, is not an observable. If we want to make a connection to actually measurable quantities, we have to compute the correlation function of the bulk field in the Bunch-Davies vacuum. In principle this can be done by taking the expectation value from the wave function. For free field theories this approach leads straightforwardly to the correct result [14]. For any interacting theory it requires non-perturbative knowledge of the wave function which, at least at the moment, seems to be completely out of reach and therefore makes this approach in praxis unrealistic.

A more promising path was started by Weinberg [15] using the Schwinger-Keldysh or in-in formalism [58, 59]. In this approach, the correlation function is computed by evolving the vacuum state from past to future infinity and back, introducing time- and anti-time ordered propagators. It has been used by various authors since, for example to discuss issues with infrared divergences in the global patch of dS [81–83].

In [84–86] it was realized that the late time correlation functions in dS in the Schwinger-Keldysh formalism can be rewritten as a linear combination of EAdS correlators. This result has led to the formulation of an auxiliary EAdS action in [87]. The perturbative calculations in dS can therefore be mapped to an equivalent computation in EAdS and as a consequence cosmological correlation functions should be given by a euclidean CFT at future infinity as well. A non-perturbative approach to quantum field theory at future infinity of dS was developed in [88], where methods from the conformal bootstrap [89] are used to obtain constraints on the QFT in the bulk.

While the above works found some general conditions and bounds on cosmological correlators at tree level, most of them still make some additional assumptions about their conformal structure at loop level. Therefore they do not provide a test of the correspondence between the cosmological correlators and a CFT beyond tree level.

One aim of this thesis is to fill this gap and consider a concrete model in the bulk and compute cosmological correlation functions including quantum corrections. The results are subject to some non-trivial consistency conditions dictated by conformal symmetry which are used to test the correspondence for the first time at one-loop level.

1.2 Content and results of this thesis

In this thesis we calculate loop corrections to cosmological correlation functions of a scalar field with quartic interaction in the Poincaré patch of four dimensional dS [90]. We achieve this goal by first performing the computation of loop corrected boundary correlators in EAdS [57] which we are able to relate to the dS calculation. For both cases we show that the correlation functions are governed by a euclidean CFT.

This approach does not claim to describe a realistic model for quantum fluctuations from the early universe. We rather intend to uncover general properties of QFT in (A)dS in an easy enough model, such that explicit calculations are possible. We compute two and four point functions up to one loop order by direct integration in position space, using Feynman parametrisation. The calculation is visualized through Feynman diagrams which in (A)dS are conventionally called Witten diagrams [22].

We start with the calculation in EAdS [57], which has been attempted before in [55, 56]. Concretely, we take a conformally coupled field in which case there are two possible choices for the boundary conditions of the bulk field ϕ, leading to two different dual operators $\mathcal{O}_\Delta$ in the CFT with scaling dimension either $\Delta = 1$ or $\Delta = 2$. It was shown in [55, 56] that the loop corrections to the two point function can be absorbed into the mass of the bulk field or, equivalently, the boundary scaling dimension Δ. We choose our renormalisation condition such that the value of Δ corresponds to that of a conformally coupled field in the bulk.

Since there are no three point functions in our model we continue with the calculation of the four point functions. The disconnected piece is completely determined by products of the two point functions of $\mathcal{O}_\Delta$. The theory on the boundary is therefore given by a generalized free field [91], which is defined by the property that the correlation functions factorize in the same way as in a free field theory. However, by a simple scaling argument, we know that the theory of $\mathcal{O}_\Delta$ cannot by given by a local action. From the bulk perspective this can be explained by the fact that we do not consider fluctuations of the metric which, according to the AdS/CFT dictionary, would result in an energy momentum tensor and require a local boundary theory. Consequently the dual CFT to our bulk field will be given by a non-local theory, similar to the long range Ising model at the critical point [92], for example. These theories were first considered in [93] in the context of AdS/CFT.

The operator product expansion (OPE) of a generalized free field theory is well known [94] and the four point function can be expanded in terms of conformal blocks of the double trace operators $:\mathcal{O}_\Delta\Box^n\partial^\ell\mathcal{O}_\Delta:$ in the CFT. From the bulk perspective these can be understood as bound states which do not appear as external operators. Introducing interactions in the bulk deforms the generalized free field at the boundary and will generate anomalous dimensions of the double trace operators, parametrized by the bulk coupling constant. To extract these we need to perform the perturbative computation of the four point function in the bulk.

By analyzing the properties of the propagator in AdS under the antipodal map and under the action of the conformal group on the boundary we are able to recast the four point function into the form of a flat space Feynman integral with three external momenta. This allows us to reproduce the results for the tree-level contribution to the four point function first calculated in [23].

At higher loop order we encounter short-distance (UV) divergences in the Witten diagrams which require regularisation and renormalisation. In [55, 56] an explicit cut-off scheme was used which has the advantage of preserving the AdS symmetries at the cost of complicating the structure of the propagator. This makes the subsequent computations technically very involved and harder to generalize.

We follow a different approach and implement an adapted version of dimensional regularisation. This is a non-trivial endeavor, since this method a priori breaks AdS invariance and as a consequence leads to non-conformally invariant boundary correlators. We develop a method to solve this problem by introducing a loop dependent analytical parameter in the integration measure which adds a finite piece to the counter-term and restores the symmetry of the renormalised correlator [57]. The advantage of this method is that most methods to solve Feynman integrals in flat space are based on dimensional regularisation (see e.g. [95–101]), making them applicable to our computation.

We show that most of the Feynman integrals we encounter are linearly reducible in the sense of [102] and can therefore be expressed in terms of single valued multiple polylogarithms [103]. The one loop diagram of the $\Delta = 1$ case contains an elliptic integral for which we find an efficient way to extract the relevant information. To simplify the calculation further we establish a decent relation in the form of several differential operators which raise the scaling dimensions of external legs by one unit.

Comparing our bulk calculation to the conformal block expansion we can extract deformations to the conformal data in the form of OPE coefficients and anomalous dimensions of the double trace operators of the generalized free field. One of the main results of this thesis is a closed expression for all anomalous dimensions at one-loop order for all double trace operators $:\mathcal{O}_\Delta \Box^n \partial^\ell \mathcal{O}_\Delta:$, which is given by

$$\gamma^{(2)}_{n>0,\ell>0}(\Delta) = \frac{\lambda_R^2}{(16\pi^2)^2} T^{\Delta}_{n,\ell}\,,$$

with

$$T^{\Delta}_{n,\ell} = -\frac{2(\ell^2 + (2\Delta + 2n - 1)(\Delta + n + \ell - 1))}{\ell(\ell+1)(2\Delta + 2n + \ell - 1)(2\Delta + 2n + \ell - 2)} - \frac{2(-1)^{\Delta}(H^{(1)}_{\ell} - H^{(1)}_{2\Delta+2n+\ell-2})}{(2\Delta + 2n + 2\ell - 1)(\Delta + n - 1)}\,,$$

where $H^{(1)}_i = \sum_{n=1}^{i} n^{-1}$ is the harmonic sum and λ_R is the renormalised bulk coupling constant. Similar results for all values of n and ℓ are derived in chapter 5, generalizing the expressions found in [56].

Using the Wick rotation from EAdS to dS as described in [14], we obtain the Bunch-Davies wave function from the partition function in EAdS. Consequently we can deduce the conformal data of the corresponding CFT directly from the EAdS results. We show that the CFTs coincide [71], where the boundary condition $\Delta = 2$ corresponds to fixing the field configuration at future infinity while $\Delta = 1$ gives the canonical momentum to the bulk field evaluated at infinity.

We are now ready to calculate the cosmological correlation functions in the late time limit [90]. Choosing as the initial condition the Bunch-Davies vacuum at past infinity we perform the computation by applying the Schwinger-Keldysh formalism. In this approach one performs a closed time integration from past to future infinity and back with field insertions on each side of the contour, therefore doubling the field content into time-ordered and anti-time ordered contributions. By Wick rotating the field insertions on each side of the contour independently and performing a change of basis in the propagators, we express the calculation as a sum over fields with either $\Delta = 1$ or $\Delta = 2$ boundary conditions in EAdS. This relation between the Schwinger-Keldysh propagators and EAdS Witten diagrams was first explained in [84–86] and reformulated into an auxiliary EAdS action in [87]. We can therefore apply the machinery developed for the EAdS calculation in [57], including the loop dependent dimensional regularisation scheme.

The results we obtain are quite remarkable. Although, at first sight, the computation looks more involved, since more diagrams have to be evaluated, the final results are actually much simpler than the corresponding expressions in the EAdS calculation. Specifically we find an interesting cancellation in the loop contributions which lead to the disappearance of any elliptic integrals. As a consequence all expressions are linearly reducible and can be expressed in terms of single valued multiple polylogarithms.

Comparing the late time cosmological correlation function to the four point function of a CFT, we show that the disconnected part is given by a generalized free field, while the interaction generates a deformation of this theory which is different from the one obtained in EAdS or, equivalently, the Bunch-Davies wave function. In this CFT, three different trajectories of double trace operators, denoted by $\mathcal{O}^S_{n,\ell}$, $\mathcal{O}^A_{n,\ell}$ and $:\!\mathcal{O}_1\Box^n\partial^\ell\mathcal{O}_2\!:$, acquire anomalous dimensions. The two different deformations of the generalized free field are schematically depicted in figure 1.1.

$$\boxed{\text{Cosmological correlator CFT}} \qquad \mathrm{CFT}(\mathcal{O}^S_{n,\ell}, \mathcal{O}^A_{n,\ell}, :\!\mathcal{O}_1\Box^n\partial^\ell\mathcal{O}_2\!:)$$

$$\uparrow$$

$$\overbrace{\mathrm{GFF}(\mathcal{O}_1)\times\mathrm{GFF}(\mathcal{O}_2)}$$

$$\swarrow \qquad \searrow$$

$$\boxed{\text{Wave function CFT}} \qquad \mathrm{CFT}_{\Psi[\pi]} \qquad \times \qquad \mathrm{CFT}_{\Psi[\phi]}$$

Figure 1.1: Deformations of the generalized free field (GFF) CFTs in the wave function CFTs (down) and cosmological correlator CFT (up). $\mathcal{O}^S_{n,\ell}$ and $\mathcal{O}^A_{n,\ell}$ are orthogonal linear combinations of $:\!\mathcal{O}_1\Box^n\partial^\ell\mathcal{O}_1\!:$ and $:\!\mathcal{O}_2\Box^n\partial^\ell\mathcal{O}_2\!:$.

We show that the cosmological correlators obey several CFT consistency conditions at different loop orders, reflecting the fact that the theory at future infinity is in fact a CFT. These conditions relate the tree-level results to the loop computation and can be interpreted as a condition on the sequential discontinuities of the Witten diagrams. An equivalent relation exists in EAdS and we show how to connect it to the flat space Cutkosky rules which extract discontinuities of Feynman integrals by putting certain internal propagators on-shell.

The main and final result of this work is the computation of all one-loop anomalous dimensions for the double trace operators $\mathcal{O}^S_{n,\ell}$, $\mathcal{O}^A_{n,\ell}$ and $:\!\mathcal{O}_1\Box^n\partial^\ell\mathcal{O}_2\!:$, given by

$$\gamma^{(2)S}_{n>0,\ell>0} = -\frac{\lambda_R^2}{(16\pi^2)^2}\frac{1}{\ell(\ell+1)}; \qquad \gamma^{(2)A}_{n>0,\ell>0} = -\frac{\lambda_R^2}{(16\pi^2)^2}\frac{1}{(2n+\ell)(2n+\ell+1)}$$
$$\gamma^{(2)}_{n,2\ell>0} = \gamma^{(2)S}_{n,2\ell>0}; \qquad \gamma^{(2)}_{n,2\ell+1>0} = \gamma^{(2)A}_{n,2\ell+2},$$

where the expressions for all values of n and ℓ are derived in chapter 6. These formulas highlight an interesting symmetry between the anomalous dimensions at different spins. From the bulk perspective, this could be a consequence of the symmetry in the auxiliary EAdS action, enforced by the Schwinger-Keldysh formalism and the fact that we take a conformally coupled scalar field. We do not expect this symmetry to hold for general masses. The equations for $\gamma^{(2)S}_{n>0,\ell>0}$ and $\gamma^{(2)}_{n,2\ell>0}$ show a degeneracy for the conformal dimensions of these operators for all values of n, which seems quite remarkable.

Outline

This thesis is structured as follows:

In chapter 2 we start with a brief review of the properties of a conformal field theory in $d > 2$ dimensions, including the OPE and conformal block expansion. We touch on the example of a generalized free field, explain how the OPE can be derived and consider the toy model of the free $O(N)$ vector model to illustrate our point. The chapter closes with a short remark about conformal perturbation theory to lay the foundation for later calculations.

The framework for the further computations in this thesis is built in chapter 3. Here we review the geometry of maximally symmetric space-times, focusing on (Anti-)de Sitter space-times and explain how to define perturbative quantum field theory in these spaces and how holography comes into play. This is crucial in understanding the similarities and differences in the QFT computations in these space-times and how they can be reduced to the evaluation of EAdS Witten diagrams.

Chapter 4 then discusses the mathematical structure and methods that we use to solve the integrals for the Witten diagrams. First, we explain how to map the diagrams to flat space Feynman integrals and how to implement a loop dependent dimensional regularisation scheme that preserves AdS invariance. We then review some well established methods of solving Feynman integrals which we will apply in the further course of the thesis. These include the Cutkosky rules to extract the discontinuity of a Feynman integral as well as multiple polylogarithms which are the solutions of linearly reducible Feynman integrals.

In chapters 5 and 6 we present the actual calculations of correlation functions, wave function coefficients and cosmological correlation functions, first published in [57,71,90].

The appendices at the end of this thesis collect useful expressions and lengthy calculations that were not included in the main body to keep the text readable.

1.3 List of publications

This thesis is partially a reproduction of some of the author's publications. Some of the results have been previously published in

[71] **T. Heckelbacher** and I. Sachs, *Loops in dS/CFT*, *JHEP* **02** (2021) 151 [2009.06511].

[57] **T. Heckelbacher**, I. Sachs, E. Skvortsov and P. Vanhove, *Analytical evaluation of AdS$_4$ Witten diagrams as flat space multi-loop Feynman integrals*, 2201.09626

[90] **T. Heckelbacher**, I. Sachs, E. Skvortsov and P. Vanhove, *Analytical evaluation of cosmological correlation functions*, 2204.07217

While working on this thesis the author contributed to the following publications, not included here

- M. Enríquez Rojo and **T. Heckelbacher**, *Asymptotic symmetries in spatially flat FRW spacetimes*, *Phys. Rev. D* **103** (2021) 064009 [2011.01960].
- M. Enríquez Rojo and **T. Heckelbacher**, *Holography and black holes in asymptotically flat FLRW spacetimes*, *Phys. Rev. D* **103** (2021) 104035 [2102.02234].
- M. Enríquez Rojo, **T. Heckelbacher** and R. Oliveri, *Asymptotic dynamics and charges for FLRW spacetimes*, 2201.07600

1.4 Acknowledgements

First and foremost I would like to thank my supervisor Ivo Sachs for the opportunity to do research under his guidance and write this thesis. I feel deeply thankful and lucky for having had the opportunity to benefit from his vast expertise and experience in various topics and thank him for his guidance, the many discussions we had and for giving me the freedom to pursue my own ideas.

Furthermore I am deeply indebted to Pierre Vanhove for the many discussions, patiently answering my questions, showing me lots of computational tools and in general for his collaboration and guidance and to Evgeny Skvortsov for his collaboration and for his regular and valuable advice.

I also would like to especially thank my office mate, colleague, collaborator and dear friend Martín Enríquez Rojo for the great times, the many discussions, collaboration and in general for going with me through the ups and downs of the experience of doing a PhD during a global pandemic.

Thanks go to all the members of the Cosmology department of LMU and all the people that crossed my path in the last years that I had the pleasure to work with. In particular, I would like to thank Ottavia Balducci, Igor Bertan, Daniel Bockisch, Ka Hei Choi, Lorenz Gärtner, Cecilia Giavoni, Katrin Hammer, Anamaria Hell, Roberto Oliveri, Tomáš Procházka, Tobias Schröder, Thomas Steingasser and Weichen Xiao. Finally I would like to thank Herta Wiesbeck-Yonis for all the administrative support.

My deepest gratitude goes to Jane Marino for all the emotional support and love she gave me during this time and for turning every moment into a joyful time (and also for the constant supply of self-made ice cream).

I also thank all my family and friends for their constant, unconditional support.

Finally I would like to thank the Hans-Böckler Stiftung for the financial support during the first part of this thesis.

Chapter 2

Aspects of conformal field theory

Conformal field theory (CFT) plays a major role in the formulation of holography in (A)dS. Since we will consider four-dimensional (A)dS, where the holographic CFT is three-dimensional it is necessary and important to review some aspects of CFTs in $d > 2$ dimensions in this chapter, especially since this topic is much less studied than two-dimensional CFTs. This chapter is mainly based on the reviews [104, 105].

2.1 CFT basics in $d > 2$

Consider a d-dimensional (pseudo-)Riemannian manifold $(M, g_{\mu\nu})$ and a smooth map $\phi : M \to M$. We call ϕ a conformal map (see e.g. [106]) if the pullback of the metric is given by

$$\phi^* g_{\mu\nu} = \Omega(x)^2 g_{\mu\nu}\,, \tag{2.1}$$

where Ω is a positive real function. If we consider a one-parameter group ϕ_t of conformal transformations, then the vector field X generating ϕ_t is called a conformal Killing field and (2.1) translates into the following condition on the Lie derivative of the metric

$$\mathcal{L}_X g_{\mu\nu} = \nabla_\mu X_\nu + \nabla_\nu X_\mu = \frac{2}{d} \nabla_\gamma X^\gamma g_{\mu\nu} \tag{2.2}$$

If M is flat (2.2) has the following solutions

$P_\mu := -i\partial_\mu$	Translations
$M_{\mu\nu} := i(x_\mu \partial_\nu - x_\nu \partial_\mu)$	Lorentz transformations
$D := -i x^\mu \partial_\mu$	Dilatations
$K_\mu := -i(2x_\mu x^\nu \partial_\nu - x^2 \partial_\mu)$	Special conformal transformations

The first two Killing vector fields are the generators of the Poincaré group, while the other two are new and have the interpretation of a local rescaling and a translation after the location of the origin and infinity have been swapped. The non-vanishing Lie brackets of these vector fields are given by

$$[D, P_\mu] = iP_\mu, \qquad [D, K_\mu] = -iK_\mu, \qquad [K_\mu, P_\nu] = 2i(\eta_{\mu\nu} D - M_{\mu\nu}), \tag{2.3a}$$
$$[K_\gamma, M_{\mu\nu}] = i(\eta_{\gamma\mu} K_\nu - \eta_{\gamma\nu} K_\mu), \qquad [P_\gamma, M_{\mu\nu}] = i(\eta_{\gamma\mu} P_\nu - \eta_{\gamma\nu} P_\mu), \tag{2.3b}$$
$$[M_{\mu\nu}, M_{\gamma\rho}] = i(\eta_{\nu\gamma} M_{\mu\rho} + \eta_{\mu\rho} M_{\nu\gamma} - \eta_{\mu\gamma} M_{\nu\rho} - \eta_{\nu\rho} M_{\mu\gamma}), \tag{2.3c}$$

where (2.3c) is just the Lorentz algebra, (2.3b) means that both P_μ and K_μ transform like vectors while (2.3a) are new.

The algebra (2.3) can be mapped to the Lorentz algebra of a $d+2$-dimensional Minkowski ambient space with metric signature $(-,+,...+,-)$ by the following isomorphism

$$M_{\mu\nu} = J_{\mu\nu}, \quad D = J_{d+1,d}, \quad P_\mu = \frac{1}{\sqrt{2}}\left(J_{\mu,d+1} - J_{\mu,d}\right), \quad K_\mu = \sqrt{2}\left(J_{\mu,d+1} + J_{\mu,d}\right),$$

where J_{AB} are the Lorentz generators in the ambient space, obeying the algebra

$$[J_{AB}, J_{CD}] = i\left(\eta_{AD}J_{BC} + \eta_{BC}J_{AD} - \eta_{AC}J_{BD} - \eta_{BD}J_{AC}\right).$$

They are the generators of the group $SO(d,2)$. To see how the ambient Minkowski space is related to the original d dimensional flat space, we restrict to the projective light-cone, given by the lines on the light-cone through the origin

$$\mathbb{LP}^d := \{[X] \in \mathbb{RP}^{d+1} : \eta_{AB}X^AX^B = 0\}.$$

It can be shown [104] that an element of $SO(d,2)$ acts on $\mathbb{LP}^d$ such that the induced metric transforms as (2.1). The embedding of Minkowski space $\mathbb{R}^{d-1,1}$ into the projective space $\mathbb{RP}^{d+1}$ is defined by

$$\begin{aligned} \iota: \quad & \mathbb{R}^{d-1,1} \to \mathbb{RP}^{d+1} \\ & x^\mu \mapsto \left(x^\mu : \frac{1-x^2}{2} : \frac{1+x^2}{2}\right), \end{aligned}$$

where $x^2 = \eta_{\mu\nu}x^\mu x^\nu$ and $\eta_{\mu\nu}$ is the standard Minkowski metric. With this embedding we have the following simple identity

$$X \cdot Y = \frac{1}{2}|x-y|^2$$

For technical reasons it is usually convenient to use the ambient space coordinates for calculations, since they transform linearly under the conformal group and only restrict to the projective lightcone at the end.

Quantizing a conformally invariant theory is most easily done in radial quantization. This means that instead of defining states on equal time slices we foliate the manifold in terms of spheres around the origin and define states as path-integrals over a sphere [105]. The exponentiation of the dilatation operator is a rescaling, which moves a state between different spheres and therefore is the equivalent to the time evolution operator in canonical quantization. The dilatation operator then takes the role of the Hamiltonian.

To fully exploit that analogy we label states by Δ and ℓ where the former is the eigenvalue of the dilatation operator and the latter the spin of the irreducible $SO(d)$ representation. The action of D and $M_{\mu\nu}$ on a state $|\Delta,\ell\rangle$ is then given by

$$D\,|\Delta,\ell\rangle = -i\Delta\,|\Delta,\ell\rangle, \qquad M_{\mu\nu}\,|\Delta,\ell\rangle = iD^{(\ell)}(M_{\mu\nu})\,|\Delta,\ell\rangle$$

where $D^{(\ell)}(M_{\mu\nu})$ is the spin ℓ representation matrix of $M_{\mu\nu}$. From the first two equations in (2.3a) we can follow that P_μ raises Δ by 1 while K_μ lowers it. The states which are annihilated by K_μ, i.e. $K_\mu |\Delta, \ell\rangle = 0$, are called primary states and states created by acting subsequently with P_μ on a primary are called descendant states.

Let us now introduce local field operators $\mathcal{O}_{\Delta,\ell}(x)$, with scaling dimension Δ and spin ℓ, such that they transform under rescaling as

$$\mathcal{O}_\Delta(\lambda x) = \frac{1}{\lambda^\Delta}\mathcal{O}_\Delta(x)\,.$$

We can define a state $|\Delta, \ell\rangle$ by inserting an operator $\mathcal{O}_{\Delta,\ell}$ on the conformally invariant vacuum at the origin. At the same time we can take any state, defined on some sphere and rescale it to a point which will behave just like a local operator insertion at that point. This is the idea behind the operator state correspondence of a CFT (see [105]). The transformation behaviour of an operator away from the origin is then completely fixed by the algebra (2.3) and is given by

$$\begin{aligned}
[D, \mathcal{O}_{\Delta,\ell}(x)] &= -i(\Delta + x^\mu \partial_\mu)\mathcal{O}_{\Delta,\ell}(x)\\
[P_\mu, \mathcal{O}_{\Delta,\ell}(x)] &= -i\partial_\mu \mathcal{O}_{\Delta,\ell}(x)\\
[K_\mu, \mathcal{O}_{\Delta,\ell}(x)] &= -i(2x_\mu \Delta + 2x_\mu x^\nu \partial_\nu - x^2\partial_\mu - 2x^\nu D^{(\ell)}(M_{\nu\mu}))\mathcal{O}_{\Delta,\ell}(x)\\
[M_{\mu,\nu}, \mathcal{O}_{\Delta,\ell}(x)] &= -i(x_\mu\partial_\nu - x_\nu\partial_\mu - iD^{(\ell)}(M_{\mu\nu}))\mathcal{O}_{\Delta,\ell}(x)
\end{aligned}$$

Following the terminology introduced above for the states we call operators which vanish under the action of K_μ primary operators, while those generated by acting with P_μ on a primary are called descendants.

What makes a CFT special compared to an ordinary QFT is the fact that large parts of the theory are already fixed by symmetry such as the two point function, the three point function up to a constant [107] and the general structure of the four point function. For scalar operators, which are most relevant for our purpose, they are given by (see e.g. [104, 105, 108] for a derivation)

$$\begin{aligned}
\langle \mathcal{O}_{\Delta_1}(x_1)\mathcal{O}_{\Delta_2}(x_2)\rangle &= \frac{\delta_{\Delta_1\Delta_2}}{x_{12}^{2\Delta_1}}\\
\langle \mathcal{O}_{\Delta_1}(x_1)\mathcal{O}_{\Delta_2}(x_2)\mathcal{O}_{\Delta_3}(x_3)\rangle &= \frac{\lambda_{123}}{x_{12}^{\Delta_1-\Delta_3+\Delta_2}x_{13}^{\Delta_1-\Delta_2+\Delta_3}x_{23}^{\Delta_2-\Delta_1+\Delta_3}}\\
\langle \mathcal{O}_{\Delta_1}(x_1)\mathcal{O}_{\Delta_2}(x_2)\mathcal{O}_{\Delta_3}(x_3)\mathcal{O}_{\Delta_4}(x_4)\rangle &= T_s(x_i)G(v,Y)\,,
\end{aligned} \tag{2.5}$$

where we introduced the shorthand notation $x_{ij} = |x_i - x_j|$ and $G(v, Y)$ is a function of the conformal cross ratios

$$v = \frac{x_{12}^2 x_{34}^2}{x_{14}^2 x_{23}^2} =; \qquad 1 - Y = \frac{x_{13}^2 x_{24}^2}{x_{14}^2 x_{23}^2}\,.$$

The kinematic prefactor is given by

$$T_s(x_i) = \frac{1}{x_{12}^{\Delta_1+\Delta_2}x_{34}^{\Delta_3+\Delta_4}}\left(\frac{x_{14}}{x_{24}}\right)^{\Delta_2-\Delta_1}\left(\frac{x_{14}}{x_{13}}\right)^{\Delta_3-\Delta_4}\,.$$

A major feature of a CFT is the convergence of the operator product expansion (OPE). For any quantum field theory we can express the product of two operators $\mathcal{O}_{\Delta_1}(x_1)\mathcal{O}_{\Delta_2}(x_2)$ in the limit $x_1 \to x_2$ as a sum over local operators at x_2 denoted as

$$\mathcal{O}_{\Delta_1}(x_1) \times \mathcal{O}_{\Delta_2}(x_2) = \sum_i C_{12i}(x_{12})\mathcal{O}_i(x_2)$$

In a general QFT this sum is only asymptotic. In a CFT this expansion is convergent, since it is equivalent to a sum over a complete set of states due to the operator state correspondence. In this case it takes the form

$$\mathcal{O}_{\Delta_1}(x_1) \times \mathcal{O}_{\Delta_2}(x_2) = \sum_{\tilde{\mathcal{O}}} a^{12}_{\tilde{\mathcal{O}}} \mathcal{D}_{12\tilde{\mathcal{O}}}(x_{12}, \partial_2)\tilde{\mathcal{O}}_i(x_2)\,.$$

where $a^{ij}_{\tilde{\mathcal{O}}}$ are called OPE coefficients and $\mathcal{D}_{12\tilde{\mathcal{O}}}$ is a differential operator whose coefficients are completely fixed by conformal symmetry. The entire information about the dynamics of the theory is therefore contained in the spectrum of operators and the OPE coefficients. Knowing those solves the theory completely and as a consequence they are referred to as the CFT data, defining the theory. Plugging the OPE into the three point function and using the orthogonality of the two point function we realize that the OPE coefficients $a^{12}_{\tilde{\mathcal{O}}}$ are given by the undetermined constants $\lambda_{12\mathcal{O}}$ in the three point function (2.5). This means that knowing the operator spectrum and all three point functions actually solves the theory completely.

The main focus of our calculations in chapters 5 and 6 will be the four point function. For any four point function we can calculate the OPE pairwise between two operators in three different ways

$$\langle(\mathcal{O}_1 \times \mathcal{O}_2)(\mathcal{O}_3 \times \mathcal{O}_4)\rangle\,, \qquad \langle(\mathcal{O}_1 \times \mathcal{O}_3)(\mathcal{O}_2 \times \mathcal{O}_4)\rangle\,, \qquad \langle(\mathcal{O}_1 \times \mathcal{O}_4)(\mathcal{O}_3 \times \mathcal{O}_2)\rangle\,, \tag{2.6}$$

where the three cases are refered to as the s, t and u channel respectively.[1] In each of the channels we can rewrite the double OPE as a sum over conformal blocks $\mathcal{G}_{\Delta,\ell}(v, Y)$. Focusing on the s channel, they are defined through

$$\langle\mathcal{O}_1(x_1)\mathcal{O}_2(x_2)\mathcal{O}_3(x_3)\mathcal{O}_4(x_4)\rangle = T_s(x_i) \sum_{\Delta,\ell} a^{12}_{\mathcal{O}_{\Delta,\ell}} a^{34}_{\mathcal{O}_{\Delta,\ell}} \mathcal{G}^s_{\Delta,\ell}(v, Y)\,. \tag{2.7}$$

The conformal blocks are eigenfunctions of the conformal casimir $C_2 = J_{AB}J^{AB}$ and a closed expression for them was first found in [109].

This derivation works in the following way [105]. Let us consider a four point function of a scalar operators $\mathcal{O}$ with equal dimensions Δ for simplicity. The double OPE of equation (2.6) can then be explicitly expressed as

$$\begin{aligned}
\langle\mathcal{O}(x_1)\mathcal{O}(x_2)\mathcal{O}(x_3)\mathcal{O}(x_4)\rangle &= \sum_{\tilde{\mathcal{O}}\tilde{\tilde{\mathcal{O}}}} a^{\mathcal{O}\mathcal{O}}_{\tilde{\mathcal{O}}} a^{\mathcal{O}\mathcal{O}}_{\tilde{\tilde{\mathcal{O}}}} \mathcal{D}_{\mathcal{O}\mathcal{O}\tilde{\mathcal{O}}}(x_{12}, \partial_2)\mathcal{D}_{\mathcal{O}\mathcal{O}\tilde{\tilde{\mathcal{O}}}}(x_{34}, \partial_4) \left\langle \tilde{\mathcal{O}}(x_2)\tilde{\tilde{\mathcal{O}}}(x_4) \right\rangle \\
&= \frac{1}{(x_{12}x_{34})^{2\Delta}} \sum_{\tilde{\mathcal{O}}} \left(a^{\mathcal{O}\mathcal{O}}_{\tilde{\mathcal{O}}}\right)^2 \mathcal{G}^s_{\tilde{\Delta},\ell}(v, Y) \qquad (2.8) \\
\Rightarrow \mathcal{G}^s_{\tilde{\Delta},\ell}(u, v) &= (x_{12}x_{34})^{2\Delta} \mathcal{D}_{\mathcal{O}\mathcal{O}\tilde{\mathcal{O}}}(x_{12}, \partial_2)\mathcal{D}_{\mathcal{O}\mathcal{O}\tilde{\mathcal{O}}}(x_{34}, \partial_4) \left\langle \tilde{\mathcal{O}}(x_2)\tilde{\mathcal{O}}(x_4) \right\rangle
\end{aligned}$$

where we chose an orthogonal basis of operators $\tilde{\mathcal{O}}$ and $\tilde{\tilde{\mathcal{O}}}$.

To see why the conformal blocks are eigenfunctions of the casimir operator let us consider the same four point function in radial quantization. The radially ordered four point function with $|x_3|, |x_4| \geq |x_1|, |x_2|$ can be written as

$$\langle\mathcal{O}(x_1)\mathcal{O}(x_2)\mathcal{O}(x_3)\mathcal{O}(x_4)\rangle = \langle 0| R\{\mathcal{O}(x_3)\mathcal{O}(x_4)\}R\{\mathcal{O}(x_1)\mathcal{O}(x_2)\} |0\rangle\,,$$

[1] Note, that this is not what we mean by the three channels in our calculation in later chapters. We will always perform the OPE in the s channel.

where $R\{...\}$ denotes radial ordering.

We can introduce an operator $\Pi_{\tilde{\mathcal{O}}}$ that projects a state into a conformal multiplet, i.e. a primary $\tilde{\mathcal{O}}$ and its descendants. The sum over all primaries then gives the unit operator because of the operator state correspondence

$$\Pi_{\tilde{\mathcal{O}}} = \sum_{\phi,\psi=\tilde{\mathcal{O}},P\tilde{\mathcal{O}},PP\tilde{\mathcal{O}}} |\phi\rangle \langle\psi| \, ; \qquad \mathbb{I} = \sum_{\tilde{\mathcal{O}}} \Pi_{\tilde{\mathcal{O}}} \, .$$

Now the four point function can be written as

$$\langle \mathcal{O}(x_1)\mathcal{O}(x_2)\mathcal{O}(x_3)\mathcal{O}(x_4)\rangle = \sum_{\tilde{\mathcal{O}}} \langle 0| \, R\{\mathcal{O}(x_3)\mathcal{O}(x_4)\}\Pi_{\tilde{\mathcal{O}}} R\{\mathcal{O}(x_1)\mathcal{O}(x_2)\} \, |0\rangle$$

and should be equivalent to equation (2.8), which means that

$$\frac{\left(a_{\tilde{\mathcal{O}}}^{\mathcal{O}\mathcal{O}}\right)^2 \mathcal{G}^s_{\tilde{\Delta},\ell}(v,Y)}{(x_{12}x_{34})^{2\Delta}} = \langle 0| \, R\{\mathcal{O}(x_3)\mathcal{O}(x_4)\}\Pi_{\tilde{\mathcal{O}}} R\{\mathcal{O}(x_1)\mathcal{O}(x_2)\} \, |0\rangle \tag{2.9}$$

The quadratic casimir is given by

$$C_2 = \frac{1}{2} J^{AB} J_{AB} = D(D-d) - \frac{1}{2} M^{\mu\nu} M_{\mu\nu}$$

and it acts on the projector $\Pi_{\mathcal{O}}$ as

$$C_2 \Pi_{\mathcal{O}} = \left[\Delta(\Delta - d) + l(l + d - 2)\right] \Pi_{\mathcal{O}} \, . \tag{2.10}$$

At the same can we define a differential operator $\mathcal{C}_2^{12}$ representing the action of the quadratic casimir on the fields $\mathcal{O}(x_1)\mathcal{O}(x_2)$ as

$$\mathcal{C}_2^{12} \mathcal{O}(x_1)\mathcal{O}(x_2) = \left[C_2, \mathcal{O}(x_1)\mathcal{O}(x_2)\right] . \tag{2.11}$$

Plugging equations (2.11), (2.10) into (2.9) we find that the conformal blocks have to obey the following differential equation

$$\mathcal{C}_2 \mathcal{G}_{\Delta,\ell}(v,Y) = \left[\Delta(\Delta - d) + l(l + d - 2)\right] \mathcal{G}_{\Delta,\ell}(v,Y) \, , \tag{2.12}$$

where the differential operator $\mathcal{C}_2$ is the differential representation of the quadratic Casimir in terms of conformal cross ratios and given in [110]. For even dimensions d equation (2.12) can be solved exactly (see [109]). For general dimensions no analytic solution is known for all spins. The spin zero conformal block has been calculated in [109] as well and in the s-channel OPE limit, defined by $v, Y \to 0$, is given by

$$\mathcal{G}_{\Delta,0}(u,v) = v^{\frac{\Delta}{2}} \sum_{m,n=0}^{\infty} \frac{\left(\frac{\Delta}{2}\right)_m^2 \left(\frac{\Delta}{2}\right)_{m+n}^2}{m!n!(\Delta + 1 - d/2)_m (\Delta)_{2m+n}} v^m Y^n$$

$$\text{with the Pochhammer symbol defined as: } (x)_n = \frac{\Gamma(x+n)}{\Gamma(x)} \, . \tag{2.13}$$

A similar expansion for general spins $\ell > 0$ was found in [111] and is given in appendix D.

The advantage of using the conformal block expansion lies in the fact that it organizes the calculation automatically in terms of conformal multiplets, since a conformal

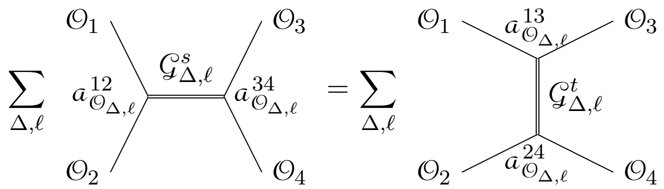

Figure 2.1: Graphical depiction of the conformal block expansion and OPE associativity. These pictures should not be confused with Feynman or Witten diagrams.

block $\mathcal{G}_{\Delta,\ell}$ contains all information about the primary operator $\mathcal{O}_{\Delta,\ell}$ and its descendants.

Note that we could have done the double OPE in the t- and u channel as well which would have given us another conformal block expansion. However, since the OPE is a convergent sum, it should not matter in which order the OPE is done and the end result for the four point function should be the same after summing over all terms. This associativity of the OPE is the basis of the conformal bootstrap, which we will not consider any further and refer the interested reader to the review [105] and references therein.

2.2 OPE of a generalized free field

A concrete example of a CFT which will play a role in subsequent calculations is a generalized free field theory [91] sometimes also referred to as mean field theory. It is given by a certain number of fields $\mathcal{O}_1, ...\mathcal{O}_n$ with scaling dimensions $\Delta_1, ..., \Delta_n$. The theory is then defined by its n-point correlation functions which vanish for odd n and for even n are given by all pairwise combinations of two point functions, which take the form

$$\langle \mathcal{O}_i(x_i)\mathcal{O}_i(x_j)\rangle = \frac{\delta_{\Delta_i \Delta_j}}{x_{ij}^{2\Delta_i}}.$$

The four point function of a generalized free field with equal scaling dimensions Δ is for example given by

$$\langle \mathcal{O}(x_1)\mathcal{O}(x_2)\mathcal{O}(x_3)\mathcal{O}(x_4)\rangle = \frac{1}{x_{12}^{2\Delta}x_{34}^{2\Delta}}\left(1 + v^{\Delta} + \left(\frac{v}{1-Y}\right)^{\Delta}\right).$$

Note that a theory like this cannot by constructed from a local action of the fields $\mathcal{O}_1, ..., \mathcal{O}_n$ for obvious dimensional reasons, unless $\Delta = \frac{d}{2} - 1$. It is therefore a free field theory in the sense that the n point functions look like they were generated by a Gaussian path-integral even though no local action exists.

A generalized free field theory can emerge as an effective description of another theory in some limit. To understand how this works let us consider the free $O(N)$ vector model, defined by the action (see e.g. [112])

$$S = \int_{\mathbb{R}^d} \mathrm{d}x^d \frac{1}{2}\sum_{i=1}^{N} \partial_\mu \phi^i \partial^\mu \phi^i\,,$$

which of course has the simple two point functions for the fundamental field ϕ^i

$$\left\langle \phi^i(x_1)\phi^j(x_2)\right\rangle = \frac{\delta_{ij}}{x_{12}^{d-2}}\,. \tag{2.14}$$

We can, however, also consider other operators, composed out more than one fundamental field. For example we can define

$$\mathcal{O}_2 := \frac{1}{\sqrt{2N}}\mathrm{Tr}(:\!\phi^2\!:) := \frac{1}{\sqrt{2N}}\sum_{i=1}^{N} :\!\phi^i\phi^i\!:= \sum_{i=1}^{N}\left(\phi^i\phi^i - \left\langle\phi^i\phi^i\right\rangle\right)\,,$$

and calculate the correlation functions of this operator. The two point function can be straightforwardly calculated from (2.14) by Wick contraction and is given by

$$\langle \mathcal{O}_2(x_1)\mathcal{O}_2(x_2)\rangle = \frac{1}{x_{12}^{2(d-2)}}\,,$$

meaning $\mathcal{O}_2$ has scaling dimension $d-2$. We can proceed in this way building operators of the form

$$\mathcal{O}_n := \frac{1}{\sqrt{n!N}}\mathrm{Tr}(:\!\phi^n\!:)\,,$$

with scaling dimension $n(d/2-1)$. The four point functions of these operators is easily obtained by Wick contraction, using equation (2.14) and in the limit $N\to\infty$ are given by

$$\langle \mathcal{O}_n(x_1)\mathcal{O}_n(x_2)\mathcal{O}_n(x_3)\mathcal{O}_n(x_4)\rangle = \frac{1}{(x_{12}x_{34})^{n(d-2)}}\left(1+v^{\frac{n(d-2)}{2}}+\left(\frac{v}{1-Y}\right)^{\frac{n(d-2)}{2}}\right)\,. \tag{2.15}$$

This shows that the free $O(N)$ vector model at infinite N is an example of a generalized free field theory. The operators $\mathcal{O}_n$ constructed in this way are called single trace operators and, following conventions in the AdS/CFT literature [113], we will refer to them as such in subsequent calculations, even if we do not know whether they are actually constructed as a trace over fundamental fields in a large N vector or matrix model. With this terminology established, we can reformulate the defining property of a generalized free field theory that all correlators are determined by the two point function of single trace operators.

The theory is therefore solved completely, which for the CFT data means that we should have access to all three point functions and operators. The three point functions of single trace operators vanish, which is obvious from the above discussion. To obtain non-vanishing three point functions we have to consider more general objects such as double trace operators.

We can construct double trace primary operators out of single trace operators, by adding combinations of $P_\mu = -i\partial_\mu$ acting on $\mathcal{O}_1$ and $\mathcal{O}_2$ in such a way that the sum is annihilated by K_μ. A general double trace operator can then be denoted by $:\!\mathcal{O}_1\Box^n\partial^\ell\mathcal{O}_2\!:$ and it has scaling dimension $\Delta_{n,\ell} = \Delta_1+\Delta_2+2n+\ell$ and has spin ℓ, where the Lorentz indices of $\partial_{\mu_1}...\partial_{\mu_\ell}$ are implicit in ∂^ℓ. An recursive algorithm on how to construct double trace primaries in this way has been developed in [94].

A more efficient way of constructing double trace operators, also described in [94], is by conglomeration which means we write them as a convolution

$$:\mathcal{O}_1\Box^n\partial^\ell\mathcal{O}_2:(x) = \int \mathrm{d}^dx_1\mathrm{d}^dx_2 f_{\Delta_1+\Delta_2+2n+\ell,\ell}(x,x_1,x_2)\mathcal{O}_{\Delta_1}(x_1)\mathcal{O}_{\Delta_2}(x_2)\,. \tag{2.16}$$

Where $f_{\Delta_1+\Delta_2+2n+\ell,\ell}(x,x_1,x_2)$ is given by the three point function of $:\mathcal{O}_1\Box^n\partial^\ell\mathcal{O}_2:(x)$ with the so called shadow operators $\mathcal{O}_{d-\Delta_1}$ and $\mathcal{O}_{d-\Delta_2}$.

As it was shown in [114] in the ambient formalism the three point function of two scalar operators with a spin ℓ operator $\mathcal{O}_{\Delta,\ell}^{A_1\ldots A_\ell}$ is given by

$$\begin{aligned}
&Y_{A_1}\ldots Y_{A_\ell}\left\langle \mathcal{O}_{\Delta_1}(X_1)\mathcal{O}_{\Delta_2}(X_2)\mathcal{O}_{\Delta,\ell}^{A_1\ldots A_\ell}(X_3)\right\rangle = \\
&\qquad = a_{\Delta,\ell}^{12}\frac{((Y\cdot X_1)X_2\cdot X_3-(Y\cdot X_2)X_1\cdot X_3)^\ell}{(X_1\cdot X_2)^{\frac{\Delta_1+\Delta_2-\Delta+\ell}{2}}(X_1\cdot X_3)^{\frac{\Delta_1+\Delta-\Delta_2-\ell}{2}}(X_2\cdot X_3)^{\frac{\Delta_2+\Delta-\Delta_1-\ell}{2}}}\,,
\end{aligned} \tag{2.17}$$

where Y is an auxiliary vector with $Y\cdot X_3 = 0$. From equation (2.17) we can see immediately that the three point function of two equal scalar operators and an operator with odd spin vanishes, meaning that there are no operators with odd spin in the OPE.

The function $f_{\Delta_1+\Delta_2+2n+\ell,\ell}(x,x_1,x_2)$ in equation (2.16) is now given by

$$f_{\Delta_1+\Delta_2+2n+\ell,\ell}(x,x_1,x_2) = Y_{A_1}\ldots Y_{A_\ell}\left\langle \mathcal{O}_{d-\Delta_1}(X_1)\mathcal{O}_{d-\Delta_2}(X_2)\mathcal{O}_{\Delta_{n,\ell},\ell}^{A_1\ldots A_\ell}(X_3)\right\rangle\,. \tag{2.18}$$

For a generalized free field we know the four point functions exactly so we can use that knowledge together with equations (2.16), (2.17) and (2.18) to extract the OPE coefficient of a specific double trace operator by setting

$$\begin{aligned}
&\int \mathrm{d}^dx_1\mathrm{d}^dx_2 f_{\Delta_1+\Delta_2+2n+\ell,\ell}(x,x_1,x_2)\left\langle \mathcal{O}_{\Delta_1}(x_1)\mathcal{O}_{\Delta_2}(x_2)\mathcal{O}_{\Delta_1}(x_3)\mathcal{O}_{\Delta_2}(x_4)\right\rangle = \\
&\qquad\qquad = \left\langle :\mathcal{O}_1\Box^n\partial^\ell\mathcal{O}_2:(x)\mathcal{O}_{\Delta_1}(x_3)\mathcal{O}_{\Delta_2}(x_4)\right\rangle
\end{aligned}$$

This integration is most easily performed in Mellin space [94, 115] where it reduces to a system of linear equations. The final result for the squared OPE coefficients

$$A^{i,j}_{[\mathcal{O}_i\mathcal{O}_j]_{n,l}} := \left(a^{i,j}_{[\mathcal{O}_i\mathcal{O}_j]_{n,l}}\right)^2$$

for the double trace operator $:\mathcal{O}_1\Box^n\partial^\ell\mathcal{O}_2:(x)$ is given by

$$A^{i,j}_{[\mathcal{O}_i\mathcal{O}_j]_{n,l}} = \frac{(-1)^l\left(\Delta_i-\frac{d}{2}+1\right)_n\left(\Delta_j-\frac{d}{2}+1\right)_n(\Delta_i)_{l+n}(\Delta_j)_{l+n}}{l!n!\left(l+\frac{d}{2}\right)_n(\Delta_i+\Delta_j+n-d+1)_n(\Delta_i+\Delta_j+2n+l-1)_l\left(\Delta_i+\Delta_j+n+l-\frac{d}{2}\right)_n}\,,$$

where the Pochhammer symbol $(x)_n$ is defined in equation (2.13).

Since we know the exact expressions for the conformal blocks and the OPE coefficients for all double trace operators we obtained all the conformal data as defined in section 2.1. In general a CFT will not be as simple as a generalized free field. However, we will see that theories which originate from a bulk theory in AdS will deform a generalized free field by their interaction terms in a very specific way namely by generating anomalous dimensions in for the double trace operators.

2.3 Perturbation theory in CFT

So far we have only discussed general features of CFTs and one particularly simple example. In general, solving a CFT exactly is usually not possible but there are certain types of CFTs, containing a parameter which can be considered small. Then we can perform a perturbative expansion in this parameter. In fact, we already encountered an example of such a theory in the previous section with the free $O(N)$ vector model. We found that the four point function behaves like a generalized free field theory in the limit $N \to \infty$ but equation (2.15) tells us that there are corrections if we go to finite values of N. We can therefore use N^{-1} as the small perturbative parameter to expand around. This approach to perturbation theory of a CFT was first described in [93].

In general, if we have a small parameter λ and know the CFT data for $\lambda = 0$, we can expand CFT data, i.e. the OPE coefficients and operator dimensions, in λ such that

$$\begin{aligned} \mathcal{A}^{\mathcal{O}_1\mathcal{O}_2}_{\mathcal{O}_3} &= \bar{A}^{\mathcal{O}_1\mathcal{O}_2}_{\mathcal{O}_3} + \lambda A^{\mathcal{O}_1\mathcal{O}_2(1)}_{\mathcal{O}_3} + \frac{1}{2}\lambda^2 A^{\mathcal{O}_1\mathcal{O}_2(2)}_{\mathcal{O}_3} + \ldots \\ \Delta &= \bar{\Delta} + \lambda\Delta^{(1)} + \frac{1}{2}\lambda^2\Delta^{(2)} + \ldots \end{aligned} \tag{2.19}$$

In this work we will mostly be concerned with four point functions and the only effect of the perturbation will be felt by the exchanged double trace operators. For this case it is most convenient to parametrize the perturbation in terms of the anomalous dimensions of the exchanged double trace operator, meaning that we absorb the expansion parameter λ in equation (2.19) into the expansion coefficients, such that equation (2.19) becomes

$$\Delta = \bar{\Delta} + \gamma^{(1)} + \gamma^{(2)} + \ldots \qquad \text{with: } \gamma^{(i)} \propto \lambda^i\,.$$

The perturbative expansion of the OPE coefficients is then given by

$$\mathcal{A}^{\mathcal{O}_1\mathcal{O}_2}_{\mathcal{O}_3} = \bar{A}^{\mathcal{O}_1\mathcal{O}_2}_{\mathcal{O}_3} + (\gamma^{(1)} + \gamma^{(2)} + \ldots) A^{\mathcal{O}_1\mathcal{O}_2(1)}_{\mathcal{O}_3} + \frac{1}{2}(\gamma^{(1)} + \gamma^{(2)} + \ldots)^2 A^{\mathcal{O}_1\mathcal{O}_2(2)}_{\mathcal{O}_3} + \ldots\,.$$

Expanding the conformal blocks in terms of anomalous dimensions as well, will provide us with the perturbative expansion of the four point function. We will use this method in chapters 5 and 6 where the small expansion parameter is given by the bulk coupling constant of the dual theory.

Chapter 3

Quantum field theory in maximally symmetric, curved space-times

Quantum field theory in curved space-time has a long history [116], however calculations beyond tree-level are hard to perform due to the lack of symmetry of a general curved space. From a technical as well as a phenomenological point of view it is therefore reasonable to restrict ones analysis to specific classes of curved space-times, which have certain symmetries. Following the treatment in flat space one can then construct a Hilbert space out of irreducible representations of that symmetry group, therefore providing a framework for a well defined quantum field theory.

The simplest non-flat space-times are arguably (Anti-)de Sitter space-times ((A)dS) since they have the same number of symmetries as Minkowski space. At the same time, dS is phenomenologically relevant since it approximately describes the inflationary stage of our Universe [9,10]. In this chapter we will show how to define an interacting scalar quantum field theory in these spaces. We will emphasize the similarities and differences and make connection to the conformal field theory on the boundary. This lays the theoretical groundwork for the computation of cosmological correlation functions. Parts of this chapter contain reproductions of [57,71,90].

3.1 Geometry of (Anti-)de Sitter space-time

Let us first specify what we mean by maximal symmetry (see e.g. [117]). For a given space-time $(M, g_{\mu\nu})$ a one parameter group of diffeomorphisms $\phi_t : M \to M$ is an isometry if $\phi_t^* g_{\mu\nu} = g_{\mu\nu}$. The vector field ξ^μ to which ϕ_t is the flow is called a Killing vector field and the fact that ϕ_t is an isometry translates to the Killing equation

$$\mathcal{L}_\xi g_{\mu\nu} = \nabla_\mu \xi_\nu + \nabla_\nu \xi_\mu = 0\,. \tag{3.1}$$

Maximal symmetry means that the number of linearly independent Killing vectors for a space-time of dimension $d+1$ is the maximum allowed by equation (3.1). Taking another derivative of the Killing equation and performing some algebra leads to the following second order differential equation for the Killing vectors

$$\nabla_\mu \nabla_\nu \xi_\alpha = -R_{\nu\alpha\mu}{}^{\lambda} \xi_\lambda\,. \tag{3.2}$$

Equation (3.2) can be turned into a system of first order differential equations determining the evolution of ξ^μ along a curve between two points a and b

$$t^\alpha \nabla_\alpha \xi_\mu = t^\alpha \Xi_{\alpha\mu}, \qquad t^\alpha \nabla_\alpha \Xi_{\mu\nu} = -R_{\mu\nu\alpha}{}^\lambda \xi_\lambda t^\alpha \,,$$

where t^α is the tangent vector along the curve and $\Xi_{\mu\nu} := \nabla_\mu \xi_\nu$. It is obvious that ξ^μ is completely determined by specifying ξ^μ and $\Xi_{\mu\nu}$ at a. Since ξ^μ can have maximally $d{+}1$ independent components and $\Xi_{\mu\nu}$ only has $(d{+}1)d/2$ components, due to equation (3.1), the maximal number of linearly independent Killing vectors is $(d+2)(d+1)/2$. The symmetries generated by ξ^μ are $d{+}1$ translations while the anti-symmetric components of $\Xi_{\mu\nu}$ generate the $d(d+1)/2$ rotations.

The Riemann tensor of a space-time with this number of symmetries should be the same in every direction and invariant under rotations at every point. The invariant symbols that obey this property are the metric $g_{\mu\nu}$ and the volume form $\sqrt{g}\epsilon^{\mu\nu\alpha\lambda}$. Considering the algebraic constraints on the Riemann tensor, the most general expression we can build out of the invariant symbols is [118]

$$R_{\mu\nu\lambda\gamma} = \frac{R}{d(d+1)}\left(g_{\mu\lambda}g_{\nu\gamma} - g_{\mu\gamma}g_{\nu\lambda}\right), \tag{3.3}$$

where R is the constant Ricci scalar. Up to the value of the Ricci scalar the geometry is therefore completely determined by the symmetries. To fix the value of R we plug (3.3) into the vacuum Einstein equations

$$R_{\mu\nu} - \frac{1}{2}g_{\mu\nu}R - \Lambda g_{\mu\nu} = 0\,,$$

to obtain

$$R = 2\frac{d+1}{d-1}\Lambda\,, \tag{3.4}$$

where Λ is the cosmological constant. Equation (3.4) tells us that there are three types of maximally symmetric space-times classified by the sign of the cosmological constant [119]. If $\Lambda = 0$ the Riemann tensor vanishes and we are left with Minkowski space, if $\Lambda > 0$ we are in dS, while $\Lambda < 0$ defines AdS. In the following we will explore the geometric properties and similarities and differences between the latter two.

3.1.1 Anti-de Sitter space-time

Let us first consider the maximally symmetric space-time with a negative cosmological constant, denoted as anti-de Sitter space-time. A $d{+}1$ dimensional AdS can be defined as a hyperboloid in a $d+2$ dimensional ambient Minkowski space $\mathbb{R}^{d,2}$ equipped with a metric η_{AB} with signature $(-,+,...,+,-)$

$$\mathbf{X}^2 := \eta_{AB}\mathbf{X}^A\mathbf{X}^B = -(\mathbf{X}^0)^2 + \sum_{i=1}^{d}(\mathbf{X}^i)^2 - (\mathbf{X}^{d+1})^2 = -\frac{1}{a^2}, \tag{3.5}$$

where $\mathbf{X} = (\mathbf{X}^A)$, $A = 0, \ldots, d+1$ and a is the inverse of the anti-de Sitter radius. From equation (3.5) it is clear that AdS is the Lorentzian version of Lobachevsky space.

The induced metric on AdS is then given by

$$\mathrm{d}s^2 = -\frac{a^2\left(\sum\limits_{i=1}^{d}\mathbf{X}^i\mathrm{d}\mathbf{X}^i - \mathbf{X}^{d+1}\mathrm{d}\mathbf{X}^{d+1}\right)^2}{1+a^2\left(\sum\limits_{i=1}^{d}(\mathbf{X}^i)^2-(\mathbf{X}^{d+1})^2\right)} + \sum_{i=1}^{d}(\mathrm{d}\mathbf{X}^i)^2 - (\mathrm{d}\mathbf{X}^{d+1})^2\,,$$

which gives the Riemann tensor

$$R_{ABCD} = -a^2(g_{AC}g_{BD} - g_{AD}g_{BC})\,. \tag{3.6}$$

This shows that the definition of AdS given by equation (3.5) is equivalent to the definition as a maximally symmetric space-time with negative cosmological constant. Comparing equation (3.6) to (3.3) and (3.4) we can relate the AdS radius to the cosmological constant through $\Lambda = -\frac{d(d-1)}{2}a^2$.

We proceed by analyzing the global structure of AdS (see e.g. [113]). There exists a conformal boundary which can be seen by taking the limit $\mathbf{X} \to \infty$. Then equation (3.5) becomes the lightcone equation for the ambient Minkowski space $\mathbb{R}^{d,2}$

$$\eta_{AB}\mathbf{X}^A\mathbf{X}^B := -(\mathbf{X}^0)^2 + \sum_{i=1}^{d}(\mathbf{X}^i)^2 - (\mathbf{X}^{d+1})^2 = 0\,. \tag{3.7}$$

The boundary of AdS is then given by the lines on the light-cone going through the origin of $\mathbb{R}^{d,2}$, which we write as

$$\partial\mathrm{AdS}_{d+1} = \{[\mathbf{X}] \in \mathbb{RP}^{d+1} : \eta_{AB}\mathbf{X}^A\mathbf{X}^B = 0\}\,.$$

It is straightforward to see that any point on $\partial\mathrm{AdS}_{d+1}$ has to fulfill

$$\sum_{i=1}^{d}(\mathbf{X}^i)^2 = 1, \quad (\mathbf{X}^0)^2 + (\mathbf{X}^{d+1})^2 = 1.$$

This means that the topology of the boundary of AdS is given by $(S^1 \times S^{d-1})/\mathbb{Z}_2$ where the quotient comes from the fact that $\mathbf{X}$ and $-\mathbf{X}$ are identified in projective space $\mathbb{RP}^{d+1}$. To see that the boundary is actually a conformal compactification of three-dimensional Minkowski space-time we define the null coordinates

$$U = \mathbf{X}^{d+1} + \mathbf{X}^d, \quad V = \mathbf{X}^{d+1} - \mathbf{X}^d$$

such that equation (3.7) becomes

$$UV = -(\mathbf{X}^0)^2 + \sum_{i=1}^{d-1}(\mathbf{X}^i)^2$$

If $V \neq 0$ this equation can always be rescaled such that $V = 1$. Then we can solve for U, showing that for $V \neq 0$ the boundary $\partial\mathrm{AdS}_{d+1}$ is a three dimensional Minkowski space. The value $V = 0$ corresponds to points at infinity which we have to add by hand. They are essential to establish the conformal symmetry, which includes the exchange of the origin with infinity. Such a construction is called a conformal compactification of Minkowski space-time [120].

The geodesic distance in AdS can be obtained by symmetry considerations. It is given by

$$d(\mathbf{X}, \mathbf{Y}) = \frac{1}{a}\text{arccosh}\left(-a^2\mathbf{X}\cdot\mathbf{Y}\right).$$

Since the appearance of the hyperbolic function complicates calculations unnecessarily, we only use the hyperbolic "angle" and define the quantity

$$K(\mathbf{X}, \mathbf{Y}) := -\frac{1}{a^2\mathbf{X}\cdot\mathbf{Y}} \tag{3.8}$$

For simplicity we will refer to this quantity as the inverse geodesic distance.

We are now ready to cover AdS with different coordinate patches. We will only discuss the two patches relevant to our analysis. The global patch is important to understand the overall causal structure and draw the conformal diagram. The Poincaré patch will be useful for the calculation we perform later since the Wick rotation to euclidean AdS is straightforward and the relation to the cosmological patch of dS is more obvious.

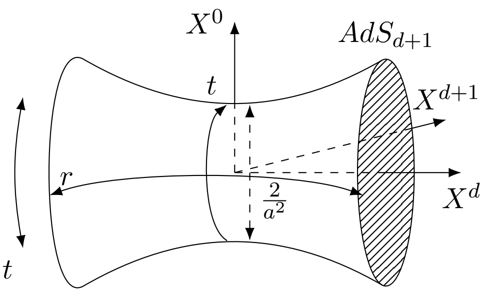

Figure 3.1: AdS_2 as a hyperboloid embedded in three dimensional Minkowski space.

The global coordinates are defined by the following parametrisation

$$\mathbf{X}^0 = \frac{1}{a}\cosh r \cos t, \quad \mathbf{X}^i = \frac{1}{a}\omega_i \sinh r, \quad \mathbf{X}^{d+1} = \frac{1}{a}\cosh r \sin t,$$

where ω_i parametrize the $d-1$ sphere S^{d-1}, while $r \in [0, \infty)$ is the radial coordinate and $t \in [0, 2\pi)$ is the time. The metric in these coordinates becomes

$$\mathrm{d}s^2 = \frac{1}{a^2}\left(-\cosh^2 r\ \mathrm{d}t^2 + \mathrm{d}r^2 + \sinh^2 r\ \mathrm{d}\Omega_{d-1}^2\right)$$

where $\mathrm{d}\Omega_{d-1}^2$ is the metric on S^{d-1}. This metric possesses a global time-like Killing vector given by ∂_t. However, the time-coordinate is circular and leads to closed time-like curves as depicted in figure 3.1. To avoid the causality problems this would cause, we consider from now on the universal cover of AdS. This means we unfold the time coordinate to $t \in \mathbb{R}$ by not identifying 0 and 2π. To analyze the causal structure we draw the conformal diagram of this space-time [113]. In order to do this we redefine the radial coordinate by $\rho = \arctan(\sinh(r))$ to obtain a metric which is given by

$$\mathrm{d}s^2 = \frac{1}{a^2\cos^2\rho}\left(-\mathrm{d}t^2 + \mathrm{d}\rho^2 + \sin^2\rho\ \mathrm{d}\Omega_{d-1}^2\right) \tag{3.9}$$

where ρ now has a finite range of $\rho \in [0, \frac{\pi}{2})$. The point $\rho = \frac{\pi}{2}$ corresponds to the conformal boundary ∂AdS at spatial infinity $\mathcal{J}$. In order to have the Cauchy problem in the bulk of AdS well-posed, i.e. guarantee global hyperbolicity, we have to add $\rho = \frac{\pi}{2}$ by hand [18]. The topology of this space is now $\mathbb{R} \times S^{d-1}$ and the conformal diagram is given by figure 3.2.

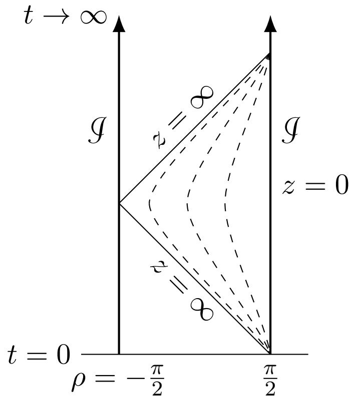

Figure 3.2: Conformal diagram of AdS with the boundary at spatial infinity denoted by $\mathcal{J}$. The Poincaré patch with $z =$ const. slicing is contained in the triangle.

The conformal diagram is infinite in the timelike direction due to the unfolding of t. A lightlike geodesic reaches the boundary in finite time and is reflected into the bulk. For further discussion of the geodesics we refer the interested reader to [121].

The second parametrisation we consider is the Poincaré patch, also depicted in figure 3.2. It has the geometry of the upper half plane

$$\mathcal{H}^{+}_{d+1} := \left\{ X := (\vec{x}, z),\, \vec{x} \in \mathbb{R}^d, z > 0 \right\}, \tag{3.10}$$

equipped with the metric

$$\mathrm{d}s^2 = \frac{1}{a^2 z^2}(\mathrm{d}z^2 + \eta_{\mu\nu}\mathrm{d}x^\mu \mathrm{d}x^\nu), \tag{3.11}$$

where $\eta_{\mu\nu}$ is the d dimensional Minkowski metric. It is defined through

$$\mathbf{X}^0 = \frac{1}{\sqrt{2}az}(1 - \frac{\eta_{\mu\nu}x^\mu x^\nu}{2} - \frac{z^2}{2}), \quad \mathbf{X}^i = \frac{x^i}{az}, \quad \mathbf{X}^{d+1} = \frac{1}{\sqrt{2}az}(1 + \frac{\eta_{\mu\nu}x^\mu x^\nu}{2} + \frac{z^2}{2}).$$

The conformal boundary now lies at $z = 0$. The metric on the boundary can be found by rescaling (3.11) with a function $\gamma(z, x^\mu)$, which must have a second order zero at $z = 0$. Taking the choice $\gamma(z, x^\mu) = a^2 z^2 \tilde{\gamma}(x^\mu)$ we get the boundary metric [122]

$$\mathrm{d}s^2_{\partial\mathrm{AdS}} = \gamma(x^\mu)\eta_{\mu\nu}\mathrm{d}x^\mu \mathrm{d}x^\nu\,,$$

which is an equivalence class of conformally Minkowski metrics reflecting the conformal symmetry on the boundary.

Another property of the Poincaré patch is the fact that it only covers half of AdS, the other half lying behind the coordinate singularity at $z \to \infty$, which corresponds to a cosmological horizon as can be seen in figure 3.2.

The other half of AdS can be accessed through the anti-podal map

$$\sigma(\vec{x}, z) := (\vec{x}, -z). \tag{3.12}$$

The fixed point of the anti-podal map, $\sigma(\vec{x}, z) = (\vec{x}, z)$ is the conformal boundary of AdS at $z = 0$. This operation exchanges the upper half space in (3.10) where $z > 0$ with the lower half space $\mathcal{H}^-_{d+1} := \left\{X := (\vec{x}, z),\ \vec{x} \in \mathbb{R}^d, z < 0\right\}$.

Just as for the global patch we find the global time-like Killing vector ∂_t. This property of AdS is a major difference with respect to dS when performing perturbative quantum field theory calculations which we will discuss in section 3.3.

3.1.2 Euclidean Anti-de Sitter space

For the calculation of boundary correlation functions we are going to work in the Wick rotated version of AdS called euclidean Anti-de Sitter (EAdS) or Lobachevsky space, the reason being that the relation to the late-time physics in dS is much more straightforward. Another advantage is the fact that the Poincaré patch actually covers the entire space since it consists of two disconnected parts.

EAdS is defined similarly to AdS as a hyperboloid embedded in a $d+2$ dimensional ambient Minkowski space-time, however, with a different signature given by the analytic continuation $\mathbf{X}^{d+1} \to i\mathbf{X}^{d+1}$, leading to

$$\mathbf{X}^2 := \eta_{AB}\mathbf{X}^A\mathbf{X}^B = -(\mathbf{X}^0)^2 + \sum_{i=1}^{d+1}(\mathbf{X}^i)^2 = -\frac{1}{a^2}, \tag{3.13}$$

This space consists of two disconnected parts as can be seen in the following way. Choose the points where $\sum_{i=1}^{d+1}(\mathbf{X}^i)^2 = 0$. Since all terms in this sum have positive signature this corresponds to choosing $\mathbf{X}^i = 0$ for all $i = 1, ..., d+1$. The solution to equation (3.13) are the two points $\mathbf{X}^0_\pm = \pm\frac{1}{a}$. Unless $a \to \infty$ the two points cannot be transformed into one another by a continuous transformation meaning they are disconnected. The same can be done for all other values of $\sum_{i=1}^{d+1}(\mathbf{X}^i)^2$, with the result depicted in figure 3.3. Note that the situation differs from Lorentzian AdS due to the sign difference of $(\mathbf{X}^{d+1})^2$, which turns the point $\sum_{i=1}^{d+1}(\mathbf{X}^i)^2 = 0$ into a null surface connecting the points $\mathbf{X}^0_\pm = \pm\frac{1}{a}$.

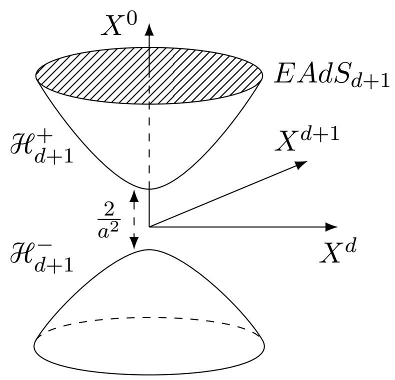

Figure 3.3: EAdS_2 as a hyperboloid embedded in three dimensional Minkowski space.

Taking the limit $\mathbf{X} \to \infty$ in equation (3.13) we find a lightcone equation

$$\mathbf{X}^2 = \eta_{AB}\mathbf{X}^A\mathbf{X}^B = -(\mathbf{X}^0)^2 + \sum_{i=1}^{d+1}(\mathbf{X}^i)^2 = 0, \tag{3.14}$$

defining a conformal boundary given by the lines on the light-cone going through the origin

$$\partial\mathrm{EAdS} := \{[\mathbf{X}] \in \mathbb{RP}^{d+1} : \eta_{AB}\mathbf{X}^A\mathbf{X}^B = 0\}.$$

The difference in the signature of the metric manifests itself on the boundary as well. We choose the null coordinates

$$U = \mathbf{X}^0 - \mathbf{X}^{d+1}, \quad V = \mathbf{X}^0 + \mathbf{X}^{d+1}$$

such that equation (3.14) turns into

$$UV = \sum_{i=1}^{d}(\mathbf{X}^i)^2 \,. \tag{3.15}$$

Equation (3.15) can be rescaled such that $V = 1$ if $V \neq 0$, so we can solve for U. This means that the boundary of EAdS_{d+1} is a d dimensional euclidean space $(\mathbb{R}^d, \delta_{\mu\nu})$ with points added at infinity corresponding to $V = 0$. We write $\partial\mathrm{EAdS} \simeq \mathbb{R}^d \cup \{\infty\}$.

As we noted above the Poincaré patch is enough to cover the entire connected part of EAdS. It is given the upper half plane as defined in (3.10) with the metric given by

$$\mathrm{d}s^2 = \frac{1}{a^2z^2}\left(\mathrm{d}z^2 + \mathrm{d}\vec{x}^2\right), \quad \text{where: } \mathrm{d}\vec{x}^2 = \sum_{i=1}^{d}(\mathrm{d}x^i)^2,$$

and parametrically defined by

$$\mathbf{X}^0 = \frac{1}{\sqrt{2}az}\left(1 - \frac{\vec{x}^2}{2} - \frac{z^2}{2}\right), \quad \mathbf{X}^i = \frac{x^i}{az}, \quad \mathbf{X}^{d+1} = \frac{1}{\sqrt{2}az}\left(1 + \frac{\vec{x}^2}{2} + \frac{z^2}{2}\right). \tag{3.16}$$

The inverse geodesic distance defined in equation (3.8) expressed in Poincaré coordinates is given by

$$K(\mathbf{X}, \mathbf{Y}) = \frac{2zw}{(\vec{x} - \vec{y})^2 + z^2 + w^2} \,.$$

For later convenience we introduce the euclidean norm in the Poincaré patch, by defining a $d+1$ vector $X = (z, \vec{x})$, such that its norm is given by

$$\|X\|^2 = z^2 + \vec{x}^2 \,. \tag{3.17}$$

Introducing an auxiliary vector $u = (1, \vec{0})$ we can express the inverse geodesic distance K in terms of the euclidean norm as

$$\frac{1}{K(\mathbf{X}, \mathbf{Y})} = 1 + \frac{\|X - Y\|^2}{2(u \cdot X)(u \cdot Y)} \,,$$

where the dot product is done with respect to the euclidean metric. We will make use of this notation in the perturbative calculation in chapters 5 and 6.

3.1.3 De-Sitter space-time

The cosmologically relevant example of a maximally symmetric space-time is the case with a positive cosmological constant, called de Sitter (dS) space-time. Very similarly to EAdS_{d+1} a $d+1$ dimensional dS can be defined as an embedding into a $d+2$ dimensional Minkowski space-time $\mathbb{R}^{d+1,1}$ equipped with a metric η_{AB} with signature $(-,+,...,+)$ (see e.g. [120])

$$\mathbf{X}^2 := \eta_{AB}\mathbf{X}^A\mathbf{X}^B = -(\mathbf{X}^0)^2 + \sum_{i=1}^{d+1}(\mathbf{X}^i)^2 = \frac{1}{a^2}. \tag{3.18}$$

From this equation it is obvious that dS is the Lorentzian version of a sphere with radius $1/a$. The induced metric is given by

$$\mathrm{d}s^2 = -\frac{a^2\left(\sum\limits_{i=1}^{d+1}\mathbf{X}^i\mathrm{d}\mathbf{X}^i\right)^2}{1+a^2\sum\limits_{i=1}^{d+1}(\mathbf{X}^i)^2} + \sum_{i=1}^{d+1}(\mathrm{d}\mathbf{X}^i)^2$$

leading to the Riemann tensor

$$R_{ABCD} = a^2(g_{AC}g_{BD} - g_{AD}g_{BC}),$$

confirming the fact that the definition of dS from equation (3.18) is equivalent to the statement that dS is a maximally symmetric space-time with a positive cosmological constant.

We can find the conformal boundary by taking $\mathbf{X} \to \infty$ leading to the lightcone equation (3.14). Note that contrary to the Lorentzian AdS case the boundary is now time-like instead of space-like as depicted in figure 3.4.

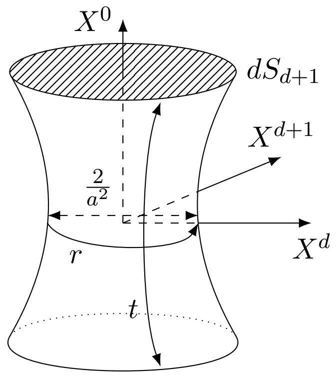

Figure 3.4: dS_2 as a hyperboloid embedded in three dimensional Minkowski space.

The boundary of dS is given by the lines on the lightcone going through the origin

$$\partial\mathrm{dS} := \{[\mathbf{X}] \in \mathbb{RP}^{d+1} : \eta_{AB}\mathbf{X}^A\mathbf{X}^B = 0\}$$

and since the defining equation is the same as for EAdS the boundary has the same geometry, i.e. is given by $\mathbb{R}^d \cup \{\infty\}$ with a euclidean metric.

The geodesic distance in dS can again be obtained from pure symmetry considerations and is given by (see e.g. [83])

$$d(\mathbf{X},\mathbf{Y}) = \frac{1}{a}\arccos(a^2\mathbf{X}\cdot\mathbf{Y})\,,$$

with the angular quantity given by

$$K(\mathbf{X},\mathbf{Y}) = \frac{1}{a^2\mathbf{X}\cdot\mathbf{Y}}\,.$$

Starting from an observer at the origin we can separate dS into causally disjoint regions based on the value of K. The region of points with $K < 1$ distance to the observer are time-like separated, while $K > 1$ corresponds to space-like and $K = 1$ to null separation.

Let us cover dS with different coordinate patches [123]. We will again only discuss the global patch and the Poincaré patch. The global patch covers the entire manifold and is important in order to analyze the causal structure and draw the conformal diagram. It has the cosmological interpretation of a Friedmann universe only filled with dark energy and positive spatial curvature. The Poincaré patch is interesting from a technical and phenomenological point of view. Technically it is appealing since it does not contain any cosmological horizons and we only see the boundary at future infinity. Phenomenologically it is relevant since it corresponds to a spatially flat Friedmann universe, filled with dark energy, which, according to current observations, is a likely scenario for the asymptotic future and the inflationary stage in the past of our universe.

The global patch is given by

$$\mathbf{X}^0 = \frac{1}{a}\sinh(at),\quad \mathbf{X}^i = \frac{1}{a}\cosh(at)\sin r\omega_i,\quad \mathbf{X}^{d+1} = \frac{1}{a}\cosh(at)\cos r\,, \tag{3.19}$$

where ω_i parametrize the $d-1$ sphere S^{d-1}, while $r \in [0,\pi]$ and $t \in (-\infty,\infty)$. The metric in this parametrisation is given by

$$\mathrm{d}s^2 = -\mathrm{d}t^2 + \frac{1}{a^2}\cosh(at)\left(\mathrm{d}r^2 + \sin^2 r\mathrm{d}\Omega^2_{d-1}\right)\,.$$

An important difference with respect to AdS is the fact that this metric does not posses a global time-like Killing vector. This will lead to major complications when we want to describe the time evolution of a scalar field, since the vacuum is not invariant under time translations anymore, as will be discussed in section 3.3.

To draw the conformal diagram we have to compactify the time direction by introducing conformal time $\tilde{\eta}$ as $\tilde{\eta} = 2\arctan(\tanh(at/2))$ to obtain a metric which is given by

$$\mathrm{d}s^2 = \frac{1}{a^2\cos^2\tilde{\eta}}\left(-\mathrm{d}\tilde{\eta}^2 + \mathrm{d}r^2 + \sin^2 r\ \mathrm{d}\Omega^2_{d-1}\right)\,.$$

The conformal time coordinate now has a finite range $\tilde{\eta} \in [0,\pi]$ where the locations $\tilde{\eta} = 0,\pi$ correspond to the conformal time-like boundary ∂dS which we will call future and past infinity $\mathcal{I}^{\pm}$ and the coordinate singularities at $r = 0,\pi$ correspond to the poles of the spherical spatial slicing. We can therefore draw the conformal diagram of dS given in figure 3.5.

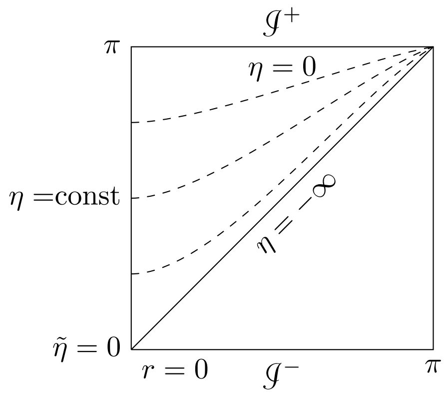

Figure 3.5: Conformal diagram of dS in the gobal patch and the Poincaré patch.

The second parametrisation we consider is the Poincaré patch which for dS is given by

$$\mathbf{X}^0 = \frac{1}{\sqrt{2}a\eta}\left(1 + \frac{\vec{x}^2}{2} - \frac{\eta^2}{2}\right), \quad \mathbf{X}^i = \frac{x^i}{a\eta}, \quad \mathbf{X}^{d+1} = \frac{1}{\sqrt{2}a\eta}\left(1 - \frac{\vec{x}^2}{2} + \frac{\eta^2}{2}\right), \tag{3.20}$$

where $\vec{x} \in \mathbb{R}^d$ and $\eta \in (-\infty, 0]$. It corresponds to the lower half space

$$\mathscr{H}^-_{d+1} := \{X := (\vec{x}, \eta) : \vec{x} \in \mathbb{R}^d, \eta < 0\}\,.$$

As depicted in figure 3.5 it only covers half of dS, while the other half is behind a cosmological horizon and therefore causally disconnected. The conformal boundary at future infinity is now located at $\eta = 0$ and by following a similar argument as for AdS, we find that the metric on the boundary is given by a class of conformally related euclidean spaces, reflecting the euclidean conformal symmetry on the boundary.

The inverse geodesic distance in this parametrisation is given by [68]

$$K(\mathbf{X}, \mathbf{Y}) := \frac{1}{a^2 \mathbf{X} \cdot \mathbf{Y}} = \frac{2\eta_x \eta_y}{\eta_x^2 + \eta_y^2 - (\vec{x} - \vec{y})^2}\,. \tag{3.21}$$

Just as for the global patch we notice that there is no globally defined time-like Killing vector.

Comparing the Poincaré patches in dS and EAdS we notice that they are related by the double Wick rotation $z \to -i\eta$ and $a \to -ia$. Even though this relation is very useful to carry over results from EAdS to dS it has to be treated with much caution since it interchanges to roles of space and time.

3.2 Irreducible representations of the (Anti-)de Sitter symmetry group

Having analyzed the geometry of (A)dS as the two maximally symmetric space-times with a non-vanishing cosmological constant we want to proceed by considering the symmetry groups of these space-times [124–126]. Our goal is to follow the example from flat space and find unitary irreducible representations of the symmetry groups which we can use to build a Hilbert space.

The defining equations (3.5), (3.13) and (3.18) are all of the form

$$\eta_{AB}\mathbf{X}^A\mathbf{X}^B = \text{const}\,, \tag{3.22}$$

where η_{AB} is the metric of the ambient Minkowski space with signature $(-,+,...,+,-)$ for Lorentzian AdS and $(-,+,...)$ for EAdS and dS. The groups, preserving equation (3.22) are the orthogonal groups $O(d,2)$ and $O(d+1,1)$. We are interested in the representations of the Lie algebra and will therefore focus on the subgroup of transformations with unit determinant, given by proper orthochronous (A)dS groups $SO(d,2)$ and $SO(d+1,1)$. Both groups have $(d+2)(d+1)/2$ generators, matching the number of Killing vectors of a maximally symmetric space-time. The Lie algebra of these groups is given by

$$[J_{AB}, J_{CD}] = -i\left(\eta_{AD}J_{BC} + \eta_{BC}J_{AD} - \eta_{AC}J_{BD} - \eta_{BD}J_{AC}\right)\,, \tag{3.23}$$

where we have to choose the correct signature for the metric η_{AB} depending on whether we consider $SO(d,2)$ or $SO(d+1,1)$. The isomorphism from the generators J_{AB} of $SO(d,2)$ to the conformal algebra on d dimensional Minkowski space, given by the generators of the Poincaré group $M_{\mu\nu}, P_\mu$, the dilatation D and the special conformal generators K_μ, is defined by

$$M_{\mu\nu} = J_{\mu\nu}, \quad D = J_{d+1,d}, \quad P_\mu = \frac{1}{\sqrt{2}}\left(J_{\mu,d+1} - J_{\mu,d}\right), \quad K_\mu = \sqrt{2}\left(J_{\mu,d+1} + J_{\mu,d}\right)\,, \tag{3.24}$$

with the indices $\mu,\nu \in \{0,...,d-1\}$. It is straightforward to check that equation (3.24) together with (3.23) gives the algebra of conformal generators given by (2.3). The unitary irreducible representations of $SO(d,2)$ can be decomposed into a product of irreducible representations of its maximal compact subgroup given by $SO(d)\times SO(2)$.

They are labeled by the spin ℓ and the scaling dimension Δ. Unitarity implies the following boundaries on the scaling dimensions [105]

$$\Delta \geq \ell + d - 2, \text{ for } \ell > 0, \text{ and } \Delta \geq \frac{d-2}{2}\,.$$

In both cases $\Delta \in \mathbb{R}$ and there is no upper limit.

This is a major difference when considering the de Sitter group $SO(d+1,1)$. The algebra of generators is again given by equation (3.23), this time, however, with the metric signature $(-,+,...,+)$. The isomorphism from the generators J_{AB} to the generators of the euclidean conformal group then becomes

$$M_{ij} = J_{ij}, \quad D = J_{0,d+1}, \quad P_i = \frac{1}{\sqrt{2}}\left(J_{i,0} - J_{i,d+1}\right), \quad K_i = \sqrt{2}\left(J_{i,0} + J_{i,d+1}\right)\,, \tag{3.25}$$

with the indices $i,j \in \{1,...,d\}$. Again we can label the irreducible representations by the spin of the $SO(d)$ part and the scaling dimension Δ. This time, however, unitarity puts some more complicated restrictions on the values of Δ. Contrary to the $SO(d,2)$ case it can now take complex values, but is restricted to fall into different classes.

The principal series exists for any spin ℓ and the scaling dimension can take values

$$\Delta = \frac{d}{2} + i\nu \text{ with } \nu \in \mathbb{R}\,. \tag{3.26}$$

As we will discuss in section 3.3 this representation corresponds to heavy fields in dS.

The complementary series, corresponding to light fields in dS, is given by

$$\Delta = \frac{d}{2} + \nu \text{ with } \nu \in \mathbb{R}\,, \tag{3.27}$$

where $-\frac{d}{2} < \nu < \frac{d}{2}$ for $\ell = 0$ and $1 - \frac{d}{2} < \nu < \frac{d}{2} - 1$ for $\ell > 0$. As we will discuss in section 3.3, this representation will be most relevant to us, since we will consider conformally coupled massless fields. For an in depth discussion of the representation theory of $SO(d+1,1)$ we refer to [125].

EAdS can be constructed from the same ambient Minkowski space as dS with the same signature of the metric. Therefore, we could conclude that the Hilbert space of EAdS should be constructed from unitary irreducible representations of $SO(d+1,1)$. But this is well-known not to be the case. The scaling dimension for EAdS can be obtained by setting $a \to ia$ in equation (3.32). The value for Δ is therefore always real and the fields transform under unitary irreducible representations of $SO(d,2)$ the symmetry group of the Lorentzian version of EAdS. This is not a problem since QFT in EAdS is a euclidean field theory. Only after Wick rotation to Lorentzian AdS the Hilbert space should be given by unitary representations which it clearly does.

The situation for dS is different. In the four-point function that we analyze in our perturbative calculation in chapter 6, we will see that there are operators appearing in the spectrum with arbitrary dimensions not obeying any $SO(d+1,1)$ unitarity constraints. However, since there is no operator state correspondence in dS, this does not really pose a problem, it just hints at the fact that the relation between the bulk and boundary degrees of freedom is more obscure in dS than in AdS. These points have been raised recently in the context of a proposed cosmological bootstrap in [87,88].

Finally we would like to express the generator of the $SO(d+1,1)$ symmetry groups in term of the local coordinates of the Poincaré patch. The action of a generator $\hat{J}_{AB}$ as an operator on a local scalar field operator $\hat{\phi}(\mathbf{X})$ is defined as

$$[\hat{J}_{AB}, \hat{\phi}(\mathbf{X})] = i\left(\mathbf{X}_A \frac{\partial}{\partial \mathbf{X}^B} - \mathbf{X}_B \frac{\partial}{\partial \mathbf{X}^A}\right)\phi(\mathbf{X})\,.$$

Using the isomorphism from equation (3.25) together with the definition of the Poincaré patch in (3.20), we can express the generators of the dS group in terms of differential operators on smooth functions

$$\begin{aligned}
J_{0,d+1} &= i\left(X_0 \frac{\partial}{\partial X^{d+1}} - X_{d+1}\frac{\partial}{\partial X^0}\right) = i\left(\eta\partial_\eta + x^i\partial_i\right) \\
J_{ij} &= i\left(X_i \frac{\partial}{\partial X^j} - X_j \frac{\partial}{\partial X^i}\right) = i(x_i\partial_j - x_j\partial_i) = M_{ij} \\
J_{i0} &= i\left(X_i \frac{\partial}{\partial X^0} - X_0 \frac{\partial}{\partial X^i}\right) = \frac{i}{\sqrt{2}}\left(-x_i\eta\partial_\eta - x_i x^j\partial_j + \left(1 + \frac{\vec{x}^2}{2} - \frac{\eta^2}{2}\right)\partial_i\right) \\
J_{i,d+1} &= i\left(X_i \frac{\partial}{\partial X^{d+1}} - X_d + 1\frac{\partial}{\partial X^i}\right) = \frac{i}{\sqrt{2}}\left(-x_i\eta\partial_\eta - x_i x^j\partial_j - \left(1 - \frac{\vec{x}^2}{2} + \frac{\eta^2}{2}\right)\partial_i\right) \\
\Rightarrow J_{i0} - J_{i,d+1} &= \sqrt{2}i\partial_i = \sqrt{2}P_i \\
\Rightarrow J_{i0} + J_{i,d+1} &= \frac{i}{\sqrt{2}}\left(-2x_i\eta\partial_\eta - 2x_i x^j\partial_j + (\vec{x}^2 - \eta^2)\partial_i\right)\,.
\end{aligned} \tag{3.28}$$

Taking the limit $\eta \to 0$ just reduces the de Sitter generators to the generators of the conformal group on $\mathbb{R}^d$

$$J_{ij} = M_{ij}, \quad J_{i0} - J_{i,d+1} = \sqrt{2} i \partial_i = \sqrt{2} P_i, \quad J_{0,d+1} \xrightarrow{\eta\to 0} i x^i \partial_i = D,$$
$$J_{i0} + J_{i,d+1} \xrightarrow{\eta\to 0} \frac{i}{\sqrt{2}} \left(\underline{x}^2 \partial_i - 2 x_i x^j \partial_j \right) = \frac{1}{\sqrt{2}} K_i \,.$$

The expressions in EAdS can be found by making the corresponding substitution $\eta \to iz$.

Finally we want to calculate the quadratic Casimir of $SO(d+1,1)$. First, consider the well known result for the Casimir of the conformal group in d dimensions [104] given by

$$C_2 = \frac{1}{2} J^{AB} J_{AB} = D^2 - \frac{1}{2} \left(K_i P^i + P_i K^i \right) - \frac{1}{2} M_{ij} M^{ij} = \Delta(\Delta - d) + \ell(\ell + d - 2) \,. \tag{3.29}$$

At the same time we can use equations (3.28) to express the quadratic Casimir as a differential operator acting on a scalar field which is given by

$$C_2 = \frac{1}{2} J^{AB} J_{AB} = \eta^2 \partial_\eta^2 - (d-1) \eta \partial_\eta - \eta^2 \nabla^2 = -\frac{1}{a^2} \Box_{dS} \,. \tag{3.30}$$

The expression for EAdS can be obtained by doing the substitutions $\eta \to iz$ and $a \to ia$. If we consider a massive scalar field in dS it will evolve according to the Klein-Gordon equation

$$(-\Box_{dS} + m^2) \phi = 0 \,. \tag{3.31}$$

Comparing equations (3.29), (3.30) and (3.31) we find the following relation between the mass of scalar field and scaling dimension on the boundary

$$\Delta(\Delta - d) = -\frac{m^2}{a^2} \quad \Leftrightarrow \quad \Delta_\pm = \frac{d}{2} \pm \sqrt{\frac{d^2}{4} - \frac{m^2}{a^2}} . \tag{3.32}$$

We immediately recognize the two unitarily equivalent representations of the principle and complementary series given in (3.26) and (3.27). For heavy fields $\frac{m^2}{a^2} > \frac{d^2}{4}$ the scaling dimension becomes complex and we are in the principal series, while for light fields we are in the complementary series. In any case, the equations of motion guarantee that any free field transforms in a unitary irreducible representation of the dS group.

The situation is slightly different for EAdS. The scaling dimension can be obtained by setting $a \to ia$ in equation (3.32). The value for Δ is therefor always real and the fields do not necessarily transform under unitary irreducible representations of $SO(d+1,1)$, but rather $SO(d,2)$. Since this is the symmetry group of the Lorentzian version of EAdS, this is to be expected.

3.3 Perturbative quantum field theory in (A)dS

Now that we analyzed the geometry of (A)dS and specified the Hilbert space, we can proceed with defining a quantum field theory in those respective space-times. We will only discuss massive scalar fields. Starting with the somewhat simpler case of

(E)AdS we will describe how the AdS/CFT correspondence arises naturally through a state operators correspondence between the bulk and the boundary. Subsequently we will consider dS where the situation is much more complicated, since no state operator correspondence exists and the time translation is not an isometry of the space-time. We have to introduce the Schrödinger picture of quantum field theory and non-equilibrium techniques in perturbation theory, known as the Schwinger-Keldysh formalism to make sense of the calculation. From now on we will always work in the Poincaré patch.

The main references for this section are given by [15, 22, 68, 83, 113, 116, 127, 128]. This section contains reproductions of [57, 71, 90].

3.3.1 Scalar field theory in (E)AdS

Let us start with the classical theory of a scalar field in AdS in the Poincaré patch. Our strategy is to start with the euclidean theory. This will give us a unique definition of the propagator, up to the choice of boundary conditions. Once we found these solutions in EAdS we can Wick rotate to Lorentzian AdS which will automatically provide us with the correct conformal vacuum and time-ordered propagator with an $i\varepsilon$ prescription.

The classical action in EAdS is given by

$$S[\phi] = \int_{\text{EAdS}} \sqrt{g}\mathrm{d}^{d+1}X \left(\frac{1}{2}(\partial\phi)^2 + \frac{1}{2}m^2\phi^2\right) . \tag{3.33}$$

The mass term m^2 in the action is in fact an effective mass, given by the expression

$$m^2 = \tilde{m}^2 + \xi R \,, \tag{3.34}$$

where $\tilde{m}$ is the actual physical mass of the field, while ξR is the non-minimal coupling to the background geometry with R being the Ricci scalar. The case $\xi = 0$ corresponds to so called minimal coupling, meaning that the only interaction of the field with the background happens through the integration measure and the metric in the kinetic term. A minimally coupled, massless field therefore has effective mass $m^2 = 0$ and, comparing to (3.32), corresponds to the scaling dimensions $\Delta \in \{d, 0\}$.

The most relevant case to us is the conformally coupled, massless field. After setting the physical mass $\tilde{m} = 0$, we demand that the trace of the energy-momentum tensor vanishes on-shell. This leads to the condition on the non-minimal coupling parameter [116]

$$\xi = \frac{1}{4}\frac{d-1}{d} \,. \tag{3.35}$$

Plugging in the Ricci scalar of AdS and using equation (3.32) with $a \to ia$ we obtain the following values for the scaling dimensions of a conformally coupled, massless field

$$\Delta_\pm = \frac{d \pm 1}{2} \,. \tag{3.36}$$

For now we will keep the value of m general and only specialize to the conformally coupled, massless case once we perform perturbative calculations of the interacting theory.

The equation of motion for the free field in the Poincaré patch of EAdS is given by

$$(-\Box_{EAdS} + m^2)\phi(z, \vec{x}) = \left(-z^2\partial_z^2 + (d-1)z\partial_z - \Delta + \frac{m^2}{a^2}\right)\phi(z, \vec{x}) = 0 \,, \tag{3.37}$$

where Δ is the usual d dimensional Laplace operator. This equation, however, is only valid in the interior of EAdS. To have a well-posed Cauchy problem we need to specify conditions at the boundary. We consider the on-shell action which is given by plugging the solution of (3.37) into the action (3.33). Upon using Green's second identity, the variation of the action becomes [127]

$$\delta S[\phi] = \int_{\mathrm{EAdS}} \sqrt{g}\mathrm{d}^{d+1}X\delta\phi \left(-\Box_{EAdS} + m^2\right)\phi + \frac{1}{2}\int\limits_{\partial EAdS} \frac{\mathrm{d}^d\vec{x}}{(az)^{d-1}}\left(\phi\partial_z\delta\phi - \delta\phi\partial_z\phi\right).$$

The first term vanishes on-shell due to the equation of motion in the bulk, while for the second term to vanish we have to impose boundary conditions the form

$$z\partial_z\phi|_{z\to 0} = A\phi|_{z\to 0}, \qquad \Rightarrow z\partial_z\delta\phi|_{z\to 0} = A\delta\phi|_{z\to 0}\,, \tag{3.38}$$

with A an arbitrary constant.

Let us now analyze the equation of motion in the bulk. The d'Alembertian $\Box_{EAdS}$ can be expressed in terms of the inverse hyperbolic distance K defined in the equation (3.8). After fixing boundary conditions the configuration of a field $\phi(X)$ will be given in terms of the configuration at an initial value $\phi_0(Y)$ as

$$\phi(X) = \int_{EAdS} \sqrt{g}\mathrm{d}^{d+1}Y\Lambda(X,Y)\phi_0(Y)$$

where $\Lambda(X, Y)$ is the euclidean Green function determined by the equation of motion in terms of K

$$\left[K^2(1-K^2)\frac{\mathrm{d}^2}{\mathrm{d}K^2} + 2K\left(1-K^2-\frac{d+1}{2}\right)\frac{\mathrm{d}}{\mathrm{d}K} + \frac{m^2}{a^2}\right]\Lambda(K) = \frac{1}{\sqrt{g}}\delta^4(\mathbf{X}-\mathbf{Y})\,. \tag{3.39}$$

It is clear that the solution only depends on K. We find the general solution

$$\begin{aligned}\Lambda(\mathbf{X},\mathbf{Y};\Delta_\pm) =& C_+(\Delta_+)K^{\Delta_+}{}_2F_1\left(\frac{\Delta_+}{2},\frac{\Delta_++1}{2};\Delta_+-\frac{d-4}{2};K^2\right)\\ &+ C_-(\Delta_+)K^{\Delta_-}{}_2F_1\left(\frac{\Delta_-}{2},\frac{\Delta_-+1}{2};\Delta_--\frac{d-4}{2};K^2\right),\end{aligned} \tag{3.40}$$

expressed in terms of Gauss' hypergeometric function ${}_2F_1(a, b; c; z)$, where Δ is given by equation (3.32) with $a \to ia$. The coefficients $C_\pm$ are fixed by the boundary conditions as defined in equation (3.38) and the flat limit. To see how this works, we expand equation (3.40) at the boundary $z \to 0$ which gives us

$$\lim_{z\to 0}\Lambda(\mathbf{X},\mathbf{Y};\Delta_+) = C_+(\Delta_+)\left(\frac{(2zw)^{\Delta_+}}{((\vec{x}-\vec{y})^2+w^2)^{\Delta_+}} + \cdots\right) + C_-(\Delta_+)\left(\frac{(2zw)^{\Delta_-}}{((\vec{x}-\vec{y})^2+w^2)^{\Delta_-}} + \cdots\right).$$

In the limit $z \to 0$ a field which solves the equation of motion will therefore be given by

$$\lim_{z\to 0}\phi(X) = \left(\phi_0(\vec{x})z^{\Delta_-} + ...\right) + \left(\tilde{\phi}_0(\vec{x})z^{\Delta_+} + ...\right),$$

where ϕ_0 and $\tilde{\phi}_0$ only depend on the boundary coordinates. If we now go back to equation (3.38) we get the following condition

$$(\Delta_- - A)\phi_0 z^{\Delta_-} + (\Delta_+ - A)\tilde{\phi}_0 z^{\Delta_+} = 0\,.$$

We immediately see, that the choice $A = \Delta_+$ requires $\phi_0 = 0$, meaning the field falls off like $\sim z^{\Delta_+}$, while $A = \Delta_-$ means $\tilde{\phi}_0 = 0$, i.e. the fall-off behaviour at the boundary is $\sim z^{\Delta_-}$. For the Green function this corresponds to either setting C_- or C_+ to zero. We will see that these two choices are the equivalent to Dirichlet and Neumann boundary conditions in flat space.

To completely fix the value of the integration constant $C_\pm$ we have to demand that we obtain the usual euclidean flat space Green function when taking the flat limit. To do this, we define the radial coordinate $r^2 = \sum_{i=1}^{d+1} (\mathbf{X}^i)^2 = -a^{-2} + (\mathbf{X}^0)^2$. Then we can express $K(\mathbf{X}, \mathbf{Y})$ in terms of r by choosing $\mathbf{Y} = (a^{-1}, 0, ..., 0)$ so K becomes

$$K(\mathbf{X}, \mathbf{Y}) = \frac{1}{a^2 \mathbf{X} \cdot \mathbf{Y}} = \frac{1}{\sqrt{1 + a^2 r^2}} \,. \tag{3.41}$$

The flat limit is given by taking the curvature radius a^{-1} to be much larger than the radial distance r, corresponding to taking the limit $ar \to 0$, such that

$$K = 1 - \frac{1}{2}(ar)^2 + \mathcal{O}((ar)^4) \,.$$

The Green function (3.40) with either Dirichlet or Neumann boundary conditions imposed in this limit is given by

$$\lim_{ar \to 0} \Lambda(\mathbf{X}, \mathbf{Y}, \Delta) = \frac{\Gamma\left(\frac{d-1}{2}\right) \Gamma\left(\Delta - \frac{d}{2} + 1\right)}{\Gamma\left(\frac{\Delta+1}{2}\right) \Gamma\left(\frac{\Delta}{2}\right)} \frac{C(\Delta)}{(ar)^{d-1}} := \frac{\Gamma\left(\frac{d+1}{2}\right)}{2(d-1)\pi^{\frac{d+1}{2}} r^{d-1}} \tag{3.42}$$

where in the last step we set the limit equal to the flat space propagator in d dimensions. We can therefore solve for $C(\Delta)$ and arrive at the canonically normalized propagator

$$\Lambda(\mathbf{X}, \mathbf{Y}, \Delta) = \mathcal{n}_\Delta K^\Delta {}_2F_1\left(\frac{\Delta}{2}, \frac{\Delta+1}{2}; \Delta - \frac{d-4}{2}; K^2\right) , \tag{3.43}$$

were the normalization constant is given by

$$\mathcal{n}_\Delta := \frac{a^{d-1}}{4\pi^{\frac{d+1}{2}}} \frac{\Gamma\left(\frac{\Delta+1}{2}\right) \Gamma\left(\frac{\Delta}{2}\right)}{\Gamma\left(\Delta - \frac{d}{2} + 1\right)} \,. \tag{3.44}$$

If we consider the singular structure of this propagator we notice that there are two singularities at $K = \pm 1$, corresponding to coinciding and antipodally coinciding points. In EAdS this is not a problem since the antipodally related points lie on disconnected parts of the space and after Wick rotating to Lorentzian AdS, are always space-like separated, as we discussed in section 3.1.

We can obtain the time-ordered Feynman propagator in the Lorentzian AdS theory in the same way as in flat space by Wick rotating the time direction from euclidean time to Lorentzian time. In the Poincaré patch this means continuing $x_d \to -ix_0$. To implement time-ordering we have to introduce an $i\varepsilon$ prescription which we will choose to be the same that gives the correct flat limit (see [18] for details). Then the time-ordered Feynman propagator is given by

$$\Lambda_F(\mathbf{X}, \mathbf{Y}, \Delta) = \frac{a^{d-1}}{4\pi^{\frac{d+1}{2}}} \frac{\Gamma\left(\frac{\Delta+1}{2}\right) \Gamma\left(\frac{\Delta}{2}\right)}{\Gamma\left(\Delta - \frac{d}{2} + 1\right)} K^\Delta {}_2F_1\left(\frac{\Delta}{2}, \frac{\Delta+1}{2}; \Delta - \frac{d-4}{2}; K^2 - i\varepsilon\right) .$$

At this point we should comment on the choice of the vacuum. As is well known the choice of a Green function, with fixed boundary conditions corresponds to choosing a vacuum state. We saw in equation (3.36) that a conformally coupled massless scalar field in $d+1=4$ bulk dimensions corresponds to $\Delta_+=2$ and $\Delta_-=1$. The propagator (3.43) for these scaling dimensions simplifies drastically and is given by

$$\Lambda(\mathbf{X},\mathbf{Y};\Delta)=\left(\frac{a}{2\pi}\right)^2\frac{K(\mathbf{X},\mathbf{Y})^\Delta}{1-K(\mathbf{X},\mathbf{Y})^2}\,. \tag{3.45}$$

Since these fields are conformally invariant and the Poincaré patch of EAdS is related to the upper half space by a Weyl transformation, a natural choice for the vacuum is the conformal vacuum which is defined through the Green function as [116]

$$\Lambda_F(X,X')=\Omega(X)^{-1}\Omega(X')^{-1}G_F(X,X')\,. \tag{3.46}$$

Here $G_F(X,X')$ is the Feynman Green function in flat space and $\Omega(X)$ is the scale factor relating AdS to flat space such that $g^{AdS}_{\mu\nu}=\Omega^2\eta_{\mu\nu}$.
To choose the correct vacuum state in the half space we have to specify boundary conditions at $z=0$. If we choose Dirichlet boundary conditions the mode functions in euclidean space have to behave like $\sin(k_z z)\mathrm{e}^{i(k_x x+k_y y+k_0 x_0)}$. The euclidean propagator in the upper half space is therefore

$$\begin{aligned}G_E^{(D)}(X,X')&\propto\int \mathrm{d}^4k\frac{\sin(k_z z)\sin(-k_w w)}{k^2}\mathrm{e}^{i(k_x(x-x')+k_y(y-y')+k_0(x_0-x_0'))}\\&=\frac{\pi}{2}\left(\frac{1}{\sum\limits_{i=0}^{2}(x_i-x_i')^2+(z-z')^2}-\frac{1}{\sum\limits_{i=0}^{2}(x_i-x_i')^2+(z+z')^2}\right)\,.\end{aligned} \tag{3.47}$$

This result can be obtained by putting an additional "source" at $\sigma(z',\vec{x}')=(-z',\vec{x}')$, which is the familiar method of mirror charges. It can be easily checked that equation (3.47) is related to (3.45) for $\Delta=2$ by (3.46). The equivalent argument holds for the Neumann propagator and a Wick rotation automatically provides us with the correct Feynman propagator. These propagators therefore correspond to the conformal vacuum with respect to the upper half space with respective boundary conditions.

State operator correspondence

A major feature for defining quantum field theory in AdS and basis for the AdS/CFT correspondence is the existence of on operator state correspondence between local operators in the bulk and states on the boundary. We follow the argumentation in [129].

Starting in the conformal global patch of AdS given by (3.9) we can Wick rotate to EAdS in global coordinates and quantize the theory on equal time-slices t. An equal time slice in the global patch corresponds to a hemisphere in the Poincaré patch given by

$$z^2+\vec{x}^2=\mathrm{e}^{2t}\,. \tag{3.48}$$

Equation (3.48) makes it clear that $t\to-\infty$ corresponds to a point. So if we place a local operator $\mathcal{O}(t,x)$ in the infinite past in the global patch, the wave function of the corresponding state at finite time represented in the Poincaré patch will be given by

$$\langle\phi_0\,|\mathcal{O}(0)|\,0\rangle=\Psi_{\mathcal{O}}[\phi_0]=\int\limits_{z^2+x^2=\mathrm{e}^{2t}}\mathcal{D}\phi\mathrm{e}^{-S[\phi]}\mathcal{O}(0) \tag{3.49}$$

where ϕ_0 is the configuration of the field on the hemisphere. This is obviously just the Schrödinger representation of a state produced by acting with an operator on the vacuum. Since we established that each bulk field in AdS corresponds to a boundary operator with a definite scaling behaviour under dilatations we conclude that equation (3.49) corresponds to a state on the boundary, where global time evolution in the bulk translates into radial evolution in $\|\vec{x}\|$.

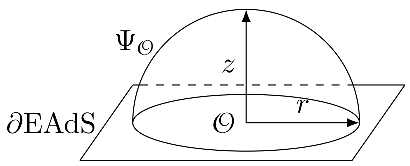

Figure 3.6: An operator inserted at past infinity in global time corresponds to a state $\Psi_{\mathcal{O}}$ on the hemisphere in the Poincaré patch. The hemisphere can be contracted to a point, defining a local operator $\mathcal{O}$ for every state on the hemisphere at the origin.

To show the other direction is straightforward as well. Consider two hemispheres as defined in equation (3.48) with radii defined through global time t_1, t_2 with $t_1 < t_2$. We define an eigenstate of the dilatation operator $\Psi_\Delta[\phi_1]$ with eigenvalue Δ as the path integral over the interior of the hemisphere with radius e^{t_1} and define a weighted path integral from t_1 to t_2 by

$$\int \mathcal{D}\phi_2 \mathcal{D}\phi_1 \mathrm{e}^{-S[\phi]} \mathrm{e}^{\Delta(t_1-t_2)} \Psi_\Delta[\phi_1] \,. \tag{3.50}$$

The integral from t_1 to t_2 corresponds to free propagation which can be undone by acting with the dilatation operator given by $\mathrm{e}^{\Delta(t_2-t_1)}$, revealing that equation (3.50) is equivalent to $\Psi_\Delta[\phi_1]$. Taking the limit $t_1 \to -\infty$ collapses the inner hemisphere to a point on the boundary which can again be thought of as a local operator on the boundary with scaling dimension Δ.

This reasoning establishes a state operator correspondence between bulk fields in AdS and states on the boundary, schematically depicted in figure 3.6. A good explanation of this point can also be found in [87].

Perturbative calculations in EAdS and Witten diagrams

Having set up the framework for quantum field theory in AdS we are now in a position to perform perturbative calculations. We are interested in obtaining correlation functions of field operators on the boundary of AdS, which is the analogue of the S-Matrix in flat space. The Poincaré patch in AdS has a globally defined time-like Killing vector, therefore making the vacuum defined on some initial time-slice invariant under time-translations. We can therefore Wick rotate to EAdS, perform all the calculations in euclidean time and interpret the result in Lorentzian AdS by Wick rotating back.

An n point correlation function of a scalar field $\phi(x)$ in euclidean field theory is uniquely defined by insertions into the path integral over the entire manifold

$$\left\langle \prod_{i=1}^{n} \phi(X_i) \right\rangle := \frac{\int \mathcal{D}\phi \mathrm{e}^{-S[\phi]} \prod_{i=1}^{n} \phi(X_i)}{\int \mathcal{D}\phi \mathrm{e}^{-S[\phi]}} = \frac{\delta^n}{\delta j(X_1)...j(X_n)} \log(Z[j])\big|_{j=0} \,, \tag{3.51}$$

with the the generating functional $Z[j]$ defined as the path integral over the euclidean action $S[\phi]$ coupled to a source $j(X)$

$$Z[j] = \int \mathcal{D}\phi \mathrm{e}^{-S[\phi]+\int \mathrm{d}^{d+1}X\phi(X)j(X)} .$$

For a free scalar field defined action (3.33) the path integral in (5.27) reduces to Gaussian integration which can be performed exactly, leading to

$$Z_{\text{free}}[j] = Z[0]\mathrm{e}^{-\frac{1}{2}\int \mathrm{d}^{d+1}X\mathrm{d}^{d+1}Y j(X)\Lambda(X,Y,\Delta)j(Y)} . \tag{3.52}$$

Plugging equation (3.52) into (3.51), we see that the free field only has correlation functions between even numbers of points, which are given by products of the two point function, which in turn is given by the Green function Λ.

Each operator in the bulk can be associated to an operator on the boundary that transforms like an eigenstate of the dilatation operator. The scaling dimension is set by the boundary condition imposed on the bulk field. The correlation function of the conformal operators at the boundary can therefore be obtained by extrapolating the bulk-to-bulk correlation functions from equation (3.51) to the boundary [21] by taking the limit

$$\left\langle \prod_{i=1}^{n} \mathcal{O}_\Delta(\vec{x}_i) \right\rangle := \lim_{z_i\to 0} z_i^{-\Delta} \left\langle \prod_{i=1}^{n} \phi(X_i) \right\rangle ,$$

where the additional rescaling by $z_i^{-\Delta}$ is done to obtain a finite result. The propagator with on external point on the boundary and one point in the bulk is the bulk-to-boundary propagator, defined as

$$\begin{aligned}\bar{\Lambda}(\vec{x},Y) := \lim_{z\to 0} z^{-\Delta}\Lambda(\mathbf{X},\mathbf{Y};\Delta) &= \frac{a^{d-1}\Gamma\left(\frac{\Delta}{2}\right)\Gamma\left(\frac{\Delta+1}{2}\right)}{4\pi^{\frac{d+1}{2}}\Gamma\left(\Delta-\frac{d}{2}+1\right)} \frac{(2w)^\Delta}{((\vec{x}-\vec{y})^2+w^2)^\Delta} \\ &= \frac{a^{d-1}\Gamma\left(\frac{\Delta}{2}\right)\Gamma\left(\frac{\Delta+1}{2}\right)}{4\pi^{\frac{d+1}{2}}\Gamma\left(\Delta-\frac{d}{2}+1\right)} \frac{2(u\cdot Y)^\Delta}{\|\vec{x}-Y\|^{2\Delta}} ,\end{aligned} \tag{3.53}$$

where in the last step we expressed K by the euclidean norm introduced in (3.17) and the auxiliary vector u is defined as $u = (0, ..., 1)$ such that $u \cdot Y = w$.

Introducing interactions is straightforward and follows the same steps as in flat space. If we add a self-interaction term of the form $\frac{1}{n!}\lambda\phi^n$ in the action of the path integral, we can expand in orders of λ and replace the ϕ of the interaction vertex with functional derivatives in terms of $j(x)$. This adds an internal vertex for each order in λ. A boundary m point correlation function at order $\mathcal{O}(\lambda^k)$ is therefore given by

$$\left.\left\langle \prod_{i=1}^{m} \mathcal{O}_\Delta(\vec{x}_i) \right\rangle\right|_{\lambda^n} = \lim_{z_i\to 0} z_i^{-\Delta} \frac{\delta^m}{\delta j(X_1)...j(X_n)} \log\left.\left((-\lambda)^k \prod_{l=1}^{k} \int \mathrm{d}^{d+1}X_l \frac{\delta^n}{\delta j(X_l)^n} Z[j] \right)\right|_{j=0}$$

There is a nice diagrammatic representation of these correlation functions, called Witten diagrams [22], which applies the concept of Feynman diagrams to AdS. Drawing a Witten diagram works the following way. The boundary of AdS is represented by a circle. For each boundary operator, draw a point on the boundary and for each bulk vertex draw a point in the bulk. Then connect the points in all possible ways allowed by the interaction vertex, where boundary points can only attach to one line. Summing over all possible diagrams drawn this way and multiplying by the corresponding symmetry factor [130] provides us with the contribution to the correlation function at the given order in λ. An example of a four point function is depicted in figure 3.7. In

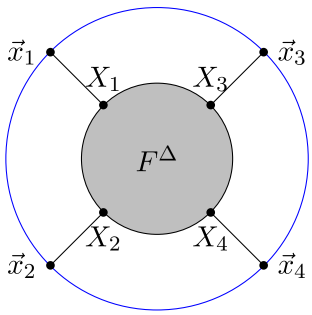

Figure 3.7: Example of a four-point Witten diagram, where F^{Δ} only depends on bulk-to-bulk propagators.

chapter 4 we will analyse the mathematical properties of these diagrams which we will use extensively in chapters 5 and 6 to calculate four point functions of $\lambda\phi^4$ theory in (A)dS.

3.3.2 Scalar field theory in dS

Defining quantum field theory in dS is somewhat more complicated than in AdS. We will start again with the classical theory of a free scalar field in the Poincaré patch of dS. To define the propagator we will go to the euclidean version of dS, which is just a sphere. This will give us a unique Green function and upon Wick rotating back and to dS and restricting to the Poincaré patch we will obtain a unique definition of a vacuum, called the Bunch-Davies or euclidean vacuum (see [65–68]).

The classical action of a free scalar field in a de Sitter space-time is given by

$$S[\phi] = \int_{\mathrm{dS}} \sqrt{g}\mathrm{d}^{d+1}X \left(-\frac{1}{2}(\partial\phi)^2 - \frac{1}{2}m^2\phi^2\right) , \tag{3.54}$$

where m^2 is the effective mass term given in equation (3.34). We can repeat the same analysis as we did for EAdS. By considering the general formula for the scaling dimension (3.32) we find that the minimally coupled massless case is given by $\Delta \in \{d, 0\}$. For the conformally coupled case we plug in equation (3.35) together with the Ricci scalar of dS. Note that the dS Ricci scalar has an opposite sign with respect to EAdS, cancelling the sign difference in the scaling dimension. This means we obtain the same values for the scaling dimension of a conformally coupled scalar field given by equation (3.36).

In the global patch of dS, given by (3.19), a Wick rotation $t \to it$ leads to $\mathbf{X}^0 \to i\mathbf{X}^0$ which turns the defining equation of dS (3.18) into the equation of the $d+1$ sphere. The conformal boundaries at future and past infinity just become the north and south pole of the sphere, since the sphere obviously does not possess any spatial boundaries. From the euclidean action we obtain the Klein-Gordon equation on the sphere, which is given by equation (3.39), with the difference that $K(\mathbf{X}, \mathbf{Y})$ is now

$$K(\mathbf{X}, \mathbf{Y}) = \frac{1}{a^2\delta_{AB}\mathbf{X}^A\mathbf{X}^B} .$$

The solutions to the equation of motion in terms of K are in principle the same as for EAdS. There is however a different basis for the solutions, related to (3.40) by an identity on the hypergeometric functions which is more appropriate for the boundary conditions imposed in dS. The solutions are given by [83]

$$\Lambda(\mathbf{X},\mathbf{Y}) = A^{+}{}_2F_1\left(\Delta_+,\Delta_-;\frac{d+1}{2};\frac{K-1}{2K}\right) + A^{-}{}_2F_1\left(\Delta_+,\Delta_-;\frac{d+1}{2};\frac{K+1}{2K}\right). \tag{3.55}$$

Since the sphere does not posses a boundary we have to find a different way to fix the integration constants $A^{\pm}$. We notice that the first term in (3.55) has a singularity at $K=1$ while the second term at $K=-1$. The former singularity corresponds to coinciding points, while the latter appears for antipodally coinciding points. As the second situation would imply non-local interactions, we choose the boundary condition $A^{-}=0$. A^{+} can be fixed by taking the flat limit equivalently to the EAdS case in equation (3.42), to get the following normalized Green function on the sphere

$$\Lambda_S(\mathbf{X},\mathbf{Y}) = \mathcal{n}_{\text{dS}}\ {}_2F_1\left(\Delta_+,\Delta_-;\frac{d+1}{2};\frac{K-1}{2K}\right), \tag{3.56}$$

with the normalization constant given by

$$\mathcal{n}_{\text{dS}} = \frac{\Gamma(\Delta_+)\Gamma(\Delta_-)}{(4\pi)^{\frac{d+1}{2}}\Gamma\left(\frac{d+1}{2}\right)}.$$

The Green function in dS is obtained from equation (3.56) by Wick rotating back and restricting to the Poincaré patch, which we will denote by $\Lambda(K(\mathbf{X},\mathbf{Y}))$. To obtain the correct time ordering for the Feynman propagator when taking the flat limit, we have to demand the correct behavior across the branch cut at $0<K<1$ which coincides with the region of time-like separation. We therefore demand that the commutator between two fields at space-like separation should vanish, while at time-like separation it should be non-vanishing. Expressed in terms of two point functions of the vacuum state defined by the analytic continuation of (3.56), this means

$$\langle 0\,|[\phi(X),\phi(Y)]|\,0\rangle = \Lambda(K(\mathbf{X},\mathbf{Y})) - \Lambda(K(\mathbf{Y},\mathbf{X}))\,.$$

For this expression to be non-vanishing for time-like separation we have to demand that we approach the branch cut from above and below depending on the time-ordering. In the Poincaré patch this leads to the replacement $K\to K-i\varepsilon\,\text{sgn}(|\eta_x|-|\eta_y|)$, where ε is an infinitesimal, positive, real parameter. The two point function with the correct behavior across the branch cut is therefore given by

$$\Lambda_{TA}(\mathbf{X},\mathbf{Y}) := \Lambda(K(\mathbf{X},\mathbf{Y}) - i\varepsilon\,\text{sgn}(|\eta_x|-|\eta_y|)\,. \tag{3.57}$$

The time ordered Feynman two point function is therefore given by

$$\begin{aligned}\Lambda_{TT}(K(\mathbf{X},\mathbf{Y})) &:= \langle 0\,|T\{\phi(X_1)\phi(X_2)\}|\,0\rangle \\ &= \theta(|\eta_x|-|\eta_y|)\Lambda_{TA}(\mathbf{X},\mathbf{Y}) + \theta(|\eta_y|-|\eta_x|)\Lambda_{TA}(\mathbf{Y},\mathbf{X})\,.\end{aligned}$$

This can be written in a more compact form replacing $K\to K+i\varepsilon$ in (3.56). The time ordered Feynman Green function in dS is therefore given by

$$\Lambda_{TT}(K(\mathbf{X},\mathbf{Y})) = \mathcal{n}_{\text{dS}}\ {}_2F_1\left(\Delta_+,\Delta_-;\frac{d+1}{2};\frac{K-1}{2K}-i\varepsilon\right), \tag{3.58}$$

while the anti-time ordered two point function is given by

$$\begin{aligned}\Lambda_{AA}(K(\mathbf{X},\mathbf{Y})) &:= \left\langle 0 \left| \bar{T}\{\phi(X_1)\phi(X_2)\} \right| 0 \right\rangle \\ &= \theta(|\eta_x| - |\eta_y|)\Lambda_{TA}(\mathbf{Y},\mathbf{X}) + \theta(|\eta_y| - |\eta_x|)\Lambda_{TA}(\mathbf{X},\mathbf{Y}) \\ &= \Lambda(K(\mathbf{X},\mathbf{Y}) + i\varepsilon)\,. \end{aligned} \tag{3.59}$$

These Green functions define the Bunch-Davies or euclidean vacuum. Let us mention that this is not the unique de Sitter invariant vacuum. There is an infinite space of de Sitter invariant vacua parametrised by two continuous parameters [68]. All these vacua have singularities at points related by the antipodal map and therefore do not provide the correct flat limit. The Bunch-Davies vacuum is therefore special from a physical perspective. Also, from a cosmological point of view, the Bunch-Davies vacuum seems to be the only reasonable choice, since it gives mode functions for the field that behave like in flat space when going to the infinite past or to wavelengths much smaller than the horizon. From now on we will only work in the Bunch-Davies vacuum and recommend [68] to the interested reader for an in depth discussion of alternative vacua.

Bunch-Davies wave function

At this point we have to discuss a major difference between quantum field theory in dS and AdS. dS does not posses a globally defined time-like Killing vector in the Poincaré or the global patch. If we prepare a vacuum state on an equal time slice, it will not stay a vacuum when we evolve it in time [116]. This complicates perturbative calculations significantly as we cannot assume that the asymptotic vacua in the infinite past and future to be the same.

There are, however, two ways to get around this problem and still define meaningful observables at future infinity. The first one is to go to the Schrödinger picture of QFT (see e.g. [131]) and consider the wave function of the universe as introduced in [61]. We start with a vacuum state on some initial time slice and project it against some out state, defining a configuration of the field and therefore providing a future boundary condition for the path integral formulation of the wave function [69, 132]

$$\Psi_0[\phi(t)] := \langle \phi(t) \,| U(t,t_0) |\, 0 \rangle = \int\limits_{\substack{\phi(t)\\ \phi(t_0)=0}} \mathcal{D}\phi \mathrm{e}^{iS[\phi]}\,.$$

To prepare the Bunch-Davies vacuum as our initial state in the infinite past we have to the Wick rotation from the sphere, which does not have an equivalent to the Poincaré patch. We consider a space which is given by dS in the Poincaré patch up the equator at $\mathbf{X}^0 = \mathbf{X}^{d+1} = 0$, which corresponds to the infinite past $\eta \to -\infty$, and glue to it a hemisphere with radius $1/a$.

The Bunch-Davies vacuum is then defined as the euclidean path integral over the hemisphere, defining the initial condition in the Poincaré patch on the initial time-slice [14]. From then on we evolve the state with the Hamiltonian in the bulk. The wave function in field configuration space $|\phi_0(\eta,\vec{x})\rangle$ on a time slice η is therefore given by

$$\Psi_{BD}[\phi(\eta,\vec{x})] := \langle \phi(\eta,\vec{x}) \,| U(\eta,-\infty) |\, 0_{BD} \rangle = \int\limits_{\substack{\phi(\eta,\vec{x})=\phi_0(\eta,\vec{x})\\ \phi(-i\infty,\vec{x})=0}} \mathcal{D}\phi \mathrm{e}^{iS[\phi]}\,.$$

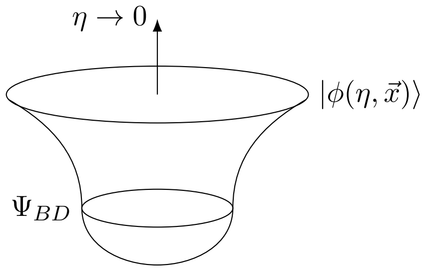

Figure 3.8: Schematical depiction of the Bunch-Davies wavefunction as a path-integral over a hemisphere attached to the Poincaré patch of dS at past infinity.

We are interested in the late-time limit of this wave function [64] which is given by taking the limit $\eta \to 0$. For a free field, given by the action (3.54) we can calculate the path integral exactly. To do this we to compute the on-shell action. Note that the projection against a configuration eigenstate $|\phi_0(\eta, \vec{x})\rangle$ acts like a Dirichlet boundary condition at future infinity.

The on-shell action for a free field in dS in the Poincaré patch is given by

$$S_{\text{on-shell}} = \frac{1}{2} \int \mathrm{d}^d\vec{x} \frac{1}{(a\eta)^{d-1}} \bar{\phi}(x) \partial_\eta \bar{\phi}(x)|_{\eta \to 0} \,. \tag{3.60}$$

Here $\bar{\phi}$ is the solution of the Klein-Gordon equation with future Dirichlet boundary condition fixing the value of the field to be ϕ_0 at future infinity

$$\bar{\phi}(\eta, \vec{x}) = \int_{\mathbb{R}^d} \mathrm{d}^d\vec{y} \bar{\Lambda}_D(\vec{y}, X) \phi_0(\vec{y})$$

where $\bar{\Lambda}_D(\vec{y}, X)$ is the Green function imposing Dirichlet boundary conditions at future infinity. Comparing the Poincaré patches in dS and EAdS we already noticed that they are related by the Wick rotation $z \to i\eta$ and $a \to -ia$. In section 3.3.1 we derived the Green functions imposing Dirichlet and Neumann boundary conditions in the Poincaré patch of EAdS. The same analysis can be repeated in the Wick rotated version. We end up with the same Green functions

$$\Lambda_{D/N}(\mathbf{X}, \mathbf{Y}, \Delta_\pm) = i\mathcal{N}_\Delta K^\Delta {}_2F_1\left(\frac{\Delta_\pm}{2}, \frac{\Delta_\pm + 1}{2}; \Delta_\pm - \frac{d-2}{2}; K^2 - i\varepsilon\right) ,$$

where this time K is given by (3.21) and similarly the bulk to boundary propagator is given by the Wick rotated version of (3.53),

$$\bar{\Lambda}_D(\vec{y}, X) = i\mathcal{N}_{\Delta_+} \frac{(2\eta_x)^{\Delta_+}}{((\vec{x} - \vec{y})^2 - \eta_x^2)^{\Delta_+}} \,. \tag{3.61}$$

Plugging equation (3.61) into the on-shell action (3.60) we obtain the result

$$\begin{aligned} S_{\text{on-shell}}[\phi_0] =& \frac{1}{2} \int_{\mathbb{R}^d} \mathrm{d}^d\vec{x} \frac{1}{(a\eta)^{d-1}} \phi_0(\vec{x}) \partial_{\eta_x} \int_{\mathbb{R}^d} \mathrm{d}^d\vec{y}\, \bar{\Lambda}_D(\vec{y}, X) \phi_0(\vec{y}) \Big|_{\eta \to 0} \\ =& \frac{i\mathcal{N}_{\Delta_+}}{2} \int_{\mathbb{R}^{2d}} \mathrm{d}^d\vec{x} \mathrm{d}^d\vec{y} \frac{\phi_0(\vec{x}) \phi_0(\vec{y})}{\|\vec{x} - \vec{y}\|^{2\Delta_+}} \,. \end{aligned} \tag{3.62}$$

By fixing the value of ϕ at future infinity, all quantum fluctuations are given by vacuum loops which do not contribute at future infinity. The free Bunch-Davies wave function in configuration space is therefore given by

$$\Psi_{BD}[\phi_0(\vec{x})] = \mathrm{e}^{iS_{\text{on-shell}}[\phi_0]}\,,$$

with $S_{\text{on-shell}[\phi_0]}$ given by (3.62).

A similar expression can be derived by imposing Neumann instead of Dirichlet boundary conditions at future infinity meaning we fix the time derivative $\partial_\eta \phi$ at future infinity. This can be thought of as going to canonical momentum space at future infinity and we call the value of the time derivative of at future infinity $\pi_0(\vec{x}) := \partial_\eta \phi(\eta, \vec{x})|_{\eta\to 0}$. The solution of the field with Neumann boundary condition at future infinity is therefore given by

$$\bar{\phi}(\eta, \vec{x}) = \int_{\mathbb{R}^d} \mathrm{d}^d\vec{y}\bar{\Lambda}_N(\vec{y}, X)\pi_0(\vec{y})\,.$$

Repeating the same steps as for the Dirichlet boundary conditions we find that the Neumann bulk to boundary propagator is given by (3.61) with $\Delta_+ \to \Delta_-$. The Bunch-Davies wave function in momentum space at future infinity is therefore given by

$$\Psi_{BD}[\pi_0(\vec{x})] = \mathrm{e}^{iS_{\text{on-shell}}[\pi_0]}; \qquad S_{\text{on-shell}}[\pi_0] = \frac{i n_{\Delta_-}}{2}\int_{\mathbb{R}^{2d}} \mathrm{d}^d\vec{x}\mathrm{d}^d\vec{y}\frac{\pi_0(\vec{x})\pi_0(\vec{y})}{\|\vec{x}-\vec{y}\|^{2\Delta_-}}$$

Having calculated the late time limit of the wave function for a free scalar field, we would like to analyse how to treat an interacting theory in this picture. Let us consider an interaction of the form $\frac{1}{n!}\lambda\phi^n$. To explain the formalism we only use Dirichlet boundary conditions and note that the Neumann wave function can be obtained by following the same steps, just replacing the Green function.

The classical equation of motion is

$$(-\Box_{dS} + m^2)\phi = -\frac{\lambda}{(n-1)!}\phi^{n-1}$$

The tree level contributions to the wave function are given by the classical solutions to the classical equation motion in perturbation, which is given by

$$\begin{aligned}
\bar{\phi}(X) &= \sum_i \lambda^i \phi_i(X) \\
\phi_0(X) &= \int_{\mathbb{R}^d} \mathrm{d}^3\vec{y}\bar{\Lambda}(\vec{y}, X)_D\phi_0(\vec{y}) \\
\phi_{i+1}(X) &= -\frac{\lambda}{(n-1)!}\int_{\mathscr{H}^-_{d+1}} \mathrm{d}^4Y\Lambda(\mathbf{X},\mathbf{Y})_D\phi_i^{n-1}(Y)
\end{aligned}$$

Solving these equations iteratively and plugging them into the on-shell action (3.60), we get an infinite expansion in terms of λ, which up to order λ, is given by

$$\begin{aligned}
S_{\text{on-shell}}[\phi_0] = {}& \frac{i n_{\Delta_+}}{2}\int_{\mathbb{R}^{2d}} \mathrm{d}^d\vec{x}\mathrm{d}^d\vec{y}\frac{\phi_0(\vec{x})\phi_0(\vec{y})}{\|\vec{x}-\vec{y}\|^{2\Delta_+}} \\
& - \frac{\lambda}{n!}\int_{\mathscr{H}^-_{d+1}} \frac{\mathrm{d}^{d+1}X}{(az)^{d+1}}\int_{\mathbb{R}^{\ltimes}} \prod_{i=1}^n \mathrm{d}^d\vec{x}_i\bar{\Lambda}_D(\vec{x}_i, X)\phi_0(\vec{x}_i) + \mathscr{O}(\lambda) \qquad (3.63)
\end{aligned}$$

This structure is very similar to the situation in EAdS. In fact, if we interpret the wave function as a generating functional of CFT and the boundary values ϕ_0 as sources, we can calculate the tree-level correlation functions of this CFT by functional differentiation with respect to the sources

$$\left\langle \prod_{i=1}^{m} \mathcal{O}(\vec{x}_i) \right\rangle = \frac{\delta^m}{\delta\phi_0(\vec{x}_1)\delta\phi_0(\vec{x}_2)...\delta\phi_0(\vec{x}_m)} \Psi_{BD}[\phi_0(\vec{x})] \,. \tag{3.64}$$

This is the basis of the dS/CFT correspondence [14,69]. As we will see, equations (3.51) and (3.64) are at least perturbatively related by the Wick rotation $z \to i\eta$ and $a \to -ia$. In chapter 6 we will show that they give rise to the same correlation functions for $\lambda\phi^4$ theory, at least in perturbation theory.

To visualize the calculation the Witten diagrams developed for AdS/CFT can be applied to this calculation in a slightly modified way.

The bulk to boundary propagator $\bar{\Lambda}_D(\vec{y}, X)$ with point $\vec{y}$ at future infinity and X at finite time is represented by

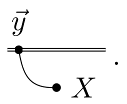

The bulk to bulk propagator $\Lambda_D(X,Y)$ with points X and X at finite time

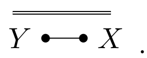

For example the tree-level contributions to the four point function of $\lambda\phi^4$ theory, generated by the terms of the on shell action given in (3.63) can be represent in terms of Witten diagrams as

$$\langle \mathcal{O}(\vec{x}_1)\mathcal{O}(\vec{x}_2)\mathcal{O}(\vec{x}_3)\mathcal{O}(\vec{x}_4)\rangle = \frac{\delta^4}{\delta\phi_0(\vec{x}_1)\delta\phi_0(\vec{x}_2)\delta\phi_0(\vec{x}_3)\delta\phi_0(\vec{x}_4)} \mathrm{e}^{iS_{on-shell}}$$

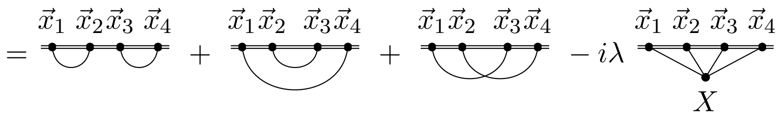

The wave function of the full quantum theory is given by the path integral over all field configurations with Bunch-Davies boundary conditions in the past and fixed boundary conditions in the future:

$$\Psi_{BD}[\phi_0(\vec{x})] = \int\limits_{\substack{\phi(0,\vec{x})=\phi_0(\vec{x}) \\ \phi(-i\infty,\vec{x})=0}} \mathcal{D}\phi \mathrm{e}^{iS[\phi]} = \mathrm{e}^{i\Gamma[\phi_0]} \,,$$

where $\Gamma[\phi_0]$ is the effective action that depends only on the boundary values of the field $\phi(0,\vec{x})$. We will calculate this effective action perturbatively in loop orders of quantum corrections by using the background field method (see e.g. [133]). This means we write our field as $\phi(X) = \varphi(X) + \chi(X)$ where $\varphi(X)$ satisfies the classical equations of motion and χ accounts for the quantum fluctuations. χ is choosen such that it vanishes on the boundary.

If we plug this ansatz into the action we get the result

$$\begin{aligned}S[\phi] =& \int \mathrm{d}^4X\sqrt{g}\left\{-\frac{1}{2}\partial_\mu\phi\partial^\mu\phi - \frac{1}{2}m^2\phi^2 - \frac{\lambda}{4!}\phi^4\right\}\\ =&S[\varphi] + \int \mathrm{d}^4X\sqrt{g}\chi\left\{\Box\varphi - m^2\varphi - \frac{\lambda}{3!}\varphi^3\right\} + \int \mathrm{d}^4X\sqrt{g}\left\{-\frac{1}{2}\partial_\mu\chi\partial^\mu\chi - \frac{1}{2}m^2\chi^2\right\}\\ &+\lambda\int \mathrm{d}^4X\sqrt{g}\left\{-\frac{1}{4}\varphi^2\chi^2 - \frac{1}{6}\varphi\chi^3 - \frac{1}{4!}\chi^4\right\}.\end{aligned}$$

The first term corresponds to the classical on shell action which we already calculated. It generates the tree-level Witten diagrams. The second term in the expansion vanishes as φ obeys the classical equations of motion. Therefore only the two remaining parts depend on χ and we are going to call the first one $S_0[\chi]$ as it corresponds to the free part of the action whereas the last term is called S_{int} as it generates the interaction terms.

Now we can plug this action into the path integral for the wave function. As the classical field is completely fixed by the equations of motion and the boundary conditions the only path integral we have to perform is over the quantum fluctuations χ:

$$\Psi_{BD}[\phi_0(\vec{x})] = \mathrm{e}^{i\Gamma[\phi_0]} = \mathrm{e}^{iS_{on-shell}[\phi_0]}\int \mathcal{D}\chi \mathrm{e}^{iS_0[\chi]+iS_{int}[\phi_0,\chi]}\,. \tag{3.65}$$

In the diagrammatic representation introduced above the quantum fluctuations generate additional loop corrections in the bulk. We will perform the explicit calculation for $\lambda\phi^4$ theory in chapter 6 as it was done in [71].

As a final note for this part, let us comment on the state operator correspondence. In section 3.3.1 we noticed that the correspondence between the Hilbert space of eigenstates of the dilatation operator in a CFT and the spectrum of operators can be generalized in AdS to a correspondence between local bulk operators and boundary states [129]. This was a consequence of the fact that time evolution in the global patch is an isometry of AdS which translates to a radial quantization in the Poincaré patch, meaning that any equal time slice can be contracted to a point by the action of the dilatation operator.

This construction obviously fails in dS for many reasons the first being that time evolution, neither in the global nor in the Poincaré patch, is an isometry of the space-time. Also from a geometrical point of view the situation is much different. An equal time slice in global patch is not given by a hemisphere in the Poincaré patch, as was the case in EAdS, but by the hyperboloid

$$\vec{x}^2 - \eta^2 = \mathrm{e}^t\,,$$

which never contracts to a point, which was essential for the state operator correspondence in AdS. These points were also raised in [87, 88].

The absence of a state operator correspondence is not a problem per se it only makes the connection between bulk physics and the theory on the boundary more obscure. At non-perturbative level at least it seems however still be possible to describe the time late wavefunction by a CFT.

Cosmological correlators

The wave function, however, is not an actual observable, but rather half the way to calculating a correlation function, which is an observable. The relation between the two is given by

$$\left\langle \prod_{i=1}^{m} \phi(\vec{x}_i) \right\rangle = \int \mathcal{D}\phi_0 \Psi^*_{BD}[\phi_0] \Psi_{BD}[\phi_0] \prod_{i=1}^{m} \phi(\vec{x}_i) \,.$$

Going from the wave function to the cosmological correlation function corresponds to inserting operators at future infinity of two Bunch-Davies wavefunctions, one having been evolved from the infinite past to the future boundary in the Poincaré patch while the other is inversely time-evolved in the contracting Poincaré patch, as depicted in figure 3.9.

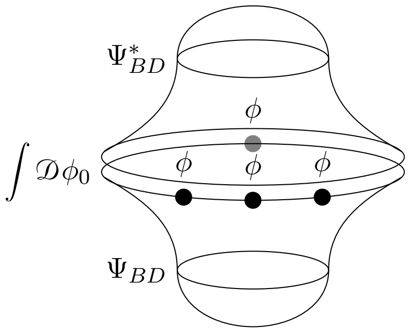

Figure 3.9: Schematical depiction of the path-integral over two Bunch-Davies wavefunctions to obtain a cosmological correlator

Even though this picture is conceptually helpful to understand the relation between the wave function and the correlator, it is practically useless for actual calculations, since it requires the non-perturbative knowledge of the wave function which we can only compute perturbatively for an interacting theory.

Instead we go from the Schrödinger to the interaction picture and consider the time evolution of the expectation value of a set of local operators on an equal time slice

$$\langle \phi(\vec{x}_1, \eta)...\phi(\vec{x}_n, \eta) \rangle_{BD} = \frac{\left\langle 0_{BD} \left| U_I^\dagger(-\infty, \eta)\phi(\vec{x}_1, \eta)...\phi(\vec{x}_n, \eta)U_I(-\infty, \eta) \right| 0_{BD} \right\rangle}{\left\langle 0_{BD} \left| U_I^\dagger(\eta_0, \eta)U_I(\eta_0, \eta) \right| 0_{BD} \right\rangle} \,. \tag{3.66}$$

Here U_I and $U_I^\dagger$ are the time-ordered and anti-time ordered evolution operator in the interaction picture given by

$$U_I(\eta_0, \eta) := T\left\{ \mathrm{e}^{-i\int_{\eta_0}^{\eta} \mathrm{d}\tilde{\eta} H_I(\tilde{\eta})} \right\}; \qquad U_I^\dagger(\eta_0, \eta) := \bar{T}\left\{ \mathrm{e}^{i\int_{\eta_0}^{\eta} \mathrm{d}\tilde{\eta} H_I(\tilde{\eta})} \right\} ,$$

where H_I is the interaction Hamiltonian and T and $\bar{T}$ denote time- and anti-time ordering, respectively. The Bunch-Davies vacuum condition is imposed at $\eta \to -\infty$. The denominator in equation (3.66) cancels vacuum bubble contributions, just as in flat space.

There are two ways to perform this calculation. We can expand the exponentials in U_I and $U_I^\dagger$ and use Wick contraction on the left and right of the insertions to calculate the correlator. Denoting the fields on the time ordered side of the integral by $\phi_T(X)$, the anti-time order fields by $\phi_A(X)$ and the field insertions on the time slice at future infinity by $\bar{\phi}(\vec{x})$, we find the following different propagators depending on the Wick contraction, given in terms of equations (3.57), (3.58) and (3.59):

$$\phi_{T/A}(X_1)\phi_{T/A}(X_2) \to \Lambda_{T/A,T/A}(K(\mathbf{X}_1,\mathbf{X}_2)); \qquad \phi_{T/A}(X_1)\bar{\phi}(\vec{x}_2) \to \bar{\Lambda}_{T/A}(X_1,\vec{x}_2)\,.$$

Where the new bulk to boundary propagator $\bar{\Lambda}_{T/A}(X_1,\vec{x}_2)$ is given by taking the limit

$$\begin{aligned}\bar{\Lambda}_{T/A}(X_1,\vec{x}_2) :&= \lim_{\eta_0:=\eta_2\to 0} \Lambda_{T/A,T/A}(K(\mathbf{X},\mathbf{Y}))\\ &= \frac{\Gamma\left(\Delta_+ - \frac{d}{2}\right)\Gamma\left(\Delta_- - \frac{d}{2}\right)\left(\Delta_+ - \frac{d}{2}\right)}{2\pi}\times\\ &\times\left(n_{\Delta_-}\frac{(2\eta_0\eta_2)^{\Delta_-}}{\|\vec{x_1}-X_2\|^{2\Delta_-}\mp i\varepsilon} + n_{\Delta_+}\frac{(2\eta_0\eta_2)^{\Delta_+}}{\|\vec{x_1}-X_2\|^{\Delta_+}\mp i\varepsilon}+\cdots\right)\,. \end{aligned} \tag{3.67}$$

It does not matter if the boundary limit is taking with time- or anti- time ordered point since there is no notion of time ordering at future infinity. The $i\varepsilon$ prescription implementing (anti-) time ordering properties, can be translated into an analytic continuation of the time on each side of the integral by denoting times on the time ordered side by $\eta_T := \eta(1-i\varepsilon)$ and on the anti time ordered side as $\eta_T := \eta(1+i\varepsilon)$.

Equation (3.67) contains two terms given by the Neumann and Dirichlet bulk to boundary propagators from EAdS (3.53), up to the signature of the metric given. This actually reflects a general relation between the Neumann and Dirichlet propagators and the Bunch-Davies propagator. By applying the following identities for the hypergeometric function

$${}_2F_1\left(a,b;\frac{a+b+1}{2};z\right) = (1-2z)^{-a}F\left(\frac{a}{2},\frac{a+1}{2};\frac{a+b+1}{2};\frac{4z(z-1)}{(1-2z)^2}\right)$$

and

$$\begin{aligned}{}_2F_1(a,b;c,z) &= \frac{\Gamma(c)\Gamma(c-a-b)}{\Gamma(c-a)\Gamma(c-b)}{}_2F_1(a,b;a+b+1-c;1-z)\\ &+\frac{\Gamma(c)\Gamma(a+b-c)}{\Gamma(a)\Gamma(b)}(1-z)^{c-a-b}{}_2F_1(c-a,c-b;1+c-a-b;1-z)\,,\end{aligned}$$

we can rewrite the hypergeometric function in (3.56) as

$$\begin{aligned}{}_2F_1\Big(\Delta_+,\Delta_-;\frac{d+1}{2};\frac{K-1}{2K}\Big) &= \frac{\Gamma\left(\frac{d+1}{2}\right)\Gamma\left(\Delta_- - \frac{d}{2}\right)}{\Gamma\left(\frac{\Delta_-}{2}\right)\Gamma\left(\frac{\Delta_-+1}{2}\right)}K^{\Delta_+}\\ &\times{}_2F_1\left(\frac{\Delta_+}{2},\frac{\Delta_++1}{2};\Delta_+-\frac{d-2}{2};K^2\right)+(\Delta_+\leftrightarrow\Delta_-)\,.\end{aligned}$$

With this formula we can express the time ordered Bunch-Davies propagator (3.58) in terms of propagators with fall-off behaviour

$$\Lambda_{TT}(K(\mathbf{X},\mathbf{Y})) = \frac{\Gamma\left(\Delta_+ - \frac{d}{2}\right)\Gamma\left(\Delta_- - \frac{d}{2}\right)\left(\Delta_+ - \frac{d}{2}\right)}{2\pi}\left(\Lambda_N(K(\mathbf{X},\mathbf{Y}))+\Lambda_D(K(\mathbf{X},\mathbf{Y}))\right)$$

and similarly for Λ_{TT} and Λ_{TA} with the respective $i\varepsilon$ term. The Dirichlet and Neumann Green function are simply related to the EAdS Green functions $\Lambda(K,\Delta_+)$ and $\Lambda(K,\Delta_-)$

by a Wick rotation. In fact, by carefully doing the rotation we can express all dS Green functions in the Poincaré patch in terms of Green functions in EAdS with fixed boundary conditions.

Time ordered points in the bulk are continued as $\eta_T \to \mathrm{e}^{-i\frac{\pi}{2}}z$, while anti-time ordered points are rotated as $\eta_A \to \mathrm{e}^{i\frac{\pi}{2}}z$, such that we do not cross any branch cuts. This trick was first emphasized in [84–86].

Doing this rotation, we observe, that the propagators transform as

$$\Lambda_{TT}(K) \to \frac{\Gamma\left(\Delta_+ - \frac{d}{2}\right)\Gamma\left(\Delta_- - \frac{d}{2}\right)\left(\Delta_+ - \frac{d}{2}\right)}{2\pi}\left(\mathrm{e}^{i\pi\Delta_-}\Lambda(K,\Delta_-) + \mathrm{e}^{i\pi\Delta_+}\Lambda(K,\Delta_+)\right) ,$$

$$\Lambda_{AA}(K) \to \frac{\Gamma\left(\Delta_+ - \frac{d}{2}\right)\Gamma\left(\Delta_- - \frac{d}{2}\right)\left(\Delta_+ - \frac{d}{2}\right)}{2\pi}\left(\mathrm{e}^{-i\pi\Delta_-}\Lambda(K,\Delta_-) + \mathrm{e}^{-i\pi\Delta_+}\Lambda(K,\Delta_+)\right) ,$$

$$\Lambda_{TT}(K) \to \frac{\Gamma\left(\Delta_+ - \frac{d}{2}\right)\Gamma\left(\Delta_- - \frac{d}{2}\right)\left(\Delta_+ - \frac{d}{2}\right)}{2\pi}\left(-\Lambda(K,\Delta_-) + \Lambda(K,\Delta_+)\right) ,$$

while the bulk to boundary propagator becomes

$$\bar{\Lambda}_{T/A}(K) \to \frac{\Gamma\left(\Delta_+ - \frac{d}{2}\right)\Gamma\left(\Delta_- - \frac{d}{2}\right)\left(\Delta_+ - \frac{d}{2}\right)}{2\pi}\Big(\eta_0^{\Delta_-}\mathrm{e}^{\pm i\frac{\pi}{2}\Delta_-}\bar{\Lambda}(K,\Delta_-) + \eta_0^{\Delta_+}\mathrm{e}^{\pm i\frac{\pi}{2}\Delta_+}\bar{\Lambda}(K,\Delta_+)\Big) . \tag{3.68}$$

To see how this formalism can be applied in practice let us take the four point function of a scalar field theory with interaction term

$$\int_{-\infty}^{\eta_0} H_{int} d\eta = \frac{\lambda}{4!}\int_{\mathcal{H}^-_{d+1}} \frac{d^4X}{(a\eta)^{d+1}}\phi^4(X).$$

The four point function evaluated at future infinity is given by

$$\lim_{\eta\to\eta_0} \phi(\eta,\vec{x}_1)\phi(\eta,\vec{x}_2)\phi(\eta,\vec{x}_3)\phi(\eta,\vec{x}_4) \equiv \phi_0(\vec{x}_1)\phi_0(\vec{x}_2)\phi_0(\vec{x}_3)\phi_0(\vec{x}_4) .$$

The disconnected term is given by the generalized free field contribution

$$\begin{aligned}\langle\phi_0(\vec{x}_1)\phi_0(\vec{x}_2)\phi_0(\vec{x}_3)\phi_0(\vec{x}_4)\rangle &= \langle\phi_0(\vec{x}_1)\phi_0(\vec{x}_2)\rangle\langle\phi_0(\vec{x}_3)\phi_0(\vec{x}_4)\rangle \\ &+ \langle\phi_0(\vec{x}_1)\phi_0(\vec{x}_3)\rangle\langle\phi_0(\vec{x}_2)\phi_0(\vec{x}_4)\rangle + \langle\phi_0(\vec{x}_1)\phi_0(\vec{x}_4)\rangle\langle\phi_0(\vec{x}_2)\phi_0(\vec{x}_3)\rangle\end{aligned}$$

where each two point function is just given by the propagator $\Lambda(K)$ with both legs taken to future infinity.

The first order term in λ has two contributions from contracting with the time-ordered and the anti-time-ordered Hamiltonian

$$\begin{aligned}W_0 = &-i\lambda\int_{\mathcal{H}^-_{d+1}}\frac{\mathrm{d}^{d+1}X}{(a\eta_T)^{d+1}}\bar{\Lambda}_T(\vec{x_1},X)\bar{\Lambda}_T(\vec{x_2},X)\bar{\Lambda}_T(\vec{x_3},X)\bar{\Lambda}_T(\vec{x_4},X) \\ &+ i\lambda\int_{\mathcal{H}^-_{d+1}}\frac{\mathrm{d}^{d+1}X}{(a\eta_A)^{d+1}}\bar{\Lambda}_A(\vec{x_1},X)\bar{\Lambda}_A(\vec{x_2},X)\bar{\Lambda}_A(\vec{x_3},X)\bar{\Lambda}_A(\vec{x_4},X).\end{aligned}$$

We perform this integral by doing the Wick rotation for η_T and η_A individually, such that we do not cross the branch cut. We set

$$\eta_T \to \mathrm{e}^{-i\frac{\pi}{2}}z; \qquad \eta_A \to \mathrm{e}^{i\frac{\pi}{2}}z$$

With this transformation we can write the cross diagram as

$$\begin{aligned}W_0 = &-\lambda \int_{\mathcal{H}^+_{d+1}} \frac{\mathrm{d}^{d+1}X}{(az)^{d+1}} \bar{\Lambda}_T(\vec{x_1}, X)\bar{\Lambda}_T(\vec{x_2}, X)\bar{\Lambda}_T(\vec{x_3}, X)\bar{\Lambda}_T(\vec{x_4}, X)\\ &- \lambda \int_{\mathcal{H}^+_{d+1}} \frac{\mathrm{d}^{d+1}X}{(az)^{d+1}} \bar{\Lambda}_A(\vec{x_1}, X)\bar{\Lambda}_A(\vec{x_2}, X)\bar{\Lambda}_A(\vec{x_3}, X)\bar{\Lambda}_A(\vec{x_4}, X).\end{aligned}$$

Focusing on the conformally coupled massless case (3.36) and using equation (3.68) to expand to the second subleading order, we obtain

$$\begin{aligned}W_0 = &- \frac{\lambda}{8} \int_{\mathcal{H}^+_4} \frac{d^{d+1}X}{(az)^{d+1}} \Big(\eta_0^{4\Delta_-} \bar{\Lambda}(K, \Delta_-)\bar{\Lambda}(K, \Delta_-)\bar{\Lambda}(K, \Delta_-)\bar{\Lambda}(K, \Delta_-)\\ &-\eta_0^{2(\Delta_-+\Delta_+)} \bar{\Lambda}(K, \Delta_+)\bar{\Lambda}(K, \Delta_+)\bar{\Lambda}(K, \Delta_-)\bar{\Lambda}(K, \Delta_-)\\ &+\eta_0^{4\Delta_+} \bar{\Lambda}(K, \Delta_+)\bar{\Lambda}(K, \Delta_+)\bar{\Lambda}(K, \Delta_+)\bar{\Lambda}(K, \Delta_+) + \cdots\Big)\end{aligned}$$

The evaluation of the tree-level four-point function is therefore reduced to a calculation in EAdS, with two different boundary conditions contributing, corresponding to conformal dimensions Δ_+ and Δ_-.

We could proceed with this calculation diagram by diagram, which is the way this relation between cosmological correlator and EAdS Witten diagrams was first written down in [84–86]. However, as shown in [87], there is an elegant way to rewrite the dS action with the Schwinger-Keldysh contour directly in terms of an auxiliary EAdS action, from which the cosmological correlation functions can be extracted by straightforward functional derivation. In the following, we will review this formulation.

The closed time evolution between two in-states from the infinite past can be expressed by a path integral with closed time curves. Then a correlation function is given by taking functional derivatives of the time and anti-time ordered sources j_T and j_A of the partition function

$$Z[j_T, j_A] = \int \mathcal{D}\phi_T \mathcal{D}\phi_A \mathrm{e}^{iS_c + i\int(\phi_T j_T + \phi_A j_A)},$$

with the closed time action given by

$$iS_c = i \int_{-\infty}^{0} \frac{\mathrm{d}\eta \mathrm{d}^d\vec{x}}{\eta^{d+1}} \left\{-\frac{1}{2}(\partial\phi_T)^2 - \frac{1}{2}m^2\phi_T^2 - V(\phi_T) + \frac{1}{2}(\partial\phi_A)^2 + \frac{1}{2}m^2\phi_A^2 + V(\phi_A)\right\}.$$

Performing the Wick rotation $\eta = z\mathrm{e}^{\pm i\frac{\pi}{2}}$ as described above, the action becomes

$$\begin{aligned}iS_c = - \int_0^\infty \frac{\mathrm{d}z\mathrm{d}^d\vec{x}}{z^{d+1}} \Bigg[&\mathrm{e}^{i\pi\frac{d-1}{2}} \left(\frac{1}{2}(\partial\phi_T)^2 - \frac{1}{2}m^2\phi_T^2 - V(\phi_T)\right)\\ &+ \mathrm{e}^{-i\pi\frac{d-1}{2}} \left(\frac{1}{2}(\partial\phi_A)^2 - \frac{1}{2}m^2\phi_A^2 - V(\phi_A)\right)\Bigg].\end{aligned}$$

As discussed above the classical solution of a free scalar field in de Sitter is given by $\phi(\eta, \vec{x}) = \phi^+(\eta, \vec{x}) + \phi^-(\eta, \vec{x})$ with

$$\phi^+(\eta, \vec{x}) := \int \mathrm{d}^3\vec{y}\, \bar{\Lambda}_{\Delta_+}(\eta, \vec{x} - \vec{y})\phi_0^+(\vec{y}),$$

$$\phi^-(\eta,\vec{x}) := \int \mathrm{d}^3\vec{y}\,\bar{\Lambda}_{\Delta_-}(\eta,\vec{x}-\vec{y})\phi_0^-(\vec{y}),$$

where $\phi^\pm(\eta,\vec{x}) \to \eta^{\Delta_\pm}$, for $\eta \to 0$. Under the Wick rotation we get

$$\phi(z\mathrm{e}^{\pm i\frac{\pi}{2}},\vec{x}) = \mathrm{e}^{\pm i\frac{\pi}{2}\Delta_+}\phi^+(z,\vec{x}) + \mathrm{e}^{\pm i\frac{\pi}{2}\Delta_-}\phi^-(z,\vec{x}), \tag{3.69}$$

which plugged in the action leads to

$$\begin{aligned}
iS_c = -\int_0^\infty \frac{\mathrm{d}z\mathrm{d}^d\vec{x}}{z^{d+1}}\Bigg[&\frac{\mathrm{e}^{-i\pi\left(\Delta_+-\frac{d-1}{2}\right)}}{2}\left((\partial\phi^+)^2 - m^2{\phi^+}^2\right)\\
&+\frac{\mathrm{e}^{-i\pi\left(\Delta_--\frac{d-1}{2}\right)}}{2}\left((\partial\phi^-)^2 - m^2{\phi^-}^2\right)\\
&+\mathrm{e}^{-i\frac{\pi}{2}}\left(\partial\phi^-\partial\phi^+ - m^2\phi^-\phi^+\right) + \frac{1}{2}\mathrm{e}^{+i\pi\left(\Delta_+-\frac{d-1}{2}\right)}\left((\partial\phi^+)^2 - m^2{\phi^+}^2\right)\\
&+\frac{1}{2}\mathrm{e}^{i\pi\left(\Delta_--\frac{d-1}{2}\right)}\left((\partial\phi^-)^2 - m^2{\phi^-}^2\right) + \mathrm{e}^{i\frac{\pi}{2}}\left(\partial\phi^-\partial\phi^+ - m^2\phi^-\phi^+\right)\\
&-\mathrm{e}^{i\pi\frac{d-1}{2}}V\left(\mathrm{e}^{-i\frac{\pi}{2}\Delta_+}\phi^+ + \mathrm{e}^{-i\frac{\pi}{2}\Delta_-}\phi^-\right) - \mathrm{e}^{-i\pi\frac{d-1}{2}}V\left(\mathrm{e}^{i\frac{\pi}{2}\Delta_+}\phi^+ + \mathrm{e}^{i\frac{\pi}{2}\Delta_-}\phi^-\right)\Bigg],
\end{aligned}$$

leading to the result, derived in [87],

$$\begin{aligned}
iS_c = -\int_0^\infty \frac{\mathrm{d}z\mathrm{d}^d\vec{x}}{z^{d+1}}\Bigg[&-\sin\left(\pi\left(\Delta_+ - \frac{d}{2}\right)\right)\left((\partial\phi^+)^2 - m^2{\phi^+}^2\right)\\
&-\sin\left(\pi\left(\Delta_- - \frac{d}{2}\right)\right)\left((\partial\phi^-)^2 - m^2{\phi^-}^2\right)\\
&-\mathrm{e}^{i\pi\frac{d-1}{2}}V\left(\mathrm{e}^{-i\frac{\pi}{2}\Delta_+}\phi^+ + \mathrm{e}^{-i\frac{\pi}{2}\Delta_-}\phi^-\right) - \mathrm{e}^{-i\pi\frac{d-1}{2}}V\left(\mathrm{e}^{i\frac{\pi}{2}\Delta_+}\phi^+ + \mathrm{e}^{i\frac{\pi}{2}\Delta_-}\phi^-\right)\Bigg].
\end{aligned} \tag{3.70}$$

We want to study a theory in dS with the potential $V(\phi) = \frac{\lambda}{4!}\phi^4$. In that case the action (3.70) becomes

$$\begin{aligned}
iS_c = -\int_0^\infty \frac{\mathrm{d}z\mathrm{d}^d\vec{x}}{z^{d+1}}\Bigg[&-\sin\left(\pi\left(\Delta_+ - \frac{d}{2}\right)\right)\left((\partial\phi^+)^2 - m^2{\phi^+}^2\right) + (\phi^+,\Delta_+ \leftrightarrow \phi^-,\Delta_-)\\
&+\frac{2\lambda}{4!}\Bigg({\phi^+}^4\sin\left(\frac{\pi}{2}(3\Delta_+ - \Delta_-)\right) + 6{\phi^+}^2{\phi^-}^2\sin\left(\frac{\pi d}{2}\right) + {\phi^-}^4\sin\left(\frac{\pi}{2}(3\Delta_- - \Delta_+)\right)\\
&+4{\phi^+}^3\phi^-\sin(\pi\Delta_+) + 4{\phi^-}^3\phi^+\sin(\pi\Delta_-)\Bigg)\Bigg].
\end{aligned} \tag{3.71}$$

In this work we consider the case of the conformally coupled scalar with $\Delta_+ = \frac{d+1}{2}$ and $\Delta_- = \frac{d-1}{2}$ with odd boundary dimensions d. The action (3.71) then becomes

$$\begin{aligned}
iS_c = -\int_0^\infty \frac{\mathrm{d}z\mathrm{d}^d\vec{x}}{z^{d+1}}\Bigg[&-\left((\partial\phi^+)^2 - m^2{\phi^+}^2\right) + \left((\partial\phi^-)^2 - m^2{\phi^-}^2\right)\\
&-(-1)^{\frac{d-1}{2}}\frac{2\lambda}{4!}\left({\phi^+}^4 - 6{\phi^+}^2{\phi^-}^2 + {\phi^-}^4\right)\Bigg].
\end{aligned} \tag{3.72}$$

This action can now be used to calculate correlation functions in dS, showing to all orders in perturbation theory, that cosmological correlators can be expressed in terms of EAdS Witten diagrams. The leading contributions in the late time expansions are given by calculating the EAdS correlators of the field ϕ^-. Note however, that this field alone will not give a consistent CFT at the boundary, since there will be mixing interaction vertices between ϕ^- and ϕ^+. To be able to describe the CFT on the boundary we have to take into account the subleading terms in the late time expansion of the cosmological correlator as well. We also notice that the kinetic term in the action is not necessarily positive, leading to ghost-like behaviour of one of the fields. This would be a problem if we wanted to interpret this action as describing a bulk theory in EAdS, however, since we only us this action as a tool to describe a theory in dS, we should treat these signs only as a way to keep track of the correct relative prefactors in the expansion.

We have shown, that perturbative calculations in (A)dS can be reduced to evaluating Witten diagrams. In the following we will analyse the mathematical structure of these diagrams and will show that under certain conditions they can be reduced to flat space Feynman integrals.

Chapter 4

Mathematical structure of Witten diagrams

In the previous chapter we concluded with the observation that the perturbative calculation of correlation functions in both EAdS and dS can be reduced to the evaluation of Witten diagrams in EAdS. Due to the complicated structure of the bulk to bulk propagator in terms of hypergeometric functions the evaluation of these diagrams for general Δ seems intractable. For certain values of Δ, however, the propagator simplifies drastically. Especially for the conformally coupled massless field we will see that there is a straightforward map to flat space propagators. This lets us take advantage of the technical methods that have been developed for the evaluation of Feynman integrals [95–101, 134, 135]. For general $\Delta \in \mathbb{N}$ we also find a form which can be mapped to flat space-like diagrams, however, with an additional analytic parameter. We will show a way to potentially calculate diagrams for these values of Δ as well.

From this chapter onward the space-time dimension will be set to $d + 1 = 4$,[1] and we will only consider the Poincaré patch as defined in equation (3.16). Section 4.1 is a partially reproduction of [57].

4.1 Witten diagrams as flat space Feynman integrals

In this work we are mainly concerned with the calculation of four point Witten diagrams, as depicted in figure 3.7. A generic four-point Witten diagram Γ_W with $L + 1$ bulk vertices and L loops is associated to the following integral:

$$W_L^{\Delta}(\vec{x}_1, \vec{x}_2, \vec{x}_3, \vec{x}_4) = 2^{4\Delta} \left(\mathcal{N}_{\Delta}\right)^{2L+4} \int\limits_{(\mathcal{H}_4^+)^{L+1}} \prod_{i=1}^{L+1} \frac{\mathrm{d}^4 X_i}{(a z_i)^4} F^{\Delta}(X_1, \ldots, X_{L+1}) \\ \times \sum_{\rho \in \mathfrak{S}_4} \frac{\delta(\Gamma_W)}{|\Gamma_W|} f^{\Delta}(X_{\rho(1)}, \ldots, X_{\rho(4)}; \vec{x}_1, \ldots, \vec{x}_4)\,, \quad (4.1)$$

where the normalization $\mathcal{N}_{\Delta}$ of the propagators in (3.44) has been pulled out of the integral. The delta-function $\delta(\Gamma_W)$ denotes the identification of the bulk points according the topology of the graph and $|\Gamma_W|$ is the symmetry factor of the graph.

[1] We will introduce dimensional regularisation later, by analytically continuing the dimension in the integration measure. This is, however, just a trick to be able to evaluate integrals and is not really a change in the space-time dimension, as we will discuss.

The term $F^{\Delta}(X_1, ..., X_{L+1})$ involves only bulk-to-bulk propagators. Its explicit form is determined by the loop order and topology of the concrete graph. Together with the integration measure it is invariant under AdS isometries. The term $f^{\Delta}(X_1, .., X_4; \vec{x}_1, ..., \vec{x}_4)$ consists of bulk-to-boundary propagators and, depending on the loop order and the topology of the graph, some of the bulk points X_i may be identical. The sum is performed over different scattering channels corresponding to permutations of the bulk points $X_1, ..., X_4$. In its most general form this term is given by

$$f^{\Delta}(X_1, \ldots, X_4; \vec{x}_1, \ldots, \vec{x}_4) = \prod_{i=1}^{4} \left(\frac{z_i}{\|X_i - \vec{x}_i\|^2} \right)^{\Delta} . \tag{4.2}$$

The integral in (4.1) is divergent in general and thus needs to be regulated before it can be manipulated. In section 4.1.2 we will consider two regularisations. The first, considered in [55,56], preserves the AdS symmetry. The dimensional regularisation discussed next, while being natural from the flat space perspective, breaks AdS invariance.

From now on, unless explicitly stated otherwise, we will consider only the conformally coupled scalar field. In $d = 3$ boundary dimensions we find from equation (3.36) that the possible values for the scaling dimension on the boundary are $\Delta \in \{1, 2\}$. Plugging this into the general equation for the EAdS propagator (3.43), we get the simplified expression

$$\Lambda(K, \Delta) = \left(\frac{a}{2\pi} \right)^2 \frac{K^{\Delta}}{1 - K^2} \qquad \text{with } \Delta \in \{1, 2\} . \tag{4.3}$$

In what follows we will establish how to map these bulk to bulk propagators to a form resembling flat space propagators in momentum space.

4.1.1 Mapping propagators to flat space

Using the euclidean norm, defined in equation (3.17) we can write equation (4.3) as

$$\begin{aligned} \Lambda(\mathbf{X}, \mathbf{Y}; 1) &= \left(\frac{a}{2\pi} \right)^2 \left(G(X, Y) - G(X, \sigma(Y)) \right) , \\ \Lambda(\mathbf{X}, \mathbf{Y}; 2) &= \left(\frac{a}{2\pi} \right)^2 \left(G(X, Y) + G(X, \sigma(Y)) \right) . \end{aligned} \tag{4.4}$$

where in (4.4) we introduced the conformal flat space propagator $G(X, Y)$, given by

$$G(X, Y) := \frac{zw}{\|X - Y\|^2} = -\frac{1}{4} {}_2F_1 \left(1, 2; 2; \frac{K - 1}{2K} \right) . \tag{4.5}$$

It has the following properties:

- Invariance under translation of boundary points, $X_0 = (\vec{x}, 0)$:

$$G(X + X_0, Y + X_0) = G(X, Y); \qquad G(X + X_0, Y) = G(X, Y - X_0).$$

- Scale invariance:

$$G(\lambda X, \lambda Y) = G(X, Y) , \quad \lambda \in \mathbb{R} \setminus \{0\} .$$

- Invariance under the inversion:

$$G\left(\frac{X'}{\|X'\|^2}, \frac{Y'}{\|Y'\|^2}\right) = G(X, Y).$$

- The antipodal map in (3.12) acts as

$$G(\sigma(X), Y) = G(X, \sigma(Y)) = -\frac{zw}{\|X - \sigma(Y)\|^2} = \frac{1}{4}\, {}_2F_1\left(1, 2; 2; \frac{K(\mathbf{X}, \mathbf{Y}) + 1}{2K(\mathbf{X}, \mathbf{Y})}\right).$$

- An identity, which will be useful when simplifying the expressions for the multi-loop Witten diagrams

$$G(X, Y)G(X, \sigma(Y)) = \frac{1}{4}\left(G(X, Y) + G(X, \sigma(Y))\right). \tag{4.6}$$

To continue we note that the inverse geodesic distance in (3.8) can be expressed in terms of the conformal flat space propagator

$$\frac{1}{K(\mathbf{X}, \mathbf{Y})} = \frac{1}{4}\left(\frac{1}{G(X, Y)} - \frac{1}{G(X, \sigma(Y))}\right). \tag{4.7}$$

Moreover, by sending $X = (\vec{x}, z)$ to the boundary point $(\vec{x}, 0)$ we have

$$\bar{K}(\vec{x}, Y) := \lim_{z \to 0} \frac{K(\mathbf{X}, \mathbf{Y})}{z} = \frac{2w}{\|\vec{x} - Y\|^2} = \lim_{z \to 0} \frac{2G(X, Y)}{z},$$

in terms of the conformal flat space propagator which is again odd under the action of the antipodal map σ.

4.1.2 Regularisation

The integrals appearing in the loop calculations are generally divergent and have to be regularised. In this section we will present two different regularisation schemes. We first review the AdS invariant scheme, introduced in [55, 56] which will serve as a double check for the calculation in the dimensional regularisation we will introduce in the second part.

AdS invariant regularisation

An AdS invariant regularisation method, given by the deformation

$$K^\delta(\mathbf{X}, \mathbf{Y}) := \frac{K(\mathbf{X}, \mathbf{Y})}{1 + \delta}, \qquad \text{with } \delta > 0,$$

where δ is a dimensionless quantity was developed and used for regulating loops in AdS space in [55, 56] and applied to loops in de Sitter space in [71].

It corresponds to a cut-off in the bulk at coinciding points. This can be seen by expressing K in terms of the radial coordinate r, as was done in equation (3.41), and taking the flat limit

$$\frac{K}{1 + \delta} = \frac{1}{1 + \delta} \frac{1}{\sqrt{1 + a^2 r^2}} \to 1 - \frac{1}{2} a^2 r^2 - \delta + \mathcal{O}(a^4 r^4, \delta^2),$$

If we write δ as $\delta = \frac{1}{2}a^2R^2$ we see that this regularisation procedure corresponds to cutting out a ball of radius R around the coinciding points.

This regularisation scheme preserves the AdS symmetry and we will use it in section 5.2.2.

For $\Delta = 1$ the regularised propagator reads

$$\Lambda(\mathbf{X},\mathbf{Y};1,\delta) = \left(\frac{a}{2\pi}\right)^2 \frac{1}{2}\left(\frac{K(\mathbf{X},\mathbf{Y})}{1+\delta-K(\mathbf{X},\mathbf{Y})} + \frac{K(\mathbf{X},\mathbf{Y})}{1+\delta+K(\mathbf{X},\mathbf{Y})}\right),$$

and for $\Delta = 2$

$$\Lambda(\mathbf{X},\mathbf{Y};2,\delta) = \left(\frac{a}{2\pi}\right)^2 \frac{1}{2}\left(\frac{K(\mathbf{X},\mathbf{Y})}{1+\delta-K(\mathbf{X},\mathbf{Y})} - \frac{K(\mathbf{X},\mathbf{Y})}{1+\delta+K(\mathbf{X},\mathbf{Y})}\right),$$

We will denote the regularised Witten diagrams (4.1) by

$$\begin{aligned} W_L^{\Delta,\delta}(\vec{x}_1,\vec{x}_2,\vec{x}_3,\vec{x}_4) = 2^{4\Delta}\frac{(\mathcal{N}_\Delta)^{2L+4}}{a^{4L+4}} \int\limits_{(\mathcal{H}_4^+)^{L+1}} \prod_{i=1}^{L+1} \frac{\mathrm{d}^4X_i}{z_i^4} F^{\Delta,\delta}(X_1,\ldots,X_{L+1}) \\ \times \sum_{\rho\in\mathfrak{S}_4} \frac{\delta(\Gamma_W)}{|\Gamma_W|} f^{\Delta}(X_{\rho(1)},\ldots,X_{\rho(4)};\vec{x}_1,\vec{x}_2,\vec{x}_3,\vec{x}_4)\,, \end{aligned} \tag{4.8}$$

with normalization $\mathcal{N}_\Delta$ given in (3.44).

Dimensional regularisation

For $\Delta = 1$ and $\Delta = 2$ we have shown in section 4.1.1, that the propagators in (4.4) can be expressed as a sum of two euclidean propagators. Therefore the bulk-to-bulk part $F^\Delta(X_1,\ldots,X_{L+1})$ (4.1) can always be expressed as a sum over products of flat space propagators.

Let us now discuss the domain of integration, which for (4.1) is the upper-half space $\mathcal{H}_4^+$. In flat momentum space on the other hand, one integrates over the entire space $\mathbb{R}^4$. It is clear from the previous discussion in section 3.3.1 that the propagator is in general not invariant under the antipodal map due to the z^Δ term in the numerator which changes the sign for odd Δ. However, since we focus on the $\lambda\phi^4$ theory, each vertex joins four propagators, meaning that each radial coordinate in the numerator only appears as $z^{4\Delta-4}$, where the -4 is due to the integration measure. For $\Delta \in \mathbb{N}$ this is always an even number and therefore invariant under the antipodal map. We thus conclude that the entire Witten diagram (4.1) is invariant under mapping every bulk point to its antipodal point and the domain of integration can be extended to $\mathbb{R}^4$. Note that this can also be done for the AdS-invariant regularisation method in equation (4.8).

To continue we note that in (4.1) powers of the radial coordinates, z_i appear in the denominator, originating from the AdS-invariant measure as well as in the numerator of the propagators. It is convenient to "covariantize" these contributions by writing them as linear propagators $z = u \cdot X_i$ with the help of the auxiliary unit vector $u = (\vec{0}, 1)$, where the dot product is understood with respect to the euclidean metric. This auxiliary vector is orthogonal to the boundary and is therefore perpendicular to any vector

$X_i = (\vec{x}_i, 0)$ parametrizing points on the boundary. In particular, for $\Delta = 1, 2$ the propagators in (4.4) take a tensorial from

$$\Lambda(\mathbf{X}, \mathbf{Y}; 1) = \left(\frac{a}{2\pi}\right)^2 \left(\frac{u\cdot X\, u\cdot Y}{\|X-Y\|^2} + \frac{u\cdot X\, u\cdot \sigma(Y)}{\|X-\sigma(Y)\|^2}\right),$$
$$\Lambda(\mathbf{X}, \mathbf{Y}; 2) = \left(\frac{a}{2\pi}\right)^2 \left(\frac{u\cdot X\, u\cdot Y}{\|X-Y\|^2} - \frac{u\cdot X\, u\cdot \sigma(Y)}{\|X-\sigma(Y)\|^2}\right). \tag{4.9}$$

We then define the dimensionally regulated Witten diagrams (4.1) by evaluating the integration measure in D dimensions,

$$W_L^{\Delta,D}(\vec{x}_1, \vec{x}_2, \vec{x}_3, \vec{x}_4) = 2^{4\Delta} \frac{(n_\Delta)^{2L+4}}{(2a^D)^{L+1}} \int\limits_{(\mathbb{R}^D)^{L+1}} \prod_{i=1}^{L+1} \frac{\mathrm{d}^D X_i}{(u\cdot X_i)^4} F^\Delta(X_1, \ldots, X_{L+1})$$
$$\times \sum_{\rho\in\mathfrak{S}_4} \frac{\delta(\Gamma_W)}{|\Gamma_W|} f^\Delta(X_{\rho(1)}, \ldots, X_{\rho(4)}; \vec{x}_1, \vec{x}_2, \vec{x}_3, \vec{x}_4), \tag{4.10}$$

where we have pulled out a factor of $(a^{-D})^{L+1}$ and rescaled every point with a such that the only dimensional dependence is in the prefactor. Upon substitution of (4.2) and (4.9) the Witten diagram (4.10) takes the form of standard flat space tensorial integrals with linear propagators.

Let us conclude the discussion of dimensional regularisation with two remarks, considering the choice of the integration measure and the concrete analytic continuation of the dimension.

First of all, note that we have used a dimensional regularisation scheme by changing the dimension of integration without changing the Jacobian from the AdS metric, which breaks the AdS invariance. An AdS preserving integration measure $\prod_{i=1}^{L+1} \frac{\mathrm{d}^D X_i}{(u\cdot X_i)^D}$ in (4.10) will not regulate the integral as a consequence of conformal symmetry.

Secondly let us comment on the concrete analytic continuation. When D approaches 4 the Witten diagrams develop divergences with leading behavior $\frac{1}{(D-4)^L}$ at L-loop order. In order to preserve the conformal symmetry, which is broken by the dimensional regularisation, we need to parametrize $D = 4 - \frac{4\epsilon}{L+1}$ at each loop order. This can be understood from the following scaling argument. Consider a four point function resulting from a bulk calculation up to one loop in the above dimensional regularisation scheme. It will consist of a term of order λ produced by a tree level graph with integration over one bulk point and an order λ^2 contribution which is given by integrating over two bulk points. If we rescale both terms with α the first term will scale with $\alpha^{4\Delta+(D-4)}$ while the second with $\alpha^{4\Delta+2(D-4)}$ due to the second bulk integral. In order for the sum to scale homogeneously and therefore describing a conformal correlation function we have to introduce a loop dependent regularisation scheme as described above.

4.1.3 Conformal mapping of the regularised integrals

We will now use invariance of the diagram under translation of the boundary points and inversion to write the four-point diagram in terms of three-dimensional conformal cross-ratios. First we apply these transformations to the integrand. The non-invariance of the regularised measure will be taken into account in a second step.

To begin with, we shift every boundary point by $\vec{x}_3$ and then invert every point. The latter leaves the bulk-to-bulk propagators invariant while the bulk-to-boundary propagators transform as

$$\frac{z}{\|X-\vec{x}\|^2} = \frac{1}{x^2}\frac{z'}{\|X'-\vec{y}\|^2} \qquad \text{with } X' = \frac{X}{\|X\|^2} \;\text{ and }\; \vec{y} = \frac{\vec{x}}{x^2}\,, \tag{4.11}$$

where we have set $\|\vec{x}\|^2 \equiv x^2$. After these transformations (4.2) becomes

$$f^{\Delta}(X_1,\ldots,X_4;\vec{x}_1,\ldots,\vec{x}_4) = \frac{z_3^{\Delta}}{(x_{13}^2 x_{23}^2 x_{34}^2)^{\Delta}}\left(\frac{z_1}{\|X_1-y_{13}\|^2}\frac{z_2}{\|X_2-y_{23}\|^2}\frac{z_4}{\|X_4-y_{43}\|^2}\right)^{\Delta},$$

where we have set $x_{ij} := \vec{x}_i - \vec{x}_j$ and $y_{ij} := x_{ij}/x_{ij}^2$. To continue we shift every bulk point as $X_i \to X_i + y_{13}$ and use scale invariance to rescale every bulk point by $X_i \to \|y_{43}-y_{13}\|\, X_i$. This gives

$$f^{\Delta}(X_1,\ldots,X_4;\vec{x}_1,\ldots,\vec{x}_4) = \frac{1}{(x_{14}^2 x_{23}^2)^{\Delta}}\left(\frac{z_1 z_2 z_3 z_4}{\|X_1\|^2\left\|X_2-\frac{y_{23}-y_{13}}{\|y_{43}-y_{13}\|}\right\|^2\left\|X_4-\frac{y_{43}-y_{13}}{\|y_{43}-y_{13}\|}\right\|^2}\right)^{\Delta}.$$

Finally, we may use the fact that the AdS group acts on points of the conformal boundary as the conformal group to implement the familiar conformal operations on the boundary points that map $\vec{x}_4$ to infinity, $\vec{x}_3$ to the origin $(0,0,0,0)$ and $\vec{x}_1 \to (-1,0,0,0)$. The remaining point $\vec{x}_2$ can be chosen to lie in the 1-4 plane, parametrized by the complex coordinate ζ, that is

$$\vec{x}_2 = \left(\frac{\zeta+\bar{\zeta}-2}{2(1-\zeta)(1-\bar{\zeta})}, \frac{\zeta-\bar{\zeta}}{2i(1-\zeta)(1-\bar{\zeta})}, 0, 0\right).$$

This takes equation (4.2) to the final form

$$f^{\Delta}(X_1,\ldots,X_4;\vec{x}_1,\ldots,\vec{x}_4) = \frac{v^{\Delta}}{(x_{12}^2 x_{34}^2)^{\Delta}}\left(\frac{z_1 z_2 z_3 z_4}{\|X_1\|^2\,\|X_2-u_\zeta\|^2\,\|X_4-u_1\|^2}\right)^{\Delta}, \tag{4.12}$$

with

$$u_1 = (1,0,0,0), \qquad u_\zeta = \left(\frac{\zeta+\bar{\zeta}}{2}, \frac{\zeta-\bar{\zeta}}{2i}, 0, 0\right), \qquad v = \zeta\bar{\zeta} = \frac{x_{12}^2 x_{34}^2}{x_{14}^2 x_{23}^2}.$$

Let us now turn to the measure. The dimensional regularisation implemented in (4.10) breaks the AdS invariance of the integration measure. We therefore have to take into account the Jacobian of the transformations implemented above. Since the regularised measure is still invariant under shifts in the $z = \text{const}$ hyperplane, the first transformation leaves the latter invariant. The second transformation in (4.11) is an inversion ($X_i \to \frac{X_i}{\|X_i\|^2}$) which induces a Jacobian

$$\prod_{i=1}^{L+1}\frac{\mathrm{d}^D X_i}{(u\cdot X_i)^4} \to \prod_{i=1}^{L+1}\frac{\mathrm{d}^D X_i}{(u\cdot X_i)^4}\frac{1}{\|X_i\|^{2(D-4)}}\,.$$

This is followed by a shift of all bulk points by y_{13}, under which

$$\prod_{i=1}^{L+1} \frac{\mathrm{d}^D X_i}{(u\cdot X_i)^4} \frac{1}{\|X_i\|^{2(D-4)}} \to \prod_{i=1}^{L+1} \frac{\mathrm{d}^D X_i}{(u\cdot X_i)^4} \frac{1}{\|X_i + y_{13}\|^{2(D-4)}} \,.$$

Finally, the rescaling by $\|y_{43}-y_{13}\|$ gives

$$\prod_{i=1}^{L+1} \frac{\mathrm{d}^D X_i}{(u\cdot X_i)^4} \frac{1}{\|X_i + y_{13}\|^{2(D-4)}} \to \prod_{i=1}^{L+1} \frac{\mathrm{d}^D X_i}{(u\cdot X_i)^4} \frac{\|y_{43}-y_{13}\|^{4-D}}{\left\|X_i + \frac{y_{13}}{\|y_{43}-y_{13}\|}\right\|^{2(D-4)}} \,.$$

Rewriting the inverted boundary points in terms of the original coordinates and choosing $\vec{x}_1, \vec{x}_2, \vec{x}_3$ and $\vec{x}_4$ as described above we get

$$\|y_{43}-y_{13}\| = \frac{\|x_{41}\|}{\|x_{43}\|\,\|x_{13}\|} \to 1 \quad \text{and} \quad \frac{y_{13}}{\|y_{43}-y_{13}\|} \to \frac{x_{13}}{\|x_{13}\|^2} = -u_1 \,,$$

and therefore the complete Jacobian is given by

$$\prod_{i=1}^{L+1} \frac{\mathrm{d}^D X_i}{(u\cdot X_i)^4} \frac{1}{\|X_i - u_1\|^{2(D-4)}} \,. \tag{4.13}$$

From (4.12) and (4.13) it is then clear that the Witten diagrams will depend only on ζ and $\bar{\zeta}$ or, equivalently, the conformal cross-ratios introduced in [55, 56]

$$v = \frac{x_{12}^2 x_{34}^2}{x_{14}^2 x_{23}^2} = \zeta\bar{\zeta}; \qquad 1 - Y = \frac{x_{13}^2 x_{24}^2}{x_{14}^2 x_{23}^2} = (1-\zeta)(1-\bar{\zeta})\,. \tag{4.14}$$

To summarize we have the δ-regularised Witten diagram (removing the prefactor $2^{4\Delta}\,(\mathcal{N}_\Delta)^{2L+4}/(a^4)^{L+1}$)

$$\begin{aligned} \mathcal{W}_L^{\Delta,\delta}(\zeta,\bar{\zeta}) := \frac{1}{2^{L+1}} \frac{v^\Delta}{(x_{12}^2 x_{34}^2)^\Delta} \int\limits_{(\mathbb{R}^4)^{L+1}} \prod_{i=1}^{L+1} \frac{\mathrm{d}^4 X_i}{z_i^4} F^{\Delta,\delta}(X_1,\ldots,X_{L+1}) \\ \times \sum_{\rho\in\mathfrak{S}_4} \frac{\delta(\Gamma_W)}{|\Gamma_W|} \left(\frac{z_{\rho(1)}}{\left\|X_{\rho(1)}\right\|^2}\right)^\Delta \left(\frac{z_{\rho(2)}}{\left\|X_{\rho(2)} - u_\zeta\right\|^2}\right)^\Delta z_{\rho(3)}^\Delta \left(\frac{z_{\rho(4)}}{\left\|X_{\rho(4)} - u_1\right\|^2}\right)^\Delta \,, \end{aligned} \tag{4.15}$$

while in dimensional regularisation, taking into account the Jacobian just derived, we have instead

$$\begin{aligned} \mathcal{W}_L^{\Delta,D}(\zeta,\bar{\zeta}) := \frac{1}{2^{L+1}} \frac{v^\Delta}{(x_{12}^2 x_{34}^2)^\Delta} \int\limits_{(\mathbb{R}^D)^{L+1}} \prod_{i=1}^{L+1} \frac{\mathrm{d}^D X_i}{(u\cdot X_i)^4} \frac{F^{\Delta}(X_1,\ldots,X_{L+1})}{\|X_i - u_1\|^{2(D-4)}} \\ \times \sum_{\rho\in\mathfrak{S}_4} \frac{\delta(\Gamma_W)}{|\Gamma_W|} \left(\frac{z_{\rho(1)}}{\left\|X_{\rho(1)}\right\|^2}\right)^\Delta \left(\frac{z_{\rho(2)}}{\left\|X_{\rho(2)} - u_\zeta\right\|^2}\right)^\Delta z_{\rho(3)}^\Delta \left(\frac{z_{\rho(4)}}{\left\|X_{\rho(4)} - u_1\right\|^2}\right)^\Delta \,. \end{aligned} \tag{4.16}$$

4.1.4 Differential operator relations

It is possible to obtain the amplitude for the Witten diagrams with external dimension $\Delta = 2$ from those with $\Delta = 1$ by acting with a suitable differential operator on the external points. This turns out to be rather useful when working with the dimensional regularisation scheme.

We use the unit vector $u = (0,0,0,1)$ perpendicular to the boundary introduced in section 4.1.2 and define the $\tilde{X}_i = (\vec{x}_i, w_i)$ associated to the external legs which, in this section, we take to lie in the bulk. We introduce the operators

$$\begin{aligned} \mathcal{H}_i &:= u^\mu \frac{\partial}{\partial \tilde{X}_i^\mu}\bigg|_{w_i=0}\,, \qquad \mathcal{H}_{ij} := u^\mu u^\nu \frac{\partial}{\partial \tilde{X}_i^\mu}\frac{\partial}{\partial \tilde{X}_j^\nu}\bigg|_{w_i=w_j=0}\,, \\ \mathcal{H}_{ijkl} &:= u^{\mu_1}u^{\mu_2}u^{\mu_3}u^{\mu_4}\frac{\partial}{\partial \tilde{X}_i^{\mu_1}}\frac{\partial}{\partial \tilde{X}_j^{\mu_2}}\frac{\partial}{\partial \tilde{X}_k^{\mu_3}}\frac{\partial}{\partial \tilde{X}_l^{\mu_4}}\bigg|_{w_i=w_j=w_k=w_l=0}\,. \end{aligned} \tag{4.17}$$

In order to define the action of these operators on Witten diagrams we move the external legs into the bulk, while keeping the form of the bulk-to-boundary propagator. We consider the generalisation of (4.2)

$$f^\Delta(X_1,\ldots,X_4;\tilde{X}_1,\ldots,\tilde{X}_4) = \prod_{i=1}^4 \left(\frac{u\cdot X_i}{\left\|X_i-\tilde{X}_i\right\|^2}\right)^\Delta\,, \tag{4.18}$$

which is not a proper product of bulk-to-bulk propagators, but should rather be understood as some generating function for bulk-to-boundary propagators obtained by moving the boundary points to a finite value of the radial coordinate. It is straightforward to check that the action of the differential operators (4.17) on the redefined bulk-to-boundary propagator (4.18) gives

$$\mathcal{H}_{1234}f^\Delta(X_1,\ldots,X_4;\tilde{X}_1,\ldots,\tilde{X}_4) = \prod_{i=1}^4 \mathcal{H}_i\left(\frac{u\cdot X_i}{\left\|X_i-\tilde{X}_i\right\|^2}\right)^\Delta\,,$$

so that

$$\begin{aligned} \mathcal{H}_{1234}f^\Delta(X_1,\ldots,X_4;\tilde{X}_1,\ldots,\tilde{X}_4) &= (2\Delta)^4\prod_{i=1}^4\left(\frac{u\cdot X_i}{\|X_i-\vec{x}_i\|^2}\right)^{\Delta+1}\,, \\ &= (2\Delta)^4 f^{\Delta+1}(X_1,\ldots,X_4;\vec{x}_1,\ldots,\vec{x}_4)\,. \end{aligned}$$

In the preceding section we have shown that the four-point Witten diagrams with external points on the conformal boundary depend only on the cross-ratios (4.14). If the external points are moved into the bulk, as above, we have to reconsider the transformations leading to this, more precisely, (4.12) and (4.13). Repeating the arguments in section 4.1.3 one can show that the integrals with external points in the bulk again depend only on the cross-ratios v and Y now expressed as

$$v = \frac{\left\|\tilde{X}_{12}\right\|^2\left\|\tilde{X}_{34}\right\|^2}{\left\|\tilde{X}_{14}\right\|^2\left\|\tilde{X}_{23}\right\|^2}\,; \qquad 1-Y = \frac{\left\|\tilde{X}_{13}\right\|^2\left\|\tilde{X}_{24}\right\|^2}{\left\|\tilde{X}_{14}\right\|^2\left\|\tilde{X}_{23}\right\|^2}\,.$$

Some of the operators in (4.17) have simple expressions in terms of the conformal cross-ratios. In particular,

$$
\begin{aligned}
x_{12}^2\mathcal{H}_{12} =& x_{34}^2\mathcal{H}_{34} = -2v\frac{\partial}{\partial v}\,, \\
x_{13}^2\mathcal{H}_{13} =& x_{24}^2\mathcal{H}_{24} = 2\,(1-Y)\,\partial_Y\,, \\
x_{14}^2\mathcal{H}_{14} =& x_{23}^2\mathcal{H}_{23} = 2v\partial_v - 2(1-Y)\partial_Y\,,
\end{aligned}
$$

and

$$
\begin{aligned}
(x_{12}x_{34})^2\mathcal{H}_{1234} =& 4v\left(v(1+v)\frac{\partial^2}{\partial v^2} + (1-Y)(2-Y)\frac{\partial^2}{\partial Y^2} - 2v(1-Y)\frac{\partial^2}{\partial v\partial Y}\right. \\
&\left. + (1+v)\frac{\partial}{\partial v} - (2-Y)\frac{\partial}{\partial Y}\right)\,.
\end{aligned}
\tag{4.19}
$$

We will use the differential operators $\mathcal{H}_{14}$ and $\mathcal{H}_{12}$ to obtain the finite part for $\Delta = 2$ at one-loop in (5.14) from the simpler auxiliary integral (5.12).

Acting with $\mathcal{H}_{1234}$ as in (4.17) on f^Δ gives

$$
\begin{aligned}
&\mathcal{H}_{1234}f^\Delta(X_1,\dots,X_4;\tilde{X}_1,\dots,\tilde{X}_4) = \frac{1}{(x_{12}^2x_{34}^2)^{\Delta+1}} \\
&\times\Big[4\Delta^2 + 2\Delta x_{12}^2\mathcal{H}_{12} + 2\Delta x_{34}^2\mathcal{H}_{34} + (x_{12}^2x_{34}^2)\mathcal{H}_{1234}\Big]\left(\frac{v\,u\cdot X_1\cdots u\cdot X_4}{\|X_1\|^2\,\|X_2-u_\zeta\|^2\,\|X_4-u_1\|^2}\right)^\Delta\,,
\end{aligned}
$$

Plugging in equations (4.19) we obtain

$$
\begin{aligned}
\mathcal{H}_{1234}f^\Delta =& \frac{4}{(x_{12}^2x_{34}^2)^{\Delta+1}}\Big[v\Big(v(1+v)\partial_v^2 + (1-Y)(2-Y)\partial_Y^2 - 2v(1-Y)\partial_v\partial_Y \\
&+ (1+v-2\Delta)\partial_v - (2-Y)\partial_Y\Big) + \Delta^2\Big]\left(\frac{v\,u\cdot X_1\cdots u\cdot X_4}{\|X_1\|^2\,\|X_2-u_\zeta\|^2\,\|X_4-u_1\|^2}\right)^\Delta\,.
\end{aligned}
$$

We will apply this differential operator for evaluating the diverging part for $\Delta = 2$ at one-loop in (5.15) from the $\Delta = 1$ result as we will describe in section 5.2.1.

4.1.5 Feynman integral form of Witten diagrams

Let us summarize the results from the previous sections and write the boundary four point function in EAdS as a superposition of flat space Feynman integrals. In section 4.1.1 we found that the propagator of a conformally coupled scalar field can always be expressed in terms of a conformal flat space propagator, which has the form of a momentum space Feynman propagator with an additional linear propagator term in the numerator. In sections 4.1.2 and 4.1.3 we used conformal symmetry and dimensional regularisation to rewrite the bulk to boundary part as the external legs of flat space three point functions. Since the domain of integration can be extended from the upper half plane to $\mathbb{R}^D$ and the Jacobian can be expressed as the linear propagator $u\cdot X$, we found that the four point function of a conformally coupled scalar field at loop order

L is a sum of terms of the form

$$I(\underline{n},\underline{m},D)=\int\prod_{i=1}^{L+1}\frac{\mathrm{d}^D X_i}{(u\cdot X_i)^{n_i}}\prod_{1\le k<j\le L+1}\frac{1}{\|X_k-X_j\|^{2n_{kj}}}$$
$$\times\frac{1}{(\|X_{a_1}\|^2)^{m_1}(\|X_{a_2}-u_1\|^2)^{m_2+2(D-4)}(\|X_{a_3}-u_\zeta\|^2)^{m_3}} \tag{4.20}$$

where $n_{kj}\in\mathbb{Z}$ are integers, n_i, m_1, m_2 and m_3 are powers depending on the conformal dimensions Δ.

These kinds of integrals have been studied for a long time and there are plenty of methods in attempting to solve them (see [101] for a recent review). The method we will apply in this work is the Feynman parametrisation (see e.g. [136]). Using the fact that for $A>0$

$$\frac{1}{A^n}=\frac{1}{\Gamma(n)}\int_0^\infty \mathrm{d}\alpha\,\mathrm{e}^{-\alpha A}\alpha^{n-1}\,,$$

and Gaussian integration we can write an integral of the form of equation (4.20) in the form

$$I=\frac{\Gamma\left(\nu-\frac{(L+1)D}{2}\right)}{\prod_{j=1}^N\Gamma(\nu_j)}\int_{(\mathbb{RP}^+)^{N-1}}\mathrm{d}^N\alpha\prod_{i=1}^N\alpha_i^{\nu_i}\frac{(U(\alpha))^{\nu-\frac{(L+2)D}{2}}}{(F(\alpha))^{\nu-\frac{(L+1)D}{2}}}\,,$$

where ν is the sum of the exponents of all propagators ν_j, α_i are the Feynman parameters and $U(\alpha)$ and $F(\alpha)$ are the Symanzik polynomials. This is a projective integral over the non-negative real projective space

$$(\mathbb{RP}^+)^N:=\left\{[\alpha_1:\ldots:\alpha_{N+1}]\in\mathbb{RP}^N:\alpha_i\ge 0\right\}\,.$$

The Symanzik polynomials are homogeneous polynomials in the Feynman parameters and contain the information about the kinematics and topology of the diagram. $U(\alpha)$ is of degree $L+1$, while $F(\alpha)$ is of degree $L+2$.

Solving these integrals in general is very complicated and there have been many methods developed to tackle them [101, 134]. We will use direct integration in the Feynman parameters. To regularise the integrals in parameter space we use an analytic regularisation procedure described in [102] and implemented in `HyperInt` [137]. We will discover that most of the regularised integrals we encounter fall in the class of linearly reducible integrals [102] and can therefore be expressed in terms of multiple polylogarithms which we will discuss in section 4.3.

Different values of Δ

So far we have only considered conformally coupled, massless fields where the propagator simplifies to equation (4.3). For general Δ the method of direct integration of Feynman parameters is not very straightforward due to the complicated structure of the hypergeometric function, appearing in the propagator in equation (3.43). For integer values of Δ there is, however, hope. We have for $\Delta=2n+1\ge 3$

$$\Lambda(\mathbf{X},\mathbf{Y};2n+1)=\Lambda(\mathbf{X},\mathbf{Y};1)+\left(\frac{a}{2\pi}\right)^2\frac{1}{K(\mathbf{X},\mathbf{Y})}P_1^{(n-2)}\left(\frac{1}{K(\mathbf{X},\mathbf{Y})^2}\right)$$
$$+\left(\frac{a}{2\pi}\right)^2 Q_1^{(n-1)}\left(\frac{1}{K(\mathbf{X},\mathbf{Y})^2}\right)\log\left(\frac{-G(X,\sigma(Y))}{G(X,Y)}\right),$$

and for $\Delta = 2n \geq 4$

$$\Lambda(\mathbf{X},\mathbf{Y};2n) = \Lambda(\mathbf{X},\mathbf{Y};2) + \left(\frac{a}{2\pi}\right)^2 P_2^{(n-2)}\left(\frac{1}{K(\mathbf{X},\mathbf{Y})^2}\right) + \\ + \left(\frac{a}{2\pi}\right)^2 \frac{1}{K(\mathbf{X},\mathbf{Y})} Q_2^{(n-2)}\left(\frac{1}{K(\mathbf{X},\mathbf{Y})^2}\right) \log\left(\frac{-G(X,\sigma(Y))}{G(X,Y)}\right),$$

where $P_i^{(r)}(x)$ and $Q_i^{(r)}(x)$ are polynomial of degree r in x. Using the relation in (4.7) these propagators can be written as a combination of the conformal flat space propagators $G(X,Y)$ and $G(X,\sigma(Y))$.

The short distance singularities for coincident bulk points or antipodal points is the same as for $\Delta = 1, 2$ but the general structure differs due to the presence of logarithms of the conformal flat space propagator. Using that $x^\eta = 1 + \eta\log(x) + O(\eta^2)$ we can consider the η-deformed propagators by making the replacement

$$\log\left(\frac{-G(X,\sigma(Y))}{G(X,Y)}\right) \to \left(\frac{-G(X,\sigma(Y))}{G(X,Y)}\right)^\eta,$$

in the above expressions for $\Lambda(\mathbf{X},\mathbf{Y};2n+1)$ and $\Lambda(\mathbf{X},\mathbf{Y};2n)$.

In this representation we end up with expressions for the Witten diagrams in terms of flat space like QFT Feynman integrals with generalized powers of the propagators

$$G(X,Y)^\eta = \left(\frac{zw}{\|X-Y\|^2}\right)^\eta, \qquad G(X,\sigma(Y))^\eta = \left(\frac{-zw}{\|X-\sigma(Y)\|^2}\right)^\eta,$$

which can be treated, using familiar analytic regularisation methods [134]. The parameter η will introduce some generalized powers of the propagators in addition to the one generated by the breaking of the conformal invariance due to the dimensional regularisation, as shown in section 4.1.3. We could therefore in principle treat those cases as well by generalizing equation (4.20) to

$$I(\underline{n},\underline{m},\underline{\eta},D) = \int \prod_{i=1}^{L} \frac{\mathrm{d}^D X_i}{(u\cdot X_i)^{n_i}} \prod_{1\leq k<j\leq L} \frac{1}{\|X_k - X_j\|^{2n_{kj}+\eta_{k,j}}} \\ \times \frac{1}{(\|X_{a_1}\|^2)^{m_1}(\|X_{a_2}-u_1\|^2)^{m_2+2(D-4)}(\|X_{a_3}-u_\zeta\|^2)^{m_3}}$$

where η_{kj} are analytic parameters. The value of the Witten diagram is the multi-linear contribution $\prod_{k,j}\partial_{\eta_{k,j}} I(\underline{n},\underline{m},\underline{\eta},D)|_{\eta_{k,j}=0}$ in the analytic parameters $\eta_{k,j}$. These integrals can in principle be reduced to master integrals using well established methods from flat space calculations, like tensor reduction and integration by parts relations [138–141]. Due to technical limitations we will leave the actual evaluation of these integrals for future work.

4.2 Unitarity methods

4.2.1 Cutting rules for flat space Feynman integrals

In this section we would like to take a closer look at the Witten diagrams in the form of a flat space Feynman integral, as written in equation (4.20). It is tempting to interpret this integral as a flat space three point function with external "momenta" $k_1 = u_1 - u_\zeta$, $k_2 = u_\zeta$, $k_3 = -u_1$. Integrating over a bulk vertex would correspond to integrating over a loop momentum. The calculation of an L loop Witten diagram in EAdS therefore is of the same complexity as an $L+1$ loop diagram in flat momentum space (see figure 4.1). We will therefore use this interpretation to apply various flat space methods to

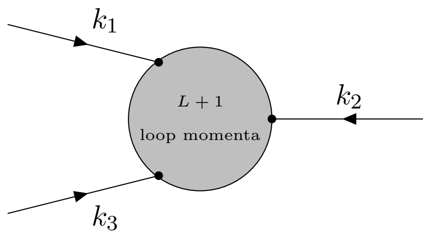

Figure 4.1: L loop Witten four point diagram represented as an $L+1$ loop three point Feynman diagram with external momenta $k_1 = u_1 - u_\zeta$, $k_2 = u_\zeta$ and $k_3 = -u_1$.

solve these integrals. Let us first review aspects of the analytic structure of Feynman integrals, which allows us to calculate discontinuities of the diagram as we describe in 5.4. See [142] for very good historical review and [101, 143] for modern references.

Consider a function $f(z)$ in the complex plane. The discontinuity of the function is defined as

$$\mathrm{Disc} f(z \pm i0) := \lim_{\varepsilon \to 0} f(z + i\varepsilon) - f(z - i\varepsilon) \tag{4.21}$$

If the discontinuity is non-vanishing it means that z is on a branch cut of the function, starting at some branch point z_0. If $f(z)$ can be expressed as an integral

$$f(z) := \int\limits_{\gamma[a,b]} h(z,w)\mathrm{d}w \tag{4.22}$$

of some analytic function $h(z,w)$ along a path $\gamma[a,b]$ from points a to b, the branch point z_0 is usually associated to a singularity of the integral. As a simple example, let us consider the logarithm $\log(z)$. On the principal sheet, it has a discontinuity across the branch cut going from $z \in (-\infty, 0]$ given by

$$\mathrm{Disc} \log(z \pm i0) = 2\pi i \theta(-z)$$

The logarithm can be defined as an integral along some path $\gamma[1,z]$

$$\log(z) = \int\limits_{\gamma[1,z]} \frac{\mathrm{d}w}{w}$$

The integral is clearly singular for $z = 0$, due to the singularity at $w = 0$ in the integrand. This is an example for an endpoint singularity. If $z < 0$ we have two possibilities of deforming the integration contour to avoid the singularity. One is going above and the other going below, which we denote by γ_+ and γ_- respectively. The discontinuity can now be defined as the difference between these two paths

$$\int_{\gamma_+[1,z]} \frac{\mathrm{d}w}{w} - \int_{\gamma_-[1,z]} \frac{\mathrm{d}w}{w} = \oint\limits_0 \frac{\mathrm{d}w}{w} = 2\pi i \,. \tag{4.23}$$

An integral like (4.23) is called the monodromy of the logarithm around the origin. The two definitions for the discontinuity (4.21) and (4.23) are equivalent if we identify

$$\log(z+i\varepsilon)=\int_{\gamma_+[1,z]}\frac{\mathrm{d}w}{w},\qquad \log(z-i\varepsilon)=\int_{\gamma_-[1,z]}\frac{\mathrm{d}w}{w}$$

In general a function like (4.22) will have singularities if the singularities $w_s(z)$ of the integrand $h(z,w)$ cannot be avoided by continuously deforming the integration contour. This happens in two cases [142]:

(i) Endpoint singularities occur if for some point z_0 the singularity of the integrand $w_s(z_0)$ coincides with one of the endpoints. Obviously there is no deformation of the contour that would avoid that. This is what happens in the case of the logarithm above.

(ii) Pinch singularities appear if at least two singularities approach the integration contour from opposite sides, therefore "trapping" the contour in the middle such that it cannot be deformed anymore. See figure 4.2

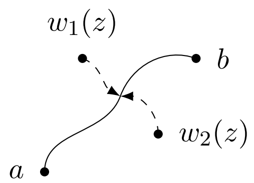

Figure 4.2: Integration contour from a to b pinched between two singularities $w_1(z)$ and $w_2(z)$ such that the singularities cannot be avoided by a deformation of the contour.

This analysis can be generalized to functions that involve several variables of integration

$$F(z)=\int_\Gamma\prod_{i=1}^n \mathrm{d}w_i H(z,w_i)\,,$$

where the integration is now performed over a multi-dimensional hyperplane Γ. The singularities in the integrand are given by equations

$$W_s(z,w_i)=0,$$

defining a $(2n-2)$-dimensional hypersurface. To find the singularities of the function $F(z)$ we follow the same reasoning as for the one dimensional case. A singularity in $F(z)$ occurs if the integration region Γ intersects with at least one singularity surface $W_s(z,w_i)$ and this intersection cannot be avoided by a continuous deformation of Γ. In principle this can happen for the same reasons as in the one-dimensional case. Either the integration region is trapped between one or more singularity surfaces or the singularity coincides with the "end point", now also described by a set analytic equations $\tilde{W}_r(z,w)=0$. The condition for a singularity of $F(z)$ can then be summarized by the following equations first found by Landau [144]:

$$\alpha_i W_i=0\ \ \forall i,\qquad \tilde{\alpha}_r\tilde{W}_r=0\ \ \forall r,\quad \frac{\partial}{\partial w_j}\left(\sum_i\alpha_i W_i+\sum_r\tilde{\alpha}_r\tilde{W}_r\right)=0\ \ \forall j. \qquad (4.24)$$

The proof of these equations goes beyond the scope of this thesis but can be found in [142, 144]. To give an intuitive explanation of (4.24) consider the following.

If a singularity surface W_1 approaches Γ we can deform Γ away in the normal direction of W_1 unless a second singularity surface W_2 approaches from the other side with the same normal direction. Γ is therefore trapped between the surfaces and the conditions for this situation are

$$W_1 = W_2 = 0, \qquad \alpha_1 \frac{\partial W_1}{\partial w_i} + \alpha \frac{\partial W_2}{\partial w_i} = 0\,.$$

Obviously this argument holds with more singularity surfaces approaching as long as there is a linear relation between the directions of their normals. Finally, since $\tilde{W}_r$ are the boundary surfaces, their normal vectors indicate the directions in which Γ cannot be deformed and therefore play a similar role in trapping Γ as the singularity surfaces W_s.

Let us now consider a general Feynman integral where for simplicity we consider the exponents of the propagators to be 1

$$A = \int \frac{\prod_{n=1}^{L} \mathrm{d}^D p_n}{\prod_{i=1}^{m} (q_i^2 - m_i^2)}\,,$$

where q_i are linear combinations of external momenta k_j and internal momenta p_n and the masses m_i can be vanishing.

Since the boundaries of the integration lie at infinity we do not have a boundary surface $\tilde{W}_r$. Then the singularities in the integrand occur when $W_i = q_i^2 - m_i^2 = 0$. Plugging this into the Landau equations (4.24) we find the conditions

$$\alpha_i (q_i^2 - m_i^2) = 0, \qquad \frac{\partial}{\partial p_j} \sum_i \alpha_i (q_i^2 - m_i^2) = 0$$

It was shown by Cutkosky in [145] that the discontinuity of the Feynman integral, given by a branch cut starting on a singularity surface W_J associated with the propagators $(q_j^2 - m_j^2)$ with $j \in J$ going on shell, is given by

$$\mathrm{Disc}_{W_J} I = \int \prod_{n=1}^{L} \mathrm{d}^D p_n \left(\prod_{j \in J} (-2\pi i) \delta(q_j^2 - m_j^2) \theta(q_j^0) \right) \prod_{i \notin J} \frac{1}{q_i^2 - m_i^2}\,. \tag{4.25}$$

In flat momentum space these singularity surfaces usually correspond to a threshold in some Mandelstam invariant, reach some value such that some real particles can be produced and the scattering amplitude develops an imaginary part.

A purely algebraic derivation based on Feynman graphs and the largest time equation was done by t'Hooft and Veltmann in [146]. They introduce the concept of a cut denoted by $\mathrm{Cut}_i A$ which means drawing lines through a diagram such that it is separated into two diagrams, where not all vertices are allowed to lie on either side of the line. The propagators which are crossed by the line are then put on-shell, by replacing them by $-2\pi i \delta(q_i^2 - m_i^2)$, while the other propagators switch the sign of the $i\varepsilon \to -i\varepsilon$ from one side of the cut to the other. In [146] it was shown that the imaginary part of the diagram A is then given by

$$A - A^* = - \sum_{\text{all cuts}} \mathrm{Cut}_i A\,. \tag{4.26}$$

The connection to the method of calculating a discontinuity by Landau and Cutkosky can drawn in the following way. If we single out a specific momentum channel P^2 of the Feynman diagram to lie on its branch cut $P^2 > 0$ and all other Mandelstam invariants are negative, the left hand side of (4.26) collapses to a single term and we get the equation for the discontinuity in across the branch cut in P^2 as

$$\mathrm{Disc}_{P^2} A = -\mathrm{Cut}_{P^2} A \,. \tag{4.27}$$

This means that the discontinuity is given by the cut that interrupts the flow of P^2 across the diagram. This region can be identified with a singularity surface in the notion of the Landau equations, making the connection between (4.25) and (4.27).

For later use let us also introduce the concepts of sequential discontinuities and cuts. A sequential discontinuity is defined as the discontinuity of a discontinuity, meaning we interpret $\mathrm{Disc}_z f$ as a an analytic function defined by the monodromy around a branch point and take the discontinuity. This concept generalizes straightforwardly to functions with multiple variables and, following the convention in [147], we define the sequential discontinuity operator recursively as

$$\mathrm{Disc}_{z_1,\ldots,z_k} f = \mathrm{Disc}_{z_k} \left(\mathrm{Disc}_{z_1,\ldots,z_{k-1}} f \right) \,. \tag{4.28}$$

In the same way we can perform sequential cuts of a diagram, by moving another Mandelstam variable on the branch cut of the already cut diagram. The sequential cut operator can be defined recursively equivalently to (4.28).The generalized relation between sequential cuts and discontinuities is then given by

$$\mathrm{Cut}_{z_1,\ldots,z_k} A = (-1)^k \mathrm{Disc}_{z_1,\ldots,z_k} A$$

So far we only considered simple poles in the integrand of the Feynman integral, by setting the exponent of the propagators to 1. In general this is not the case and therefore to cut a propagator with a different exponent we have to generalize our definition of a cut. The derivation of (4.25) is based on the residue theorem so the cut of a propagator with higher power should be given by the residue of a higher order pole, meaning the we replace the δ function in (4.25) by $\partial^{n-1}_{m_i^2} \delta(q_i^2 - m_i^2)$, where n is the exponent of the propagator.

As a final note, let us return to the actual Witten diagrams. For flat space Feynman integrals the physical interpretation of the branch cuts is that certain particles are able to become real so that their virtual propagators go on-shell. For the Witten diagrams this interpretation is not so straightforward. We merely use the structure of the integral and its similarity to Feynman integrals. The cutting rules were merely a technical tool. We will further discuss this in section 5.4.

4.2.2 Cutting Witten diagrams directly

A different approach at using analytic properties of the conformal four point functions has been developed in [148] and related to cutting rules of a Witten diagram in [48,49]. The advantage of this method is, that the results are presented in terms of conformal blocks right away. However, the cutting rules only allow one to calculate the double discontinuity of the Witten diagram, which for our purpose only gives us access to a consistency check between tree-level and one-loop calculations as we will discuss in section 5.5. Nevertheless we would like to briefly review that method and compare the results obtained that way to our method in chapter 5.

Recalling the general formula (2.5) for the four point function of a CFT, expressed in terms of ζ and $\bar{\zeta}$, we can write down the double discontinuity in the s-channel, introduced in [148], of $G(\zeta,\bar{\zeta})$ as

$$\mathrm{dDisc}_s G(\zeta,\bar{\zeta}) = \cos(\alpha) G(\zeta,\bar{\zeta}) - \frac{1}{2}\left(\mathrm{e}^{i\alpha} G(\zeta + i\varepsilon,\bar{\zeta}) + \mathrm{e}^{-i\alpha} G(\zeta - i\varepsilon,\bar{\zeta})\right)$$

with $\alpha = \frac{\pi}{2}(\Delta_3 + \Delta_4 - \Delta_1 - \Delta_2)$. Plugged into the conformal block expansion of equation (2.7) we obtain the following formula

$$\mathrm{dDisc}_s G(\zeta,\bar{\zeta}) = 2\sum_{\Delta,\ell} \sin\left(\frac{\pi}{2}(\Delta - \Delta_1 - \Delta_2)\right) \sin\left(\frac{\pi}{2}(\Delta - \Delta_3 - \Delta_4)\right) a^{12}_{\mathcal{O}_\Delta} a^{34}_{\mathcal{O}_\Delta} \mathcal{G}_{\Delta,\ell}(v,Y)\,,$$

where $\mathrm{dDisc} f$ is given in terms of the sequential discontinuities defined in the previous section as $(2\pi i)^{-2}\mathrm{Disc}(\mathrm{Disc} f)$ in the same variable.

This immediately tells us that if only double trace operators of a generalized free field with dimension $\Delta_i + \Delta_j + 2n + \ell$ are exchanged, there is no double discontinuity. It only exists if these operators have anomalous dimensions.

The double discontinuity of the four point function can now be directly related to the calculation in the bulk by introducing the concept of a "cut" of the Witten diagrams. This is possible due to the split representation of the bulk to bulk propagator (3.43), given by the following integral [149]

$$\Lambda(X_1, X_2, \Delta) = \int_{-\infty}^{+\infty} \mathrm{d}\nu P(\nu,\Delta) \int_{\partial AdS} \mathrm{d}^d\vec{x}\,\bar{\Lambda}\left(\vec{x}, X_1, \frac{d}{2} + \nu\right) \bar{\Lambda}\left(\vec{x}, X_2, \frac{d}{2} - \nu\right)\,, \quad (4.29)$$

where the spectral function $P(\nu,\Delta)$ is given by

$$P(\nu,\Delta) = \frac{i}{\nu^2 - (\Delta - \frac{d}{2})}\frac{\nu^2}{\pi}\,,$$

which has poles at $\nu_\pm = \pm(\Delta - \frac{d}{2})$. In any loop integral we can now replace the bulk to bulk propagators by the split representation of equation (4.29) as depicted in figure 4.3 for the one-loop diagram.

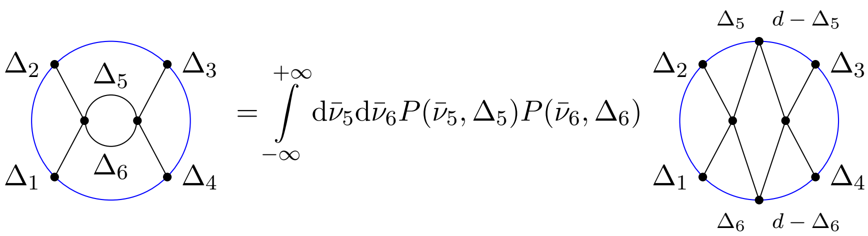

Figure 4.3: One-loop Witten diagram as an integral over the cut diagram

A cut is then defined in the same spirit as for the flat space Feynman integrals by dropping the integral over ν and replacing the spectral function $P(\nu,\Delta)$ by the residue times $2\pi i$ at the pole $\nu = -(\Delta - \frac{d}{2})$, given by

$$2\pi i \mathrm{Res}_{\nu = -(\Delta - \frac{d}{2})} 2P(\nu,\Delta) = 2\Delta - d\,.$$

As depicted in figure 4.3 this corresponds to replacing a bulk to bulk propagator by two bulk to boundary propagators with external dimensions Δ and $d-\Delta$. This method has been applied in [49] in the spectral representation of Witten diagrams [48] given by

$$\langle \mathcal{O}_{\Delta_1}(\vec{x}_1)\mathcal{O}_{\Delta_2}(\vec{x}_2)\mathcal{O}_{\Delta_3}(\vec{x}_3)\mathcal{O}_{\Delta_4}(\vec{x}_4)\rangle = \sum_{\ell=0}^{\infty}\int_{\frac{d}{2}-i\infty}^{\frac{d}{2}+i\infty}\frac{\mathrm{d}\Delta}{2\pi i}\rho_{\Delta_1\Delta_2\Delta_3\Delta_4}(\Delta,\ell)\mathcal{G}_{\Delta,\ell}(\vec{x}_i)\,, \tag{4.30}$$

where $\rho_{\Delta_1\Delta_2\Delta_3\Delta_4}(\Delta,\ell)$ is the spectral function which has poles in Δ and ℓ at the positions of operators appearing in the OPE, such that the integral collapses to the sum of equation (2.7). The spectral function can be calculated from the split representation for the propagator and the coefficients of the three point functions $\langle\mathcal{O}_{\Delta_1}\mathcal{O}_{\Delta_2}\mathcal{O}_{\Delta,\ell}\rangle$ by integrating over bulk to boundary propagators. By performing a cut as depicted in figure 4.3 the Witten diagram is reduced to the product of two tree-level four point functions. This is especially obvious in the spectral representation where the one-loop spectral function is given by

$$\rho^{1-\mathrm{loop}}_{\Delta_1\Delta_2\Delta_3\Delta_4} \sim \int \mathrm{d}\nu_5\nu_6 P(\bar{\nu}_5,\Delta_5)P(\bar{\nu}_6,\Delta_6)\rho^{\mathrm{tree}}_{\Delta_1,\Delta_2,\bar{\Delta}_5,\bar{\Delta}_6}\rho^{\mathrm{tree}}_{d-\bar{\Delta}_5,d-\bar{\Delta}_6,\Delta_3,\Delta_4}\,, \tag{4.31}$$

where $\bar{\Delta}_{5/6}=\frac{d}{2}+\bar{\nu}_{5/6}$ denotes the “off-shell” scaling dimension. Cutting a one-loop diagram means in practice that we evaluate the integrand of equation (4.31) at the on-shell dimension Δ_5 and Δ_6 and equation (4.30) then tells us that the location of the poles of the cut four point function will be the same as for the tree level diagram. This is just a different formulation of the consistency relation between the tree-level and one-loop calculation discussed in section 5.5.

If we denote the cut by Cut_{56}, it was shown in [49] that the cut of the diagram is related to the double discontinuity by

$$\begin{aligned}\mathrm{dDisc}_s(W_1^{\Delta_1,\Delta_2,\Delta_3,\Delta_4,D}) = 2\sin&\left(\frac{\pi}{2}(\Delta_5+\Delta_6-\Delta_1-\Delta_2)\right)\\ &\sin\left(\frac{\pi}{2}(\Delta_5+\Delta_6-\Delta_3-\Delta_4)\right)\mathrm{Cut}_{56}(W_1^{\Delta_1,\Delta_2,\Delta_3,\Delta_4,D})\,,\end{aligned}$$

therefore making a connection between the analytic structure and unitarity similarly to the cutting rules in flat space.

The advantage of this formulation is that the four point functions are expressed in terms of conformal blocks right away and the theory is naturally formulated for arbitrary Δ. However, as we saw, we only have access to the double discontinuity, which can only provide us with a consistency check between first and second order calculations, while for new data from the second order contribution we would need the single discontinuity. We will therefore not use the above described method in this work any further and merely leave this brief discussion for completeness.

4.3 Multiple Polylogarithms

In this section we will briefly review the method of expressing certain classes of Feynman integrals in terms of multiple polylogarithms as it was developed and implemented in the `HyperInt` package (see [137]). For further information we refer to [103, 150–152].

A multiple polylogarithm is defined recursively as the iterated integral

$$G(\sigma_1, ..., \sigma_n; z) := \int_0^z \frac{\mathrm{d}z_1}{z_1 - \sigma_1} G(\sigma_2, ..., \sigma_n; z_1)\,. \tag{4.32}$$

If $\sigma_n \neq 0$ this is equivalent to the definition

$$G(\sigma_1, ..., \sigma_n; z) := \int_0^z \frac{\mathrm{d}z_1}{z_1 - \sigma_1} \int_0^{z_1} \frac{\mathrm{d}z_2}{z_2 - \sigma_2} ... \int_0^{z_{n-1}} \frac{\mathrm{d}z_n}{z_n - \sigma_n}\,, \tag{4.33}$$

where the number n is called the weight of the multiple polylogarithm. In this case we have the additional useful property

$$G(\sigma_1, ..., \sigma_n; z) = G(\lambda\sigma_1, ..., \lambda\sigma_n; \lambda z) \qquad \forall \lambda \in \mathbb{C} \setminus \{0\}\,. \tag{4.34}$$

Upon total differentiation with respect to all arguments they obey the relation

$$\mathrm{d}G(\sigma_1, ..., \sigma_n; z) = \sum_{i=1}^{n} G(\sigma_1, ..., \hat{\sigma}_i, ..., \sigma_n)(\mathrm{d}\log(\sigma_{i-1} - \sigma_i) - \mathrm{d}\log(\sigma_{i+1} - \sigma_i))\,, \tag{4.35}$$

which can by straightforwardly derived from equation (4.33) through integration by parts. The hat means that the corresponding variable is omitted and we set $\sigma_0 = z$ and $\sigma_{n+1} = 0$.

Multiple polylogarithms have an equivalent representation as a nested sum given by

$$\mathrm{Li}_{s_1,...,s_k}(x_1, \ldots, x_k) := \sum_{0<p_1<\cdots<p_k}^{\infty} \frac{x_1^{p_1}}{p_1^{s_1}} \cdots \frac{x_k^{p_k}}{p_k^{s_k}} \quad \text{for } |x_1 \cdots x_i| < 1, \quad \forall i \in \{1, .., k\}\,. \tag{4.36}$$

where $\mathrm{Li}_{s_1,...,s_n}(x_1, \ldots, x_n)$ and $G(\sigma_1, ..., \sigma_n; z)$ are related by the following formula

$$(-1)^n \mathrm{Li}_{s_1,...,s_n}(x_1, \ldots, x_n) = G(\underbrace{0, ..., 0}_{s_n-1 \text{ times}}, \sigma_n, ..., \sigma_2, \underbrace{0, ..., 0}_{s_1-1 \text{ times}}, \sigma_1)(z)\,,$$

with $x_i = \frac{\sigma_{i+1}}{\sigma_i}$, with $x_n = \frac{z}{\sigma_n}$. The multiple polylogarithm $\mathrm{Li}_{s_1,...,s_n}(x_1, \ldots, x_n)$ therefore has weight $s_1 + ... + s_n$.

Some familiar expressions can be directly expressed as special cases of multiple polylogarithms. The ordinary logarithm and classical polylogarithm are for example given by

$$\log(x) = G(0; x); \qquad \mathrm{Li}_n(x) = -G(\underbrace{0, ..., 0}_{n-1 \text{ times}}, 1; x)\,.$$

They obey a shuffle algebra, which allows us to express two multiple polylogarithms of weight n and m as the superposition of multiple polylogarithms of weight $n + m$. This works the following. Consider two multiple polylogarithms $G(\sigma_1, ..., \sigma_n, z)$ and $G(\sigma_{n+1}, ..., \sigma_{n+m}, z)$. Their product is then given by

$$G(\sigma_1, ..., \sigma_n; z) \cdot G(\sigma_{n+1}, ..., \sigma_{n+m}; z) = \sum_{\pi \in \Omega(n,m)} G(\sigma_{\pi(1)}, ..., \sigma_{\pi(n+m)}; z)\,,$$

where $\Omega(N, M)$ is the set of all permutations of the elements of the index sets N and M, that leaves the relative order in N and M invariant.

The representation of equation (4.36) is especially useful for us to expand the results of our Witten diagrams. The strategy is now to bring a Witten diagram in its Feynman parametric representation into the form of a nested integral as given in equation (4.32). The integrand of the next integration is always given by a multiple polylogarithm times a rational function where the denominator is linear in the next integration variable, i.e. of the form (4.32). An integral obeying these conditions is called linearly reducible and we refer the interested reader to [96, 102] and references therein for a thorough discussion of these integrals.

To see how this works in practice we go through the evaluation of the tree level four point function depicted in figure 5.1 with the parametric representation given by equation (5.2). For simplicity we only consider the case with external dimension $\Delta = 1$. Setting $\alpha_3 = 1$ due to the projectivity of the integral, equation (5.2) becomes

$$I(\zeta, \bar{\zeta}) = \int_0^\infty \mathrm{d}\alpha_1 \mathrm{d}\alpha_2 \frac{1}{(1+\alpha_1+\alpha_2)(\alpha_1\alpha_2+\alpha_1\zeta\bar{\zeta}+\alpha_2(1-\zeta)(1-\bar{\zeta}))}\,.$$

Since the Symanzik polynomials are linear in both Feynman parameters, we can integrate α_1 straight away and obtain

$$\begin{aligned} I &= \int_0^\infty \mathrm{d}\alpha_2 \frac{1}{(\alpha_2+\zeta)(\alpha_2+\bar{\zeta})} \log\left(\frac{(\alpha_2+\zeta\bar{\zeta})(1+\alpha_2)}{\alpha_2(1-\zeta)(1-\bar{\zeta})}\right) \\ &= \frac{1}{\zeta-\bar{\zeta}} \int_0^\infty \mathrm{d}\alpha_2 \left(\frac{1}{\alpha_2+\zeta} - \frac{1}{\alpha_2+\bar{\zeta}}\right) \log\left(\frac{(\alpha_2+\zeta\bar{\zeta})(1+\alpha_2)}{\alpha_2(1-\zeta)(1-\bar{\zeta})}\right)\,, \end{aligned}$$

where in the second step we used partial fraction decomposition to express the integrand in a form that is suitable for equation (4.32). Let us focus on the first summand in the integrand. We express the logarithm in terms of polylogarithms as

$$\begin{aligned} &\frac{\mathrm{d}\alpha_2}{\alpha_2+\zeta} \log\left(\frac{(\alpha_2+\zeta\bar{\zeta})(1+\alpha_2)}{\alpha_2(1-\zeta)(1-\bar{\zeta})}\right) = \\ &= \mathrm{d}\log(\alpha_2+\zeta)\left(\mathrm{Li}_1\left(\frac{\zeta}{\alpha_2+\zeta}\right) - \mathrm{Li}_1\left(\frac{\zeta-1}{\alpha_2+\zeta}\right) - \mathrm{Li}_1\left(\frac{\zeta(1-\bar{\zeta})}{\alpha_2+\zeta}\right) + \log(\alpha_2+\zeta) - \log((1-\zeta)(1-\bar{\zeta}))\right) \\ &\qquad = \mathrm{d}\log(\alpha_2+\zeta)\left(-G(\alpha_2+\zeta,\zeta) + G(\alpha_2+\zeta,\zeta-1) + G(\alpha_2+\zeta,\zeta(1-\bar{\zeta}))\right. \\ &\qquad\qquad \left. + \log(\alpha_2+\zeta) - \log((1-\zeta)(1-\bar{\zeta}))\right)\,, \end{aligned}$$

where we used (4.34). Comparing to equation (4.35) we can immediately write down the primitive for this part of the integral

$$\begin{aligned} P_\zeta(\alpha_2) &= -G(0,\alpha_2+\zeta,\zeta) + G(0,\alpha_2+\zeta,\zeta-1) + G(0,\alpha_2+\zeta,\zeta(1-\bar{\zeta})) \\ &\quad + \frac{1}{2}\log^2(\alpha_2+\zeta) - \log(\alpha_2+\zeta)\log((1-\zeta)(1-\bar{\zeta})) \\ &= \mathrm{Li}_2\left(\frac{\zeta}{\zeta+\alpha_2}\right) - \mathrm{Li}_2\left(\frac{\zeta-1}{\alpha_2+\zeta}\right) - \mathrm{Li}_2\left(\frac{\zeta(1-\bar{\zeta})}{\alpha_2+\zeta}\right) \\ &\quad + \frac{1}{2}\log^2(\alpha_2+\zeta) - \log(\alpha_2+\zeta)\log((1-\zeta)(1-\bar{\zeta}))\,. \end{aligned}$$

The second term is given by replacing $\zeta \leftrightarrow \bar{\zeta}$ and we denote the resulting primitive as $P_{\bar{\zeta}}(\alpha_2)$. Therefore the result of the integral is given by

$$I = \frac{1}{\zeta-\bar{\zeta}} \left(P_\zeta(\alpha_2) - P_{\bar{\zeta}}(\alpha_2)\right)\Big|_0^\infty$$

Using the fact that the polylogarithm vanishes at vanishing argument, the diverging terms $\log^2(\alpha_2+\zeta)$ and $\log(\alpha+\zeta)$ cancel with the contribution from $P_{\bar{\zeta}}(\alpha_2)$ and applying identities (A.1) the final result is given by

$$I = \frac{1}{\zeta-\bar{\zeta}}\left(2\mathrm{Li}_2\left(\zeta\right) - 2\mathrm{Li}_2\left(\bar{\zeta}\right) + \log\zeta\bar{\zeta}\left(\log(1-\zeta)-\log(1-\bar{\zeta})\right)\right) = \frac{4iD(\zeta,\bar{\zeta})}{\zeta-\bar{\zeta}}\,,$$

where $D(\zeta,\bar{\zeta})$ is the Bloch-Wigner dilogarithm [150] given in equation (A.2). This is actually the well known result for the one-loop three point function for a flat space diagram in momentum space.

The cross diagram is arguably the simplest diagram we evaluate, where we can do the calculation by hand. For more complicated diagrams we use the program `HyperInt` [137], which automatically expresses linearly reducible Feynman integrals in terms of multiple polylogarithms.

Interestingly most of the diagrams we encounter in EAdS and all diagrams in dS up to one loop order happen to be linearly reducible and therefore can be expressed in terms of multiple polylogarithms.

Chapter 5

Loop corrections to scalar field theory in Anti de Sitter space-time

We are now ready to calculate loop corrections to Witten diagrams for a $\lambda\phi^4$ theory and make their dependence on conformal cross ratios explicit. Below we will use two different regularisation schemes to establish scheme independence of our results. This chapter is a partial reproduction of [57].

5.1 The tree-level cross diagram

We start with the evaluation of the cross diagram for general integer dimensions $\Delta \geq 1$.[1] This is the first order perturbation in $\lambda\phi^4$ theory and depicted in figure 5.1.

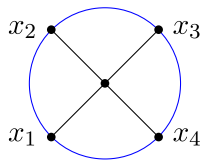

Figure 5.1: Cross diagram

5.1.1 General dimensions

The integral corresponding to this Witten diagram as defined in (4.16) is finite and therefore does not have to be regulated. Since this diagram only involves bulk-to-boundary propagators it takes a simple form in any dimension D and for general Δ,

$$\mathcal{W}_0^{\Delta,D}(\zeta,\bar{\zeta}) = \frac{1}{2}\frac{v^{\Delta}}{(x_{12}^2 x_{34}^2)^{\Delta}} \int_{\mathbb{R}^D} \frac{\mathrm{d}^D X}{(u\cdot X)^D} \left(\frac{(u\cdot X)^4}{\|X\|^2\,\|X-u_\zeta\|^2\,\|X-u_1\|^2}\right)^{\Delta} . \tag{5.1}$$

[1]The cross diagram is referred to as the D-function in [109]. We will not use this notation, reserving the name of $D(\zeta,\bar{\zeta})$ for the Bloch-Wigner single-valued dilogarithm function defined in (A.2).

We can evaluate this integral by using the parametric representation which is based on the fact that for $A > 0$

$$\frac{1}{A^n} = \frac{1}{\Gamma(n)} \int_0^\infty \mathrm{d}\alpha \, \mathrm{e}^{-\alpha A} \alpha^{n-1} \,.$$

In this representation (5.1) becomes

$$\mathcal{W}_0^{\Delta,D} = \frac{1}{2} \frac{i^{4\Delta - D} \pi^{\frac{D+1}{2}}}{\Gamma\left(\frac{D+1}{2} - 2\Delta\right) \Gamma(\Delta)^2} \frac{v^\Delta}{(x_{12}^2 x_{34}^2)^\Delta} I_\times^\Delta(\zeta, \bar\zeta) \,, \tag{5.2}$$

with

$$I_\times^\Delta(\zeta,\bar\zeta) = \int\limits_{(\mathbb{RP}^+)^2} \frac{\prod\limits_{i=1}^{3} \mathrm{d}\alpha_i \alpha_i^{\Delta-1}}{(\alpha_1+\alpha_2+\alpha_3)^\Delta (\alpha_1\alpha_2 + \alpha_1\alpha_3\zeta\bar\zeta + \alpha_2\alpha_3(1-\zeta)(1-\bar\zeta))^\Delta} \,, \tag{5.3}$$

where $(\mathbb{RP}^+)^2$ indicates that the integral is taken over the positive real projective space defined as

$$(\mathbb{RP}^+)^{n-1} := \{[\alpha_1, \dots, \alpha_n] \in \mathbb{RP}^{n-1} : \alpha_1, \dots, \alpha_n \geq 0\} \,.$$

Note that the only dependence on the spacetime dimension is contained in the prefactor.

We show in the appendix B.1 that for $\Delta \geq 1$ the cross integral takes the form

$$\begin{aligned} I_\times^\Delta(\zeta,\bar\zeta) =& \frac{c_1^\Delta(\zeta,\bar\zeta)}{(\zeta-\bar\zeta)^{4(\Delta-1)}} \frac{4iD(\zeta,\bar\zeta)}{\zeta-\bar\zeta} + \frac{c_2^\Delta(\zeta,\bar\zeta)}{(\zeta-\bar\zeta)^{4(\Delta-1)}} \log(\zeta\bar\zeta) \\ &+ \frac{c_3^\Delta(\zeta,\bar\zeta)}{(\zeta-\bar\zeta)^{4(\Delta-1)}} \log((1-\zeta)(1-\bar\zeta)) + \frac{c_4^\Delta(\zeta,\bar\zeta)}{(\zeta-\bar\zeta)^{4(\Delta-1)}} . \end{aligned}$$

where $c_r^\Delta(\zeta,\bar\zeta)$ are polynomial in ζ and $\bar\zeta$, and with $D(\zeta,\bar\zeta)$ is the Bloch-Wigner dilogarithm defined in equation (A.2). Despite the apparent singularity for $\bar\zeta = \zeta$ the expression is regular on the real slice. As expected $I_\times^\Delta(\zeta,\zeta^\cdot)$, with $\bar\zeta = \zeta^\cdot$ being complex conjugate of ζ, is a single-valued function on $\mathbb{C} \setminus \{0,1\}$.

In the rest of the paper we will make use of the result for $\Delta = 1$ which reads

$$\mathcal{W}_0^{1,4}(\zeta,\bar\zeta) = \frac{\pi^2}{x_{12}^2 x_{34}^2} \zeta\bar\zeta \frac{2iD(\zeta,\bar\zeta)}{\zeta-\bar\zeta} , \tag{5.4}$$

and for $\Delta = 2$, given by

$$\begin{aligned} \mathcal{W}_0^{2,4}(\zeta,\bar\zeta) =& \frac{3\pi^2(\zeta\bar\zeta)^2}{4x_{12}^4 x_{34}^4} \\ &\times \Bigg(\frac{4\zeta^2\bar\zeta^2 - (\zeta+\bar\zeta)^3 + 2\zeta\bar\zeta(\zeta+\bar\zeta)^2 + 2(\zeta+\bar\zeta)^2 - 8\zeta\bar\zeta(\zeta+\bar\zeta) + 4\zeta\bar\zeta}{(\zeta-\bar\zeta)^4} \frac{2iD(\zeta,\bar\zeta)}{\zeta-\bar\zeta} \\ &+ \frac{(\zeta+\bar\zeta)^2 - 3\zeta\bar\zeta(\zeta+\bar\zeta) + 2\zeta\bar\zeta}{(\zeta-\bar\zeta)^4} \log(\zeta\bar\zeta) \\ &+ \frac{3\zeta\bar\zeta(\zeta+\bar\zeta) - 2(\zeta+\bar\zeta)^2 + 3(\zeta+\bar\zeta) - 4\zeta\bar\zeta}{(\zeta-\bar\zeta)^4} \log((1-\zeta)(1-\bar\zeta)) + \frac{1}{(\zeta-\bar\zeta)^2} \Bigg) . \end{aligned} \tag{5.5}$$

$\mathcal{W}_0^{2,4}(\zeta,\bar\zeta)$ can equivalently be obtained by acting on $\mathcal{W}_0^{1,4}(\zeta,\bar\zeta)$ with the differential operator $\mathcal{H}_{1234}$ in (4.17). This is a simple application of the method described in section 4.1.4.

5.1.2 Dimensional regularisation

Even though the Witten cross diagram is finite and does not need to be regularised, we will need the higher terms in the $D-4$ expansion, for the renormalisation of the one-loop diagrams. In order to restore AdS-invariance after regularisation, we need to evaluate the cross diagram in $D = 4-4\epsilon$ dimensions.[2] For $\Delta = 1$ the integral is

$$\mathcal{W}_0^{1,4-4\epsilon}(\zeta,\bar\zeta) = \frac{1}{2}\frac{\zeta\bar\zeta}{(x_{12}x_{34})^2}\int_{\mathbb{R}^4}\frac{\mathrm{d}^{4-4\epsilon}X}{\|X\|^2\,\|X-u_1\|^{2(1-4\epsilon)}\,\|X-u_\zeta\|^2}\,. \tag{5.6}$$

Making use of the parametric representation (B.2) we can expand in ϵ. Again the resulting integrand is linearly reducible and we can evaluate the integral by using `HyperInt` [137], resulting in

$$W_0^{1,4-4\epsilon}(\zeta,\bar\zeta) = \frac{2^4a^{4+4\epsilon}}{(2\pi)^8}\mathcal{W}_0^{1,4-4\epsilon}(\zeta,\bar\zeta) = \frac{2^4a^{4+4\epsilon}}{(2\pi)^8}\left(\mathcal{W}_0^{1,4}(\zeta,\bar\zeta)+\epsilon\mathcal{W}_{0,\epsilon}^{1,4}(\zeta,\bar\zeta)+O(\epsilon^2)\right)\,,$$

with $W_0^{1,4}(\zeta,\bar\zeta)$ given in (5.4) and

$$\mathcal{W}_{0,\epsilon}^{1,4}(\zeta,\bar\zeta) = \frac{\zeta\bar\zeta\pi^2}{x_{12}^2x_{34}^2}\left(\frac{f_1(\zeta,\bar\zeta)}{\zeta-\bar\zeta}-\frac{2iD(\zeta,\bar\zeta)}{\zeta-\bar\zeta}\log(\zeta\bar\zeta)+\frac{2iD(\zeta,\bar\zeta)}{\zeta-\bar\zeta}\log((1-\zeta)(1-\bar\zeta))\right)\,,$$

where the function $f_1(\zeta,\bar\zeta)$ can be found in equation (A.3). The corresponding result for $\Delta = 2$ can then be obtained by acting on the parametric representation for $\Delta = 1$ with $\mathcal{H}_{1234}$ before expanding in ϵ. After integration over the Feynman parameters (see (B.3)) we find

$$W_0^{2,4-4\epsilon}(\zeta,\bar\zeta) = \frac{2^8a^{4+4\epsilon}}{(2\pi)^8}\mathcal{W}_0^{2,4-4\epsilon}(\zeta,\bar\zeta) = \frac{2^8a^{4+4\epsilon}}{(2\pi)^8}\left(\mathcal{W}_0^{2,4}(\zeta,\bar\zeta)+\epsilon\mathcal{W}_{0,\epsilon}^{2,4}(\zeta,\bar\zeta)+O(\epsilon^2)\right)\,, \tag{5.7}$$

with $\mathcal{W}_0^{2,4}(\zeta,\bar\zeta)$ given in (5.5) and $\mathcal{W}_{0,\epsilon}^{2,4}(\zeta,\bar\zeta)$ given by equation (B.4).

5.2 The one-loop diagram

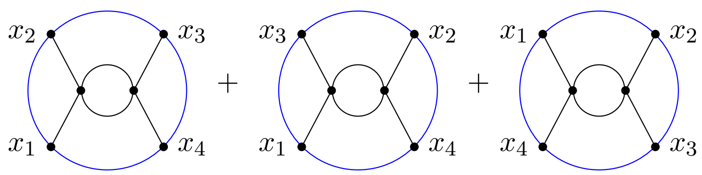

Figure 5.2: One-loop Witten diagrams

At one-loop level there are numerous diagrams to be evaluated but, as was found out in [55, 56], tadpoles and self-energy corrections only contribute to the mass shift at this level so we can reabsorb them into the conformal dimension of the boundary operator. In this section we fix this dimension to $\Delta = 1$ and $\Delta = 2$ and the only remaining connected one-loop diagrams in $\lambda\phi^4$ theory are the three channels of the one-loop bubble diagram depicted in figure 5.2.

[2] See Remark 2 at the end of section 4.1.2.

5.2.1 Dimensional regularisation

In order to restore conformal invariance after regularisation, we calculate these diagrams in dimensional regularisation with $D = 4 - 2\epsilon$ using the general formula (4.16) with $\delta(\Gamma_W) = \delta(X_{\sigma(1)} = X_{\sigma(2)})\delta(X_{\sigma(3)} = X_{\sigma(4)})$ to obtain

$$W_1^{\Delta,4-2\epsilon}(\zeta,\bar\zeta) = \frac{a^{4+4\epsilon}2^{4\Delta}(\zeta\bar\zeta)^\Delta}{4(x_{12}^2x_{34}^2)^\Delta(2\pi)^8}\int\limits_{(\mathbb{R}^D)^2} \mathrm{d}^{4-2\epsilon}X_1\mathrm{d}^{4-2\epsilon}X_2 \cdot$$
$$\cdot\frac{(u\cdot X_1)^{2\Delta-4}(u\cdot X_2)^{2\Delta-4}\tilde\Lambda(\mathbf{X}_1,\mathbf{X}_2;\Delta)^2}{\|X_1-u_1\|^{-4\epsilon}\|X_2-u_1\|^{-4\epsilon}}\Bigg(\frac{1}{\|X_1\|^{2\Delta}\|X_2-u_1\|^{2\Delta}\|X_2-u_\zeta\|^{2\Delta}}$$
$$+\frac{1}{\|X_2\|^{2\Delta}\|X_2-u_1\|^{2\Delta}\|X_1-u_\zeta\|^{2\Delta}}+\frac{1}{\|X_2\|^{2\Delta}\|X_1-u_1\|^{2\Delta}\|X_2-u_\zeta\|^{2\Delta}}\Bigg),$$

where $\tilde\Lambda$ is the propagator (4.9) without the normalization factor $a^2/4\pi^2$ which has been pulled out of the integral. Expanding the square with the help of the identity in (4.6) one finds

$$\tilde\Lambda(\mathbf{X}_1,\mathbf{X}_2;\Delta)^2 = \frac{(u\cdot X_1)^2\,(u\cdot X_2)^2}{\|X_1-X_2\|^4}+\frac{(u\cdot X_1)^2\,(u\cdot\sigma(X_2))^2}{\|X_1-\sigma(X_2)\|^4}$$
$$-\frac{(-1)^\Delta}{2}\left(\frac{u\cdot X_1\,u\cdot X_2}{\|X_1-X_2\|^2}+\frac{u\cdot X_1\,u\cdot\sigma(X_2)}{\|X_1-\sigma(X_2)\|^2}\right).$$

Upon substitution into (5.2.1) we arrive at

$$W_1^{\Delta,4-2\epsilon}(\zeta,\bar\zeta) = \frac{2^{4\Delta}a^{4+4\epsilon}}{(2\pi)^{12}}\sum_{i\in\{s,t,u\}}\left(\mathcal{W}_{1,\mathrm{div}}^{\Delta,4-2\epsilon,i}(\zeta,\bar\zeta)-\frac{(-1)^\Delta}{2}\mathcal{W}_{1,\mathrm{fin}}^{\Delta,4,i}(\zeta,\bar\zeta)\right), \tag{5.8}$$

where the integral in $W_{1,\mathrm{div}}^{\Delta,4-2\epsilon,i}(\zeta,\bar\zeta)$ requires regularisation while $W_{1,\mathrm{fin}}^{\Delta,4,i}(\zeta,\bar\zeta)$ does not. For instance, in the s-channel

$$\mathcal{W}_{1,\mathrm{div}}^{\Delta,4-2\epsilon,s}(\zeta,\bar\zeta) = \frac{1}{2}\frac{(\zeta\bar\zeta)^\Delta}{(x_{12}^2x_{34}^2)^\Delta}\int\limits_{\mathbb{R}^{2D}}\frac{\mathrm{d}^{4-2\epsilon}X_1\mathrm{d}^{4-2\epsilon}X_2(u\cdot X_1)^{2\Delta-2}(u\cdot X_2)^{2\Delta-2}\|X_1-u_1\|^{4\epsilon}}{\|X_1\|^{2\Delta}\|X_1-u_\zeta\|^{2\Delta}\|X_2-u_1\|^{2\Delta-4\epsilon}\|X_1-X_2\|^4},$$

and

$$\mathcal{W}_{1,\mathrm{fin}}^{\Delta,4,s}(\zeta,\bar\zeta) = \frac{1}{2}\frac{(\zeta\bar\zeta)^\Delta}{(x_{12}^2x_{34}^2)^\Delta}\int_{\mathbb{R}^8}\frac{\mathrm{d}^4X_1\mathrm{d}^4X_2(u\cdot X_1)^{2\Delta-3}(u\cdot X_2)^{2\Delta-3}}{\|X_1\|^{2\Delta}\|X_1-u_\zeta\|^{2\Delta}\|X_2-u_1\|^{2\Delta}\|X_1-X_2\|^2}, \tag{5.9}$$

with similar expression for the other channels listed in equation (C.1).

For Δ=1 the evaluation of the divergent part is straightforward. In the parametric representation (see (C.4)) we can integrate using `HyperInt` [137] giving

$$\mathcal{W}_{1,\mathrm{div}}^{\Delta,4-2\epsilon,s}(\zeta,\bar\zeta) = -\frac{\pi^{4-2\epsilon}\mathrm{e}^{-2\gamma\epsilon}\zeta\bar\zeta}{2x_{12}^2x_{34}^2}\Big(\frac{1}{\epsilon}\frac{4iD(\zeta,\bar\zeta)}{\zeta-\bar\zeta}+\frac{f_1(\zeta,\bar\zeta)}{\zeta-\bar\zeta}-\frac{2iD(\zeta,\bar\zeta)}{\zeta-\bar\zeta}\log(\zeta\bar\zeta)$$
$$+\frac{4iD(\zeta,\bar\zeta)}{\zeta-\bar\zeta}\log((1-\zeta)(1-\bar\zeta))\Big). \tag{5.10}$$

Adding the corresponding contributions form the t- and u-channel from appendix C.1.1 we end up with

$$W_{1,\text{div}}^{1,4-2\epsilon}(\zeta,\bar\zeta) = \frac{2^4 a^{4+4\epsilon}}{(2\pi)^{12}} \sum_{i\in\{s,t,u\}} \mathcal{W}_{1,\text{div}}^{1,4-2\epsilon,i}(\zeta,\bar\zeta)$$
$$= \frac{2^4 a^{4+4\epsilon}}{(2\pi)^{12}} \left(-\frac{3\pi^2}{\epsilon} \mathcal{W}_0^{1,4-4\epsilon}(\zeta,\bar\zeta) + \frac{\pi^4 v}{2x_{12}^2 x_{34}^2} \sum_{i\in\{s,t,u\}} L_0^{1,i}(\zeta,\bar\zeta) \right) ,$$

where the $L_0^{\Delta,i}(\zeta,\bar\zeta)$ terms are regular for $\epsilon \to 0$. Their expressions are given in appendix C.1.3.

The finite piece $\mathcal{W}_{1,\text{fin}}^{1,4,i}$ is harder to solve exactly. In the parametric representation it can be rewritten as (see appendix C.1.4 for details)

$$\mathcal{W}_{1,\text{fin}}^{1,4,i}(v,Y) = \frac{2\pi^4 v^\Delta}{(x_{12}x_{34})^\Delta} \begin{cases} L_0'(v,1-Y,1) & i=s \\ L_0'(1-Y,1,v) & i=t \\ L_0'(1,v,1-Y) & i=u \end{cases} ,$$

with

$$L_0'(x,y,z) = \int_1^\infty d\lambda \int_0^\infty ds \int_0^1 dr \frac{\log(1+\lambda s)}{4\lambda\sqrt{(1+s)(1+\lambda s)}(sr(1-r)x + ry + (1-r)z)} ,$$

and $v = \zeta\bar\zeta$ and $\zeta + \bar\zeta = v + Y$.

The integral is an elliptic polylogarithm obtained by integrating the dilogarithm in (C.15) over the elliptic curve (C.17). Since we want to calculate anomalous dimensions, which are related to the coeffcients of the terms proportional to $\log(v)$, we are not actually interested in the complete result of the integral. In appendix C.1.4 we provide an efficient way to extract the coefficients of the $\log(v)^2$ and $\log(v)$ terms and do an expansion in v and Y.

Altogether, the total one-loop Witten diagram for $\Delta = 1$ is given by

$$W_1^{1,4-2\epsilon}(v,Y) = \frac{2^4 a^{4+4\epsilon}}{(2\pi)^{12}} \Big(-\frac{3\pi^2}{\epsilon} \mathcal{W}_0^{1,4-4\epsilon}(v,Y) + \frac{\pi^4 v}{2x_{12}^2 x_{34}^2} \sum_{i\in\{s,t,u\}} L_0^{1,i}(v,Y) +$$
$$\frac{\pi^4 v}{x_{12}^2 x_{34}^2} \sum_{i\in\{s,t,u\}} L_0'^{\,i}(v,Y) + \mathcal{O}(\epsilon) \Big). \quad (5.11)$$

For $\Delta = 2$ we start with the calculation of the finite part. There are no elliptic integrals to compute and we can find closed form expressions in terms of single-valued polylogarithms of weight up to three.

To obtain the parametric representation of the finite part (5.9) we introduce the auxiliary integrals $\tilde{\mathcal{W}}_{1,\text{fin}}^{2,4,i}$ for each channel, with the s-channel given by

$$\tilde{\mathcal{W}}_{1,\text{fin}}^{2,4,s} = \frac{1}{8} \int_{\mathbb{R}^8} \frac{\mathrm{d}^4 X_1 \mathrm{d}^4 X_2}{\|X_1 - \vec{x}_1\|^2 \|X_1 - \vec{x}_2\|^4 \|X_2 - \vec{x}_3\|^4 \|X_2 - \vec{x}_4\|^2 \|X_1 - X_2\|^2}$$
$$= \frac{1}{8} \frac{x_{14}^2}{x_{12}^4 x_{34}^4} (\zeta\bar\zeta)^2 \int_{\mathbb{R}^8} \frac{\mathrm{d}^4 X_1 \mathrm{d}^4 X_2}{\|X_1\|^2 \|X_1 - u_\zeta\|^4 \|X_2 - u_1\|^2 \|X_1 - X_2\|^2} , \quad (5.12)$$

and the other channels displayed in (C.2). The second line in equation (5.12) is obtained by performing the conformal mappings as described in section 4.1.3. Considering the discussion in section 4.1.4 it is straightforward to see, that the finite part of the one-loop integral in each channel is given by the action of the differential operator $\mathcal{H}_{ij}$ on the corresponding auxiliary integral by

$$\mathcal{W}_{1,\text{fin}}^{2,4,s} = \mathcal{H}_{14}\tilde{\mathcal{W}}_{1,\text{fin}}^{2,4,s}; \qquad \mathcal{W}_{1,\text{fin}}^{2,4,t} = \mathcal{H}_{12}\tilde{\mathcal{W}}_{1,\text{fin}}^{2,4,t}; \qquad \mathcal{W}_{1,\text{fin}}^{2,4,u} = \mathcal{H}_{12}\tilde{\mathcal{W}}_{1,\text{fin}}^{2,4,u}. \tag{5.13}$$

In equation (C.9) we give the result of (5.13) in the parametric representation. Integrating over the Feynman parameters we obtain

$$\begin{aligned}\mathcal{W}_{1,\text{fin}}^{2,4,s}(\zeta,\bar\zeta) = \frac{\pi^4}{8}\frac{(\zeta\bar\zeta)^2}{(x_{12}^2x_{34}^2)^2}\Bigg(&\frac{(\zeta+\bar\zeta-2)8iD(\zeta,\bar\zeta)}{(\zeta-\bar\zeta)^3}\\ &+\frac{2(2\zeta\bar\zeta-\zeta-\bar\zeta)}{\zeta\bar\zeta(\zeta-\bar\zeta)^2}\log((1-\zeta)(1-\bar\zeta)) - \frac{4\log(\zeta\bar\zeta)}{(\zeta-\bar\zeta)^2}\Bigg),\end{aligned} \tag{5.14}$$

for the s channel. The results for the other channels are given in appendix C.1.2.

The divergent integrals in (5.8) can be calculated by acting with $\mathcal{H}_{1234}$ on the corresponding expressions for $\Delta = 1$. Some care has to be taken since the action of $\mathcal{H}_{1234}$ and the ϵ expansion do not commute: We have to act on the parametric representation of the $\Delta = 1$ expressions which gives us the parametric representation of the $\Delta = 2$ expressions. These can then be expanded in ϵ. The explicit expressions are given in equation (C.11). Integrating over the Feynman parameters and summing over the three channels we end up with

$$\begin{aligned}W_{1,\text{div}}^{2,4-2\epsilon}(\zeta,\bar\zeta) = \frac{2^8a^{4+4\epsilon}}{(2\pi)^{12}}\Big(&-\frac{3\pi^2}{\epsilon}\mathcal{W}_0^{2,4-4\epsilon} + 3\pi^2\mathcal{W}_0^{2,4}\\ &+\frac{1}{2}\sum_{j\in\{s,t,u\}}\mathcal{W}_{1,\text{fin}}^{2,4,j} + \frac{3\pi^4v^2}{8(x_{12}^2x_{34}^2)^2}\sum_{i\in\{s,t,u\}}L_0^{2,i} + \mathcal{O}(\epsilon)\Big).\end{aligned} \tag{5.15}$$

In sum, the total one-loop Witten diagram for $\Delta = 2$ is given by

$$W_1^{2,4-2\epsilon}(\zeta,\bar\zeta) = \frac{2^8a^{4+4\epsilon}}{(2\pi)^{12}}\left(-\frac{3\pi^2}{\epsilon}\mathcal{W}_0^{2,4-4\epsilon} + 3\pi^2\mathcal{W}_0^{2,4} + \frac{3\pi^4v^2}{8(x_{12}^2x_{34}^2)^2}\sum_{i\in\{s,t,u\}}L_0^{2,i} + \mathcal{O}(\epsilon)\right), \tag{5.16}$$

with the expressions for $L_0^{\Delta,i}$ given in appendix C.1.3.

Renormalisation: In order to subtract the UV-divergences in our dimensional regularisation we define the bare coupling constant λ as usual through $\lambda = \lambda_R\,(a\mu)\mu^{2\epsilon} + \delta\lambda$. The bare coupling is divergent but gives finite four-point functions by choosing the divergent counter-term $\delta\lambda$ accordingly. The renormalised coupling λ_R is finite and dimensionless in any dimension due to the factor $\mu^{2\epsilon}$ where μ has the dimension of length, which accounts for the scaling correction due to dimensional regularisation. Summing the tree-level (cross) and the one-loop (bubble) diagram contributions from (5.7) and (5.16) above, we have, for the connected part of the four-point function, up to finite terms,

$$\begin{aligned}\lambda_R\mu^{4\epsilon}W_0^{\Delta,4-4\epsilon} - \frac{\lambda_R^2\mu^{4\epsilon}}{2}W_1^{\Delta,4-2\epsilon} &= \frac{2^{4\Delta}a^4}{(2\pi)^8}\lambda_R\cdot(a\mu)^{4\epsilon}\left(1+\frac{3\lambda_R}{32\pi^2}\frac{1}{\epsilon}\right)\mathcal{W}_0^{\Delta,4-4\epsilon}\\ &\equiv \mu^{2\epsilon}\lambda\mathcal{W}_0^{\Delta,4-4\epsilon}.\end{aligned}$$

The extra factor $\mu^{2\epsilon}$ in front of λ arises since we have chosen the measure $d^{4-4\epsilon}X$, rather than $d^{4-2\epsilon}X$ for the cross diagram in (5.6). Focusing on the $1/\epsilon$ pole then fixes the value of the counter-term

$$\delta\lambda = -\frac{3\lambda_R^2\mu^{2\epsilon}}{32\pi^2}\frac{1}{\epsilon}\,.$$

On the other hand the $\log\mu$ contribution to the finite part in $\delta\lambda$ gives rise to the Callan-Symanzik equation

$$0 = \mu\frac{\mathrm{d}}{\mathrm{d}\mu}\lambda = 2\epsilon\mu^{2\epsilon}\left(\lambda_R - \frac{3\lambda_R^2}{32\pi^2}\frac{1}{\epsilon}\right) + \mu^{2\epsilon}\mu\frac{\partial\lambda_R}{\partial\mu}\frac{\partial}{\partial\lambda_R}\left(\lambda_R - \frac{3\lambda_R^2}{32\pi^2}\frac{1}{\epsilon}\right),$$

from which we read of the beta function

$$\beta = \frac{3\lambda_R^2}{16\pi^2} + \mathcal{O}(\lambda^3)\,.$$

This coincides with the β function of $\lambda\phi^4$ theory in flat space.

5.2.2 AdS invariant regularisation

Let us compare the results obtained so far to the AdS-invariant regularisation method described in section 4.1.2, which was used in [55, 56, 71]. The one-loop Witten diagram associated to the graphs in figure 5.2, with the regularisation given by (4.15), again consists of the sum over the contributions from the three channels

$$W_1^{\Delta,\delta}(\zeta,\bar\zeta) = \frac{2^{4\Delta}a^4}{(2\pi)^{12}}\sum_{i\in\{s,t,u\}}\mathcal{W}_1^{\Delta,\delta,i}(\zeta,\bar\zeta)\,,$$

with the contribution to the s-channel given by

$$\mathcal{W}_1^{\Delta,\delta,s} = \frac{1}{4}\frac{(\zeta\bar\zeta)^\Delta}{(x_{12}^2x_{34}^2)^\Delta}\int_{\mathbb{R}^8}\frac{\mathrm{d}^4X_1\mathrm{d}^4X_2 z_1^{2\Delta-4}z_2^{2\Delta-4}}{\|X_1\|^{2\Delta}\,\|X_1-u_\zeta\|^{2\Delta}\,\|X_2-u_1\|^{2\Delta}}\left(\frac{K^\delta(\mathbf{X}_1,\mathbf{X}_2)^\Delta}{1-K^\delta(\mathbf{X}_1,\mathbf{X}_2)^2}\right)^2, \tag{5.17}$$

and the integrals for the other channels given in (C.3).

In order to simplify the calculation we will separate these double integrals into an integral with the two external legs connected to X_1 and perform the integration over X_2 later as

$$\mathcal{W}_1^{\Delta,\delta,i} = \frac{1}{2}\int_{\mathbb{R}^4}\mathrm{d}^4X_2\hat{\mathcal{W}}_1^{\Delta,\delta,i}(\vec w_1,\vec w_2,X_2)\frac{z_2^{2\Delta-4}}{\|\vec w_3-X_2\|^{2\Delta}}\,, \tag{5.18}$$

with the intermediate integral

$$\hat{\mathcal{W}}_1^{\Delta,\delta,i}(\vec w_1,\vec w_2,X_2) = \frac{1}{2}\frac{v^\Delta}{(x_{12}^2x_{34}^2)^\Delta}\int_{\mathbb{R}^4}\frac{\mathrm{d}^4X_1\;\; z_1^{2\Delta-4}}{\|\vec w_1-X_1\|^{2\Delta}\,\|\vec w_2-X_1\|^{2\Delta}}\left(\frac{K^\delta(\mathbf{X}_1,\mathbf{X}_2)^\Delta}{1-K^\delta(\mathbf{X}_1,\mathbf{X}_2)^2}\right)^2,$$

associated to the fish diagram in figure 5.3.

Comparing to the expressions in equation (5.17) it is straightforward to identify the three channels as:

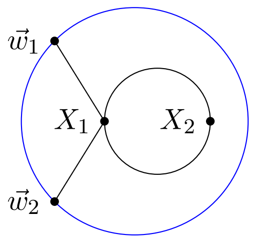

Figure 5.3: Fish diagram

- s-channel: $\vec{w}_1 \to 0$, $\vec{w}_2 \to u_\zeta$ and $\vec{w}_3 \to u_1$
- t-channel: $\vec{w}_1 \to u_\zeta$, $\vec{w}_2 \to u_1$ and $\vec{w}_3 \to 0$
- u-channel: $\vec{w}_1 \to 0$, $\vec{w}_2 \to u_1$ and $\vec{w}_3 \to u_\zeta$

For $\Delta = 1$ and $\Delta = 2$, this integral can be further simplified by rewriting the square of the bulk-to-bulk propagator in (5.17) in terms of euclidean propagators as described in 4.1. The fish diagram is then given by

$$\begin{aligned}\hat{\mathcal{W}}_1^{\Delta,\delta,i}(\vec{w}_1, \vec{w}_2, X_2) = &\frac{v^\Delta}{(x_{12}^2 x_{34}^2)^\Delta} \frac{1}{4} \int_{\mathbb{R}^4} \frac{\mathrm{d}^4 X_1}{z_1^4} \prod_{i=1}^{2} \frac{z_1^\Delta}{\|\vec{w}_i - X_1\|^{2\Delta}} \\ &\times \left(\frac{K^\delta(\mathbf{X}_1, \mathbf{X}_2)^2}{(1 - K^\delta(\mathbf{X}_1, \mathbf{X}_2))^2} - (-1)^\Delta \frac{K^\delta(\mathbf{X}_1, \mathbf{X}_2)}{1 - K^\delta(\mathbf{X}_1, \mathbf{X}_2)} \right) . \end{aligned} \tag{5.19}$$

For $\Delta = 2$: We split the integral into a first piece that diverges when $\delta \to 0$

$$\begin{aligned}\hat{\mathcal{W}}_1^{\Delta,\delta,i}(\vec{w}_1, \vec{w}_2, X_2)|_1 :=& \frac{v^2}{(x_{12}^2 x_{34}^2)^2} \frac{1}{4} \int_{\mathbb{R}^4} \mathrm{d}^4 X_1 \prod_{i=1}^{2} \frac{1}{\|\vec{w}_i - X_1\|^4} \frac{K(\mathbf{X}_1, \mathbf{X}_2)^2}{(1 - K(\mathbf{X}_1, \mathbf{X}_2) + \delta)^2} \\ =& \frac{\pi^2 v^2}{(x_{12}^2 x_{34}^2)^2} \left[\frac{1}{8} \prod_{i=1}^{2} \frac{z_2}{\|\vec{w}_i - X_2\|^2} - \prod_{i=1}^{2} \frac{z_2^2}{\|\vec{w}_i - X_2\|^4} \cdot \right. \\ & \left. \left(\log \left(\frac{z_2^2 \, |\vec{w}_1 - \vec{w}_2|^2}{\|\vec{w}_1 - X_2\|^2 \, \|\vec{w}_2 - X_2\|^2} \right) + \log 2\delta + 2 \right) \right]\end{aligned}$$

and a second piece that is finite when $\delta \to 0$:

$$\begin{aligned}\hat{\mathcal{W}}_1^{\Delta,\delta,i}(\vec{w}_1, \vec{w}_2, X_2)|_2 :=& \lim_{\delta \to 0} \frac{v^2}{(x_{12}^2 x_{34}^2)^2} \frac{1}{4} \int_{\mathbb{R}^4} \mathrm{d}^4 X_1 \prod_{i=1}^{2} \frac{1}{\|\vec{w}_i - X_1\|^4} \frac{K(\mathbf{X}_1, \mathbf{X}_2)}{1 - K(\mathbf{X}_1, \mathbf{X}_2) + \delta} \\ =& \frac{\pi^2 v^2}{(x_{12}^2 x_{34}^2)^2} \frac{1}{8} \prod_{i=1}^{2} \frac{z_2}{\|\vec{w}_i - X_2\|^2} ,\end{aligned}$$

so that the complete result for the fish diagram becomes

$$\begin{aligned}\hat{\mathcal{W}}_1^{\Delta,\delta,i}(\vec{w}_1, \vec{w}_2, X_2) &= \hat{\mathcal{W}}_1^{\Delta,\delta,i}(\vec{w}_1, \vec{w}_2, X_2)|_1 - \hat{\mathcal{W}}_1^{\Delta,\delta,i}(\vec{w}_1, \vec{w}_2, X_2)|_2 \\ &= -\frac{\pi^2 v^2}{(x_{12}^2 x_{34}^2)^2} \prod_{i=1}^{2} \frac{z_2^2}{\|\vec{w}_i - X_2\|^4} \left(\log \left(\frac{z_2^2 \, |\vec{w}_1 - \vec{w}_2|^2}{\|\vec{w}_1 - X_2\|^2 \, \|\vec{w}_2 - X_2\|^2} \right) + \log 2\delta + 2 \right) .\end{aligned}$$

Finally, using (5.18) we attach the remaining bulk-to-boundary propagator to obtain the integral for the one-loop diagram for $\Delta = 2$

$$\mathcal{W}_1^{\Delta,\delta,i} = -\frac{v^2}{(x_{12}^2 x_{34}^2)^2}\frac{\pi^2}{2}\int_{\mathbb{R}^4} \mathrm{d}^4 X z^4 \prod_{i=1}^{3} \frac{1}{\|X - \vec{w}_i\|^4} \cdot \left(\log\left(\frac{z_2^2\,|\vec{w}_1 - \vec{w}_2|^2}{\|\vec{w}_1 - X\|^2\,\|\vec{w}_2 - X\|^2}\right) + \log 2\delta + 2\right),$$

which evaluates to

$$\mathcal{W}_1^{\Delta,\delta,i} = -\pi^2\Big(\log\left(\frac{\delta}{2}\right) + \frac{11}{3}\Big)\mathcal{W}_0^{2,\delta} + \frac{3\pi^4 v^2}{8(x_{12}^2 x_{34}^2)^2} L_0^{2,i}.$$

Restoring the prefactors, the complete one-loop diagram is thus

$$W_1^{2,\delta} = \frac{2^8 a^4 \pi^2}{(2\pi)^{12}}\left(-3\log\left(\frac{\delta}{2}\right)\mathcal{W}_0^{2,\delta} - 11\mathcal{W}_0^{2,\delta} + \frac{3\pi^4 v^2}{8(x_{12}^2 x_{34}^2)^2}\sum_{i\in\{s,t,u\}} L_0^{2,i}\right), \tag{5.20}$$

where the $L_0^{\Delta,i}$ terms are given in C.1.3 and $\mathcal{W}_0^{\Delta,\delta}$ is the cross diagram evaluated in section 5.1.1.

For $\Delta = 1$: We split the integral in a first piece that diverges when $\delta \to 0$

$$\begin{aligned}\hat{\mathcal{W}}_1^{1,\delta,i}(\vec{w}_1,\vec{w}_2,X_2)|_1 &:= \frac{v}{(x_{12}^2 x_{34}^2)}\frac{1}{4}\int_{\mathbb{R}^4}\mathrm{d}^4 X_1 \prod_{i=1}^{2}\frac{1}{\|\vec{w}_i - X_1\|^2}\frac{K(\mathbf{X}_1,\mathbf{X}_2)^2}{(1-K(\mathbf{X}_1,\mathbf{X}_2)+\delta)^2} \\ &= -\frac{\pi^2 v}{(x_{12}^2 x_{34}^2)}\prod_{i=1}^{2}\frac{z_2}{\|\vec{w}_i - X_2\|^2}\left(\log\left(\frac{z_2^2\,|\vec{w}_1-\vec{w}_2|^2}{\|\vec{w}_1 - X_2\|^2\,\|\vec{w}_2 - X_2\|^2}\right) + \log 2\delta\right),\end{aligned}$$

and the finite piece when $\delta \to 0$:

$$\begin{aligned}\hat{\mathcal{W}}_1^{1,\delta,i}(\vec{w}_1,\vec{w}_2,X_2)|_2 &:= \lim_{\delta\to 0}\frac{v}{(x_{12}^2 x_{34}^2)}\frac{1}{4}\int_{\mathbb{R}^4}\frac{\mathrm{d}^4 X_1}{z_1^2}\prod_{i=1}^{2}\frac{1}{\|\vec{w}_i - X_1\|^2}\frac{K(\mathbf{X}_1,\mathbf{X}_2)}{1-K(\mathbf{X}_1,\mathbf{X}_2)+\delta} \\ &= \frac{2\pi^2 v^2}{(x_{12}^2 x_{34}^2)^2}\prod_{i=1}^{2}\frac{z_2}{\|\vec{w}_i - X_2\|^2}\int_0^1 \mathrm{d}u\frac{\mathrm{arctanh(u)}}{4u^2 + (1-u^2)\frac{|\vec{w}_1-\vec{w}_2|^2 4z_2^2}{\|\vec{w}_1-X_2\|^2\|\vec{w}_2-X_2\|^2}}.\end{aligned}$$

Thus the complete integral for the fish diagram is

$$\begin{aligned}\hat{\mathcal{W}}_1^{\Delta,\delta,i}(\vec{w}_1,\vec{w}_2,X_2) &= \hat{\mathcal{W}}_1^{1,\delta,i}(\vec{w}_1,\vec{w}_2,X_2)|_1 - \hat{\mathcal{W}}_1^{1,\delta,i}(\vec{w}_1,\vec{w}_2,X_2)|_2 \\ &= -\frac{\pi^2 v}{(x_{12}^2 x_{34}^2)}\prod_{i=1}^{2}\frac{z_2}{\|\vec{w}_i - X_2\|^2}\Bigg[\left(\log\left(\frac{z_2^2\,|\vec{w}_1-\vec{w}_2|^2}{\|\vec{w}_1 - X_2\|^2\,\|\vec{w}_2 - X_2\|^2}\right) + \log 2\delta\right) \\ &\qquad - 2\int_0^1 \mathrm{d}u\frac{\mathrm{arctanh(u)}}{4u^2 + (1-u^2)\frac{|\vec{w}_1-\vec{w}_2|^2 4z_2^2}{\|\vec{w}_1-X_2\|^2\|\vec{w}_2-X_2\|^2}}\Bigg].\end{aligned}$$

Finally we attach the remaining bulk-to-boundary propagator to obtain the full one-loop diagram for $\Delta = 1$

$$\mathcal{W}_1^{1,\delta,i} = \frac{1}{2}\frac{\pi^2 v}{(x_{12}^2 x_{34}^2)} \int_{\mathbb{R}^4} \mathrm{d}^4 X_2 \prod_{i=1}^{3} \frac{1}{\|\vec{w}_i - X_2\|^2} \Bigg[2\int_0^1 \mathrm{d}u \frac{\operatorname{arctanh}(\mathrm{u})}{4u^2 + (1-u^2)\frac{|\vec{w}_1-\vec{w}_2|^2 4z_2^2}{\|\vec{w}_1-X_2\|^2\|\vec{w}_2-X_2\|^2}} - \left(\log\left(\frac{z_2^2\,|\vec{w}_1-\vec{w}_2|^2}{\|\vec{w}_1-X_2\|^2\,\|\vec{w}_2-X_2\|^2}\right) + \log 2\delta\right)\Bigg],$$

with the result

$$\mathcal{W}_1^{1,\delta,i} = -\pi^2 \log\left(\frac{\delta}{2}\right)\mathcal{W}_0^{1,\delta} + \frac{\pi^4 v}{2x_{12}^2 x_{34}^2} L_0^{1,i} + \frac{\pi^4 v}{x_{12}^2 x_{34}^2} L_0'^{\,i}\,.$$

Restoring the prefactors, the complete one-loop diagram is then

$$W_1^{1,\delta} = \frac{2^4 a^4 \pi^2}{(2\pi)^{12}}\left(-3\log\left(\frac{\delta}{2}\right)\mathcal{W}_0^{1,\delta} + \frac{\pi^2 v}{2x_{12}^2x_{34}^2}\sum_{i\in\{s,t,u\}} L_0^{1,i} + \frac{\pi^2 v}{x_{12}^2 x_{34}^2}\sum_{i\in\{s,t,u\}} L_0'^{\,i} + \mathcal{O}(\delta)\right), \tag{5.21}$$

where $L_0^{\Delta,i}$ and $L_0'^{\,i}$ are given in C.1.3 and C.1.4 respectively and $\mathcal{W}_0^{\Delta,\delta}$ is the cross diagram evaluated in section 5.1.1.

Note that since the finite terms in both regulariation schemes corresponding to $W_{1,\mathrm{fin}}^{\Delta,4,i}$ and the second term in (5.19) are the same, we can conclude immediately that L_0' is the same in both regularisation schemes.

Renormalisation: As expected the UV divergent part is proportional to the cross diagram and can therefore be absorbed in the coupling constant λ, which makes the coupling constant scale dependent.

To understand how this works in the AdS-invariant regularisation we expand the regularised inverse geodesic distance around the coincidence points

$$\frac{K}{1+\delta} = \frac{1}{1+\delta}\frac{1}{\sqrt{1+a^2R^2}} \to 1 - \frac{1}{2}a^2R^2 - \delta + \mathcal{O}(a^4R^4, \delta^2),$$

where δ is a dimensionless quantity and $R = \sqrt{(\mathbf{X}^0 - \mathbf{Y}^0)^2 + \cdots + (\mathbf{X}^3 - \mathbf{Y}^3)^2}$. If we write it as $\delta = \frac{1}{2}a^2r^2$ we see that this regularisation procedure corresponds to cutting out a ball of radius r around the coinciding points. The quantity a would be the renormalisation scale in usual flat space renormalisation theory, corresponding to the energy at which the physical scattering experiment is performed. In our case, where we are merely interested in boundary to boundary correlation functions, the only physically relevant length scale is the AdS radius and we can therefore identify a with the inverse AdS radius.

To perform the renormalisation we write the connected part of the four-point correlator up to order λ^2:

$$\lambda W_0^{\Delta,\delta} - \frac{\lambda^2}{2}W_1^{\Delta,\delta} = \frac{2^{4\Delta}a^4}{(2\pi)^8}\left[\lambda_R\cdot\left(1+\frac{3\lambda_R}{32\pi^2}\log\left(\frac{\delta}{2}\right)\right)\mathcal{W}_0^{\Delta,\delta} + \text{finite terms}\right]. \tag{5.22}$$

To absorb the divergent part, it is straightforward to see that we can choose a counterterm of the form

$$\delta\lambda\,\mathcal{W}_0^{\Delta,\delta} = -\frac{3\lambda_R^2}{32\pi^2}\log\delta\,\mathcal{W}_0^{\Delta,4}\,.$$

The renormalised coupling is then related to the bare coupling λ through

$$\lambda = \lambda_R - \frac{3\lambda_R^2}{2(4\pi)^2}\log\delta + \mathcal{O}(\lambda_R^3)\,.$$

This regularises the expression (5.22) up to order λ_R^2. The beta function can now be calculated as

$$\beta(\lambda) = -\frac{\mathrm{d}\lambda}{\mathrm{d}\log r} = \frac{3\lambda^2}{16\pi^2} + \mathcal{O}(\lambda^3)\,,$$

which is again consistent with the flat space $\lambda\phi^4$ theory. In this equation we used the fact that δ is defined as $\delta = \frac{1}{2}r^2a^2$ as described above.

Comparing (5.21) and (5.20) with (5.16) and (5.11) makes it clear that both regularisation schemes are equivalent up to addition of a cross diagram W_0^Δ. Since these are the tree-level contributions they can always be absorbed into the coupling constant by choosing a non-minimal subtraction scheme.

In the following we will choose our counter-term such that the finite piece only contains the L_0^Δ and $L_0'^{\,\Delta}$ terms. Therefore the renormalised one-loop contributions are given by:

$$\begin{aligned}
W_1^{1,\mathrm{ren}} &= \frac{2^4a^4\pi^4}{(2\pi)^{12}}\frac{v}{x_{12}^2x_{34}^2}\left(\frac{1}{2}\sum_{i\in\{s,t,u\}}L_0^{1,i} + \sum_{i\in\{s,t,u\}}L_0'^{\,i}\right)\\
W_1^{2,\mathrm{ren}} &= \frac{2^8a^4\pi^4}{(2\pi)^{12}}\frac{3v^2}{8(x_{12}^2x_{34}^2)^2}\sum_{i\in\{s,t,u\}}L_0^{2,i}\,.
\end{aligned}$$

Note that this differs from the scheme used in [55, 56, 71] where contributions from the cross diagram have been integrated into the finite piece. For the anomalous dimensions the effect of different renormalisation schemes can always be absorbed into a redefinition of the coupling constant, that is, a change in parametrization, as we will discuss in section 5.5.

5.3 Two loop diagrams

To give an outlook on how to proceed to higher-loop integrals, we present the integral expressions of the two-loop contributions to the four-point function in terms of the euclidean propagators from section 4.1.1 but leave the evaluations of the integrals for future work.

There are two topologies contributing, which we will refer to as the necklace and the ice cream diagram.

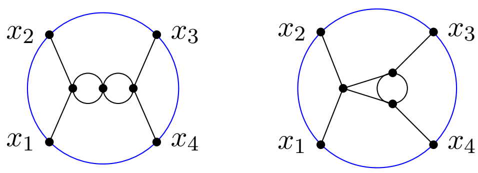

Figure 5.4: One channel of the two-loop Necklace (left) and Ice cream (right) diagram. The other channels can be obtained by permutations of the boundary points.

The necklace diagram is depicted in figure 5.4 on the left. In dimensional regularisation it leads to the integral

$$\mathcal{W}^{\Delta,D}_{2,\circ\circ}(\zeta,\bar\zeta) = \frac{v^\Delta}{8(x_{12}^2x_{34}^2)^\Delta}\int\limits_{(\mathbb{R}^D)^3}\prod_{i=1}^{3}\frac{\mathrm{d}^D X_i}{(u\cdot X_i)^4\,\|X_i-u_1\|^{2(D-4)}} f^\Delta_{\circ\circ}(X_1,X_3;\zeta,\bar\zeta)$$
$$\left(\frac{(u\cdot X_1)^2(u\cdot X_2)^2}{\|X_1-X_2\|^4}+\frac{(-1)^\Delta}{2}\frac{(u\cdot X_1)(u\cdot X_2)}{\|X_1-X_2\|^2}\right)\left(\frac{(u\cdot X_2)^2(u\cdot X_3)^2}{\|X_2-X_3\|^4}+\frac{(-1)^\Delta}{2}\frac{(u\cdot X_2)(u\cdot X_3)}{\|X_2-X_3\|^2}\right),$$

where the bulk-to-boundary part

$$f^\Delta_{\circ\circ}(X_1,X_3;\zeta,\bar\zeta) = \frac{(u\cdot X_1)^{2\Delta}(u\cdot X_3)^{2\Delta}}{\|X_1\|^{2\Delta}\,\|X_3-u_1\|^{2\Delta}\,\|X_3-u_\zeta\|^{2\Delta}}$$
$$\frac{(u\cdot X_1)^{2\Delta}(u\cdot X_3)^{2\Delta}}{\|X_3\|^{2\Delta}\,\|X_3-u_1\|^{2\Delta}\,\|X_1-u_\zeta\|^{2\Delta}}+\frac{(u\cdot X_1)^{2\Delta}(u\cdot X_3)^{2\Delta}}{\|X_3\|^{2\Delta}\,\|X_1-u_1\|^{2\Delta}\,\|X_3-u_\zeta\|^{2\Delta}},$$

is the same as for the one loop diagram in equation (5.2.1).

The ice-cream diagram is depicted in figure 5.4 on the right. In dimensional regularisation it corresponds to the integral

$$\mathcal{W}^{\Delta,D}_{2,\triangleleft\circ}(\zeta,\bar\zeta) = \frac{v^\Delta}{8(x_{12}^2x_{34}^2)^\Delta}\int\limits_{(\mathbb{R}^D)^3}\prod_{i=1}^{3}\frac{\mathrm{d}^D X_i}{(u\cdot X_i)^4\,\|X_i-u_1\|^{2(D-4)}} f^\Delta_{\triangleleft\circ}(X_1,X_2,X_3;\zeta,\bar\zeta)$$
$$\times\frac{(u\cdot X_1)^4(u\cdot X_2)^2(u\cdot X_3)^2}{\|X_1-X_2\|^4\,\|X_1-X_3\|^4}\left(\frac{(u\cdot X_2)^2(u\cdot X_3)^2}{\|X_2-X_3\|^4}+\frac{(-1)^\Delta}{2}\frac{(u\cdot X_2)(u\cdot X_3)}{\|X_2-X_3\|^2}\right),$$

where the bulk-to-boundary part can easily be read-off from the general formula (4.12).

It is easy to see, that when D approaches 4, these diagrams diverge like $(D-4)^{-2}$, with coefficients proportional to the cross diagram, and a sub-leading divergence of order $(D-4)^{-1}$ proportional to the one-loop Witten diagram. In order to restore the AdS invariance of the renormalised four-point function, we will need to evaluate these divergences in $D=4-4\epsilon/3$ dimensions.

In principle, solving these integrals can be done by following the same steps as for the one-loop case, the main difference being that the integrals are more complicated and that we will have elliptic polylogarithms appearing for the $\Delta=2$ case in the necklace diagram integrals. For $\Delta=1$ we meet integrals beyond elliptic integrals whose analysis is beyond the scope of the present work.

5.4 Discontinuities and unitarity of Witten diagrams

In this section we discuss how unitarity can be used to extract the prefactors of the $\log(v)^n$ terms in Witten diagrams, by calculating the discontinuity in v using the flat space Cutkosky rules [145] as reviewed in section 4.2.

5.4.1 Discontinuities

On general grounds, to any loop order the Witten diagrams have a small v expansion of the form

$$\mathcal{W}^\Delta_L(v,Y) = \frac{1}{2^{L+1}}\frac{v^\Delta}{(x_{12}^2x_{34}^2)^\Delta}\sum_{n=0}^{L+1}\log^n(v)p^{(n)}_L(v,Y;\Delta)+O(v)\,,$$

where $p_L^{(n)}(v, Y; \Delta)$ is an analytic function in v and Y for v and Y small. The (sequential) discontinuity in v of the Witten diagram is therefore contained in the $\log^n(v)$ terms. More precisely,

$$\mathrm{Disc}_v \mathcal{W}_L^\Delta(v, Y) = \frac{1}{2^{L+1}} \frac{v^\Delta}{(x_{12}^2 x_{34}^2)^\Delta} \sum_{n=1}^{L+1} \mathrm{Disc}_v \left(\log^n(v)\right) p_L^{(n)}(v, Y; \Delta) \,. \tag{5.23}$$

Recalling the definition of the discontinuity of a function $f(v)$ from equation (4.21)

$$\mathrm{Disc}_v f(v \pm i0) := \lim_{\varepsilon \to 0} \left(f(v + i\varepsilon) - f(v - i\varepsilon)\right).$$

We use the *principal branch* for the logarithm which is a continuous function on the complex plane except for the negative real axis. Thus, the discontinuities of $\log(v)$ and $\log^2(v)$ are

$$\begin{aligned}
\mathrm{Disc}_v \log(v) &= \lim_{\varepsilon \to 0} \left(\log(v + i\varepsilon) - \log(v - i\varepsilon)\right) = 2\pi i \Theta(-v) \,, \\
\mathrm{Disc}_v \log^2(v) &= 4\pi i \Theta(-v) \log(|v|) \,,
\end{aligned}$$

while the sequential double discontinuity is given by

$$\begin{aligned}
\mathrm{Disc}_v \mathrm{Disc}_v \log(v) &= 0 \,, \\
\mathrm{Disc}_v \mathrm{Disc}_v \log^2(v) &= 2(2\pi i)^2 \Theta(-v) \,.
\end{aligned}$$

Here we are only concerned with Witten diagrams up to loop order $L = 1$, therefore only terms which are maximally quadratic in $\log(v)$ can appear. In this case the (sequential) discontinuities with respect to v, applied to the one-loop Witten diagrams in (5.23), lead to

$$\begin{aligned}
\mathrm{Disc}_v \mathcal{W}_0^\Delta(v, Y) &= \frac{1}{2} \frac{v^\Delta}{(x_{12}^2 x_{34}^2)^\Delta} 2\pi i \Theta(-v) p_0^{(1)}(v, Y; \Delta), \\
\mathrm{Disc}_v \mathcal{W}_1^\Delta(v, Y) &= \frac{1}{4} \frac{v^\Delta}{(x_{12}^2 x_{34}^2)^\Delta} 2\pi i \Theta(-v) \left(2 \log(|v|) p_1^{(2)}(v, Y; \Delta) + p_1^{(1)}(v, Y; \Delta)\right), \\
\mathrm{Disc}_v \mathrm{Disc}_v \mathcal{W}_1^\Delta(v, Y) &= \frac{1}{2} \frac{v^\Delta}{(x_{12}^2 x_{34}^2)^\Delta} (2\pi i)^2 \Theta(-v) p_1^{(2)}(v, Y; \Delta).
\end{aligned} \tag{5.24}$$

From these expressions we can read-off the coefficients of $\log(v)^2$ and $\log(v)$ which, in turn, provide us with the information about the second order anomalous dimensions of the double-trace operators of the boundary theory.

As we will discuss in section 5.5 a direct consequence of the conformal symmetry at the boundary is the fact, that the sequential discontinuities of the Witten diagrams can be expanded in terms of conformal blocks of a generalized free field

$$\frac{1}{2\pi i} \mathrm{Disc}_v \mathcal{W}_0^\Delta = \sum_{n,l \geq 0} c_{0,n,l}^\Delta G_{\Delta_{n,l}}; \qquad \frac{1}{2(2\pi i)^2} \mathrm{Disc}_v \mathrm{Disc}_v \mathcal{W}_1^\Delta = \sum_{n,l \geq 0} c_{1,n,l}^\Delta G_{\Delta_{n,l}} \,.$$

and furthermore, that the expansion coefficients of the renormalised Witten diagrams are related by the simple relation

$$c_{1,n,l}^\Delta = -\frac{1}{4} \left(c_{0,n,l}^\Delta\right)^2 \,, \tag{5.25}$$

This relation (and its generalisation to higher-loop order) follows directly from the way the perturbative bulk interactions generate the anomalous dimensions in (5.29). For example in the $\Delta = 2$ case, since $c^2_{1,n,l} = c^2_{0,n,l} = 1$, we have the following relation between the discontinuities of the tree-level and one-loop Witten diagram

$$\frac{1}{2\pi i}\mathrm{Disc}_v \mathcal{W}_0^{\Delta}(v,Y) = -\frac{1}{4}\frac{1}{2(2\pi i)^2}\mathrm{Disc}_v\mathrm{Disc}_v \mathcal{W}_1^{\Delta}(v,Y)\,.$$

In the following we will show how to use the relation between the sequential discontinuities and multiple unitarity cuts developed in [143, 145, 147] for flat space Feynman integrals in momentum space to extract the coefficient of the $\log(v)$. We will demonstrate the success of the method with two examples and compare them to our exact results from sections 5.1 and 5.2. Note that we did not have to use this method, since we were able to solve the integrals for the Witten diagrams exactly. However, for higher loops and different conformal weights Δ, where solving the integrals exactly might be more challenging, this method could turn out to be useful.

5.4.2 Unitarity cuts

We notice that we can interpret the dimensionally regulated L-loop Witten diagrams in (4.10) as three-point momentum Feynman integrals in flat space, with external “momenta” $k_1 = u_1 - u_\zeta, k_2 = u_\zeta$ and $k_3 = -u_1$ where we integrate over $L+1$ loop momenta.

Because of this interpretation, we want to apply the relation between the discontinuity of the Witten diagrams with respect to the variable v and unitarity cuts $\mathrm{Disc}_v W_L^{\Delta}(v,Y) = \mathrm{Cut} W_L^{\Delta}(v,Y)$ along the lines of [145, 147]. For being able to apply the standard methods of calculating the Cutkosky discontinuities to the Witten diagrams, we need to perform a Wick rotation to go to Lorentzian AdS, meaning, that in this section the conformal flat propagator in (4.5) is given by

$$G(X,Y) := \frac{zw}{\|X-Y\|^2 - i\varepsilon}, \qquad \|X-Y\|^2 = (X_1-Y_1)^2 - \sum_{i=2}^{4}(X_i-Y_i)^2,$$

and $u_\zeta = \frac{1}{2}(\zeta+\bar\zeta, \zeta-\bar\zeta, 0, 0)$. We have introduced a Feynman $-i\varepsilon$ prescription following [18], which provides the correct flat limit.

We only consider the case $\Delta = 1$ because the $\Delta = 2$ case is obtained by acting with $\mathcal{H}_{1234}$ introduced in section 4.1.4.

Unitarity cuts of the cross Witten diagram

As an example, consider the tree-level cross diagram in AdS from equation (5.6). Identifying the bulk point X with the loop momentum l, this is equivalent to the flat space diagram depicted in figure 5.5. We are interested in the unitarity cut with respect to $k_2^2 = u_\zeta^2 = \zeta\bar\zeta = v$. The corresponding cut we have to perform is indicated in figure 5.5. The cut diagram is now given by [147]

$$\mathrm{Cut}_{u_\zeta}\mathcal{W}_0^{1,4-4\epsilon} = \frac{1}{2}\frac{v}{x_{12}^2 x_{34}^2}(2\pi i)^2\int \mathrm{d}^{4-4\epsilon}X\,\frac{\delta^+(\|X\|^2)\delta^+(\|X-u_\zeta\|^2)}{\left(\|X-u_1\|^2 - i\varepsilon\right)^{1-4\epsilon}}\,,$$

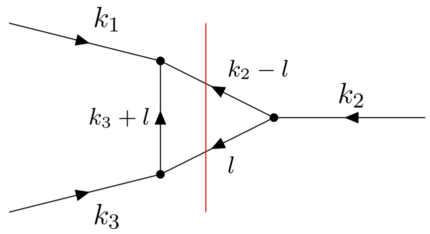

Figure 5.5: Cross diagram as a flat space three point function with $k_1 = u_1 - u_\zeta$, $k_2 = u_\zeta$, $k_3 = -u_1$ and $l = X$. The red line corresponds to the unitarity cut in the $k_2^2 = \zeta\bar{\zeta}$-channel.

where $\delta^+(\|X\|^2) = \delta(\|X\|^2)\Theta(X_1)$.
We parametrize the loop momentum X by $X = (x_0, r\cos\theta, 0, r\sin\theta)$. The integration measure is then given by

$$\int_{\mathbb{R}^4} \mathrm{d}^4 X \delta^+(\|X\|^2) = 2\pi^{1-2\epsilon}\mathrm{e}^{-2\gamma\epsilon} \int_0^\infty \mathrm{d}x_0 \int_0^\infty \mathrm{d}r r^{2-4\epsilon} \int_{-1}^{+1} \mathrm{d}\cos\theta \delta(x_0^2 - r^2)\,.$$

With this, the cut diagram becomes

$$\begin{aligned}
\mathrm{Cut}_{u_\zeta} \mathcal{W}_0^{1,4-4\epsilon} &= \frac{(2\pi)^3}{4} \frac{(\pi \mathrm{e}^\gamma)^{-2\epsilon} v}{x_{12}^2 x_{34}^2} \int_0^\infty \mathrm{d}x_0 \int_{-1}^{+1} \mathrm{d}\cos\theta x_0^{1-4\epsilon} (\sin\theta)^{4\epsilon} \frac{\delta\left(\zeta\bar{\zeta} - x_0\left(\zeta + \bar{\zeta} - \cos\theta(\zeta - \bar{\zeta})\right)\right)}{(1-2x_0)^{1-4\epsilon}} \\
&= \frac{(2\pi)^3}{4} \frac{(\pi \mathrm{e}^\gamma)^{-2\epsilon} v}{x_{12}^2 x_{34}^2} \int_{-1}^{+1} \mathrm{d}x \frac{(1-x^2)^{-2\epsilon}(\zeta\bar{\zeta})^{1-4\epsilon}}{(\zeta + \bar{\zeta} - x(\zeta - \bar{\zeta}))(\zeta + \bar{\zeta} - 2\zeta\bar{\zeta} - x(\zeta - \bar{\zeta}))^{1-4\epsilon}}\,,
\end{aligned} \tag{5.26}$$

which evaluates to

$$\mathrm{Cut}_{u_\zeta} \mathcal{W}_0^{1,4-4\epsilon} = -\frac{v\pi^3}{x_{12}^2 x_{34}^2} \frac{1}{(\zeta - \bar{\zeta})} \log\left(\frac{1-\zeta}{1-\bar{\zeta}}\right) + \mathcal{O}(\epsilon)\,,$$

where the $\mathcal{O}(\epsilon)$ term is given in the appendix by equation (C.20). Comparing the $\mathcal{O}(\epsilon^0)$ expression to (5.23) we see that the coefficient of $\log(v)$ is given by

$$p_0^{(1)}(v, Y) = \frac{x_{12}^2 x_{34}^2}{v} \frac{1}{2\pi i} \mathrm{Cut}_{u_\zeta} \mathcal{W}_0^{1,4} = \frac{i\pi^2}{2} \frac{1}{\zeta - \bar{\zeta}} \log\left(\frac{1-\zeta}{1-\bar{\zeta}}\right)\,,$$

which coincides with the exact calculation in (5.4) up to the additional factor of i which is due to the Lorentzian signature. This is a direct verification of the relation between the v discontinuities and the unitarity cuts.

The result for $\Delta = 2$ can easily be obtained by acting with $\mathcal{H}_{1234}$ on the $\Delta = 1$ result, since there are no terms in the Witten diagram that would produce extra $\log(v)$ terms due to differentiation.

Unitarity cuts of the one-loop Witten diagram

The same method can be applied at one loop, given by the integrals (C.1). As an example we consider the divergent part of the s-channel diagram given by $\mathcal{W}_{1,\mathrm{div}}^{1,4-2\epsilon,s}$.

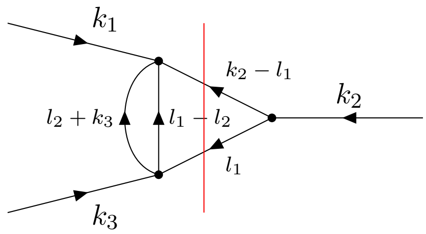

Figure 5.6: One-loop s-channel diagram as a two-loop flat space three point function with $k_1 = u_1 - u_\zeta$, $k_2 = u_\zeta$, $k_3 = -u_1$, $l_2 = X_2$ and $l_1 = X_1$. The red line corresponds to the unitarity cut in the $k_2^2 = \zeta\bar{\zeta}$ channel.

The corresponding flat space diagram is now given by a two-loop momentum space integral depicted in figure 5.6.

The discontinuity in v can then be calculated by performing the cut as shown in figure 5.6 and we get

$$\begin{aligned}
\mathrm{Cut}_{u_\zeta}\mathscr{W}^{1,4-2\epsilon,s}_{1,\mathrm{div}} =& \frac{1}{4}\frac{(2\pi i)^2 v}{x_{12}^2 x_{34}^2}\int \mathrm{d}^{4-2\epsilon}X_1 \mathrm{d}^{4-2\epsilon}X_2 \frac{\delta^+(\|X_1\|^2)\delta^+(\|X_1-u_\zeta\|^2)\,\|X_1-u_1\|^{4\epsilon}}{(\|X_2-u_1\|^2)^{1-2\epsilon}(\|X_1-X_2\|^2)^2} \\
=& -\frac{\pi^{2-\epsilon}\Gamma(\epsilon)}{\Gamma(1-2\epsilon)}\frac{1}{4}\frac{(2\pi i)^2 v}{x_{12}^2 x_{34}^2}\int \mathrm{d}^{4-2\epsilon}X_1 \frac{\delta^+(\|X_1\|^2)\delta^+(\|X_1-u_\zeta\|^2)}{(\|X_1-u_1\|^2)^{1-3\epsilon}}\,,
\end{aligned}$$

evaluating the delta-function constraints we have

$$\begin{aligned}
\mathrm{Cut}_{u_\zeta}\mathscr{W}^{1,4-2\epsilon,s}_{1,\mathrm{div}} =& -\frac{\pi^{4-2\epsilon}\Gamma(\epsilon)}{\Gamma(1-2\epsilon)\Gamma(1-\epsilon)}\frac{1}{4}\frac{(2\pi i)^2 v}{x_{12}^2 x_{34}^2} \\
&\times \int_{-1}^{+1}\mathrm{d}x \frac{(1-x^2)^{-\epsilon}(\zeta\bar{\zeta})^{1-2\epsilon}}{(\zeta+\bar{\zeta}-x(\zeta-\bar{\zeta}))^{1+\epsilon}(\zeta+\bar{\zeta}-2\zeta\bar{\zeta}-x(\zeta-\bar{\zeta}))^{1-3\epsilon}} \\
=& -\pi^{4-2\epsilon}\mathrm{e}^{-4\gamma\epsilon}\frac{1}{4}\frac{(2\pi i)^2 v}{x_{12}^2 x_{34}^2}\left[\frac{1}{\epsilon}I^1_{1,\mathrm{div}} + I^{1,\epsilon}_{1,\mathrm{div}} + \mathscr{O}(\epsilon)\right].
\end{aligned}$$

By comparing the integrand with equation (5.26) it is obvious, that $I^1_{1,\mathrm{div}}$ is given by the ϵ^0 term of the cut of the cross diagram in that equation. The expression for $I^{1,\epsilon}_{1,\mathrm{div}}$ is given in the appendix by equation (C.21).

The coefficient of the $\log(v)$ term of the uncut diagram can be extracted from this by comparing $I^{1,\epsilon}_{1,\mathrm{div}}$ to equation (5.24).

$$p_1^{(1)}(v,Y) = \frac{2}{i\pi}\, I^{1,\epsilon}_{1,\mathrm{div}}\Big|_{\log(v=\zeta\bar{\zeta})=0}\,.$$

Comparing to the exact result in equation (5.10) we see that the $\log(v)$ coefficients coincide, which is direct verification of the relation between the v discontinuities and the unitarity cuts.

This method can be applied to all other integrals to extract the $\log(v)$ coefficients. As mentioned above we will not proceed here since we were able to calculate the exact expressions. We merely want to propose this technique, since it might be useful in future work to go to higher-loop orders, where calculating the exact expressions is much harder.

We note, in passing, that this approach differs from the AdS unitarity methods developed in [48–50, 52] where the double discontinuity of a Witten diagram is calculated using the split representation of the propagator and the Lorentzian inversion formula [148]. While that method generalizes straightforwardly to general Δ and gives the result in terms of conformal blocks right away, it is much harder to compute anomalous dimensions beyond tree-level since they would involve cuts in the external bulk to boundary propagators.

In the language of [49] we are performing external cuts and therefore calculate the single discontinuity, which lets us extract the information about loop corrections to the anomalous dimensions.

5.5 Conformal block expansion

In order to extract the conformal dimensions of the "double-trace" operators in the conformal field dual to ϕ^4-theory in AdS we now compare the bulk calculation of the latter to the conformal block expansion of the former. First, let us note that the free part of the four-point correlation function, i.e. the disconnected part has the form of a generalized free field, meaning that it consists of the sum over all permutations of products of two point functions, but no classical CFT action exists which would generate these two-point correlation functions

$$\langle \mathcal{O}_\Delta(\vec{x}_1)\mathcal{O}_\Delta(\vec{x}_2)\rangle = \lim_{z_1,z_2\to 0}(z_1 z_2)^{-\Delta}\Lambda(\mathbf{X}_1,\mathbf{X}_2,\Delta) = 2^\Delta \mathcal{N}_\Delta \frac{1}{(x_{12}^2)^\Delta}\,.$$

Summing over the three permutations of external points, the disconnected part of the four-point correlation function becomes

$$\begin{aligned}\langle \mathcal{O}_\Delta(\vec{x}_1)\mathcal{O}_\Delta(\vec{x}_2)\mathcal{O}_\Delta(\vec{x}_3)\mathcal{O}_\Delta(\vec{x}_4)\rangle_{\text{disc}} &= \frac{2^{2\Delta}\mathcal{N}_\Delta^2}{(x_{12}^2x_{34}^2)^\Delta}\left(1+v^\Delta+\left(\frac{v}{1-Y}\right)^\Delta\right) \\ &= \frac{2^{2\Delta}\mathcal{N}_\Delta^2}{(x_{12}^2x_{34}^2)^\Delta}\left(1+v^\Delta\left(2+\sum_{n=1}^\infty\frac{\Gamma(\Delta+n)}{\Gamma(\Delta)\Gamma(n+1)}Y^n\right)\right)\,.\end{aligned} \tag{5.27}$$

In the last step we expand in $\vec{x}_1\to\vec{x}_2$ and $\vec{x}_3\to\vec{x}_4$, which translates into a small v and Y expansion

$$v=\frac{x_{12}^2x_{34}^2}{x_{14}^2x_{23}^2},\qquad Y=1-\frac{x_{13}^2x_{24}^2}{x_{14}^2x_{23}^2}.$$

From the perspective of the CFT this corresponds to the double operator product expansion (OPE)

$$\begin{aligned}\mathcal{O}_\Delta(\vec{x}_1)\mathcal{O}_\Delta(\vec{x}_2) &= \sum_{\tilde{\mathcal{O}}} a_{\Delta_{\tilde{\mathcal{O}}}}\mathcal{D}_{\tilde{\mathcal{O}}}(x_{12},\partial_2)\tilde{\mathcal{O}}(\vec{x}_2)\,,\\ \mathcal{O}_\Delta(\vec{x}_3)\mathcal{O}_\Delta(\vec{x}_4) &= \sum_{\tilde{\mathcal{O}}} a_{\Delta_{\tilde{\mathcal{O}}}}\mathcal{D}_{\tilde{\mathcal{O}}}(x_{34},\partial_4)\tilde{\mathcal{O}}(\vec{x}_4)\,,\end{aligned}$$

where $\mathcal{D}_{\tilde{\mathcal{O}}}(x_{ij},\partial_i)$ is a differential operator given by a power series in ∂_i of the form

$$\mathcal{D}_{\tilde{\mathcal{O}}}(x_{ij},\partial_j) = (x_{ij}^2)^{-\Delta+\frac{1}{2}\Delta_{\tilde{\mathcal{O}}}}\left(1+a\,x_{ij}\cdot\partial_j+b\,x_{ij}^2\partial_j^2+\cdots\right),$$

where the expansion coefficients $a, b, \ldots$ are completely fixed by conformal symmetry. The four-point function then becomes

$$\begin{aligned}\langle \mathcal{O}_\Delta(\vec{x}_1)\mathcal{O}_\Delta(\vec{x}_2)\mathcal{O}_\Delta(\vec{x}_3)\mathcal{O}_\Delta(\vec{x}_4)\rangle &= \sum_{\tilde{\mathcal{O}},\tilde{\tilde{\mathcal{O}}}} a_{\Delta_{\tilde{\mathcal{O}}}} a_{\Delta_{\tilde{\tilde{\mathcal{O}}}}} \mathcal{D}(x_{12},\partial_2)\mathcal{D}(x_{34},\partial_4)\langle \tilde{\mathcal{O}}(\vec{x}_2)\tilde{\tilde{\mathcal{O}}}(\vec{x}_4)\rangle \\ &= \frac{2^{2\Delta}\eta_\Delta^2}{(x_{12}^2 x_{34}^2)^\Delta}\left(1+\sum_{\tilde{\mathcal{O}}} A_{\Delta_{\tilde{\mathcal{O}}}} G_{\Delta_{\tilde{\mathcal{O}}},l}(v,Y)\right),\end{aligned}$$

where we used that $\langle \tilde{\mathcal{O}}(\vec{x}_2)\tilde{\tilde{\mathcal{O}}}(\vec{x}_4)\rangle$ vanishes for $\tilde{\mathcal{O}} \neq \tilde{\tilde{\mathcal{O}}}$. Here $G_{\Delta_{\tilde{\mathcal{O}}},l}(v,Y)$ are conformal blocks, see e.g. [109], that contain the information about the entire multiplet of a primary operator $\tilde{\mathcal{O}}$ and its descendants appearing in the OPE. They are eigenfunctions of the quadratic Casimir of the conformal group and depend on the conformal dimension $\Delta_{\tilde{\mathcal{O}}}$ and the spin l of $\tilde{\mathcal{O}}$. In three dimensions the conformal blocks can be obtained from the formula for general dimensions, which has been calculated in [111]. We list the relevant formula from this calculation in appendix D. In the following we will refer to $A_{\Delta_{\mathcal{O}}} \equiv a^2_{\Delta_{\mathcal{O}}}$ as the OPE coefficients. The normalization of the expansion is fixed by our bulk theory.

For a generalized free field the conformal block expansion can be determined exactly: The spectrum of primary "double-trace" operators is given by $:\mathcal{O}_\Delta \Box^n \partial^l \mathcal{O}_\Delta:$, with conformal dimension $\Delta_{(n,l)} = 2\Delta + 2n + l$, where $n, l/2 \in \mathbb{N}$. The OPE coefficients $A_{n,l}$ for these operators are known as well [94] and given in appendix D. We can therefore immediately write down the conformal block expansion for the generalized free field

$$\langle \mathcal{O}_\Delta(\vec{x}_1)\mathcal{O}_\Delta(\vec{x}_2)\mathcal{O}_\Delta(\vec{x}_3)\mathcal{O}_\Delta(\vec{x}_4)\rangle = \frac{2^{2\Delta}\eta_\Delta^2}{(x_{12}^2 x_{34}^2)^\Delta}\left(1+\sum_{n,l} A_{n,l} G_{\Delta_{(n,l)},l}(v,Y)\right).$$

By adding the interaction term $\lambda\phi^4$ in the bulk we deform the four-point function, such that the deformation is parametrized by an expansion in the renormalized bulk coupling constant λ_R. From the calculation in sections 5.1 and 5.2 we obtained the following four-point function up to $\mathcal{O}(\lambda_R^2)$:

$$\begin{aligned}\langle \mathcal{O}_\Delta(\vec{x}_1)\mathcal{O}_\Delta(\vec{x}_2)\mathcal{O}_\Delta(\vec{x}_3)\mathcal{O}_\Delta(\vec{x}_4)\rangle &= \frac{2^{2\Delta}\eta_\Delta^2}{(x_{12}^2 x_{34}^2)^\Delta}\Bigg[1+v^\Delta\Bigg(2+\sum_{n=1}^{\infty}\frac{\Gamma(\Delta+n)}{\Gamma(\Delta)\Gamma(n+1)}Y^n \\ -\frac{\lambda_R}{(4\pi)^2}\frac{2^{2\Delta}\sqrt{\pi}}{2\Gamma(\frac{5}{2}-2\Delta)\Gamma(\Delta)^2}I_\times^\Delta(v,Y) &+ \frac{\lambda_R^2}{(4\pi)^4}\sum_{i\in\{s,t,u\}}\begin{cases} L_0^{1,i}+2L_0'^{\,i} & \text{for } \Delta=1 \\ 3L_0^{2,i} & \text{for } \Delta=2\end{cases}\Bigg)\Bigg],\end{aligned} \tag{5.28}$$

From the CFT side the deformation generated by the bulk interaction term generates anomalous dimensions for the double-trace operators

$$\Delta_{(n,l)} \to \Delta_{(n,l)} + \sum_{p=0}^{\infty}\gamma_{n,l}^{(p)}(\Delta), \tag{5.29}$$

where $\gamma_{n,l}^{(p)}(\Delta)$ is of order λ_R^p in the renormalized bulk coupling constant λ_R. In order to match the conformal block expansion to the deformed four-point correlation function in equation (5.28), we expand both, the OPE coefficients and conformal blocks in powers of the anomalous dimensions up to $\mathcal{O}(\lambda_R^2)$

$$\begin{aligned}\mathcal{A}_{n,l}(\Delta) =& A_{n,l}(\Delta) + (\gamma^{(1)}_{n,l}(\Delta) + \gamma^{(2)}_{n,l}(\Delta))A^{(1)}_{n,l} + \frac{1}{2}(\gamma^{(1)}_{n,l}(\Delta))^2 A^{(2)}_{n,l} + \cdots \\ \mathcal{G}_{\Delta_{(n,l)},l} =& G_{\Delta(n,l),l} + (\gamma^{(1)}_{n,l}(\Delta) + \gamma^{(2)}_{n,l}(\Delta)) \underbrace{\frac{\partial G_{\Delta,l}}{\partial \Delta}\bigg|_{\Delta(n,l)}}_{G'_{\Delta(n,l),l}} + \frac{1}{2}(\gamma^{(1)}_{n,l}(\Delta))^2 \underbrace{\frac{\partial^2 G_{\Delta,l}}{\partial \Delta^2}\bigg|_{\Delta(n,l)}}_{G''_{\Delta(n,l),l}} + \cdots ,\end{aligned}$$

so that

$$\begin{aligned}\mathcal{A}_{n,l}\mathcal{G}_{\Delta(n,l),l} =& A_{n,l}G_{\Delta(n,l),l} + \gamma^{(1)}_{n,l}(\Delta)\left(A_{n,l}G'_{\Delta(n,l),l} + A^{(1)}_{n,l}G_{\Delta(n,l),l}\right) \\ &+ \frac{1}{2}(\gamma^{(1)}_{n,l}(\Delta))^2\left(A_{n,l}G''_{\Delta(n,l),l} + A^{(2)}_{n,l}G_{\Delta(n,l),l} + 2A^{(1)}_{n,l}G'_{\Delta(n,l),l}\right) \\ &+ \gamma^{(2)}_{n,l}(\Delta)\left(A_{n,l}G'_{\Delta(n,l),l} + A^{(1)}_{n,l}G_{\Delta(n,l),l}\right) + \mathcal{O}(\lambda^3)\,. \end{aligned} \tag{5.30}$$

The conformal blocks are of the form $G_{\Delta,l}(v,Y) = v^{\Delta/2}f(v,Y)$ so that the derivatives contain terms like

$$G'_{\Delta,l}(v,Y) = v^{\Delta/2}\log(v)f(v,Y) + \cdots ; \quad G''_{\Delta,l}(v,Y) = v^{\Delta/2}\log^2(v)f(v,Y) + \cdots$$

Comparing this to equation (5.30) we realize that the terms proportional to $\log(v)$ in (5.30) give us access to the anomalous dimensions at a given order in λ_R, while the $\log^2(v)$ term provides a consistency check that the boundary Witten diagrams correspond to a consistent CFT. Consistency between the first and second order calculation in λ_R require that the $\log^2(v)$ term has to be proportional $(\gamma^{(1)}_{n,l})^2$. This is the basis for equation (5.25) as well. The contributions without log's then provide information about the OPE coefficients. Thus we can expand the exact expressions for the Witten diagrams we calculated in sections 5.1 and 5.2 in v, Y and compare them to the conformal block expansion to extract the anomalous dimensions and OPE coefficients.

By extracting the coefficient of $\log(v) = \log(\zeta\bar{\zeta})$ in the analytic expressions for Witten diagrams up to one-loop order, and comparing with the expansion of the four-point correlation function, we can extract the L-loop contributions to the anomalous dimensions $\gamma^{(L)}_{n,l}(\Delta)$. These contributions to the anomalous dimensions depend on the renormalised coupling

$$\gamma := \frac{\lambda_R}{16\pi^2},$$

such that at loop order L the ratio $\gamma^{(L)}_{n,l}(\Delta)/\gamma^L$ is independent of the renormalised coupling. We will comment more about the renormalisation scheme dependence below.

Anomalous dimensions for $\boldsymbol{\Delta = 1}$ The anomalous dimensions for $\Delta = 1$ are given by

$$\begin{aligned}\gamma^{(1)}_{n,l}(1) &= \gamma\,(1+\delta_{n,0})\delta_{l,0}; \\ \gamma^{(2)}_{n,l>0}(1) &= \gamma^2 \begin{cases} \frac{-2}{l(l+1)} + \frac{4}{2l+1}\left(H^{(2)}_l - \zeta(2)\right) & \text{for } n=0 \\ T^1_{n,l} & \text{for } n>0 \end{cases}\end{aligned}$$

$$\gamma^{(2)}_{n,0}(1) = \gamma^2 \begin{cases} -4 + \frac{4}{2l+1}\left(H_l^{(2)} - \zeta(2)\right) & \text{for } n = 0 \\ \frac{(6n^2-3n-2)}{n(2n+1)} H^{(1)}_{2n} - 1 & \text{for } n > 0 \end{cases},$$

where the generalized harmonic numbers are given by $H_i^{(k)} = \sum_{n=1}^{i} n^{-k}$ and the rational piece $T^{\Delta}_{n,l}$ is given by

$$T^{\Delta}_{n,l} = -\frac{2(l^2 + (2\Delta + 2n - 1)(\Delta + n + l - 1))}{l(l+1)(2\Delta + 2n + l - 1)(2\Delta + 2n + l - 2)} - \frac{2(-1)^{\Delta}(H_l^{(1)} - H^{(1)}_{2\Delta+2n+l-2})}{(2\Delta + 2n + 2l - 1)(\Delta + n - 1)}. \tag{5.31}$$

The tree level results agree with [93]. The OPE coefficients at order λ for $l = 0$ are given by the known formula [93, 94]

$$A^{(1)}_{n,0}(\Delta) = \frac{1}{2}\frac{\partial A_{n,0}(\Delta)}{\partial n},$$

For the second order OPE coefficients and the first order OPE coefficients at $l > 0$ one needs to expand the finite piece of the L_0' integral, which we leave to a further study.

Anomalous dimensions for $\boldsymbol{\Delta = 2}$ Similarly we have the following results for the anomalous dimensions

$$\gamma^{(1)}_{n,l}(2) = \gamma\, \delta_{l,0} \quad \text{for } n \geq 0;$$

$$\gamma^{(2)}_{n,l}(2) = \gamma^2 \begin{cases} T^2_{n,l} & \text{for } l > 0 \\ \frac{2\left(6n^2+15n+11\right) H^{(1)}_{2n+2} - \left(26n^2+65n+41\right)}{2(n+1)(2n+3)} & \text{for } l = 0 \end{cases}$$

where $T^2_{n,l}$ is given by equation (5.31).We thus obtained closed expressions for the anomalous dimensions of all double trace operators appearing in the OPE expansion of the single trace operator $\mathcal{O}_\Delta$ for $\Delta = 1, 2$. To our knowledge, these have not been obtained before.

Renormalisation scheme dependence Note, that the first order anomalous dimension, which is generated by the cross Witten diagram, has only a non-zero constant contribution for $l = 0$. Changing the renormalisation scheme, i.e. adding a cross term to the finite piece of the one loop contribution therefore only shifts the $\gamma^{(2)}_{n,0}(\Delta)$ part of the second order anomalous dimensions by a constant, which can always be absorbed by redefining the coupling constant. The anomalous dimensions for $l > 0$ are completely scheme independent.

In the $\Delta = 1$ case we find an anomalous piece in the $n = 0$ trajectory given by

$$\frac{4\gamma^2}{2l+1}\left(H_l^{(2)} - \zeta(2)\right) = -\frac{4\gamma^2 \psi^{(1)}(l+1)}{2l+1},$$

where $\psi^{(1)}(l+1)$ is the digamma function, which is absent in the $\Delta = 2$ case. This is consistent with the result obtained in [56].

In both cases the anomalous dimensions of the scalar operators $:\mathcal{O}\Box^n\mathcal{O}:$ are positive and have different behaviour compared to the operators with non-vanishing spin. The behaviour for the latter can be summarized into equation (5.31), applicable to both cases. It is consistent with previous results for the $n = 0$ trajectory in [55, 56] and for the subleading trajectories obtained in [71].

Regge trajectories We can use equation (5.31) to compare our result to previous results for large l obtained by bootstrap methods [29, 153, 154]. Expanding around $l \to \infty$ we obtain

$$\gamma^{(2)}_{n,l}(\Delta) = \gamma^2 \sum_{k=0}^{\infty} \frac{q_k^{\Delta}(n)}{l^{2\Delta+k}},$$

where the $q_k^{\Delta}(n)$ are polynomials in n of order $2\Delta + k - 2$, which can easily be extracted from the exact expressions.

It is also straightforward to express the anomalous dimensions in terms of the conformal spin

$$J^2 = (l + \Delta + n)(l + \Delta + n - 1).$$

Expanding the anomalous dimensions in large J we obtain

$$\gamma^{(2)}_{n,J}(\Delta) = \gamma^2 \sum_{k=0}^{\infty} \frac{Q_k^{\Delta}(n)}{J^{2\Delta+2k}},$$

where the $Q_k^{\Delta}(n)$ are polynomials in n of order $2\Delta+2k-2$. For $\Delta = 1$ these polynomials only contain even powers of n. These behaviours are in agreement with the results from [153–155].

Another interesting limit to explore would be the behaviour at $n \to \infty$. Taking the limit $n \to \infty$ in equation (5.31) we obtain

$$\lim_{n\to\infty} \gamma^{(2)}_{n,l>0}(\Delta) = -\gamma^2 \frac{1}{l(1+l)}.$$

For $\Delta = 1$ the limit is approached from below, while for $\Delta = 2$ it is reached from above, as can be understood from the $(-1)^{\Delta}$ factor in (5.31) in agreement with general observations made in [93, 156]. It would be interesting to test this observation for other values of Δ.

Chapter 6

Loop corrections to scalar field theory in de Sitter space-time

In this chapter we calculate perturbative observables of a $\lambda\phi^4$ theory in dS. We start with Bunch-Davies wave function and continue with the cosmological correlator, building on the formalism described in chapter 3. As it turns out we will be able to use many of the results, already obtained in chapter 5.

6.1 Bunch-Davies wave function and dS/CFT

In this section we perform the semi classical expansion of the Bunch-Davies wave function. This section is partially a reproduction of parts of [71] and we partially stick to the notational conventions introduced there.

To make a semiclassical expansion up to second loop order, we expand $\mathrm{e}^{iS_{int}[\varphi,\chi]}$ in (3.65) up to second order in the coupling constant λ. For better readability we write $\varphi(X) = \varphi_X$:

$$\begin{aligned}\mathrm{e}^{iS_{int}[\varphi,\chi]} =& 1 - i\lambda \int \mathrm{d}^4X\sqrt{g(X)}\left\{\frac{1}{4}\varphi_X^2\chi_X^2 + \frac{1}{6}\varphi_X\chi_X^3 + \frac{1}{4!}\chi_X^4\right\}\\ &- \frac{\lambda^2}{2}\iint \mathrm{d}^4X\mathrm{d}^4Y\sqrt{g(X)g(Y)}\left\{\frac{1}{16}\varphi_X^2\varphi_Y^2\chi_X^2\chi_Y^2 + \frac{1}{4!2}\varphi_X^2\chi_X^2\chi_Y^4\right.\\ &\left.+\frac{1}{36}\varphi_X\varphi_Y\chi_X^3\chi_Y^3 + \frac{1}{4!3}\varphi_X\chi_X^3\chi_Y^4 + \frac{1}{12}\varphi_X^2\varphi_Y\chi_X^2\chi_Y^3 + \frac{1}{(4!)^2}\chi_X^4\chi_Y^4\right\} + \mathcal{O}(\lambda^3)\end{aligned}$$

The second last two terms in the λ^2 integral have an odd number of χ insertions and therefore vanish when performing the path integral. The last term just gives a contribution in the bulk and is independent of the classical part of the field φ. Therefore the functional derivatives with respect to the fields on the boundary vanish and the term does not contribute to the conformal correlation functions (3.64). The same is true for the last two terms in the $i\lambda$ contribution. Now we can calculate the effective action perturbatively by using Wick's theorem to calculate the path integral over χ:

$$
\begin{aligned}
\Psi[\phi_0(\vec{x})] =& \mathrm{e}^{iS_{on-shell}[\varphi]}\Bigg(1-\frac{i\lambda}{4}\int \mathrm{d}^4X\sqrt{g(X)}\varphi_X^2 i\Lambda_D(X,X)\\
&-\frac{\lambda^2}{2}\iint \mathrm{d}^4X\mathrm{d}^4Y\sqrt{g(X)g(Y)}\Big\{\frac{1}{16}\varphi_X^2\varphi_Y^2 i\Lambda_D(X,X)i\Lambda_D(Y,Y)\\
&+\frac{1}{8}\varphi_X^2\varphi_Y^2 i^2\Lambda_D^2(X,Y)++\frac{1}{4}\varphi_X^2 i^2\Lambda_D^2(X,Y)i\Lambda_D(Y,Y)+\frac{1}{6}\varphi_X\varphi_Y i^3\Lambda_D^3(X,Y)\\
&+\frac{1}{4}\varphi_X\varphi_Y i\Lambda_D(X,X)i\Lambda_D(X,Y)i\Lambda_D(Y,Y)\Big\}\Bigg)
\end{aligned}
$$

Plugging in the tree-level solution for φ we can regroup the terms in the effective action to give the contributions to the 2 and 4 point functions. To simplify the notation we write in this section $\int \mathrm{d}^4X\sqrt{g(X)}=\int \mathrm{d}^4\tilde{X}$ and $\Lambda_D(X,Y)=\Lambda_{xy}$:

$$
\begin{aligned}
\Psi[\phi_0(\vec{x})] =& \mathrm{e}^{i\Gamma[\phi_0]}=\mathrm{e}^{iS_{\text{on-shell}}}\Bigg(1-\iint \mathrm{d}^3\vec{x}_1\mathrm{d}^3\vec{x}_2\phi_0(\vec{x}_1)\phi_0(\vec{x}_2)\Big[\frac{i\lambda}{4}\int \mathrm{d}^4\tilde{X} i\Lambda_{XX}\bar{\Lambda}_{X\vec{x}_1}\bar{\Lambda}_{X\vec{x}_2}\\
&+\lambda^2\iint \mathrm{d}^4\tilde{X}\mathrm{d}^4\tilde{Y}\Big\{\frac{1}{8}i^2\Lambda_{XY}^2 i\Lambda_{YY}\bar{\Lambda}_{X\vec{x}_1}\bar{\Lambda}_{X\vec{x}_2}+\frac{1}{12}i^3\Lambda_{XY}^3\bar{\Lambda}_{X\vec{x}_1}\bar{\Lambda}_{Y\vec{x}_2}\\
&+\frac{1}{8}i\Lambda_{XX}i\Lambda_{XY}i\Lambda_{YY}\bar{\Lambda}_{X\vec{x}_1}\bar{\Lambda}_{X\vec{x}_2}\Big\}\Big]\\
&-\lambda^2\iiiint\prod_{i=1}^{4}\mathrm{d}^3\vec{x}_i\phi_0(\vec{x}_i)\Big[\iint \mathrm{d}^4\tilde{X}\mathrm{d}^4\tilde{Y}\Big\{\frac{1}{3!2}i\Lambda_{XX}i\Lambda_{XY}\bar{\Lambda}_{X\vec{x}_1}\bar{\Lambda}_{X\vec{x}_2}\bar{\Lambda}_{Y\vec{x}_3}\bar{\Lambda}_{Y\vec{x}_4}\\
&+\frac{1}{32}i\Lambda_{XX}i\Lambda_{YY}\bar{\Lambda}_{X\vec{x}_1}\bar{\Lambda}_{X\vec{x}_2}\bar{\Lambda}_{Y\vec{x}_3}\bar{\Lambda}_{Y\vec{x}_4}+\frac{1}{16}i^2\Lambda_{XY}^2\bar{\Lambda}_{X\vec{x}_1}\bar{\Lambda}_{X\vec{x}_2}\bar{\Lambda}_{Y\vec{x}_3}\bar{\Lambda}_{Y\vec{x}_4}\Big\}\Big]+\mathcal{O}(\lambda^3)\Bigg)
\end{aligned}
$$

By functional differentiating we can now calculate the two point and and four point function of the dual CFT up to second order in λ. In what follows we focus on these correlators rather than the wave function since they contain the relevant information about the CFT. We will write them in terms of the corresponding Witten diagrams:

$$\langle\mathcal{O}(\vec{x}_1)\mathcal{O}(\vec{x}_2)\rangle=\frac{\delta^2\Psi[\phi_0]}{\delta\phi_0(\vec{x}_1)\delta\phi_0(\vec{x}_2)}=$$

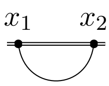

$-\frac{i\lambda}{2}$

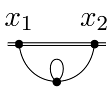

$-\frac{\lambda^2}{4}$

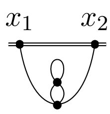

$-\frac{\lambda^2}{4}$

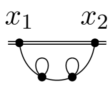

$-\frac{\lambda^2}{6}$

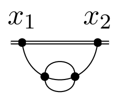

$$\langle\mathcal{O}(\vec{x}_1)\mathcal{O}(\vec{x}_2)\mathcal{O}(\vec{x}_3)\mathcal{O}(\vec{x}_4)\rangle=\frac{\delta^4\Psi[\phi_0]}{\delta\phi_0(\vec{x}_1)\delta\phi_0(\vec{x}_2)\delta\phi_0(\vec{x}_3)\delta\phi_0(\vec{x}_4)}$$

$=3\times$

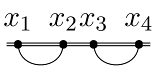

$-i\lambda\Big(3\times$

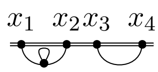

$+$

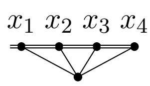

$\Big)$

$-3\times\lambda^2\Big(\frac{1}{2}$

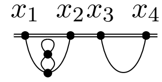

$+\frac{1}{2}$

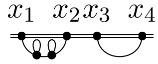

$+\frac{1}{3}$

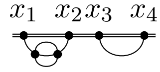

$+\frac{1}{4}$

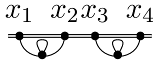

$+4\times\frac{1}{2}$

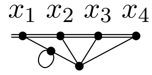

$+3\times\frac{1}{2}$

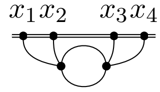

$\Big)$

6.1.1 Two point function

Now we have all the parts in place to calculate the two point function of the dual conformal field theory by explicitly integrating over the vertices in the diagrams. We will perform all the calculations directly in de Sitter space however we will find out that all the results are exactly what you would get from taking the results from [55,56] and do the analytic continuation.

Tadpole The second diagram in the two point function is the tadpole and is given by the following integral:

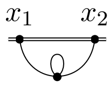

$$= \int \mathrm{d}^4 X \sqrt{g(X)} \bar{\Lambda}_D(\vec{x}_1, X) i\Lambda_D(X,X) \bar{\Lambda}_D(X, \vec{x}_2) = i\Lambda_D(X,X) M(\vec{x}_1, \vec{x}_2) \tag{6.1}$$

First we calculate the mass shift $M(\vec{x}_1, \vec{x}_2)$ which is given by the integral:

$$M(\vec{x}_1, \vec{x}_2) = -\frac{1}{a^4 \pi^4} \int_{-\infty}^{0} \frac{\mathrm{d}\eta}{\eta^4} \int \mathrm{d}^3 \vec{x} \frac{\eta^4}{(\eta^2 - (\vec{x}_1 - \vec{x})^2 - i\varepsilon)^2 (\eta^2 - (\vec{x}_2 - \vec{x})^2 - i\varepsilon)^2}$$

To simplify the calculation we use translation invariance to shift $\vec{x}_1$ and $\vec{x}_2$ by $\vec{x}_2$ and we get $\vec{x}_1' = \vec{x}_1 - \vec{x}_2$ and $\vec{x}_2' = 0$. Now we can go to spherical coordinates with $r = |\vec{x}|$ and the determinant becomes $\sqrt{g(x)} = \frac{1}{a^4 \eta^4} r^2 \sin\theta$:

$$\begin{aligned}
M(\vec{x}_1, \vec{x}_2) &= -\frac{1}{a^4 \pi^4} \int_{-\infty}^{0} \mathrm{d}\eta \int_0^{\pi} \mathrm{d}\theta \int_0^{\infty} \mathrm{d}r \frac{2\pi r^2 \sin\theta}{(\eta^2 - |\vec{x}_1'|^2 + 2|\vec{x}_1'| r \cos\theta - r^2 - i\varepsilon)^2 (\eta^2 - r^2 - i\varepsilon)^2} \\
&= -\frac{2}{a^4 \pi^3} \int_{-\infty}^{0} \mathrm{d}\eta \int_{-1}^{+1} \mathrm{d}u \int_0^{\infty} \mathrm{d}r \frac{2\pi r^2}{(\eta^2 - |\vec{x}_1'|^2 + 2|\vec{x}_1'| r u - r^2 - i\varepsilon)^2 (\eta^2 - r^2 - i\varepsilon)^2} \\
&= -\frac{4}{a^4 \pi^3} \int_{-\infty}^{0} \mathrm{d}\eta \int_0^{\infty} \mathrm{d}r \frac{r^2}{(\eta^2 - (|\vec{x}_1'| + r)^2 - i\varepsilon)(\eta^2 - (|\vec{x}_1'| - r)^2 - i\varepsilon)(\eta^2 - r^2 - i\varepsilon)^2}
\end{aligned}$$

It is clear that the argument of the integral is invariant under $r \to -r$ so the integration can be done over the whole real axis. By continuing the domain of r to the complex plane we see that the integrand of M has the following poles in r:

$$M(\vec{x}_1, \vec{x}_2) = -\frac{4}{a^4 \pi^3} \int_{-\infty}^{0} \mathrm{d}\eta \int_{-\infty}^{\infty} \mathrm{d}r r^2 \frac{1}{2} \frac{(\eta - i\varepsilon - |\vec{x}_1'| - r)^{-1} (\eta - i\varepsilon + |\vec{x}_1'| - r)^{-1} (\eta - i\varepsilon - r)^{-2}}{(\eta - i\varepsilon + |\vec{x}_1'| + r)(\eta - i\varepsilon - |\vec{x}_1'| + r)(\eta - i\varepsilon + r)^2}$$

$$\begin{aligned}
r_1 &= -\eta - x_1 + i\varepsilon & r_2 &= -\eta + x_1 + i\varepsilon \\
r_3 &= -\eta + i\varepsilon & r_4 &= \eta - x_1 - i\varepsilon \\
r_5 &= \eta + x_1 - i\varepsilon & r_6 &= \eta - i\varepsilon
\end{aligned}$$

By either closing the integration contour in the upper or lower half we see that we include either the poles r_1, r_2, r_3 or r_4, r_5, r_6 as the sign of $i\varepsilon$ is fixed by the sign convention of the metric. The choice does not matter so we pick the last three poles and integrate along the following contour:

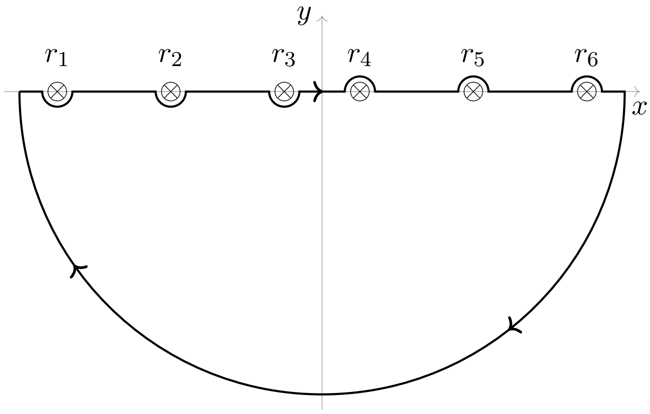

We use the Residue theorem to solve the r integral:

$$
\begin{aligned}
M(\vec{x}_1,\vec{x}_2) =& -\frac{4}{a^4\pi^3}\int\limits_{-\infty}^{\epsilon} \mathrm{d}\eta(-2\pi i)\left(\frac{(|\vec{x}_1'|-\eta)}{16\eta\,|\vec{x}_1'|^3\,(|\vec{x}_1'|-2\eta)^2}+\frac{(\eta+|\vec{x}_1'|)}{16\eta\,|\vec{x}_1'|^3\,(2\eta+|\vec{x}_1'|)^2}\right.\\
&\left.+\frac{1}{8\eta(|\vec{x}_1'|-2\eta)^2(2\eta+|\vec{x}_1'|)^2}\right)\\
=&\frac{2i}{a^4\pi^2}\int_{-\infty}^{\epsilon}\mathrm{d}\eta\frac{1}{\eta\left(|\vec{x}_1'|^2-4\eta^2\right)^2}=\frac{i}{a^4\pi^2\,|\vec{x}_1'|^4}\left(1+\ln\left(-\frac{4\epsilon^2}{|\vec{x}_1'|^2}\right)\right)+\mathcal{O}(\epsilon)\\
=&\frac{i}{a^4\pi^2\,|\vec{x}_1-\vec{x}_2|^4}\left(1+\ln\left(-\frac{4\epsilon^2}{|\vec{x}_1-\vec{x}_2|^2}\right)\right)+\mathcal{O}(\epsilon)
\end{aligned}
$$

where ϵ in this case is the cutoff before $\eta\to 0$ and the expansion is done around $\epsilon=0$.

Now that we calculated the mass shift we can take a closer look at the first part of (6.1) which is the propagator on the lightcone. In case of null separated points the geodesic distance (3.21) goes to 1. Therefore the propagator diverges at coinciding points. To regularize this divergence we do impose the dS invariant δ regularisation scheme described in section 4.1.2 (as it was done in [55, 56]):

$$
\begin{aligned}
&K\to K^\delta=\frac{K}{1+\delta}\\
\Rightarrow\; & i\Lambda_D(X,Y)\to-\frac{a^2}{4\pi^2}\frac{K^2}{(1+\delta+K)(1+\delta-K)}\xrightarrow{K\to 1}-\frac{a^2}{4\pi^2\delta(2+\delta)}
\end{aligned}
$$

As described in section 4.1.2 this regularization corresponds to carving out a ball of radius δ around the coinciding point and rescaling everything by $(1+\delta)^{-1}$. The complete one-loop tadpole diagram is then given by:

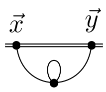

$$
\begin{aligned}
T_1(\vec{x},\vec{y})= \ldots =& i\Lambda_D(X,X)\frac{M(\vec{x},\vec{y})}{(1+\delta)^4}=-\frac{i}{4a^2\pi^4(1+\delta)^4\delta(2+\delta)}\frac{1}{|\vec{x}-\vec{y}|^4}\left(1+\ln\left(-\frac{4\epsilon^2}{|\vec{x}-\vec{y}|^2}\right)\right)\\
&\xrightarrow{\delta\to 0} i\left(\frac{1}{\delta}-\frac{9}{2}\right)\frac{1}{8a^2\pi^4}\frac{1}{|\vec{x}-\vec{y}|^4}\left(1+\ln\left(-\frac{4\epsilon^2}{|\vec{x}-\vec{y}|^2}\right)\right)
\end{aligned}
$$

Double tadpole The next term in the expansion of the two point function is the double tadpole which is given by:

$T_2(\vec{x}_1, \vec{x}_2) =$ 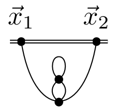

$$= \int \mathrm{d}^4 X \sqrt{g(X)} \int \mathrm{d}^4 Y \sqrt{g(Y)} \bar{\Lambda}_D(\vec{x}_1, X) i^2 \Lambda_D^2(X,Y) i\Lambda_D(Y,Y) \bar{\Lambda}_D(X, \vec{x}_2)$$

Again we use the regularization $K \to K/(1+\delta)$. Then the different parts in the integral become:

$$\begin{aligned} i\Lambda_D(Y,Y) &\to -\frac{a^2}{4\pi^2\delta(2+\delta)} \\ i^2\Lambda_D^2(X,Y) &\to \frac{a^4}{(4\pi^2)^2} \frac{K_{xy}^4}{((1+\delta)^2 - K_{xy}^2)^2} \\ \bar{\Lambda}_D(\vec{x}_1, X)\bar{\Lambda}_D(X, \vec{x}_2) &\to \frac{1}{(1+\delta)^4} \bar{\Lambda}_D(\vec{x}_1, X)\bar{\Lambda}_D(X, \vec{x}_2) \end{aligned}$$

The whole integral becomes:

$$\begin{aligned} T_2(\vec{x}_1, \vec{x}_2) = &- \frac{a^6}{(4\pi^2)^3} \frac{1}{\delta(2+\delta)(1+\delta)^4} \int \mathrm{d}^4 X \sqrt{g(X)} \bar{\Lambda}_D(\vec{x}_1, X)\bar{\Lambda}_D(X, \vec{x}_2) \\ &\times \underbrace{\int \mathrm{d}^4 Y \sqrt{g(Y)} \frac{K_{xy}^4}{(1+\delta-K_{xy})^2(1+\delta+K_{xy})^2}}_{:=\mathcal{K}} \end{aligned}$$

We concentrate now on the last part of the integral. In local coordinates this is given by:

$$\begin{aligned} \mathcal{K} &= a^{-4} \int \mathrm{d}^4 Y \sqrt{g(Y)} \frac{K_{xy}^4}{(1+\delta-K_{xy})^2(1+\delta+K_{xy})^2} \\ &= \int \mathrm{d}^4 Y \frac{16\eta_x^4}{\Big((1+\delta)^2(\eta_x^2+\eta_y^2-(x-y)^2)^2 - 4\eta_x^2\eta_y^2\Big)^2} \end{aligned}$$

To show that this part is independent of (η_x, x) we use translation invariance to shift the spatial part of the integral to $(\eta_y, y') = (\eta_y, y+x)$. Then $\mathcal{K}$ becomes:

$$\begin{aligned} \mathcal{K} &= a^{-4} \int \mathrm{d}^4 Y' \frac{16\eta_x^4}{\Big((1+\delta)^2(\eta_x^2+\eta_y^2-y'^2)^2 - 4\eta_x^2\eta_y^2\Big)^2} \\ &= a^{-4} \int \mathrm{d}^4 Y \frac{16\eta_x^4}{\Big[((1+\delta)(\eta_x^2+\eta_y^2-y'^2) + 2\eta_x\eta_y)((1+\delta)(\eta_x^2+\eta_y^2-y'^2) - 2\eta_x\eta_y)\Big]} \end{aligned}$$

To see that this is also independent of η_x we use scale invariance. It is easy to see that any rescaling of $\eta_x \to \lambda\eta_x$ can be undone be rescaling $(\eta_y, y') \to (\lambda\eta_y, \lambda y')$. Therefore we can fix η_x to any random value so we choose $\eta_x = -1$. Therefore we get:

$$\mathcal{K} = a^{-4} \int \mathrm{d}^4 Y \frac{16}{\Big[((1+\delta)(1+\eta_y^2-y'^2) + 2\eta_y)((1+\delta)(1+\eta_y^2-y'^2) - 2\eta_y)\Big]}$$

So T_2 factorizes into:

$$T_2(\vec{x}_1, \vec{x}_2) = \frac{a^6}{(4\pi^2)^3} \frac{1}{\delta(2+\delta)(1+\delta)^4} \times M(\vec{x}_1, \vec{x}_2) \times \mathcal{K}$$

As the integral $\mathcal{K}$ is symmetric under $\eta_y \to -\eta_y$ we can write it as an integral over $\eta_y \in]-\infty, \infty[$. We can do the spatial part of the integral in spherical coordinates. After integrating over the angular part we get:

$$\mathcal{K} = \frac{32\pi}{a^4} \int_{-\infty}^{\infty} \mathrm{d}\eta \int_0^{\infty} \mathrm{d}r \frac{r^2}{\left[((1+\delta)(\eta^2+1-r^2)+2\eta)((1+\delta)(\eta^2+1-r^2)-2\eta)\right]^2}$$

To execute the r integral we use again the residue theorem. After that the η integral can be calculated straightforwardly:

$$\begin{aligned}
\mathcal{K} &= \frac{32\pi}{a^4} i \int_{-\infty}^{\infty} \mathrm{d}\eta \frac{1}{64(1+\delta)^{3/2}\eta^3} \left(\frac{(1+\delta)(1+\eta^2)-\eta}{\sqrt{(\eta-1)^2+\delta(1+\eta^2)}} - \frac{(1+\delta)(1+\eta^2)+\eta}{\sqrt{(\eta+1)^2+\delta(1+\eta^2)}} \right) \\
&= \frac{i\pi^2}{2a^4(1+\delta)^{3/2}} \int_{-\infty}^{\infty} \mathrm{d}\eta \frac{1}{\eta^3} \left(\frac{(1+\delta)(1+\eta^2)-\eta}{\sqrt{(\eta-1)^2+\delta(1+\eta^2)}} - \frac{(1+\delta)(1+\eta^2)+\eta}{\sqrt{(\eta+1)^2+\delta(1+\eta^2)}} \right) \\
&= \frac{-i\pi^2}{a^4} \frac{2(1+\delta) + (2+\delta(2+\delta)) \ln\left(\frac{\delta}{2+\delta}\right)}{2(1+\delta)^3}
\end{aligned}$$

Therefore the complete double tadpole integral becomes:

$$T_2(\vec{x}_1, \vec{x}_2) = -\frac{i\pi^2 a^2}{(4\pi^2)^3} \frac{2(1+\delta) + (2+\delta(2+\delta)) \ln\left(\frac{\delta}{2+\delta}\right)}{2\delta(2+\delta)(1+\delta)^7} \times M(\vec{x}_1, \vec{x}_2)$$

For small δ this becomes:

$$\begin{aligned}
T_2(\vec{x}_1, \vec{x}_2) &= \frac{i\pi^2 a^2}{2(4\pi^2)^3} \left(\frac{14 + 13\ln\frac{\delta}{2}}{2} - \frac{1+\ln\frac{\delta}{2}}{\delta} \right) \times M(\vec{x}_1, \vec{x}_2) + \mathcal{O}(\delta) \\
&= -\frac{1}{2a^2(4\pi^2)^3} \left(\frac{14 + 13\ln\frac{\delta}{2}}{2} - \frac{1+\ln\frac{\delta}{2}}{\delta} \right) \frac{1}{\left|\underline{x}-\underline{y}\right|^4} \left(1 + \ln\left(-\frac{4\epsilon^2}{\left|\underline{x}-\underline{y}\right|^2} \right) \right)
\end{aligned}$$

Sunrise diagram The next second order diagram is the so called sunrise diagram. It is given by the following integral:

$$S(\vec{x}_1, \vec{x}_2) =$$

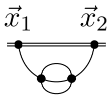

$$= \int \mathrm{d}^4X \int \mathrm{d}^4Y \sqrt{g(X)g(Y)} \bar{\Lambda}_D(\vec{x}_1, X) i^3 \Lambda_D^3(X, Y) \bar{\Lambda}_D(Y, \vec{x}_2)$$

Again using the same regularization as above this integral becomes:

$$S(\vec{x}_1, \vec{x}_2) = \frac{a^6}{(4\pi^2)^3(1+\delta)^4} \frac{1}{\pi^4} \int \mathrm{d}^4X \sqrt{g(X)} \bar{K}_{\vec{x}_1 Y}^2 \underbrace{\int \mathrm{d}^4Y \sqrt{g(Y)} \frac{K_{xy}^6}{(1+\delta+K_{xy})^3(1+\delta-K_{xy})^3} \bar{K}_{\vec{x}_2 x}^2}_{:=J}$$

We can split off one leg from the integral and calculate J first and then attaching the missing leg in the final step:

$$J(Y,\vec{x}_2)=\frac{a^6}{(4\pi^2)^3(1+\delta)^4}\frac{1}{\pi^4}\int \mathrm{d}^4Y\sqrt{g(Y)}\frac{K_{xy}^6}{(1+\delta+K_{xy})^3(1+\delta-K_{xy})^3}\bar{K}^2_{y,\vec{x}'_2}$$

We shift $\vec{x}_2$ and $\vec{x}$ by $-\vec{x}_2$ to $\vec{x}'_2=\vec{x}_2-\vec{x}_2=0$ and $\vec{x}'=\vec{x}-\vec{x}_2$. The integral then becomes:

$$J=\frac{a^6}{(4\pi^2)^3(1+\delta)^4}\frac{1}{\pi^4}\int \mathrm{d}^4Y\sqrt{g(Y)}\frac{K_{x'y}^6}{(1+\delta+K_{x'y})^3(1+\delta-K_{x'y})^3}\bar{K}^2_{y\vec{x}'_2}$$

Using inversion invariance to simplify the integral even further. Inversion in de Sitter space is given by (similarly to the transformations on the four point function in 4.1):

$$\begin{aligned}
&\eta\to\frac{\eta'}{\eta'^2-\vec{x}'^2};\qquad x_i\to\frac{x'_i}{\eta'^2-\vec{x}'^2}\\
&\Rightarrow K_{xy}=\frac{2\eta_x\eta_y}{\eta_x^2+\eta_y^2-(\vec{x}-\vec{y})^2}\to\frac{2\eta'_x\eta'_y}{{\eta'_x}^2+{\eta'_y}^2-(\vec{x}'-\vec{y}')^2}=K_{x'y'}\\
&\Rightarrow \bar{K}_{y\vec{x}_2}=\frac{\eta_y}{\eta_y^2-(\vec{y}-\vec{x}_2)^2}\to\frac{\eta'}{{\eta'_y}^2-\vec{y}'^2}=\left|\vec{x}'_2\right|^2\bar{K}_{y'\vec{x}'_2}
\end{aligned}$$

As the propagator in de Sitter space time is invariant under inversion we can use these identities to further simplify our integral for J. By shifting $\vec{x}$ and $\vec{x}_2$ by $-\vec{x}_2$ we set $\vec{x}'_2=0$. Now applying inversion of every point we send $\vec{x}'_2\to\vec{x}''_2=\frac{\vec{x}'_2}{\left|\vec{x}'_2\right|^2}=\infty$. Then the bulk-to-boundary propagator becomes:

$$\bar{K}_{y\vec{x}'_2}\to|\vec{x}''_2|^2\bar{K}_{y'\vec{x}''_2}\overset{|\vec{x}''_2|\to\infty}{\longrightarrow}\eta'_y$$

After shifting $\vec{y}''=\vec{y}'+\vec{x}''$ we can write J as:

$$\begin{aligned}
J=&\frac{2^6a^2\eta''^6_x}{(4\pi^2)^3(1+\delta)^4}\frac{1}{\pi^4}\int\frac{\mathrm{d}^4y'}{{\eta'_y}^4}\frac{{\eta'_y}^8((1+\delta)(\eta''^2_x+{\eta'_y}^2-\left|\underline{y}'\right|^2)+2\eta''_x\eta'_y)^{-3}}{((1+\delta)(\eta''^2_x+{\eta'_y}^2-\left|\underline{y}'\right|^2)-2\eta''_x\eta'_y)^3}\\
=&\frac{4a^2\eta''^6_x}{\pi^5(1+\delta)^4}\frac{1}{\pi^4}\int_{-\infty}^{0}\mathrm{d}\eta'_y\int_0^\infty\mathrm{d}r\frac{r^2{\eta'_y}^4((1+\delta)(\eta''^2_x+{\eta'_y}^2-r^2)+2\eta''_x\eta'_y)^{-3}}{((1+\delta)(\eta''^2_x+{\eta'_y}^2-r^2)-2\eta''_x\eta'_y)^3}\\
=&\frac{2a^2\eta''^6_x}{\pi^5(1+\delta)^4}\frac{1}{\pi^4}\int_{-\infty}^{+\infty}\mathrm{d}\eta'_y\int_0^\infty\mathrm{d}r\frac{r^2{\eta'_y}^4((1+\delta)(\eta''^2_x+{\eta'_y}^2-r^2)+2\eta''_x\eta'_y)^{-3}}{((1+\delta)(\eta''^2_x+{\eta'_y}^2-r^2)-2\eta''_x\eta'_y)^3}
\end{aligned}$$

In the last step the fact was used that the integral is symmetric under $\eta_y\to-\eta_y$ to extend the limits of the integral.

The integrand has four poles of third order:

$$r_{\pm1}=\pm\sqrt{\frac{(1+\delta)(\eta''^2_x+\eta_y^2)+2\eta''_x\eta_y}{1+\delta}}$$

$$r_{\pm 2} = \pm\sqrt{\frac{(1+\delta)(\eta_x''^2+\eta_y^2)-2\eta_x''\eta_y}{1+\delta}}$$

We extend the integral to the complex plane and choose an integral contour such that the two poles with positive sign are included. Then performing the η_y' integral gives:

$$\begin{aligned}J =& \frac{4ia^2\eta_x''^6}{\pi^8(1+\delta)^4}\frac{6\delta(\delta+2)+3\delta(\delta+1)(\delta+2)(\log(\delta)-\log(\delta+2))+2}{512\eta_x''^4\delta(\delta+1)^2(\delta+2)} \\ =& \frac{4ia^2\eta_x''^2}{\pi^8}\frac{6\delta(\delta+2)+3\delta(\delta+1)(\delta+2)\ln\frac{\delta}{\delta+2}+2}{512\delta(\delta+1)^6(\delta+2)}\end{aligned}$$

For the first order in δ this is:

$$J = \frac{4ia^2\eta_x''^2}{\pi^8}\frac{1}{2\cdot 4^4}\left(\frac{1}{\delta}+\frac{6\ln\frac{\delta}{2}-1}{2}\right) = \frac{2ia^2\eta_x''^2}{(4\pi^2)^4}\left(\frac{1}{\delta}+\frac{6\ln\frac{\delta}{2}-1}{2}\right)$$

Now we can revert the inversion we did before the integration and take back the shift by $-\vec{x}_2$:

$$\begin{aligned}\eta_x'' \to \frac{\eta_x}{\eta_x^2-\vec{x}'^2} &= \frac{\eta_x}{\eta_x^2-(\vec{x}-\vec{x}_2)^2} = \bar{K}_{x\vec{x}_2} \\ \Rightarrow J &= \frac{2ia^2}{(4\pi^2)^4}\left(\frac{1}{\delta}+\frac{6\ln\frac{\delta}{2}-1}{2}\right)\bar{K}^2_{x\vec{x}_2}\end{aligned}$$

So finally by attaching the missing leg to J we get the complete sunrise diagram:

$$\begin{aligned}S(\vec{x}_1,\vec{x}_2) &= \int \mathrm{d}^4X\sqrt{g(X)}\bar{K}^2_{\vec{x}_1x}J(x,\vec{x}_2) = \frac{2ia^2}{(4\pi^2)^4}\left(\frac{1}{\delta}+\frac{6\ln\frac{\delta}{2}-1}{2}\right)\int \mathrm{d}^4x\sqrt{g(x)}\bar{K}^2_{\vec{x}_1x}\bar{K}^2_{x\vec{x}_2} \\ &= \frac{ia^2\pi^2}{2(4\pi^2)^3}\left(\frac{1}{\delta}+\frac{6\ln\frac{\delta}{2}-1}{2}\right)M(\vec{x}_1,\vec{x}_2) \\ &= \frac{1}{4(4\pi^2)^3a^2}\left(\frac{1}{\delta}+\frac{6\ln\frac{\delta}{2}-1}{2}\right)\frac{1}{|\vec{x}-\vec{y}|^4}\left(1+\ln\left(\frac{4\epsilon^2}{|\vec{x}-\vec{y}|^2}\right)\right)\end{aligned}$$

We see that all the quantum corrections to the two point function can be absorbed into a mass shift counterterm. In quantum field theory in flat space time the common renormalization scheme requires then, that the on shell mass is fixed to be the physical mass. In this case the relevant on-shell quantity is the conformal dimension of the dual operator which is fixed to be $\Delta = 2$.

6.1.2 Four point function

The tree level contributions to the four point function is given by the second term in (3.63) with $n = 4$. It is obvious that doing the analytic continuation $\eta \to -iz$ this will correspond to the cross diagram from EAdS given in 5.1.

A similar argument holds for the one loop contribution to the second order four point function which is given by the diagram

$W_1(\vec{x}_1,\vec{x}_2,\vec{x}_3,\vec{x}_4) =$ 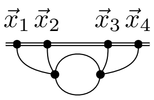

$$= \int \mathrm{d}^4X\mathrm{d}^4Y\sqrt{g(X)g(Y)}\bar{\Lambda}_D(\vec{x}_1,X)\bar{\Lambda}_D(\vec{x}_3,X)i^2\Lambda_D^2(X,Y)\bar{\Lambda}_D(Y,\vec{x}_2)\bar{\Lambda}_D(Y,\vec{x}_4)$$

We have done the explicit computation in de Sitter space for all the previous diagrams and we figured out that they give the same results as the ones obtained for Euclidean Anti-de-Sitter with an additional prefactor of $-i$ for each vertex. This makes sense from the point of view that de Sitter in Poincaré coordinates is just the double analytic continuation $z \to -i\eta$ and $a \to -ia$. Therefore we can simply use the results from EAdS chapter 5 and use this continuation to get the result. After renormalisation the one loop contribution to the four point function will therefore be just given by equation (5.28).

Consequently the dual CFT and the anomalous dimensions and OPE coefficients will be exactly the same as for the EAdS case. Note that we only did the explicit calculation for the two point function for the $\Delta = 2$ case, but the result for $\Delta = 1$ is just the same as can easily be checked by just replacing the propagators from the Dirichlet to Neumann boundary conditions in the above calculation.

Just as in EAdS we therefore have two deformed generalized free fields as the conformal duals to the wave function with different boundary conditions. Since there is now interaction between them, the two CFTs can be considered as direct product even after the deformation. As we will see in the following section this is not going to the case anymore for the cosmological correlator.

6.2 Cosmological correlator CFT

Finally we are going to calculate loop corrections to the cosmological correlators, by applying all the methods developed up to this point. This section is a partial reproduction of [90].

In this section we again focus entirely on the conformally coupled scalar field. As we noticed in section 3.3.2, perturbatively, this can be treated like a theory of two interacting scalar fields with boundary dimensions Δ_+ and Δ_- in EAdS, governed by the action (3.70). For the conformally coupled scalar field with $\Delta_+ = \frac{d+1}{2}$ and $\Delta_- = \frac{d-1}{2}$ with odd boundary dimensions d the action (3.71) then becomes

$$iS_c = -\int_0^\infty \frac{\mathrm{d}z\mathrm{d}^d\vec{x}}{z^{d+1}}\Big[-\left((\partial\phi^+)^2 - m^2{\phi^+}^2\right) + \left((\partial\phi^-)^2 - m^2{\phi^-}^2\right)$$
$$-(-1)^{\frac{d-1}{2}}\frac{2\lambda}{4!}\left({\phi^+}^4 - 6{\phi^+}^2{\phi^-}^2 + {\phi^-}^4\right)\Big]. \quad (6.2)$$

We will then be able to use the formalism from chapter 4 for evaluating the Witten diagrams.

The L-loop Witten diagrams between sets of fields of dimensions Δ_1 and Δ_2 are denoted by

$$W^{\Delta_1\Delta_2\Delta_3\Delta_4,D}_{L,dS}(\vec{x}_1,\vec{x}_2,\vec{x}_2,\vec{x}_4).$$

The case $(\Delta_1,\Delta_2,\Delta_3,\Delta_4) = (1,1,1,1)$ is evaluated in section 6.2.2, $(\Delta_1,\Delta_2,\Delta_3,\Delta_4) = (2,2,2,2)$ is evaluated in section 6.2.2, and the mixed correlators with $(\Delta_1,\Delta_2,\Delta_3,\Delta_4) = (2,2,1,1)$ and permutations are evaluated in section 6.2.2.

Using the normalization of the fields and the coupling constant introduced in (6.2) and the conformal mappings as described in section 4.1, we can write a generic EAdS four-point Witten diagram with equal external dimensions Δ as

$$W^{\Delta\Delta\Delta\Delta,D}_{L,\text{dS}}(\vec{x}_1,\ldots,\vec{x}_4) = \frac{a^4}{(4\pi^2)^{2L+4}} \mathcal{W}^{\Delta\Delta\Delta\Delta,D}_{L}(\vec{x}_1,\ldots,\vec{x}_4),$$

where $\mathcal{W}^{\Delta\Delta\Delta\Delta,D}_{L}$ is the corresponding Witten diagram in EAdS with standard normalization of the propagator as defined in section 3.3. The four-point function with mixed boundary conditions will be given by acting with the differential operator, defined in section 4.1.4, onto the corresponding legs of the $\Delta = 1$ Witten diagrams. All calculations will be done in the loop dependent dimensional regularisation scheme introduced and described in section 4.1.2.

6.2.1 Two-point functions

If we represent the propagators as

$\Lambda(X,Y;1) =$ 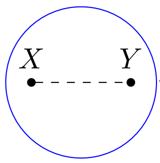

, $\Lambda(X,Y;2) =$ 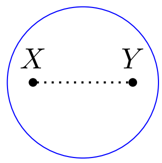

then the loop corrections to the boundary two-point function up to order λ^2 for $\Delta = 1$ correspond to the diagrams

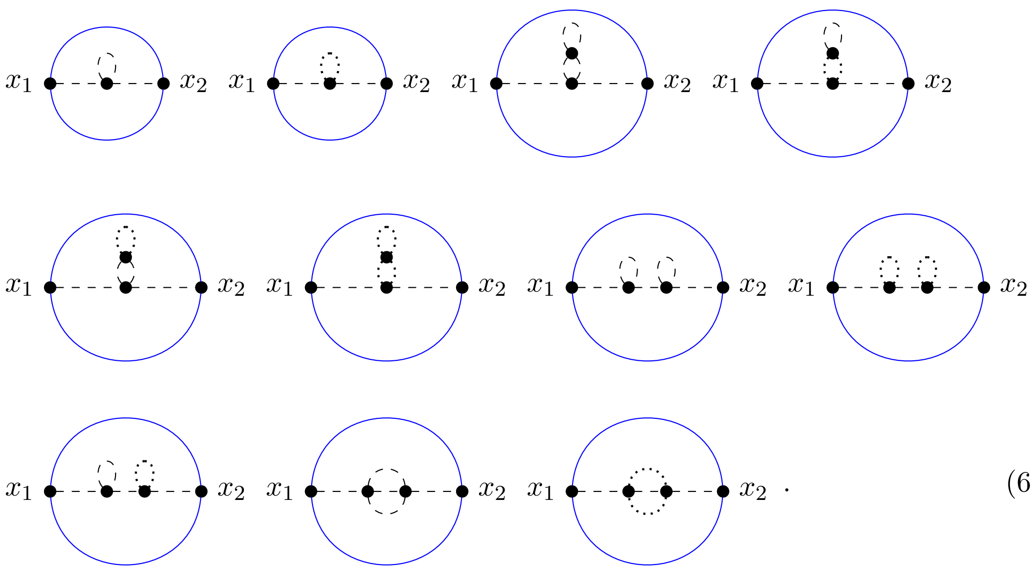

. (6.3)

For $\Delta = 2$ the diagrams are the same up to replacing the external lines by the $\Delta = 2$ bulk to boundary propagator.

Using the results from [55], it can be checked that the integrals appearing in (6.3) all reduce to a divergent piece times a mass-shift term. We can therefore use the same argument that the renormalized mass should be fixed at the value “measured” at the boundary, which in our case fixes the leading order fall off behaviour at future infinity to $\Delta = 1$. As a result, we can ignore the loop corrections to the two point function in the following calculation of the four-point function, and we will draw the renormalised propagators as

$\Lambda(X,Y;1) =$ 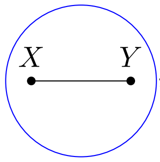

, $\Lambda(X,Y;2) =$ 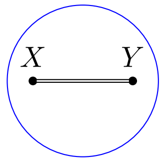

.

6.2.2 Four-point functions

Recalling (3.69), the dominant term contribution to the bulk scalar field ϕ is contained in ϕ^-. From this one may conclude that the four-point correlation function at future infinity is given by calculating the correlation functions of the auxiliary field ϕ^- at the boundary of EAdS, with action (6.2). However considering only ϕ^- as a boundary field one will not be able retrieve all the information of the dual CFT. This can also be seen form the bulk action (6.2) in which ϕ^- and ϕ^+ are coupled. To access the full CFT information we rather have to expand the four-point function to second subleading order in η_0, that is

$$\begin{aligned}
&\langle \phi_0(\vec{x_1})\phi_0(\vec{x_2})\phi_0(\vec{x_3})\phi_0(\vec{x_4})\rangle = \eta_0^{4\Delta_-}\left\langle \phi^-(\vec{x_1})\phi^-(\vec{x_2})\phi^-(\vec{x_3})\phi^-(\vec{x_4})\right\rangle \\
&+\eta_0^{2(\Delta_-+\Delta_+)}\left(\left\langle \phi^+(\vec{x_1})\phi^+(\vec{x_2})\phi^-(\vec{x_3})\phi^-(\vec{x_4})\right\rangle + \left\langle \phi^+(\vec{x_1})\phi^-(\vec{x_2})\phi^+(\vec{x_3})\phi^-(\vec{x_4})\right\rangle\right. \\
&\left.+\left\langle \phi^+(\vec{x_1})\phi^-(\vec{x_2})\phi^-(\vec{x_3})\phi^+(\vec{x_4})\right\rangle\right) + \eta_0^{4\Delta_+}\left\langle \phi^+(\vec{x_1})\phi^+(\vec{x_2})\phi^+(\vec{x_3})\phi^+(\vec{x_4})\right\rangle . \qquad (6.4)
\end{aligned}$$

$\langle \phi^-\phi^-\phi^-\phi^-\rangle$

The contributions to the leading term of the late time expansion of the four-point correlation function in equation (6.4) is given by

$\langle \phi^-(x_1)\phi^-(x_2)\phi^-(x_3)\phi^-(x_4)\rangle = \Bigg($ 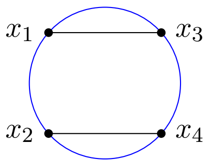

$+\,2$ perm.$\Bigg) - \lambda$ 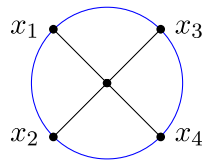

$+\dfrac{\lambda^2}{2}\Bigg($ 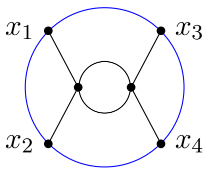

$+\,2$ perm.$\Bigg) + \dfrac{\lambda^2}{2}\Bigg($ 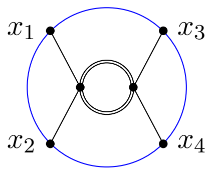

$+\,2$ perm.$\Bigg) + \mathcal{O}(\lambda^3)$.

(6.5)

- The disconnected part is given by the product of two-point functions

$$\begin{aligned}
&\langle \phi^-(x_1)\phi^-(x_2)\rangle\langle \phi^-(x_3)\phi^-(x_4)\rangle + \langle \phi^-(x_1)\phi^-(x_3)\rangle\langle \phi^-(x_2)\phi^-(x_4)\rangle \\
&\qquad + \langle \phi^-(x_1)\phi^-(x_4)\rangle\langle \phi^-(x_2)\phi^-(x_3)\rangle = \frac{2^2a^4}{(4\pi^2)^2}\frac{1}{x_{12}^2x_{34}^2}\left(1+v+\frac{v}{(1-Y)}\right) .
\end{aligned}$$

Here we follow the notation and conventions of [57] for the cross-ratio

$$v = \frac{x_{12}^2x_{34}^2}{x_{14}^2x_{23}^2} = \zeta\bar{\zeta}; \qquad 1-Y = \frac{x_{13}^2x_{24}^2}{x_{14}^2x_{23}^2} = (1-\zeta)(1-\bar{\zeta})\,.$$

where $x_{ij}^2 = |\vec{x_i} - \vec{x_j}|^2$.
• The cross terms is given by the $\Delta = 1$ term in EAdS

$$\mathcal{W}_0^{1111,D}(\zeta,\bar{\zeta}) = \frac{1}{2}\frac{v^\Delta}{x_{12}^2 x_{34}^2}\int_{\mathbb{R}^D} \frac{\mathrm{d}^D X}{\|X-u_1\|^{2(D-4)}} \frac{1}{\|X\|^2\,\|X-u_\zeta\|^2\,\|X-u_1\|^2}\,, \tag{6.6}$$

where the norm is defined with a euclidean signature

$$\|X\|^2 = z^2 + \vec{x}^2$$

and the radial coordinate z is expressed with the help of the normal vector to the boundary $u = (0,0,0,1)$ such that

$$u \cdot X = z.$$

• For the one-loop contributions we use the following expression for the square of the propagator:

$$\begin{aligned}\tilde{\Lambda}(X_1,X_2;\Delta)^2 = \frac{(u\cdot X_1)^2\,(u\cdot X_2)^2}{\|X_1-X_2\|^4} + \frac{(u\cdot X_1)^2\,(u\cdot \sigma(X_2))^2}{\|X_1-\sigma(X_2)\|^4}\\ -\frac{(-1)^\Delta}{2}\left(\frac{u\cdot X_1\,u\cdot X_2}{\|X_1-X_2\|^2}+\frac{u\cdot X_1\,u\cdot\sigma(X_2)}{\|X_1-\sigma(X_2)\|^2}\right),\end{aligned}$$

where $\sigma(X)$ is the antipodal map after Wick rotation

$$\sigma(\vec{x},z) = (\vec{x},-z).$$

Then, by regrouping contributions from the $\Delta = 1$ and $\Delta = 2$ fields propagating in the loops in (6.5), one can see that for the sum, over Δ, of the propagators squared the cross-terms cancel so that

$$\tilde{\Lambda}(X_1,X_2;1)^2 + \tilde{\Lambda}(X_1,X_2;2)^2 = 2\frac{(u\cdot X_1)^2\,(u\cdot X_2)^2}{\|X_1-X_2\|^4} + 2\frac{(u\cdot X_1)^2\,(u\cdot\sigma(X_2))^2}{\|X_1-\sigma(X_2)\|^4}. \tag{6.7}$$

After unfolding the integral to the whole space $\mathbb{R}^4$ the one-loop contribution, in the s-channel, for four external scalars of the same dimension Δ adds up to

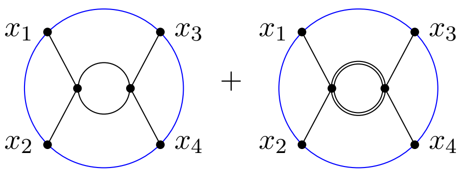

(6.8)

$$= \frac{2^{4\Delta}a^4}{(4\pi^2)^6}\int_{(\mathbb{R}^D)^2} \mathrm{d}^D X \mathrm{d}^D Y \frac{(u\cdot X)^{2\Delta-2}(u\cdot Y)^{2\Delta-2}}{\|X-Y\|^4\,\|X-x_1\|^2\,\|X-x_2\|^2\,\|Y-x_3\|^2\,\|Y-x_4\|^2}\,,$$

with similar expressions for the other channels. Finally, performing the conformal mappings as described in [57] the integrand of equation (6.8) takes the form

$$\mathcal{W}_{1,\mathrm{div}}^{\Delta,4-2\epsilon,\underline{s}} = \frac{(\zeta\bar{\zeta})^\Delta}{(x_{12}^2 x_{34}^2)^\Delta}\int_{\mathbb{R}^{2D}} \frac{\mathrm{d}^{4-2\epsilon}X_1 \mathrm{d}^{4-2\epsilon}X_2 (u\cdot X_1)^{2\Delta-2}(u\cdot X_2)^{2\Delta-2}}{\|X_1\|^{2\Delta}\,\|X_1-u_\zeta\|^{2\Delta}\,\|X_2-u_1\|^{2\Delta-4\epsilon}\,\|X_1-u_1\|^{-4\epsilon}\,\|X_1-X_2\|^4}\,,$$

where the subscript "div" indicates that the integral is divergent and $\epsilon = \frac{4-D}{2}$ is a regulator. The contributions to the other channels are given in the appendix in equation (C.1).

These integrals were already calculated in chapter 5 and the results are given in appendix C.1. Note that, because of (6.7), the elliptic sector, which was present in the one-loop EAdS computation for $\Delta = 1$, cancels out. By consequence, the loop integrals are linearly reducible [102] and thus can be expressed in terms of multiple polylogarithms using the program `HyperInt` [137]. The entire four-point function then becomes

$$\left\langle \phi^-(x_1)\phi^-(x_2)\phi^-(x_3)\phi^-(x_4)\right\rangle = \frac{2^2 a^4}{(4\pi^2)^2}\Bigg[\frac{1}{x_{12}^2 x_{34}^2}\left(1+v+\frac{v}{1-Y}\right) - \frac{2^2\lambda}{(4\pi^2)^2}\mathcal{W}_0^{1111,4-4\epsilon}(v,Y)$$
$$+\frac{2^2\lambda^2}{(4\pi^2)^4}\left(-\frac{3\pi^2}{\epsilon}\mathcal{W}_0^{1111,4-4\epsilon}(v,Y)+\frac{\pi^4 v}{2x_{12}^2x_{34}^2}\sum_{i\in\{s,t,u\}}L_0^{1,i}(v,Y)\right)+\mathcal{O}(\lambda^3)\Bigg].$$

The integrals $\mathcal{W}_0^{1111,4-4\epsilon}(v,Y)$ and $L_0^{1,i}$ have been evaluated in chapter 5. We have recalled their expressions in (C.13) for $L_0^{1,i}$.

$\langle \phi^+\phi^+\phi^+\phi^+\rangle$

The contributions to the $\phi^+\phi^+\phi^+\phi^+$ term of the late time expansion of the four point correlation function in equation (6.4) are given by

$\left\langle \phi^+(x_1)\phi^+(x_2)\phi^+(x_3)\phi^+(x_4)\right\rangle = \Bigg($ 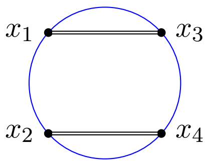 $+\,2$ perm.$\Bigg) - \lambda$ 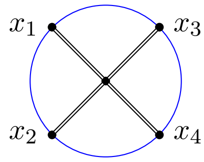

$+\,\frac{\lambda^2}{2}\Bigg($ 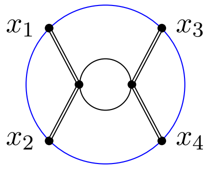 $+\,2$ perm.$\Bigg) + \frac{\lambda^2}{2}\Bigg($ 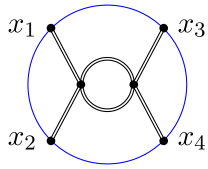 $+\,2$ perm.$\Bigg) + \mathcal{O}(\lambda^3)$.

• The cross term is again just given by the same expression as the $\Delta = 2$ cross in EAdS, given in appendix B.
• Since the squares of the bulk-to-bulk propagators are the same, similar arguments as for the $\Delta = 1$ case hold, i.e. the result can be written as a sum of the divergent and finite parts of the one-loop Witten diagrams with $\Delta = 2$. The details are given in appendix C.1.

The entire four-point function at this order is therefore given by

$$\left\langle \phi^+(x_1)\phi^+(x_2)\phi^+(x_3)\phi^+(x_4)\right\rangle = \frac{2^4 a^4}{(4\pi^2)^2}\Bigg[\frac{1}{x_{12}^4 x_{34}^4}\left(1+v^2+\frac{v^2}{(1-Y)^2}\right)$$
$$-\frac{2^4\lambda}{(4\pi^2)^2}\mathcal{W}_0^{2,4-4\epsilon} - \frac{2^4\lambda^2}{(4\pi^2)^4}\Bigg(-\frac{3\pi^2}{\epsilon}\mathcal{W}_0^{2222,4-4\epsilon}(v,Y)$$
$$+3\pi^2\mathcal{W}_0^{2222,4}(v,Y)+\frac{1}{2}\sum_{j\in\{s,t,u\}}\mathcal{W}_{1,\mathrm{fin}}^{2222,j}(v,Y)+\frac{\pi^4 v}{2x_{12}^2x_{34}^2}\sum_{i\in\{s,t,u\}}L_0^{2,i}(v,Y)\Bigg)+\mathcal{O}(\lambda^3)\Bigg]$$

where $\mathcal{W}_{1,\mathrm{fin}}^{2222,j}$ and $L_0^{2,i}$ have been calculated in chapter 5 and recalled in (C.10) and (C.14) respectively. In fact, as described in chapter 4 there is a differential relation between the correlators with ϕ^+ and ϕ^- external legs. We will make use of this in the next subsection.

Mixed correlators

Additionally, we have the correlation functions of ϕ^+ with ϕ^-, which are sub-leading in the late-time expansion. They are equivalent up to permutation of the operators $\phi^-(x_i), \phi^+(x_j)$ so we will only calculate $\langle \phi^+(x_1)\phi^+(x_2)\phi^-(x_3)\phi^-(x_4)\rangle$ and discuss the other combinations at the end of section 6.2.3.

The diagrams we calculate are given by

$$\Big\langle \phi^+(x_1)\phi^+(x_2)\phi^-(x_3)\phi^-(x_4)\Big\rangle =$$
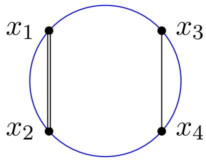

$$+\lambda$$
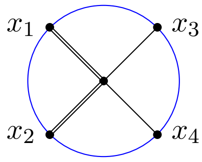

$$-\lambda^2 \Bigg(\frac{1}{2}$$
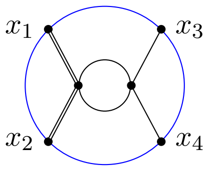

$$+\frac{1}{2}$$
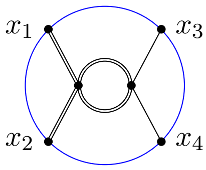

$$+$$
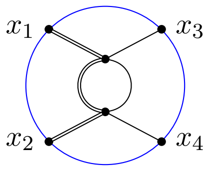

$$+$$
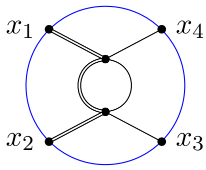

$$\Bigg).$$

• The disconnected part only contains the product of two propagators and is therefore given by

$$\Big\langle \phi^+(x_1)\phi^+(x_2)\phi^-(x_3)\phi^-(x_4)\Big\rangle = \frac{2^3 a^4}{2^2(4\pi^2)^2}\frac{1}{x_{12}^4 x_{34}^2}$$

• The tree-level contribution can be inferred from (6.6) by acting on the latter with

$$\mathcal{H}_{12} = \frac{1}{x_{12}^2}\left(2\Delta - 2v\frac{\partial}{\partial v}\right).$$

Thus,

$$W_{0,\mathrm{dS}}^{2211,4-4\epsilon}(\vec{x}_1,\ldots,\vec{x}_4) = \frac{2^6 a^4}{(4\pi^2)^4}\frac{1}{4}\mathcal{H}_{12}\mathcal{W}_0^{1111,4-4\epsilon}(\vec{x}_1,\ldots,\vec{x}_4). \tag{6.9}$$

To compute the right-hand-side we express $\mathcal{W}_0^{1111,4-4\epsilon}(\vec{x}_1,\ldots,\vec{x}_4)$ in parametric representation and act with $\mathcal{H}_{12}$ before expanding the result in ϵ. See section 4.1.4 and appendix B for more details with $\mathcal{W}_0^{2211,4-4\epsilon}(\vec{x}_1,\ldots,\vec{x}_4)$ there, related to (6.9) as

$$W_{0,\mathrm{dS}}^{2211,4-4\epsilon}(\vec{x}_1,\ldots,\vec{x}_4) = \frac{2^6 a^4}{(4\pi^2)^4}\mathcal{W}_0^{2211,4-4\epsilon}(\vec{x}_1,\ldots,\vec{x}_4)\,.$$

The one-loop contributions can be obtained in the same way. We observe that the sum of the first two terms contains a term like equation (6.7). The same arguments apply therefore for the cancellation of the mixed terms and, we get

$\frac{1}{2}$ 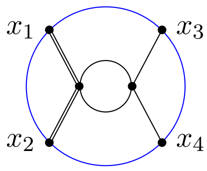

$+\frac{1}{2}$ 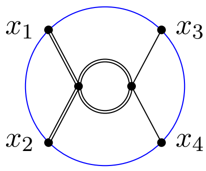

$$= \frac{1}{2}\frac{2^6 a^4}{(4\pi^2)^6}\int_{(\mathbb{R}^D)^2} \mathrm{d}^D X \mathrm{d}^D Y \frac{(u\cdot X)^2}{\|X-Y\|^4\,\|X-x_1\|^4\,\|X-x_2\|^4\,\|Y-x_3\|^2\,\|Y-x_4\|^2}\,.$$

It is not hard to see that this integral is given by acting with $\mathscr{H}_{12}$ on $\mathscr{W}^{1,4-2\epsilon,s}_{1,\mathrm{div}}$ giving

$$\begin{aligned} W^{2211,4-2\epsilon,s}_{1,\mathrm{dS}}(\vec{x}_1,\dots,\vec{x}_4) &= \frac{1}{2}\frac{2^6a^4}{(4\pi^2)^6}\frac{1}{4}\mathscr{H}_{12}\mathscr{W}^{1,4-2\epsilon,s}_{1,\mathrm{div}}(\vec{x}_1,\dots,\vec{x}_4),\\ &=: \frac{2^6a^4}{(4\pi^2)^6}\mathscr{W}^{2211,4-2\epsilon,s}_{1}(\vec{x}_1,\dots,\vec{x}_4) \end{aligned}$$

where $\mathscr{W}^{2211,4-2\epsilon,s}_{1}$ is given in appendix C.2.

For the last two terms we use the fact that the propagators can be expressed as (see section 4.1 for details):

$$\begin{aligned} \Lambda(X,Y;1) &= -\left(\frac{a}{2\pi}\right)^2\left(\frac{zw}{\|X-Y\|^2}+\frac{zw}{\|X-\sigma(Y)\|^2}\right),\\ \Lambda(X,Y;2) &= -\left(\frac{a}{2\pi}\right)^2\left(\frac{zw}{\|X-Y\|^2}-\frac{zw}{\|X-\sigma(Y)\|^2}\right). \end{aligned}$$

Therefore the product appearing in the Witten diagrams is given by:

$$\Lambda(X,Y;1)\Lambda(X,Y;2) = \left(\frac{a}{2\pi}\right)^4\left[\frac{(zw)^2}{\|X-Y\|^4}-\frac{(zw)^2}{\|X-\sigma(Y)\|^4}\right] \tag{6.10}$$

We can unfold the region of integration of the last two diagrams from $(\mathscr{H}^+_D)^2$ to $\mathbb{R}^{2D}$ by using that the measure of integration is odd under the action of the antipodal map, like the product of propagators in (6.10). We then have

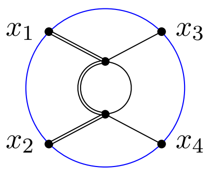

$$\propto \int_{(\mathscr{H}^+_D)^2}\frac{\mathrm{d}^DX\mathrm{d}^DY}{z^4w^4}\left(\frac{(zw)^2}{\|X-Y\|^4}-\frac{(zw)^2}{\|X-\sigma(Y)\|^4}\right) \times\frac{(zw)^3}{\|X-x_1\|^4\,\|Y-x_2\|^4\,\|X-x_3\|^2\,\|Y-x_4\|^2} \tag{6.11}$$

since $\|X-\sigma(Y)\|^2 = (\vec{x}-\vec{y})^2+(z+w)^2$ we unfold the Y integral to the full space $\mathbb{R}^D$ to get

$$(6.11) = \int_{\mathscr{H}^+_D}\frac{\mathrm{d}^DX}{z^4}\int_{\mathbb{R}^D}\frac{\mathrm{d}^DY}{w^4}\frac{(zw)^2}{(\|X-Y\|^2)^2}\frac{(zw)^3}{(\|X-x_1\|^2\,\|Y-x_2\|^2)^2\,\|X-x_3\|^2\,\|Y-x_4\|^2}.$$

We then unfold the z integration to the full space $\mathbb{R}^D$ to get

$$(6.11) = \frac{1}{2}\int_{\mathbb{R}^D}\frac{\mathrm{d}^D X}{z^4}\int_{\mathbb{R}^D}\frac{\mathrm{d}^D Y}{w^4}\frac{(zw)^2}{(\|X-Y\|^2)^2}\frac{(zw)^3}{(\|X-x_1\|^2\,\|Y-x_2\|^2)^2\,\|X-x_3\|^2\,\|Y-x_4\|^2}.$$

Including the correct normalization we end up with

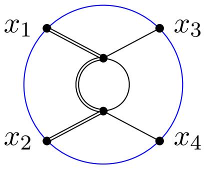

$$= \frac{1}{2}\frac{2^6 a^4}{(4\pi^2)^6}\int_{(\mathbb{R}^D)^2}\mathrm{d}^D X \mathrm{d}^D Y$$

$$\times\frac{(u\cdot X)(u\cdot Y)}{\|X-Y\|^4\,\|X-x_1\|^4\,\|Y-x_2\|^4\,\|X-x_3\|^2\,\|Y-x_4\|^2}.$$

Again, this integral is given by acting with $\mathcal{H}_{12}$ on $\mathcal{W}^{1,4-2\epsilon,t}_{1,\mathrm{div}}$ in equation (C.1). The same applies to the last diagram with respect to $\mathcal{W}^{1,4-2\epsilon,u}_{1,\mathrm{div}}$ and we obtain for these two contributions

$$\begin{aligned} W^{2211,4-2\epsilon,i}_{1,\mathrm{dS}}(\vec{x}_1,\ldots,\vec{x}_4) &= \frac{1}{2}\frac{2^6 a^4}{(4\pi^2)^6}\frac{1}{4}\mathcal{H}_{12}\mathcal{W}^{1,4-2\epsilon,i}_{1,\mathrm{div}}(\vec{x}_1,\ldots,\vec{x}_4),\\ &=: \frac{2^6 a^4}{(4\pi^2)^6}\mathcal{W}^{2211,4-2\epsilon,i}_{1}(\vec{x}_1,\ldots,\vec{x}_4)\end{aligned}$$

where $\mathcal{W}^{2211,4-2\epsilon,i}_1$ with $i\in\{s,t,u\}$ is given in appendix C.2. The complete four-point function is therefore given by

$$\begin{aligned}\left\langle\phi^+(x_1)\phi^+(x_2)\phi^-(x_3)\phi^-(x_4)\right\rangle = \frac{2^3 a^4}{(4\pi^2)^2}\Bigg[&\frac{1}{x_{12}^4 x_{34}^2}+\frac{2^3\lambda}{(4\pi^2)^2}\mathcal{W}^{2211,4-4\epsilon}_0\\ &-\frac{2^3\lambda^2}{(4\pi^2)^4}\left(-\frac{3\pi^2}{\epsilon}\mathcal{W}^{2211,4-4\epsilon}_0+\sum_{i\in\{s,t,u\}}\mathcal{W}^{2211,4,i}_{1,\mathrm{finite}}\right)\Bigg].\end{aligned}$$

with $\mathcal{W}^{2211,4,i}_{1,\mathrm{finite}}$ given in equations (C.19).
The correlation functions $\langle\phi^+(x_1)\phi^-(x_2)\phi^+(x_3)\phi^-(x_4)\rangle$ and $\langle\phi^+(x_1)\phi^-(x_2)\phi^-(x_3)\phi^+(x_4)\rangle$ can be obtained from this result by exchanging external points accordingly. This, however, only works after regularisation as we will discuss in the next section.

6.2.3 Renormalization and finite result

To simplify the calculation in EAdS we changed the normalisation of the fields $\phi^\pm$ and the coupling constant λ in the auxiliary action (6.2). However if we want to interpret our result in terms of a de Sitter calculation we have to reverse that procedure, especially if we want to compare the β function with the well-known flat-space result. At leading order they should coincide, since the leading short distance divergence does not depend on the global geometry.

Following the same arguments as in section 5.2.1, we introduce the renormalized coupling constant λ_R through the divergent bare coupling as $\lambda = \lambda_R(a\mu)\mu^{2\epsilon}+\delta\lambda$.

Then, up to finite terms, the connected part of the four-point functions is given by

$$
\begin{aligned}
&\frac{2^{\sum_i \Delta_i} a^4}{(8\pi^2)^4}(\mu a)^{4\epsilon}\Big(2\lambda_R \mathcal{W}_0^{\Delta_1\Delta_2\Delta_3\Delta_4,4-4\epsilon} + \frac{\lambda_R^2}{16\pi^4}\frac{3\pi^2}{\epsilon}\mathcal{W}_0^{\Delta_1\Delta_2\Delta_3\Delta_4,4-4\epsilon}\Big)\\
&\qquad = \frac{2^{\Delta_1+\cdots+\Delta_4}a^4 2}{(8\pi^2)^4}(\mu a)^{4\epsilon}\left(\lambda_R + \frac{3\lambda_R^2}{32\pi^2\epsilon}\right)\mathcal{W}_0^{\Delta_1\Delta_2\Delta_3\Delta_4,4-4\epsilon}\\
&\qquad =: \frac{2^{\Delta_1+\cdots+\Delta_4}a^4 2}{(8\pi^2)^4}\mu^{2\epsilon}\lambda \mathcal{W}_0^{\Delta_1\Delta_2\Delta_3\Delta_4,4-4\epsilon}.
\end{aligned}
\tag{6.12}
$$

This determines the counter-term

$$
\delta\lambda = -\frac{3\lambda_R^2\mu^{2\epsilon}}{32\pi^2\epsilon}
$$

while the finite $\log\mu$ contribution to λ gives rise to the Callan-Symanzik equation

$$
0 = \frac{\mathrm{d}}{\mathrm{d}\log\mu}\lambda,
$$

which leads to the leading order contribution to the beta function

$$
\beta = \frac{3\lambda_R^2}{16\pi^2} + \mathcal{O}(\lambda_R^3)
$$

coinciding with the flat space result.

After renormalisation with a minimal subtraction scheme and restoring the canonical normalisation of the fields and coupling constant, from a dS point of view, we obtain the following finite results for the four-point functions with equal external dimensions $\Delta_- = 1$ or $\Delta_+ = 2$

$$
\begin{aligned}
\langle\phi^\pm(x_1)\phi^\pm(x_2)\phi^\pm(x_3)\phi^\pm(x_4)\rangle = \frac{2^{2\Delta_\pm}a^4}{(8\pi^2)^2}\Bigg[&\frac{1}{x_{12}^{2\Delta_\pm}x_{34}^{2\Delta_\pm}}\left(1 + v^{\Delta_\pm} + \frac{v^{\Delta_\pm}}{(1-Y)^{\Delta_\pm}}\right)\\
&- \frac{2^{2\Delta_\pm}2\lambda_R}{(8\pi^2)^2}\mathcal{W}_0^{\Delta_\pm\Delta_\pm\Delta_\pm\Delta_\pm,4} + \frac{2^{2\Delta_\pm}4\lambda_R^2}{(8\pi^2)^4}\sum_{i\in\{s,t,u\}}\mathcal{W}_{1,\text{finite}}^{\Delta_\pm\Delta_\pm\Delta_\pm\Delta_\pm,i}\Bigg],
\end{aligned}
$$

where $\mathcal{W}_0^{1111,4}$ is given in (5.4), $\mathcal{W}_0^{2222,4}$ is given in (5.5), $\mathcal{W}_{1,\text{finite}}^{1111,i}$ are given in (C.8) and $\mathcal{W}_{1,\text{finite}}^{2222,i}$ are given in (C.12). The mixed correlator is given by

$$
\left\langle\phi^+(x_1)\phi^+(x_2)\phi^-(x_3)\phi^-(x_4)\right\rangle = \frac{a^4}{8\pi^4}\left[\frac{1}{x_{12}^4x_{34}^2} + \frac{\lambda_R}{4\pi^4}\mathcal{W}_0^{2211,4} + \frac{\lambda_R^2}{128\pi^8}\sum_{i\in\{s,t,u\}}\mathcal{W}_{1,\text{finite}}^{2211,i}\right],
\tag{6.13}
$$

where the term $\mathcal{W}_0^{2211,4}$ is given in (B.1) and $\mathcal{W}_{1,\text{finite}}^{2211,i}$ are given in (C.19).

Note, that we considered the tree-level four-point function in $D = 4-4\epsilon$ dimensions in equation (6.12), meaning that the counter term contains a finite piece, given by the coefficient of the $\mathcal{O}(\epsilon)$ contribution to $\mathcal{W}_0^{\Delta_1\Delta_2\Delta_3\Delta_4,4-4\epsilon}$. As discussed in section 5.2.1 this is done to restore the global AdS symmetry in the bulk, guaranteeing that the renormalized four-point function transforms homogeneously under dilatations on the boundary. As a consequence one should be able to obtain the four-point functions $\langle\phi^+(x_1)\phi^-(x_2)\phi^+(x_3)\phi^-(x_4)\rangle$ and $\langle\phi^+(x_1)\phi^-(x_2)\phi^-(x_3)\phi^+(x_4)\rangle$ by simple permutation of the external points in equation (6.13), resulting in transformations on the conformal cross-ratios.

Concretely, the correlation function $\langle\phi^+(x_1)\phi^-(x_2)\phi^+(x_3)\phi^-(x_4)\rangle$ is obtained from (6.13) by making the replacements $x_2 \leftrightarrow x_3$ which corresponds to $\zeta \to 1-\zeta, \bar{\zeta} \to 1-\bar{\zeta}$ or $(v, 1-Y) \to (1-Y, v)$. Similarly, $\langle\phi^+(x_1)\phi^-(x_2)\phi^-(x_3)\phi^+(x_4)\rangle$ is obtained from (6.13) by making the replacements $x_2 \leftrightarrow x_4$ which corresponds to $\zeta \to \frac{1}{\zeta}, \bar{\zeta} \to \frac{1}{\bar{\zeta}}$ or $(v, 1-Y) \to (1/v, (1-Y)/v)$. We checked explicitly, that this holds for our result, providing an additional test for the loop dependent regularisation scheme introduced in section 5.2.1 to restore the conformal symmetry on the boundary, which is a priori broken by naive dimensional regularisation.

6.3 Conformal block expansion

We have seen in the last section that we can interpret the leading- and subleading expansion coefficients of the field at late times as operators, $\mathcal{O}_1$ and $\mathcal{O}_2$, of dimension $\Delta = 1$ and $\Delta = 2$ respectively, living on the euclidean $\mathbb{R}^3$ hypersurface at future infinity. Furthermore, since we have an auxiliary EAdS action for the correlation functions of the latter, we conclude that the theory on the boundary should, at least perturbatively, be described by a dual CFT.

In total there are five different four-point functions to be considered for describing this CFT. We write the possible OPEs between the operators $\mathcal{O}_1$ and $\mathcal{O}_2$ schematically as

$$\begin{aligned}
\mathcal{O}_1(x_1) \times \mathcal{O}_1(x_2) &\sim \sum_{\tilde{\mathcal{O}}} a^{11}_{\tilde{\mathcal{O}}} \tilde{\mathcal{O}}(x_2), \\
\mathcal{O}_2(x_1) \times \mathcal{O}_2(x_2) &\sim \sum_{\tilde{\mathcal{O}}} a^{22}_{\tilde{\mathcal{O}}} \tilde{\mathcal{O}}(x_2), \\
\mathcal{O}_1(x_1) \times \mathcal{O}_2(x_2) &\sim \sum_{\tilde{\mathcal{O}}} a^{12}_{\tilde{\mathcal{O}}} \tilde{\mathcal{O}}(x_2)\,,
\end{aligned} \tag{6.14}$$

where $a^{ij}_{\tilde{\mathcal{O}}}$ are OPE coefficients and "$\sim$" means that the contributions of descendant operators are implicit.

In terms of conformal blocks [109], the general form of the five four-point functions we have to consider is

$$\langle\mathcal{O}_1(x_1)\mathcal{O}_1(x_2)\mathcal{O}_1(x_3)\mathcal{O}_1(x_4)\rangle = \frac{1}{x_{12}^2 x_{34}^2} \sum_{\tilde{\mathcal{O}},l} (a^{11}_{\tilde{\mathcal{O}}})^2 \mathcal{G}_{\tilde{\mathcal{O}},l}, \tag{6.15a}$$

$$\langle\mathcal{O}_2(x_1)\mathcal{O}_2(x_2)\mathcal{O}_1(x_3)\mathcal{O}_1(x_4)\rangle = \frac{1}{x_{12}^4 x_{34}^2} \sum_{\tilde{\mathcal{O}},l} a^{22}_{\tilde{\mathcal{O}}} a^{11}_{\tilde{\mathcal{O}}} \mathcal{G}_{\tilde{\mathcal{O}},l}, \tag{6.15b}$$

$$\langle\mathcal{O}_2(x_1)\mathcal{O}_1(x_2)\mathcal{O}_2(x_3)\mathcal{O}_1(x_4)\rangle = \frac{1}{(x_{12}^2 x_{34}^2)^{\frac{3}{2}}} \left(\frac{x_{24}^2}{x_{13}^2}\right)^{\frac{1}{2}} \sum_{\tilde{\mathcal{O}},l} (a^{12}_{\tilde{\mathcal{O}}})^2 \mathcal{G}_{\tilde{\mathcal{O}},l},$$

$$\langle\mathcal{O}_2(x_1)\mathcal{O}_1(x_2)\mathcal{O}_1(x_3)\mathcal{O}_2(x_4)\rangle = \frac{1}{(x_{12}^2 x_{34}^2)^{\frac{3}{2}}} \frac{(x_{24}^2 x_{13}^2)^{\frac{1}{2}}}{x_{14}^2} \sum_{\tilde{\mathcal{O}},l} (a^{12}_{\tilde{\mathcal{O}}})^2 \mathcal{G}_{\tilde{\mathcal{O}},l},$$

$$\langle\mathcal{O}_2(x_1)\mathcal{O}_2(x_2)\mathcal{O}_2(x_3)\mathcal{O}_2(x_4)\rangle = \frac{1}{x_{12}^4 x_{34}^4} \sum_{\tilde{\mathcal{O}},l} (a^{22}_{\tilde{\mathcal{O}}})^2 \mathcal{G}_{\tilde{\mathcal{O}},l}. \tag{6.15c}$$

where $\mathcal{G}_{\tilde{\mathcal{O}},l}$ is the conformal block for the primary field $\tilde{\mathcal{O}}$. In the following we will denote the square of the OPE coefficients by capital letters, that is

$$A^{\Delta_1\Delta_2}_{\mathcal{O}} := \left(a^{\Delta_1\Delta_2}_{\mathcal{O}}\right)^2 .$$

Since we have no three-point functions due to the quartic vertex none of the "single trace" operators $\mathcal{O}_1$ and $\mathcal{O}_2$ will appear in the OPE.

The spectrum of "double trace" operators for the disconnected part can be read off from the corresponding four-point functions by conglomeration as described in [94]. The possible primary operators are given by

$$:\!\mathcal{O}_1\Box^n\partial^l\mathcal{O}_1\!:, \;\; :\!\mathcal{O}_2\Box^n\partial^l\mathcal{O}_2\!:, \;\; :\!\mathcal{O}_2\Box^n\partial^l\mathcal{O}_1\!: \tag{6.16}$$

which we will denote by

$$[\mathcal{O}_1\mathcal{O}_1]_{n,l}\,, [\mathcal{O}_2\mathcal{O}_2]_{n,l}\,, [\mathcal{O}_2\mathcal{O}_1]_{n,l}$$

respectively. They have the corresponding scaling dimension $2+2n+l$, $4+2n+l$ and $3+2n+l$ with $n,l\in\mathbb{N}$. Recall that in the scalar four-point function we can only distinguish operators by their scaling dimension, which may be the same for different values of n and l. Furthermore, while the dimensions of $\mathcal{O}_1$ and $\mathcal{O}_2$ are determined by the (renormalized) mass m, which is fixed for a conformally coupled bulk scalar, we may expect that the "double trace" operators pick up anomalous dimensions due to the bulk interaction term.

6.3.1 Correlation functions with degenerate conformal block expansion

Let us first consider the four-point functions (6.15a), (6.15b) and (6.15c). By examining the bulk diagrams we notice, that we will have mixing between the double trace operators in the double OPE. If the two-point function between the operators $[\mathcal{O}_1\mathcal{O}_1]_{n+1,l}$ and $[\mathcal{O}_2\mathcal{O}_2]_{n,l}$ does not vanish they are not a good basis for the conformal block expansion. Instead, we choose a basis of operators $\mathcal{O}^S_{n,l}$ and $\mathcal{O}^A_{n,l}$ both with scaling dimension $\Delta^{S/A}_{n,l} = 2+2n+l+\mathcal{O}(\lambda)$ and spin l such that they are orthogonal, i.e. at $\mathcal{O}(\lambda^0)$ they have the two point functions

$$\begin{aligned}
&\left\langle \mathcal{O}^S_{n,l}(x_1)\mathcal{O}^A_{n,l}(x_2)\right\rangle = 0;\\
&\left\langle \mathcal{O}^S_{n,l}(x_1)\mathcal{O}^S_{n,l}(x_2)\right\rangle = \left\langle \mathcal{O}^A_{n,l}(x_1)\mathcal{O}^A_{n,l}(x_2)\right\rangle = \frac{1}{2}\left\langle [\mathcal{O}_1\mathcal{O}_1]_{n,l}(x_1)[\mathcal{O}_1\mathcal{O}_1]_{n,l}(x_2)\right\rangle ,
\end{aligned} \tag{6.17}$$

where the additional factor of $1/2$ guarantees canonical normalization of the final result. Combining (6.14), (6.16) and (6.17) we then write

$$\begin{aligned}
\mathcal{O}_1\times\mathcal{O}_1 &\sim 1 + \sum_{n,\frac{l}{2}\in\mathbb{N}} a^{1,1}_{[\mathcal{O}_1\mathcal{O}_1]_{n,l}}[\mathcal{O}_1\mathcal{O}_1]_{n,l} \equiv 1 + \sum_{n,\frac{l}{2}\in\mathbb{N}} \big(a^{1,1}_{\mathcal{O}^S_{n,l}}\,\mathcal{O}^S_{n,l} + a^{1,1}_{\mathcal{O}^A_{n,l}}\,\mathcal{O}^A_{n,l}\big)\\
\mathcal{O}_2\times\mathcal{O}_2 &\sim 1 + \sum_{n,\frac{l}{2}\in\mathbb{N}} a^{2,2}_{[\mathcal{O}_2\mathcal{O}_2]_{n,l}}[\mathcal{O}_2\mathcal{O}_2]_{n,l} \equiv 1 + \sum_{n,\frac{l}{2}\in\mathbb{N}} \big(a^{2,2}_{\mathcal{O}^S_{n,l}}\,\mathcal{O}^S_{n,l} + a^{2,2}_{\mathcal{O}^A_{n,l}}\,\mathcal{O}^A_{n,l}\big)\,,
\end{aligned}$$

where the OPE coefficients $a^{\Delta,\Delta}_{[\mathcal{O}_\Delta\mathcal{O}_\Delta]_{n,l}}$ for the generalized free field are given in section 2.2.

To find the OPE coefficients of the operators in the orthogonal basis we can express the four-point functions of the generalized free field in terms of conformal blocks as

$$\langle \mathcal{O}_1(x_1)\mathcal{O}_1(x_2)\mathcal{O}_1(x_3)\mathcal{O}_1(x_4)\rangle|_{\lambda^0} = \frac{1}{x_{12}^2 x_{34}^2}\left(1+\sum_{n,\frac{l}{2}\in\mathbb{N}}\left(A^{1,1}_{\mathcal{O}^S_{n,l}}+A^{1,1}_{\mathcal{O}^A_{n,l}}\right)\frac{1}{2}G^{0,0}_{\Delta_{n,l}}\right),$$
$$\langle \mathcal{O}_2(x_1)\mathcal{O}_2(x_2)\mathcal{O}_2(x_3)\mathcal{O}_2(x_4)\rangle|_{\lambda^0} = \frac{1}{x_{12}^4 x_{34}^4}\left(1+\sum_{n,\frac{l}{2}\in\mathbb{N}}\left(A^{2,2}_{\mathcal{O}^S_{n,l}}+A^{2,2}_{\mathcal{O}^A_{n,l}}\right)\frac{1}{2}G^{0,0}_{\Delta_{n,l}}\right),$$
$$\langle \mathcal{O}_2(x_1)\mathcal{O}_2(x_2)\mathcal{O}_1(x_3)\mathcal{O}_1(x_4)\rangle|_{\lambda^0} = \frac{1}{x_{12}^4 x_{34}^2}\left(1+\sum_{n,\frac{l}{2}\in\mathbb{N}}\left(a^{2,2}_{\mathcal{O}^S_{n,l}}a^{1,1}_{\mathcal{O}^S_{n,l}}+a^{2,2}_{\mathcal{O}^A_{n,l}}a^{1,1}_{\mathcal{O}^A_{n,l}}\right)\frac{1}{2}G^{0,0}_{\Delta_{n,l}}\right),$$

with the equation for the conformal blocks $G^{a,b}_{\Delta_{n,l}}$ given in the appendix D. We used the fact that the conformal blocks for operators with the same dimension and spin are identical, meaning they coincide for $\mathcal{O}^S_{n,l}$ and $\mathcal{O}^A_{n,l}$. Comparing this expansion to the generalized free field, we see immediately that the OPE coefficients in the new basis must obey the following conditions

$$\begin{aligned} A^{1,1}_{\mathcal{O}^S_{n,l}}+A^{1,1}_{\mathcal{O}^A_{n,l}} &= 2A^{1,1}_{[\mathcal{O}_1\mathcal{O}_1]_{n,l}}; \quad A^{2,2}_{\mathcal{O}^S_{n,l}}+A^{2,2}_{\mathcal{O}^A_{n,l}} = 2A^{2,2}_{[\mathcal{O}_2\mathcal{O}_2]_{n-1,l}}; \\ a^{2,2}_{\mathcal{O}^S_{n,l}}a^{1,1}_{\mathcal{O}^S_{n,l}}+a^{2,2}_{\mathcal{O}^A_{n,l}}a^{1,1}_{\mathcal{O}^A_{n,l}} &= 0\,. \end{aligned} \tag{6.19}$$

Note, that from the second condition it follows that $a^{2,2}_{\mathcal{O}^S_{0,l}} = a^{2,2}_{\mathcal{O}^A_{0,l}} = 0$, since $A^{2,2}_{[\mathcal{O}_2\mathcal{O}_2]_{-1,l}} = 0$.

Equation (6.19) does not determine the zeroth order OPE coefficients uniquely. We have to proceed to first order in λ to obtain additional conditions to fix them. We expect the operators $\mathcal{O}^S_{n,l}$ and $\mathcal{O}^A_{n,l}$ to receive anomalous dimensions from the interaction term in the bulk

$$\Delta^{S/A} = 2+2n+l+\sum_{i=0}^{\infty}\gamma^{(i)S/A}_{n,l}$$

with $\gamma^{(i)S/A}_{n,l}$ of order λ^i in the coupling constant. A convenient parametrization is to expand the squared OPE coefficients and conformal blocks in γ [93, 94]:

$$\begin{aligned} \mathcal{A}^{\Delta,\Delta}_{\mathcal{O}^{S/A}_{n,l}} &= A^{\Delta,\Delta}_{\mathcal{O}^{S/A}_{n,l}} + (\gamma^{(1)S/A}_{n,l}+\gamma^{(2)S/A}_{n,l})A^{\Delta,\Delta(1)}_{\mathcal{O}^{S/A}_{n,l}} + \frac{1}{2}(\gamma^{(1)S/A}_{n,l})^2 A^{(2)\Delta,\Delta}_{\mathcal{O}^{S/A}_{n,l}} + \cdots \\ a^{1,1}_{\mathcal{O}^S_{n,l}}a^{2,2}_{\mathcal{O}^S_{n,l}} &= a^{1,1}_{\mathcal{O}^{S/A}_{n,l}}a^{2,2}_{\mathcal{O}^{S/A}_{n,l}} + (\gamma^{(1)S/A}_{n,l}+\gamma^{(2)S/A}_{n,l})a^{1,1(1)}_{\mathcal{O}^{S/A}_{n,l}}a^{2,2(1)}_{\mathcal{O}^{S/A}_{n,l}} + \frac{1}{2}(\gamma^{(1)S/A}_{n,l})^2 a^{1,1(2)}_{\mathcal{O}^{S/A}_{n,l}}a^{2,2(2)}_{\mathcal{O}^{S/A}_{n,l}} + \cdots \\ \mathcal{G}^{0,0}_{\Delta_{(n,l)},l} &= G^{0,0}_{\Delta(n,l),l} + (\gamma^{(1)S/A}_{n,l}+\gamma^{(2)S/A}_{n,l})\underbrace{\left.\frac{\partial G^{0,0}_{\Delta,l}}{\partial\Delta}\right|_{\Delta(n,l)}}_{G'^{0,0}_{\Delta(n,l),l}} + \frac{1}{2}(\gamma^{(1)S/A}_{n,l})^2\underbrace{\left.\frac{\partial^2 G^{0,0}_{\Delta,l}}{\partial\Delta^2}\right|_{\Delta(n,l)}}_{G''^{0,0}_{\Delta(n,l),l}} + \cdots, \end{aligned}$$

where the expansion of $a^{1,1}_{\mathcal{O}^S_{n,l}}a^{2,2}_{\mathcal{O}^S_{n,l}}$ can be obtained by expanding $\sqrt{\mathcal{A}^{2,2}_{\mathcal{O}^{S/A}_{n,l}}\mathcal{A}^{1,1}_{\mathcal{O}^{S/A}_{n,l}}}$, providing us with an additional consistency check for our calculation.

In the following we will go in detail through the process of extracting the anomalous dimensions and OPE coefficients up to second order in λ. Since this part is quite technical, we highlighted the main result, which are the first and second order anomalous dimensions.

First order calculation The first order contributions in λ to the four-point functions (6.18) are then given by

$$\langle \mathcal{O}_\Delta(x_1)\mathcal{O}_\Delta(x_2)\mathcal{O}_\Delta(x_3)\mathcal{O}_\Delta(x_4)\rangle|_{\lambda^1} = \frac{1}{(x_{12}^2 x_{34}^2)^\Delta}\times$$
$$\sum_{n,\frac{l}{2}\in\mathbb{N}} \left((\gamma_{n,l}^{(1)S} A^{\Delta,\Delta}_{\mathcal{O}^S_{n,l}} + \gamma_{n,l}^{(1)A} A^{\Delta,\Delta}_{\mathcal{O}^A_{n,l}}) G'^{0,0}_{\Delta_{(n,l)},l} + \left(\gamma_{n,l}^{(1)S} A^{\Delta,\Delta(1)}_{\mathcal{O}^S_{n,l}} + \gamma_{n,l}^{(1)A} A^{\Delta,\Delta(1)}_{\mathcal{O}^A_{n,l}}\right) G^{0,0}_{\Delta_{(n,l)},l}\right) \tag{6.20a}$$
$$\langle \mathcal{O}_2(x_1)\mathcal{O}_2(x_2)\mathcal{O}_1(x_3)\mathcal{O}_1(x_4)\rangle|_{\lambda^1} = \frac{1}{x_{12}^4 x_{34}^2} \sum_{n,\frac{l}{2}\in\mathbb{N}} \left((\gamma_{n,l}^{(1)S} a^{1,1}_{\mathcal{O}^S_{n,l}} a^{2,2}_{\mathcal{O}^S_{n,l}} + \gamma_{n,l}^{(1)A} a^{1,1}_{\mathcal{O}^A_{n,l}} a^{2,2}_{\mathcal{O}^A_{n,l}}) G'^{0,0}_{\Delta_{(n,l)},l}\right.$$
$$\left. + \left(\gamma_{n,l}^{(1)S} a^{2,2(1)}_{\mathcal{O}^S_{n,l}} a^{1,1(1)}_{\mathcal{O}^S_{n,l}} + \gamma_{n,l}^{(1)A} a^{2,2(1)}_{\mathcal{O}^A_{n,l}} a^{1,1(1)}_{\mathcal{O}^A_{n,l}}\right) G^{0,0}_{\Delta_{(n,l)},l}\right). \tag{6.20b}$$

We compare this expansion to the bulk calculation. Keeping in mind that the derivative of a conformal block produces a term $\propto \log v$ we notice that the logarithmic terms in the four-point functions give us three additional conditions on the free OPE coefficients $a^{1,1}_{\mathcal{O}^{S/A}_{n,l}}$ and $a^{2,2}_{\mathcal{O}^{S/A}_{n,l}}$, while also introducing two new unknown quantities in the first order anomalous dimensions $\gamma_{n,l}^{(1)S}$ and $\gamma_{n,l}^{(1)A}$. Comparing to the bulk results, the additional conditions for $l=0$ are

$$\begin{aligned}
\gamma_{n,l}^{(1)S} A^{1,1}_{\mathcal{O}^S_{n,l}} + \gamma_{n,l}^{(1)A} A^{1,1}_{\mathcal{O}^A_{n,l}} &= \frac{\lambda}{16\pi^2} A^{1,1}_{[\mathcal{O}_1\mathcal{O}_1]_{n,l}},\\
\gamma_{n,l}^{(1)S} A^{2,2}_{\mathcal{O}^S_{n,l}} + \gamma_{n,l}^{(1)A} A^{2,2}_{\mathcal{O}^A_{n,l}} &= \frac{\lambda}{16\pi^2} A^{2,2}_{[\mathcal{O}_2\mathcal{O}_2]_{n-1,l}}\\
\gamma_{n,l}^{(1)S} a^{2,2}_{\mathcal{O}^S_{n,l}} a^{1,1}_{\mathcal{O}^S_{n,l}} + \gamma_{n,l}^{(1)A} a^{2,2}_{\mathcal{O}^A_{n,l}} a^{1,1}_{\mathcal{O}^A_{n,l}} &= \frac{\lambda}{16\pi^2} a^{1,1}_{[\mathcal{O}_1\mathcal{O}_1]_{n,l}} a^{2,2}_{[\mathcal{O}_2\mathcal{O}_2]_{n-1,l}}.
\end{aligned} \tag{6.21}$$

For $n>0$, equations (6.19) and (6.21) require either $\gamma_{n,l}^{(1)S}$ or $\gamma_{n,l}^{(1)A}$ to vanish. This choice is a matter of convention as $\mathcal{O}^S$ and $\mathcal{O}^A$ have not been defined separately so far. We choose $\gamma_{n>0,l}^{(1)A}=0$. Then the solution for the zeroth order OPE coefficients and first order anomalous dimensions is

$$\begin{aligned}
A^{1,1}_{\mathcal{O}^S_{n,l}} = A^{1,1}_{\mathcal{O}^A_{n,l}} = A^{1,1}_{[\mathcal{O}_1\mathcal{O}_1]_{n,l}};\quad A^{2,2}_{\mathcal{O}^S_{n,l}} = A^{2,2}_{\mathcal{O}^A_{n,l}} = A^{2,2}_{[\mathcal{O}_2\mathcal{O}_2]_{n-1,l}},\\
a^{1,1}_{\mathcal{O}^S_{n,l}} a^{2,2}_{\mathcal{O}^S_{n,l}} = -a^{1,1}_{\mathcal{O}^A_{n,l}} a^{2,2}_{\mathcal{O}^A_{n,l}} = \sqrt{A^{1,1}_{[\mathcal{O}_1\mathcal{O}_1]_{n,l}} A^{2,2}_{[\mathcal{O}_2\mathcal{O}_2]_{n-1,l}}},
\end{aligned}$$

$$\boxed{\gamma_{n,l}^{(1)S} = \gamma\delta_{0,l};\qquad \gamma_{n,l}^{(1)A} = 0 \qquad \text{with } \gamma := \frac{\lambda}{16\pi^2}\,.}$$

From the pieces without logarithmic terms we can access information about the first order OPE coefficients. Since we chose $\gamma_{n,l}^{(1)A}=0$ this determines only the OPE coefficients for $\mathcal{O}^S_{n,l}$:

$$A^{1,1(1)}_{\mathcal{O}^S_{n,0}} = \frac{1}{2}\frac{\partial}{\partial n} A^{1,1}_{\mathcal{O}^S_{n,0}};\qquad A^{2,2(1)}_{\mathcal{O}^S_{n,0}} = \frac{1}{2}\frac{\partial}{\partial n} A^{2,2}_{\mathcal{O}^S_{n,0}}\qquad \text{for } n\geq 1\,.$$

Note that the first order OPE coefficients of the four-point function with mixed external dimensions are determined by the four-point functions with equal dimensions as

$$a^{2,2(1)}_{\mathcal{O}^{S/A}_{n,0}} a^{1,1(1)}_{\mathcal{O}^{S/A}_{n,0}} = \frac{A^{2,2(1)}_{\mathcal{O}^{S/A}_{n,0}} A^{1,1}_{\mathcal{O}^{S/A}_{n,0}} + A^{2,2}_{\mathcal{O}^{S/A}_{n,0}} A^{1,1(1)}_{\mathcal{O}^{S/A}_{n,0}}}{2\sqrt{A^{1,1}_{\mathcal{O}^{S/A}_{n,0}} A^{2,2}_{\mathcal{O}^{S/A}_{n,0}}}}\,, \quad \text{for } n \geq 1\,,$$

therefore providing an additional consistency check for the calculation, which our result passes.

For $n = 0$ the situation is a bit more complicated. Since $a^{2,2}_{\mathcal{O}^{S/A}_{0,l}} = 0$ we do not have the additional condition on the difference of the anomalous dimensions coming from equation (6.20b). We therefore find from equation (6.20a) that

$$\gamma^{(1)S}_{0,0} A^{1,1}_{\mathcal{O}^S_{0,0}} + \gamma^{(1)A}_{0,0} A^{1,1}_{\mathcal{O}^A_{0,0}} = 2\gamma A^{1,1}_{[\mathcal{O}_1\mathcal{O}_1]_{0,0}}\,,$$

and since the expansion of equation (6.20a) with $\Delta = 2$ starts with $\mathcal{O}(v^2)$ we need to have

$$\gamma^{(1)S}_{0,0} A^{2,2(1)}_{\mathcal{O}^S_{0,0}} + \gamma^{(1)A}_{0,0} A^{2,2(1)}_{\mathcal{O}^A_{0,0}} = 0. \tag{6.22}$$

The expansion of the bulk result for equation (6.20b) starts already at order $\mathcal{O}(v)$ but since it does not contain any $\log(v)$ terms at that order we get the additional condition

$$\gamma^{(1)S}_{0,0} a^{2,2(1)}_{\mathcal{O}^S_{0,0}} a^{1,1(1)}_{\mathcal{O}^S_{0,0}} + \gamma^{(1)A}_{0,0} a^{2,2(1)}_{\mathcal{O}^A_{0,0}} a^{1,1(1)}_{\mathcal{O}^A_{0,0}} = 2\gamma. \tag{6.23}$$

Second order calculation At second order in λ, the contributions from the conformal block expansion are given by

$$\begin{aligned}
\langle\mathcal{O}_\Delta(x_1)\mathcal{O}_\Delta(x_2)\mathcal{O}_\Delta(x_3)\mathcal{O}_\Delta(x_4)\rangle|_{\lambda^2} &= \frac{1}{(x_{12}^2x_{34}^2)^\Delta}\sum_{n,\frac{l}{2}\in\mathbb{N}}\Bigg(\frac{1}{2}\left((\gamma^{(1)S}_{n,l})^2 + (\gamma^{(1)A}_{n,l})^2\right)A^{\Delta,\Delta}_{\mathcal{O}^S_{n,l}} G''^{0,0}_{\Delta_{(n,l)},l}\\
&+\left((\gamma^{(1)S}_{n,l})^2 A^{\Delta,\Delta(1)}_{\mathcal{O}^S_{n,l}} + (\gamma^{(1)A}_{n,l})^2 A^{\Delta,\Delta(1)}_{\mathcal{O}^A_{n,l}}\right) G'^{0,0}_{\Delta_{(n,l)},l} + \frac{1}{2}\left((\gamma^{(1)S}_{n,l})^2 A^{\Delta,\Delta(2)}_{\mathcal{O}^S_{n,l}} + (\gamma^{(1)A}_{n,l})^2 A^{\Delta,\Delta(2)}_{\mathcal{O}^A_{n,l}}\right) G^{0,0}_{\Delta_{(n,l)},l}\\
&+(\gamma^{(2)S}_{n,l} + \gamma^{(2)A}_{n,l})A^{\Delta,\Delta}_{\mathcal{O}^S_{n,l}} G'^{0,0}_{\Delta_{(n,l)},l} + \left(\gamma^{(2)S}_{n,l} A^{\Delta,\Delta(1)}_{\mathcal{O}^S_{n,l}} + \gamma^{(2)A}_{n,l} A^{\Delta,\Delta(1)}_{\mathcal{O}^A_{n,l}}\right) G^{0,0}_{\Delta_{(n,l)},l}\Bigg)
\end{aligned}$$

and

$$\begin{aligned}
\langle\mathcal{O}_2(x_1)\mathcal{O}_2(x_2)\mathcal{O}_1(x_3)\mathcal{O}_1(x_4)\rangle|_{\lambda^2} &= \frac{1}{x_{12}^4x_{34}^2}\sum_{n,\frac{l}{2}\in\mathbb{N}}\Bigg(\frac{1}{2}\left((\gamma^{(1)S}_{n,l})^2 - (\gamma^{(1)A}_{n,l})^2\right) a^{1,1}_{\mathcal{O}^S_{n,l}} a^{2,2}_{\mathcal{O}^S_{n,l}} G''^{0,0}_{\Delta_{(n,l)},l}\\
&+\left((\gamma^{(1)S}_{n,l})^2 a^{1,1(1)}_{\mathcal{O}^S_{n,l}} a^{2,2(1)}_{\mathcal{O}^S_{n,l}} + (\gamma^{(1)A}_{n,l})^2 a^{1,1(1)}_{\mathcal{O}^A_{n,l}} a^{2,2(1)}_{\mathcal{O}^A_{n,l}}\right) G'^{0,0}_{\Delta_{(n,l)},l}\\
&+(\gamma^{(2)S}_{n,l} - \gamma^{(2)A}_{n,l}) a^{1,1}_{\mathcal{O}^S_{n,l}} a^{2,2}_{\mathcal{O}^S_{n,l}} G'^{0,0}_{\Delta_{(n,l)},l} + \left(\gamma^{(2)S}_{n,l} a^{1,1(1)}_{\mathcal{O}^A_{n,l}} a^{2,2(1)}_{\mathcal{O}^S_{n,l}} + \gamma^{(2)A}_{n,l} a^{1,1(1)}_{\mathcal{O}^A_{n,l}} a^{2,2(1)}_{\mathcal{O}^A_{n,l}}\right) G^{0,0}_{\Delta_{(n,l)},l}\\
&+\frac{1}{2}\left((\gamma^{(1)S}_{n,l})^2 a^{1,1(2)}_{\mathcal{O}^S_{n,l}} a^{2,2(2)}_{\mathcal{O}^S_{n,l}} + (\gamma^{(1)A}_{n,l})^2 a^{1,1(2)}_{\mathcal{O}^A_{n,l}} a^{2,2(2)}_{\mathcal{O}^A_{n,l}}\right) G^{0,0}_{\Delta_{(n,l)},l}\Bigg)\,,
\end{aligned} \tag{6.24}$$

where all single trace primaries have the same weight in the first equation. Again we compare this to the results from the bulk calculation. The terms proportional to $\log(v)^2$

provide us with a consistency check between the first and second order calculation. We find

$$\frac{\left(\gamma_{0,0}^{(1)S}\right)^2 A^{1,1}_{\mathcal{O}^S_{0,0}} + \left(\gamma_{0,0}^{(1)A}\right)^2 A^{1,1}_{\mathcal{O}^A_{0,0}}}{\left(\gamma_{0,0}^{(1)S} A^{1,1}_{\mathcal{O}^S_{0,0}} + \gamma_{0,0}^{(1)A} A^{1,1}_{\mathcal{O}^A_{0,0}}\right)^2} = \frac{1}{2A^{1,1}_{[\mathcal{O}_1\mathcal{O}_1]_{0,0}}};$$

$$\frac{\left(\gamma_{n>0,0}^{(1)S}\right)^2 + \left(\gamma_{n>0,0}^{(1)A}\right)^2}{\left(\gamma_{n>0,0}^{(1)S} + \gamma_{n>0,0}^{(1)A}\right)^2} = \frac{\left(\gamma_{n>0,0}^{(1)S}\right)^2 - \left(\gamma_{n>0,0}^{(1)A}\right)^2}{\left(\gamma_{n>0,0}^{(1)S} - \gamma_{n>0,0}^{(1)A}\right)^2} = 1$$

from which it follows that $\gamma_{n>0,0}^{(1)A} = 0$ in consistency with the first order calculation, while for $n = 0$ we find that

$$\gamma_{0,0}^{(1)S} = \gamma_{0,0}^{(1)A} = \gamma; \qquad A^{1,1}_{\mathcal{O}^S_{0,0}} + A^{1,1}_{\mathcal{O}^A_{0,0}} = 2A^{1,1}_{[\mathcal{O}_1\mathcal{O}_1]_{0,0}}.$$

From condition (6.22) it follows then, that

$$A^{2,2(1)}_{\mathcal{O}^S_{0,0}} + A^{2,2(1)}_{\mathcal{O}^A_{0,0}} = 0,$$

and from equation (6.23) we get

$$a^{2,2(1)}_{\mathcal{O}^S_{0,0}} a^{1,1(1)}_{\mathcal{O}^S_{0,0}} + a^{2,2(1)}_{\mathcal{O}^A_{0,0}} a^{1,1(1)}_{\mathcal{O}^A_{0,0}} = 2.$$

The expansion of equation (6.24) starts at order $\mathcal{O}(v)$, where the terms at that order contain $\log(v)$ terms and terms purely polynomial in v, Y. The logarithmic terms can be absorbed by imposing equation (6.23) providing an additional consistency check between the first and second order calculation. The polynomial parts give $\gamma_{0,0}^{(2)S} a^{2,2(1)}_{\mathcal{O}^S_{0,0}} a^{1,1(1)}_{\mathcal{O}^S_{0,0}} + \gamma_{0,0}^{(2)A} a^{2,2(1)}_{\mathcal{O}^A_{0,0}} a^{1,1(1)}_{\mathcal{O}^A_{0,0}}$, which can only be solved, if we go to the next order in λ.

The expansion of $\langle \mathcal{O}_2(x_1)\mathcal{O}_2(x_2)\mathcal{O}_2(x_3)\mathcal{O}_2(x_4)\rangle|_{\lambda^2}$ starts at $\mathcal{O}(v)$, where the terms at this order are purely polynomial in v and Y. These terms can be absorbed by choosing

$$A^{2,2(2)}_{\mathcal{O}^S_{0,0}} + A^{2,2(2)}_{\mathcal{O}^A_{0,0}} = 1.$$

The coefficients of the $\log(v)$ terms give us access to the sum and difference between the second order anomalous dimensions. We obtain the following results

$$\gamma^{(2)S}_{n>0,l>0} + \gamma^{(2)A}_{n>0,l>0} = -\frac{\gamma^2}{l(l+1)} - \frac{\gamma^2}{2n+l} + \frac{\gamma^2}{2n+l+1},$$

$$\gamma^{(2)S}_{n>0,l>0} - \gamma^{(2)A}_{n>0,l>0} = -\frac{\gamma^2}{l(l+1)} + \frac{\gamma^2}{2n+l} - \frac{\gamma^2}{2n+l+1},$$

If $l = 0$ we find the following

$$\gamma^{(2)S}_{n>0,0} + \gamma^{(2)A}_{n>0,0} = 3H^{(1)}_{2n}\gamma^2 - \frac{\gamma^2}{2n(2n+1)} - \gamma^2,$$

$$\gamma^{(2)S}_{n>0,0} - \gamma^{(2)A}_{n>0,0} = 3H^{(1)}_{2n}\gamma^2 + \frac{\gamma^2}{2n(2n+1)} - 7\gamma^2,$$

with $H_n^{(1)} = \sum_{m=1}^{n} 1/m$ the harmonic number, which implies that

$$\boxed{\begin{aligned} \gamma^{(2)S}_{n>0,l>0} &= -\frac{\gamma^2}{l(l+1)}; \qquad \gamma^{(2)A}_{n>0,l>0} = -\frac{\gamma^2}{(2n+l)(2n+l+1)}, \\ \gamma^{(2)S}_{n>0,0} &= 3\gamma^2 \sum_{m=1}^{2n} \frac{1}{m} - 4\gamma^2; \qquad \gamma^{(2)A}_{n>0,0} = -\frac{\gamma^2}{2n(2n+1)} + 3\gamma^2. \end{aligned}}$$

Remarkably the anomalous dimensions for $\mathcal{O}^S_{n>0,l>0}$ seem to be completely degenerate for all values of n and the dimension for $\mathcal{O}^A_{n,l>0}$ can be brought into the general form

$$\boxed{\Delta^A_{n,l>0} = \bar{\Delta}^A_{n,l} - \frac{\gamma^2}{(\bar{\Delta}^A_{n,l}-2)(\bar{\Delta}^A_{n,l}-1)} + \mathcal{O}(\gamma^3)} \tag{6.25}$$

where $\bar{\Delta}^A_{n,l} = \Delta^A_{n,l}|_{\lambda=0} = 2+2n+l$. For the $n=0$ trajectory we can again only make a statement about the sum

$$\boxed{\gamma^{(2)S}_{0,0} + \gamma^{(2)A}_{0,0} = -2\gamma^2; \quad \gamma^{(2)S}_{0,l>0} + \gamma^{(2)A}_{0,l>0} = -\frac{\gamma^2}{l(l+1)}.}$$

6.3.2 Correlation functions with non-degenerate conformal block expansion

The four-point functions $\langle \mathcal{O}_2(x_1)\mathcal{O}_1(x_2)\mathcal{O}_2(x_3)\mathcal{O}_1(x_4)\rangle$ and $\langle \mathcal{O}_2(x_1)\mathcal{O}_1(x_2)\mathcal{O}_1(x_3)\mathcal{O}_2(x_4)\rangle$ provide us with the OPE of

$$\mathcal{O}_1 \times \mathcal{O}_2 \sim \sum_{n,l\in\mathbb{N}} a^{1,2}_{[\mathcal{O}_1\mathcal{O}_2]_{n,l}} [\mathcal{O}_1\mathcal{O}_2]_{n,l}.$$

Since the two-point function between these operators vanishes, the OPE will be regular. The double trace operators appearing in the free four-point function are the double trace operators $[\mathcal{O}_1\mathcal{O}_2]_{n,l}$ with scaling dimension $\Delta_{n,l} = 3+2n+l$. Since they have odd dimensions for even spin and even dimensions for odd spin, they can be distinguished from the operators $\mathcal{O}^S_{n,l}$ and $\mathcal{O}^A_{n,l}$ in the OPE and the conformal block expansion will be non-degenerate.

The free four-point functions are given by

$$\begin{aligned} \langle \mathcal{O}_2(x_1)\mathcal{O}_1(x_2)\mathcal{O}_2(x_3)\mathcal{O}_1(x_4)\rangle|_{\lambda^0} &= \frac{1}{(x_{12}^2 x_{34}^2)^{\frac{3}{2}}} \left(\frac{x_{24}^2}{x_{13}^2}\right)^{\frac{1}{2}} \left(\frac{v}{1-Y}\right)^{\frac{3}{2}}, \\ \langle \mathcal{O}_2(x_1)\mathcal{O}_1(x_2)\mathcal{O}_1(x_3)\mathcal{O}_2(x_4)\rangle|_{\lambda^0} &= \frac{1}{(x_{12}^2 x_{34}^2)^{\frac{3}{2}}} \frac{(x_{24}^2 x_{13}^2)^{\frac{1}{2}}}{x_{14}^2} \frac{v^{\frac{3}{2}}}{\sqrt{1-Y}}. \end{aligned}$$

Expanding in terms of conformal blocks gives

$$\begin{aligned} \langle \mathcal{O}_2(x_1)\mathcal{O}_1(x_2)\mathcal{O}_2(x_3)\mathcal{O}_1(x_4)\rangle|_{\lambda^0} &= \frac{1}{(x_{12}^2 x_{34}^2)^{\frac{3}{2}}} \left(\frac{x_{24}^2}{x_{13}^2}\right)^{\frac{1}{2}} \sum_{n,l\in\mathbb{N}} A^{2,1}_{[\mathcal{O}_2\mathcal{O}_1]_{n,l}} G^{\frac{1}{2},\frac{1}{2}}_{\Delta_{n,l}}, \\ \langle \mathcal{O}_2(x_1)\mathcal{O}_1(x_2)\mathcal{O}_1(x_3)\mathcal{O}_2(x_4)\rangle|_{\lambda^0} &= \frac{1}{(x_{12}^2 x_{34}^2)^{\frac{3}{2}}} \frac{(x_{24}^2 x_{13}^2)^{\frac{1}{2}}}{x_{14}^2} \sum_{n,l\in\mathbb{N}} A^{2,1}_{[\mathcal{O}_2\mathcal{O}_1]_{n,l}} G^{\frac{1}{2},-\frac{1}{2}}_{\Delta_{n,l}}, \end{aligned}$$

where the squared OPE coefficients are given in the appendix D. A major difference with respect to the OPE of the correlation functions in the previous section is the fact that now also operators with odd spin l contribute.

At first order in the bulk coupling λ we can determine the first order anomalous dimensions and OPE coefficients through

$$
\begin{aligned}
&\langle \mathcal{O}_2(x_1)\mathcal{O}_1(x_2)\mathcal{O}_2(x_3)\mathcal{O}_1(x_4)\rangle|_{\lambda^1} = \frac{1}{(x_{12}^2 x_{34}^2)^{\frac{3}{2}}}\left(\frac{x_{24}^2}{x_{13}^2}\right)^{\frac{1}{2}} \times \\
&\sum_{n,l\in\mathbb{N}} \gamma_{n,l}^{(1)}\left(A_{[\mathcal{O}_2\mathcal{O}_1]_{n,l}}^{2,1} G'^{\frac{1}{2},\frac{1}{2}}_{\Delta_{n,l}} + A_{[\mathcal{O}_2\mathcal{O}_1]_{n,l}}^{2,1(1)} G^{\frac{1}{2},\frac{1}{2}}_{\Delta_{n,l}}\right), \\
&\langle \mathcal{O}_2(x_1)\mathcal{O}_1(x_2)\mathcal{O}_2(x_3)\mathcal{O}_1(x_4)\rangle|_{\lambda^1} = \frac{1}{(x_{12}^2 x_{34}^2)^{\frac{3}{2}}}\frac{(x_{24}^2 x_{13}^2)^{\frac{1}{2}}}{x_{14}^2} \times \\
&\sum_{n,l\in\mathbb{N}} \gamma_{n,l}^{(1)}\left(A_{[\mathcal{O}_2\mathcal{O}_1]_{n,l}}^{2,1} G'^{\frac{1}{2},-\frac{1}{2}}_{\Delta_{n,l}} + A_{[\mathcal{O}_2\mathcal{O}_1]_{n,l}}^{2,1(1)} G^{\frac{1}{2},-\frac{1}{2}}_{\Delta_{n,l}}\right).
\end{aligned}
$$

Comparing with the bulk calculation gives the result

$$
\gamma_{n,l}^{(1)} = \gamma\delta_{0,l}; \qquad A_{[\mathcal{O}_2\mathcal{O}_1]_{n,0}}^{2,1(1)} = \frac{1}{2}\frac{\partial}{\partial n} A_{[\mathcal{O}_2\mathcal{O}_1]_{n,0}}^{2,1}.
$$

The result is the same for both of the above four-point functions showing the consistency of the calculation.

At second order in λ we get the following conformal block expansion

$$
\begin{aligned}
&\langle \mathcal{O}_2(x_1)\mathcal{O}_1(x_2)\mathcal{O}_2(x_3)\mathcal{O}_1(x_4)\rangle|_{\lambda^2} = \frac{1}{(x_{12}^2 x_{34}^2)^{\frac{3}{2}}}\left(\frac{x_{24}^2}{x_{13}^2}\right)^{\frac{1}{2}} \times \\
&\sum_{n,l\in\mathbb{N}} \Bigg[\gamma_{n,l}^{(2)}\left(A_{[\mathcal{O}_2\mathcal{O}_1]_{n,l}}^{2,1} G'^{\frac{1}{2},\frac{1}{2}}_{\Delta_{n,l}} + A_{[\mathcal{O}_2\mathcal{O}_1]_{n,l}}^{2,1(1)} G^{\frac{1}{2},\frac{1}{2}}_{\Delta_{n,l}}\right) \\
&+\frac{1}{2}\left(\gamma_{n,l}^{(1)}\right)^2\left(A_{[\mathcal{O}_2\mathcal{O}_1]_{n,l}}^{2,1} G''^{\frac{1}{2},\frac{1}{2}}_{\Delta_{n,l}} + 2A_{[\mathcal{O}_2\mathcal{O}_1]_{n,l}}^{2,1(1)} G'^{\frac{1}{2},\frac{1}{2}}_{\Delta_{n,l}} + A_{[\mathcal{O}_2\mathcal{O}_1]_{n,l}}^{2,1(2)} G^{\frac{1}{2},\frac{1}{2}}_{\Delta_{n,l}}\right)\Bigg], \qquad (6.29a) \\
&\langle \mathcal{O}_2(x_1)\mathcal{O}_1(x_2)\mathcal{O}_1(x_3)\mathcal{O}_2(x_4)\rangle|_{\lambda^2} = \frac{1}{(x_{12}^2 x_{34}^2)^{\frac{3}{2}}}\frac{(x_{24}^2 x_{13}^2)^{\frac{1}{2}}}{x_{14}^2} \times \\
&\sum_{n,l\in\mathbb{N}} \Bigg[\gamma_{n,l}^{(2)}\left(A_{[\mathcal{O}_2\mathcal{O}_1]_{n,l}}^{2,1} G'^{\frac{1}{2},-\frac{1}{2}}_{\Delta_{n,l}} + A_{[\mathcal{O}_2\mathcal{O}_1]_{n,l}}^{2,1(1)} G^{\frac{1}{2},-\frac{1}{2}}_{\Delta_{n,l}}\right) \\
&+\frac{1}{2}\left(\gamma_{n,l}^{(1)}\right)^2\left(A_{[\mathcal{O}_2\mathcal{O}_1]_{n,l}}^{2,1} G''^{\frac{1}{2},-\frac{1}{2}}_{\Delta_{n,l}} + 2A_{[\mathcal{O}_2\mathcal{O}_1]_{n,l}}^{2,1(1)} G'^{\frac{1}{2},-\frac{1}{2}}_{\Delta_{n,l}} + A_{[\mathcal{O}_2\mathcal{O}_1]_{n,l}}^{2,1(2)} G^{\frac{1}{2},-\frac{1}{2}}_{\Delta_{n,l}}\right)\Bigg]. \qquad (6.29b)
\end{aligned}
$$

Again the coefficient of the $\log(v)^2$ term provides us with a consistency check between the first and second order calculation which our results pass. From either (6.29a) or (6.29b) we can determine the second order anomalous dimensions. As it should be they lead to identical results given by the following formulas:

$$
\boxed{
\begin{aligned}
\gamma_{n,0}^{(2)} &= 3\gamma^2 \sum_{m=1}^{2n+1}\frac{1}{m} - 7\gamma^2, \\
\gamma_{n,l>0}^{(2)} &= \begin{cases} -\frac{\gamma^2}{l(1+l)} & \text{for } l \mod 2 = 0 \\ -\frac{\gamma^2}{(l+2n+2)(l+2n+1)} & \text{for } l \mod 2 = 1. \end{cases}
\end{aligned}
}
$$

Comparing to the results from the previous section we notice a striking similarity. The anomalous dimensions of $[\mathcal{O}_1\mathcal{O}_2]_{n,2l>0}$ and $\mathcal{O}^S_{n,2l>0}$ are the same while for $[\mathcal{O}_1\mathcal{O}_2]_{n,2l+1}$ we find a form similar to $\mathcal{O}^A_{n,2l}$

$$\boxed{\Delta_{n,2l+1} = \bar{\Delta}_{n,2l+1} - \frac{\gamma^2}{(\bar{\Delta}_{n,2l+1}-2)(\bar{\Delta}_{n,2l+1}-1)} + \mathcal{O}(\gamma^3), \qquad l \geq 0} \tag{6.30}$$

with $\bar{\Delta}_{n,l} = \Delta_{n,l}|_{\lambda=0} = 3 + 2n + l$. Note that $\Delta^A_{n,l>0}$ in (6.25) only has contributions for even spin, while (6.30) applies to odd spins.

6.4 The whole picture

Let us summarize the results of this rather technical section: We confirmed the proposal in [87], that cosmological four-point functions can be described by a CFT dual to an effective field theory in Euclidean AdS, by describing explicitly the CFT dual to conformally coupled scalar ϕ^4 theory at loop level. The CFT consists of two scalar single-trace operators $\mathcal{O}_1$ and $\mathcal{O}_2$ with scaling dimension $\Delta \in \{1, 2\}$ and an infinite tower of three types of double-trace operators $\mathcal{O}^S_{n,l}$, $\mathcal{O}^A_{n,l}$ with dimension $\bar{\Delta}^{S/A}_{n,l} = 2 + 2n + l$ and $[\mathcal{O}_1\mathcal{O}_2]_{n,l}$ with dimension $\bar{\Delta}_{n,l} = 3 + 2n + l$. For $\mathcal{O}^S_{n,l}$ and $\mathcal{O}^A_{n,l}$ the spin l can only take even integer values, while for $[\mathcal{O}_1\mathcal{O}_2]_{n,l}$ it can take all integer values.

The operator $\mathcal{O}^S_{n,l}$ receives anomalous dimensions encoded in the four-point functions
$\langle \mathcal{O}_\Delta(x_1)\mathcal{O}_\Delta(x_2)\mathcal{O}_\Delta(x_3)\mathcal{O}_\Delta(x_4)\rangle$ and $\langle \mathcal{O}_2(x_1)\mathcal{O}_2(x_2)\mathcal{O}_1(x_3)\mathcal{O}_1(x_4)\rangle$ and so does $\mathcal{O}^A_{n,l}$. Similarly, the operator $[\mathcal{O}_1\mathcal{O}_2]_{n,l}$ receives anomalous dimensions from the four-point function
$\langle \mathcal{O}_2(x_1)\mathcal{O}_1(x_2)\mathcal{O}_2(x_3)\mathcal{O}_1(x_4)\rangle$ or, equivalently, $\langle \mathcal{O}_2(x_1)\mathcal{O}_1(x_2)\mathcal{O}_1(x_3)\mathcal{O}_2(x_4)\rangle$. However, the spectrum contains operators with all integer spins instead of only even spins, which was the case for $\mathcal{O}^S_{n,l}$ and $\mathcal{O}^A_{n,l}$. Interestingly, there is a simple relation between the anomalous dimensions of $\mathcal{O}^S_{n,l}$, $\mathcal{O}^A_{n,l}$ and $[\mathcal{O}_1\mathcal{O}_2]_{n,l}$ given by

$$\boxed{\gamma^{(2)}_{n,2l>0} = \gamma^{(2)S}_{n,2l>0}, \qquad \gamma^{(2)}_{n,2l+1>0} = \gamma^{(2)A}_{n,2l+2} \qquad l > 0.}$$

This relation seems to suggest a symmetry between the operators $\mathcal{O}^A_{n,l}$, $\mathcal{O}^S_{n,l}$ and $[\mathcal{O}_1\mathcal{O}_2]_{n,l}$, which could have several origins. One possible explanation is the special choice for the scaling dimension of the single-trace operators, $\Delta_\pm \in \{1, 2\}$. It is easily checked that for different values of $\Delta_\pm$ the relative coefficients between the vertices in (3.71) change and even new vertices of the form ${\phi^+}^3\phi^-$ are generated. The cancellation of the elliptic sector, discussed in section 6.2.2, does not occur anymore, and we expect the integrals to have a very different structure. As we do not have a simple form for the propagator for general values of Δ the technical implementation of the explicit loop calculation, necessary to check this claim, is much more involved, and we leave it for future studies. For conformal coupling in odd d the propagator simplifies to a rational function of K and the auxiliary EAdS action (6.2) is always the same. We therefore expect the general structure of the results, including the apparent symmetry to hold for those cases as well.

On the other hand, for generic scaling dimension of the single trace operators, the action (3.71) still displays a symmetry due to the fact that all vertices have the same coupling constant λ, which look fine-tuned in the general class of ϕ^4 theories in EAdS. Possibly, the apparent symmetry in the anomalous dimensions of the double trace operators is related to this.

Comparing with the results from section 6.1 and chapter 5 we can draw the following picture. Starting from the theory in the bulk we can calculate either the Bunch-Davies wave function as in section 6.1 or the cosmological correlation functions as we did here. The Bunch-Davis wavefunction is defined as

$$\begin{aligned}\Psi[\phi_0(x)] &= \lim_{\eta'\to-\infty(1+i\varepsilon)} \int\limits_{\substack{\phi(0,x)=\phi_0(x)\\ \phi(\eta',x)=0}} \mathcal{D}\phi \mathrm{e}^{iS[\phi]} \quad \text{or} \\ \tilde{\Psi}[\pi_0(x)] &= \int \mathcal{D}\phi_0 \mathrm{e}^{i\int \mathrm{d}^3x \phi_0(x)\pi_0(x)}\Psi[\phi_0]\,, \end{aligned} \tag{6.31}$$

where ϕ_0 and $\pi_0(x)$ denote the value of the bulk field and its canonically conjugate momentum at the boundary respectively. From a dS point of view $\Psi[\pi_0]$ corresponds to choosing Neumann instead of Dirichlet boundary conditions at future infinity.

Performing a semiclassical expansion of (6.31) one finds that the Bunch-Davis wave function has an interpretation as a generating functional for a CFT at future infinity. A conformally coupled scalar field in dS, without self-interactions, will give rise to a direct product of CFTs of two generalized free fields, where $\Psi[\phi_0(x)]$ corresponds to the external dimension $\Delta = 2$ while $\Psi[\pi_0(x)]$ to $\Delta = 1$. Introducing interactions in the bulk theory deforms the theory on the boundary. However, no non-trivial OPEs between $\mathcal{O}_1$ and $\mathcal{O}_2$ are introduced. Thus, the deformations will only affect the $\Delta = 1$ and $\Delta = 2$ sector separately and the theory keeps its product structure. In section 6.1 it was shown that the deformed CFT obtained in this way is identical to that obtained from a bulk theory in EAdS considered in [55–57] and chapter 5.

The cosmological correlator CFT introduces non-trivial OPE's between $\mathcal{O}_1$ and $\mathcal{O}_2$. Thus, the deformed CFT looses its product structure. Additionally, a new tower of double trace operators $[\mathcal{O}_1\mathcal{O}_2]_{n,l}$ receives anomalous dimensions due to the new mixing vertex introduced by the Schwinger-Keldysh formalism. Curiously we noticed, that the anomalous dimensions generated for these new operators are the same as the ones already found for $\mathcal{O}^S_{n,l}$ and $\mathcal{O}^A_{n,l}$.

There is, however, a relation between the CFT of the Bunch-Davies wave function and that of cosmological correlators. This can be seen by expressing a cosmological correlation function as

$$\langle\phi_0(x_1)\phi_0(x_2)\phi_0(x_3)\phi_0(x_4)\rangle = \int \mathcal{D}\phi_0 \Psi^*[\phi_0]\Psi[\phi_0]\phi_0(x_1)\phi_0(x_2)\phi_0(x_3)\phi_0(x_4) \tag{6.32}$$

or, equivalently,

$$\langle\phi_0(x_1)\phi_0(x_2)\phi_0(x_3)\phi_0(x_4)\rangle = \int \mathcal{D}\phi_0\mathcal{D}\pi_0 \mathrm{e}^{i\int \mathrm{d}^3x\phi_0(x)\pi_0(x)}\tilde{\Psi}[\pi_0]\Psi[\phi_0]\phi_0(x_1)\phi_0(x_2)\phi_0(x_3)\phi_0(x_4)\,,$$

where in the second step we used the inverse Fourier transformation of (6.31) as is explained in [87]. Analogous expressions exist for $\pi_0(x)$. The CFT of cosmological correlators can therefore be understood as a functional integral over the wavefunction CFTs with all possible boundary conditions, where the mixing between the two kinds boundary conditions contained in the Fourier exponential. This is analogous to the mixing vertex that was introduced in section 3.3.2 resulting from the Schwinger-Keldysh contour.

Finally, let us note, that the expression (6.32) is merely of conceptual value since it requires the exact knowledge of the wavefunctionals to perform the integral. From (6.32) it is not even clear that the result of the functional integration should preserve conformal symmetry. Computationally, the way to go is through the Schwinger-Keldysh formalism and the auxiliary EAdS action, introduced in [87] and reviewed in section 3.3.2. The two different ways to deform the generalized free field is schematically depicted in figure 1.1.

Chapter 7

Conclusion and Outlook

In this thesis we derived analytic expressions for cosmological correlation functions in the late time limit of a conformally coupled scalar field with $\lambda\phi^4$ interaction in the Poincaré patch of dS up to one-loop order [90]. On the way we also computed boundary correlation functions of the same theory in EAdS [57], generalizing the results of [55, 56]. It turns out that in both cases the results are determined by a dual CFT which consists of two different deformations of a generalized free field theory. We extract the OPE coefficients and anomalous dimensions to all primary double trace operators and find closed expressions for the latter. This result is equivalent to finding the masses of all resonances in a scattering process in flat space. By utilizing the dS/CFT correspondence [14, 69], we also showed that the expansion coefficients of the Bunch-Davis wave function for this theory in dS are governed by the same CFT as in EAdS [71]. Our results are consistent with the asymptotic fall-off behavior of the anomalous dimensions which were obtained by conformal bootstrap methods [36, 153–155] and we manage to generalize them.

We performed this computation by mapping the four point Witten diagrams to an equivalent calculation of flat space Feynman integrals with three external momenta. To obtain finite results we needed to regularise UV divergences that appear at one-loop level. We implemented a dimensional regularisation scheme that restores the (A)dS invariance of the theory which we checked by comparing the results to the covariant cut-off regularisation, developed in [55, 56]. To our knowledge, this has not been achieved before and we showed that our method produces consistent CFT correlation functions on the boundary. This allowed us to use the techniques from [96, 102, 137] to solve most of the integrals analytically.

By evaluating the Witten diagrams for EAdS we noticed that most of them are linearly reducible [102] and can therefore be expressed in terms of single valued multiple polylogarithms. Only one subclass of integrals turned out to contain an elliptic sector, which we managed to expand efficiently in terms of conformal cross ratios. The dual CFT we obtain is a deformed generalized free field with external dimensions either $\Delta = 1$ or $\Delta = 2$ with no nontrivial mixing between the two. The effect of the elliptic integrals manifests itself in the form of a non-rational contribution to the leading Regge trajectory of the anomalous dimensions.

We then considered the Bunch-Davies wave function in dS with the same bulk theory. Following the conjectured dS/CFT correspondence [69] we used the wave function as a generating functional to calculate CFT correlators at the future boundary of dS up to one loop order. As it turns out this CFT is exactly the same as the one in EAdS, considered before.

This result could potentially affect the conjectured higher spin/CFT correspondence in dS. In [80] a duality between an interacting $Sp(N)$ model and Vasiliev higher spin theory in dS [157] was conjectured in analogy to the duality between an interacting $O(N)$ model and higher spin theory in AdS [158]. Going from $O(N)$ to $Sp(N)$ corresponds to continuing $N \to -N$. As N is the parameter controlling the quantum fluctuations in the $1/N$ expansion it is the prefactor of the action in the partition function. This would mean that the action should switch the sign and it was argued in [80] that, as a consequence, every connected tree level n point function would acquire an extra minus sign when going from EAdS to dS. By looking at the analysis performed in [71] and in this thesis we see that the two point function does in fact change sign while the four point function does not. For the two point function this is just a normalization issue. After this normalization is fixed the relative sign of all the higher order contributions to the n point functions are fixed and we get the same result as for EAdS, i.e. no change of sign in the four point function. In order to have a sign change one has to additionally change the sign of the ϕ^4 coupling.

However, this is no statement about the higher spin theory, since we do not know the exact form of the quartic interaction term for higher spin fields. Our analysis in this thesis does not consider higher spin fields and we only consider quartic self-interactions. Thus the only implication we can make is that if such a quartic scalar interaction were present in the higher spin theory it would change sign when passing from EAdS to dS.

Finally we computed loop corrections to the actual cosmological correlation functions in dS. We did this by taking advantage of a relation between the Witten diagrams in EAdS and the cosmological correlators in the Schwinger-Keldysh formalism, first explained in [84–86] and formulated in terms of an auxiliary EAdS action in [87]. The correlators are therefore best described by an effective theory in EAdS with a doubled field content, corresponding to the $\Delta = 1$ and $\Delta = 2$ boundary terms. We were able to use the methods and many of the results from the EAdS calculation to evaluate the cosmological correlators. Curiously, due to some non-trivial cancellations in the loop diagrams, the elliptic sector that was present in the EAdS calculations vanishes and the results can all be expressed in terms of single valued multiple polylogarithms. In contrast to the EAdS and wave function CFT, we observed non-trivial mixing between the fields with different boundary conditions. This reflects itself in the conformal block expansion as well, where three different trajectories of double trace operators receive anomalous dimensions. Interestingly, there is a symmetry between the anomalous dimensions of operators with different spin, as well as a degeneracy in twist, which we did not observe in the EAdS case. Furthermore the data of OPE coefficients and anomalous dimensions obeys several CFT consistency conditions between the tree level and one-loop level data, therefore showing that, at least perturbatively, the cosmological correlation functions are in fact described by a CFT.

The consequences and further applications of our results are manifold. On the technical side we can proceed with the calculation at higher loops, which would be the next straightforward application of the formalism described in this thesis. For the EAdS case we expect the integrals to become much more complicated, meaning, that different elliptic integrals and even more complicated structures will appear. To extract anomalous dimensions we therefore would stick to calculating the discontinuity by applying flat space Cutkosky rules [145,147]. For the cosmological correlation functions we expect the higher loop corrections to be simpler with respect to the corresponding

EAdS expressions, since similar cancellations as described before are expected. In that case it would be most interesting to check if the symmetries and degeneracies we discovered, hold at higher loop level as well. If this is the case, one would expect that this effect is connected to some deeper property of the theory at future infinity.

Another straightforward next step would be the application of the above formalism to different values of the external scaling dimensions Δ, i.e. to consider a bulk field with a different mass. This is especially relevant for the EAdS calculation, where Δ can take almost any real value. We found that by introducing an additional analytic parameter in the propagator we can in principle map the computation with any integer value of Δ to a flat space calculation. For these cases one could apply the method of mapping the Feynman integrals to master integrals by applying tensor reduction, integration by parts relations [95, 135, 138–141] and intersection theory [100, 159, 160].

For dS, however, the situation is a bit more complicated since unitarity puts severe restrictions on the value of Δ, forcing it to be complex for high masses. Especially in four dimensions, the only allowed integer values of Δ are the ones we already considered in this thesis and for other values no general simplifications of the hypergeometric functions in the propagator exist, at least to our knowledge. How to apply our method to those cases therefore remains an open question.

So far everything we did was done in an exact (A)dS background. This is an important step in understanding how QFT behaves in a cosmological scenario, however, not a realistic model for our universe. From a physical perspective the next logical step would be to try to apply this formalism to space-times with a slightly broken dS symmetry, like inflation. Under the cosmological bootstrap program some interesting results have been obtained recently, by trying to reconstruct the inflationary cosmological correlators from physical principles like locality, unitarity and symmetries (see e.g. [17, 73, 161]. A relevant question for us to ask in that context is, which properties of the dS symmetry are preserved and can be carried over. On the one hand this is a technical issue, since our formalism is based heavily on the fact that we have a maximally symmetric space-time. On the other hand it is also conceptually interesting since going away from an exact dS symmetry should reflect itself in a breaking of the conformal symmetry in the dual theory. It has been conjectured in [162] that this should trigger an inverse renormalisation group flow of the boundary theory from an IR to a UV fixed point in the future. As we expect our universe to behave like an exact dS space in the far future it is tempting to think about this renormalisation group flow as a holographic dual to cosmic time evolution, from inflation in the past to dark energy domination in the future. This statement is obviously highly speculative and leaves many open questions, most importantly how the concept of causality would be implemented in that description of time evolution. Nevertheless it is a fascinating idea and we leave its further investigation to future work.

Appendix A

Multiple polylogarithms

A.1 Definitions

In the evaluation of the Witten diagrams, we encountered multiple polylogarithms as the results of linearly reducible Witten diagrams in the parametric representation as described in section 4.3. Following the convention used by Panzer in `HyperInt` [137], they are defined by the nested sum

$$\mathrm{Li}_{s_1,\ldots,s_k}(x_1,\ldots,x_k) := \sum_{0<p_1<\cdots<p_k}^{\infty} \frac{x_1^{p_1}}{p_1^{s_1}} \cdots \frac{x_k^{p_k}}{p_k^{s_k}} \quad \text{for } |x_1\cdots x_i| < 1, \quad \forall i \in \{1,..,k\}\,.$$

The sum $s_1 + s_2 + \cdots + s_k$ is referred to as the weight of the multiple polylogarithm.

Some useful definitions and identities are

$$\begin{aligned}
\mathrm{Li}_1(x) &= -\log(1-x)\,,\\
\mathrm{Li}_{1,1}(y,x) &= \mathrm{Li}_2\left(\frac{x(y-1)}{1-x}\right) - \mathrm{Li}_2\left(\frac{x}{x-1}\right) - \mathrm{Li}_2(xy)\;,\\
\mathrm{Li}_2(1-x) &= -\mathrm{Li}_2(x) - \log(x)\log(1-x) + \zeta(2)\,,\\
\mathrm{Li}_2\left(1-\frac{1}{x}\right) &= \mathrm{Li}_2(x) - \frac{1}{2}\log^2(x) + \log(x)\log(1-x) - \zeta(2)
\end{aligned} \tag{A.1}$$

and the Bloch-Wigner dilogarithm given by:

$$D(\zeta,\bar\zeta) = \frac{1}{2i}\left(\mathrm{Li}_2(\zeta) - \mathrm{Li}_2\left(\bar\zeta\right) - \frac{1}{2}\log(\zeta\bar\zeta)\left(\mathrm{Li}_1(\zeta) - \mathrm{Li}_1\left(\bar\zeta\right)\right)\right). \tag{A.2}$$

For a detailed discussion of these functions and their properties we refer the interested reader to [103, 150–152].

A.2 Some recurring expressions

We collect recurring expressions that enter the evaluation of the Witten diagrams:

$$\begin{aligned}
f_1(\zeta,\bar\zeta) = \log(\zeta\bar\zeta)&\left(\mathrm{Li}_{1,1}\left(\bar\zeta,\frac{\zeta}{\bar\zeta}\right) - \mathrm{Li}_{1,1}\left(\zeta,\frac{\bar\zeta}{\zeta}\right) + \mathrm{Li}_1(\zeta)\,\mathrm{Li}_1\left(\frac{\bar\zeta}{\zeta}\right) - \mathrm{Li}_1\left(\bar\zeta\right)\mathrm{Li}_1\left(\frac{\zeta}{\bar\zeta}\right)\right)\\
&+ \mathrm{Li}_3(\zeta) - \mathrm{Li}_3\left(\bar\zeta\right) + \mathrm{Li}_{2,1}(1,\zeta) - \mathrm{Li}_{2,1}\left(1,\bar\zeta\right)\\
&+ 2\,\mathrm{Li}_{2,1}\left(\zeta,\frac{\bar\zeta}{\zeta}\right) - 2\,\mathrm{Li}_{2,1}\left(\bar\zeta,\frac{\zeta}{\bar\zeta}\right) + \mathrm{Li}_{1,2}\left(\zeta,\frac{\bar\zeta}{\zeta}\right) - \mathrm{Li}_{1,2}\left(\bar\zeta,\frac{\zeta}{\bar\zeta}\right)\\
&- 2\,\mathrm{Li}_1\left(\frac{\bar\zeta}{\zeta}\right)\mathrm{Li}_2(\zeta) - \mathrm{Li}_2\left(\frac{\bar\zeta}{\zeta}\right)\mathrm{Li}_1(\zeta) + 2\,\mathrm{Li}_1\left(\frac{\zeta}{\bar\zeta}\right)\mathrm{Li}_2\left(\bar\zeta\right) + \mathrm{Li}_1\left(\bar\zeta\right)\mathrm{Li}_2\left(\frac{\zeta}{\bar\zeta}\right)
\end{aligned} \tag{A.3}$$

$$\begin{aligned}
f_2(\zeta,\bar\zeta) &= -\frac{1}{2}f_1(\zeta,\bar\zeta) + \frac{1}{2}\left(\mathrm{Li}_2\left(\zeta\right)\mathrm{Li}_1\left(\bar\zeta\right) - \mathrm{Li}_2\left(\bar\zeta\right)\mathrm{Li}_1\left(\zeta\right)\right) \\
&\quad + \mathrm{Li}_{1,2}\left(1,\zeta\right) - \mathrm{Li}_{1,2}\left(1,\bar\zeta\right) + \frac{1}{2}\left(\mathrm{Li}_{2,1}\left(1,\zeta\right) - \mathrm{Li}_{2,1}\left(1,\bar\zeta\right)\right) \\
&\quad + \frac{1}{2}\log(\zeta\bar\zeta)\left(\mathrm{Li}_2\left(\zeta\right) - \mathrm{Li}_2\left(\bar\zeta\right) - \mathrm{Li}_{1,1}\left(1,\zeta\right) + \mathrm{Li}_{1,1}\left(1,\bar\zeta\right)\right) \\
&\quad - \frac{1}{4}\log^2(\zeta\bar\zeta)\left(\mathrm{Li}_1\left(\zeta\right) - \mathrm{Li}_1\left(\bar\zeta\right)\right), \\
f_3(\zeta,\bar\zeta) &= 4i\frac{\zeta+\bar\zeta-2}{\zeta-\bar\zeta}D(\zeta,\bar\zeta) + \log(\zeta\bar\zeta)\log\left(\frac{(1-\zeta)(1-\bar\zeta)}{\zeta\bar\zeta}\right), \\
f_4(\zeta,\bar\zeta) &= -4i\frac{\zeta+\bar\zeta}{\zeta-\bar\zeta}D(\zeta,\bar\zeta) - \log((1-\zeta)(1-\bar\zeta))\log\left(\frac{(1-\zeta)(1-\bar\zeta)}{\zeta\bar\zeta}\right) \\
f_5(\zeta,\bar\zeta) &= \frac{4i(\zeta+\bar\zeta-2\zeta\bar\zeta)}{\zeta-\bar\zeta}D(\zeta,\bar\zeta) - \log(\zeta\bar\zeta)\log((1-\zeta)(1-\bar\zeta)), \\
f_6(\zeta,\bar\zeta) &= \frac{1}{2}\left(\mathrm{Li}_2\left(\zeta\right)\mathrm{Li}_1\left(\bar\zeta\right) - \mathrm{Li}_2\left(\bar\zeta\right)\mathrm{Li}_1\left(\zeta\right)\right) + \mathrm{Li}_{1,2}\left(1,\zeta\right) - \mathrm{Li}_{1,2}\left(1,\bar\zeta\right) \\
&\quad + \frac{1}{2}\left(\mathrm{Li}_{2,1}\left(1,\zeta\right) - \mathrm{Li}_{2,1}\left(1,\bar\zeta\right)\right) + \frac{1}{2}\log\left(\zeta\bar\zeta\right)\left(-\mathrm{Li}_{1,1}\left(1,\zeta\right) + \mathrm{Li}_{1,1}\left(1,\bar\zeta\right)\right), \\
f_7(\zeta,\bar\zeta) &= -(\mathrm{Li}_{1,1}\left(1,\zeta\right) + \mathrm{Li}_{1,1}\left(1,\bar\zeta\right)) + \frac{1}{2}\left(\log(\zeta\bar\zeta)+4\right)\log((1-\zeta)(1-\bar\zeta)) \\
&\quad - \log(1-\zeta)\log(1-\bar\zeta)
\end{aligned}$$

Appendix B

Evaluation of the Witten cross diagram

In this appendix we collect exact evaluations of the Witten cross diagram. In section B.1 we given an analytic evaluation of the cross diagram for all Δ, in section B.2 we give the results for the evaluation of the cross diagram in dimensional regularisation for $\Delta = 1$ and $\Delta = 2$ and in section B.3 we give the v and Y expansion of the cross diagram for all values of Δ.

B.1 The analytic evaluation of cross diagram for all Δ

The case of Δ integer. When Δ is a positive integer we have that for $\Delta \geq 5$

$$I_\times^\Delta(\zeta,\bar\zeta) = \sum_{r=0}^{3} \frac{\sum_{0\leq a,b\leq \Delta+1} n_r^{a,b}(\Delta)(\zeta\bar\zeta)^a(\zeta+\bar\zeta)^b}{(\zeta-\bar\zeta)^{4(\Delta-4)}} I_\times^{1+r}(\zeta,\bar\zeta).$$

The evaluation of the integrals $I_\times^r(\zeta,\bar\zeta)$ with $1 \leq r \leq 4$ is easily done with `HyperInt` [137], with the results

$$I_\times^1(\zeta,\bar\zeta) = \frac{4iD(\zeta,\bar\zeta)}{\zeta-\bar\zeta},$$

and

$$\begin{aligned} I_\times^2(\zeta,\bar\zeta) = {} & \frac{4i\left(-(\zeta+\bar\zeta)^3 + 2(\zeta+\bar\zeta)^2\zeta\bar\zeta + 2(\zeta+\bar\zeta)^2 - 8(\zeta+\bar\zeta)\zeta\bar\zeta + 4\zeta^2\bar\zeta^2 + 4\zeta\bar\zeta\right)}{(\zeta-\bar\zeta)^4}\frac{D(\zeta,\bar\zeta)}{\zeta-\bar\zeta} \\ & + \frac{4\left(\left(\zeta+\bar\zeta\right)^2 - 3\left(\zeta+\bar\zeta\right)\zeta\bar\zeta + 2\zeta\bar\zeta\right)}{(\zeta-\bar\zeta)^4}\log(\zeta\bar\zeta) \\ & + \frac{4\left(-2\left(\zeta+\bar\zeta\right)^2 + 3\left(\zeta+\bar\zeta\right)\zeta\bar\zeta + 3\zeta + 3\bar\zeta - 4\zeta\bar\zeta\right)}{(\zeta-\bar\zeta)^4}\log((1-\zeta)(1-\bar\zeta)) + \frac{2}{(\zeta-\bar\zeta)^2} \end{aligned}$$

and

$$I_\times^3(\zeta,\bar\zeta) = \frac{c_1^3(\zeta,\bar\zeta)}{(\zeta-\bar\zeta)^8}\frac{4iD(\zeta,\bar\zeta)}{\zeta-\bar\zeta} + \frac{c_2^3(\zeta,\bar\zeta)}{(\zeta-\bar\zeta)^8}\log(\zeta\bar\zeta) + \frac{c_3^3(\zeta,\bar\zeta)}{(\zeta-\bar\zeta)^8}\log((1-\zeta)(1-\bar\zeta)) + \frac{c_4^3(\zeta,\bar\zeta)}{(\zeta-\bar\zeta)^8},$$

with

$$
\begin{aligned}
c_1^3(\zeta,\bar\zeta) &= \left(\zeta+\bar\zeta\right)^6 - 6\left(\zeta+\bar\zeta\right)^5\zeta\bar\zeta + 6\left(\zeta+\bar\zeta\right)^4\zeta^2\bar\zeta^2 - 6\left(\zeta+\bar\zeta\right)^5 + 66\left(\zeta+\bar\zeta\right)^4\zeta\bar\zeta \\
&- 132\left(\zeta+\bar\zeta\right)^3\zeta^2\bar\zeta^2 + 72\left(\zeta+\bar\zeta\right)^2\zeta^3\bar\zeta^3 + 6\left(\zeta+\bar\zeta\right)^4 - 132\left(\zeta+\bar\zeta\right)^3\zeta\bar\zeta + 324\left(\zeta+\bar\zeta\right)^2\zeta^2\bar\zeta^2 \\
&- 216\left(\zeta+\bar\zeta\right)\zeta^3\bar\zeta^3 + 36\zeta^4\bar\zeta^4 + 72\left(\zeta+\bar\zeta\right)^2\zeta\bar\zeta - 216\left(\zeta+\bar\zeta\right)\zeta^2\bar\zeta^2 + 104\zeta^3\bar\zeta^3 + 36\zeta^2\bar\zeta^2 \\
c_2^3(\zeta,\bar\zeta) &= -3\left(\zeta+\bar\zeta\right)^5 + 22\left(\zeta+\bar\zeta\right)^4\zeta\bar\zeta - 25\left(\zeta+\bar\zeta\right)^3\zeta^2\bar\zeta^2 + 6\left(\zeta+\bar\zeta\right)^4 - 96\left(\zeta+\bar\zeta\right)^3\zeta\bar\zeta \\
&+ 204\left(\zeta+\bar\zeta\right)^2\zeta^2\bar\zeta^2 - 110\left(\zeta+\bar\zeta\right)\zeta^3\bar\zeta^3 + 72\left(\zeta+\bar\zeta\right)^2\zeta\bar\zeta - 198\left(\zeta+\bar\zeta\right)\zeta^2\bar\zeta^2 + 92\zeta^3\bar\zeta^3 + 36\zeta^2\bar\zeta^2 \\
c_3^3(\zeta,\bar\zeta) &= -6\left(\zeta+\bar\zeta\right)^5 + 28\left(\zeta+\bar\zeta\right)^4\zeta\bar\zeta - 25\left(\zeta+\bar\zeta\right)^3\zeta^2\bar\zeta^2 + 28\left(\zeta+\bar\zeta\right)^4 - 192\left(\zeta+\bar\zeta\right)^3\zeta\bar\zeta \\
&+ 276\left(\zeta+\bar\zeta\right)^2\zeta^2\bar\zeta^2 - 110\left(\zeta+\bar\zeta\right)\zeta^3\bar\zeta^3 - 25\left(\zeta+\bar\zeta\right)^3 + 276\left(\zeta+\bar\zeta\right)^2\zeta\bar\zeta - 396\left(\zeta+\bar\zeta\right)\zeta^2\bar\zeta^2 \\
&+ 128\zeta^3\bar\zeta^3 - 110\left(\zeta+\bar\zeta\right)\zeta\bar\zeta + 128\zeta^2\bar\zeta^2 \\
c_4^3(\zeta,\bar\zeta) &= \frac{-13\left(\zeta+\bar\zeta\right)^3 + 26\left(\zeta+\bar\zeta\right)^2\zeta\bar\zeta + 26\left(\zeta+\bar\zeta\right)^2 - 88\left(\zeta+\bar\zeta\right)\zeta\bar\zeta + 36\zeta^2\bar\zeta^2 + 36\zeta\bar\zeta}{2}
\end{aligned}
$$

and

$$
I_\times^4(\zeta,\bar\zeta) = \frac{c_1^4(\zeta,\bar\zeta)}{(\zeta-\bar\zeta)^{12}}\frac{4iD(\zeta,\bar\zeta)}{\zeta-\bar\zeta} + \frac{c_2^3(\zeta,\bar\zeta)}{(\zeta-\bar\zeta)^{12}}\log(\zeta\bar\zeta) + \frac{c_3^3(\zeta,\bar\zeta)}{(\zeta-\bar\zeta)^{12}}\log((1-\zeta)(1-\bar\zeta)) + \frac{c_4^3(\zeta,\bar\zeta)}{(\zeta-\bar\zeta)^{12}}
$$

with

$$
\begin{aligned}
c_1^4(\zeta,\bar\zeta) &= 400\zeta^3\bar\zeta^3 - 5076\left(\zeta+\bar\zeta\right)^5\zeta^2\bar\zeta^2 + 9312\left(\zeta+\bar\zeta\right)^4\zeta^3\bar\zeta^3 - 6900\left(\zeta+\bar\zeta\right)^3\zeta^4\bar\zeta^4 \\
&+ 1800\left(\zeta+\bar\zeta\right)^2\zeta^5\bar\zeta^5 - 19304\left(\zeta+\bar\zeta\right)^3\zeta^3\bar\zeta^3 + 15528\left(\zeta+\bar\zeta\right)^2\zeta^4\bar\zeta^4 - 4800\left(\zeta+\bar\zeta\right)\zeta^5\bar\zeta^5 \\
&- 11136\left(\zeta+\bar\zeta\right)\zeta^4\bar\zeta^4 + 12\left(\zeta+\bar\zeta\right)^8\zeta\bar\zeta - 30\left(\zeta+\bar\zeta\right)^7\zeta^2\bar\zeta^2 + 20\left(\zeta+\bar\zeta\right)^6\zeta^3\bar\zeta^3 \\
&- 234\left(\zeta+\bar\zeta\right)^7\zeta\bar\zeta + 948\left(\zeta+\bar\zeta\right)^6\zeta^2\bar\zeta^2 - 1320\left(\zeta+\bar\zeta\right)^5\zeta^3\bar\zeta^3 + 600\left(\zeta+\bar\zeta\right)^4\zeta^4\bar\zeta^4 \\
&+ 948\left(\zeta+\bar\zeta\right)^6\zeta\bar\zeta - 1320\left(\zeta+\bar\zeta\right)^5\zeta\bar\zeta + 9312\left(\zeta+\bar\zeta\right)^4\zeta^2\bar\zeta^2 + 600\left(\zeta+\bar\zeta\right)^4\zeta\bar\zeta \\
&- 6900\left(\zeta+\bar\zeta\right)^3\zeta^2\bar\zeta^2 + 15528\left(\zeta+\bar\zeta\right)^2\zeta^3\bar\zeta^3 + 1800\left(\zeta+\bar\zeta\right)^2\zeta^2\bar\zeta^2 \\
&- 4800\left(\zeta+\bar\zeta\right)\zeta^3\bar\zeta^3 - \left(\zeta+\bar\zeta\right)^9 + 12\left(\zeta+\bar\zeta\right)^8 - 30\left(\zeta+\bar\zeta\right)^7 + 20\left(\zeta+\bar\zeta\right)^6 + 2352\zeta^5\bar\zeta^5 \\
&+ 400\zeta^6\bar\zeta^6 + 2352\zeta^4\bar\zeta^4 \\
c_2^4(\zeta,\bar\zeta) &= \frac{1}{3}\Big(11\left(\zeta+\bar\zeta\right)^8 - 150\left(\zeta+\bar\zeta\right)^7\zeta\bar\zeta + 411\left(\zeta+\bar\zeta\right)^6\zeta^2\bar\zeta^2 - 294\left(\zeta+\bar\zeta\right)^5\zeta^3\bar\zeta^3 - 60\left(\zeta+\bar\zeta\right)^7 \\
&+ 1444\left(\zeta+\bar\zeta\right)^6\zeta\bar\zeta - 6390\left(\zeta+\bar\zeta\right)^5\zeta^2\bar\zeta^2 + 9306\left(\zeta+\bar\zeta\right)^4\zeta^3\bar\zeta^3 - 4368\left(\zeta+\bar\zeta\right)^3\zeta^4\bar\zeta^4 \\
&+ 60\left(\zeta+\bar\zeta\right)^6 - 3060\left(\zeta+\bar\zeta\right)^5\zeta\bar\zeta + 18786\left(\zeta+\bar\zeta\right)^4\zeta^2\bar\zeta^2 - 34920\left(\zeta+\bar\zeta\right)^3\zeta^3\bar\zeta^3 \\
&+ 24264\left(\zeta+\bar\zeta\right)^2\zeta^4\bar\zeta^4 - 5544\left(\zeta+\bar\zeta\right)\zeta^5\bar\zeta^5 + 1800\left(\zeta+\bar\zeta\right)^4\zeta\bar\zeta - 18000\left(\zeta+\bar\zeta\right)^3\zeta^2\bar\zeta^2 \\
&+ 37984\left(\zeta+\bar\zeta\right)^2\zeta^3\bar\zeta^3 - 25680\left(\zeta+\bar\zeta\right)\zeta^4\bar\zeta^4 + 4944\zeta^5\bar\zeta^5 + 5400\left(\zeta+\bar\zeta\right)^2\zeta^2\bar\zeta^2 \\
&- 13800\left(\zeta+\bar\zeta\right)\zeta^3\bar\zeta^3 + 6656\zeta^4\bar\zeta^4 + 1200\zeta^3\bar\zeta^3\Big) \\
c_3^4(\zeta,\bar\zeta) &= \frac{1}{3}\Big(6144\zeta^3\bar\zeta^3 - 9450\left(\zeta+\bar\zeta\right)^5\zeta^2\bar\zeta^2 + 11106\left(\zeta+\bar\zeta\right)^4\zeta^3\bar\zeta^3 - 4368\left(\zeta+\bar\zeta\right)^3\zeta^4\bar\zeta^4 \\
&- 52920\left(\zeta+\bar\zeta\right)^3\zeta^3\bar\zeta^3 + 29664\left(\zeta+\bar\zeta\right)^2\zeta^4\bar\zeta^4 - 5544\left(\zeta+\bar\zeta\right)\zeta^5\bar\zeta^5 - 39480\left(\zeta+\bar\zeta\right)\zeta^4\bar\zeta^4 \\
&- 210\left(\zeta+\bar\zeta\right)^7\zeta\bar\zeta + 471\left(\zeta+\bar\zeta\right)^6\zeta^2\bar\zeta^2 - 294\left(\zeta+\bar\zeta\right)^5\zeta^3\bar\zeta^3 + 2888\left(\zeta+\bar\zeta\right)^6\zeta\bar\zeta \\
&- 9450\left(\zeta+\bar\zeta\right)^5\zeta\bar\zeta + 37572\left(\zeta+\bar\zeta\right)^4\zeta^2\bar\zeta^2 + 11106\left(\zeta+\bar\zeta\right)^4\zeta\bar\zeta - 52920\left(\zeta+\bar\zeta\right)^3\zeta^2\bar\zeta^2 \\
&+ 75968\left(\zeta+\bar\zeta\right)^2\zeta^3\bar\zeta^3 - 4368\left(\zeta+\bar\zeta\right)^3\zeta\bar\zeta + 29664\left(\zeta+\bar\zeta\right)^2\zeta^2\bar\zeta^2 - 39480\left(\zeta+\bar\zeta\right)\zeta^3\bar\zeta^3
\end{aligned}
$$

$$- 5544\left(\zeta+\bar\zeta\right)\zeta^2\bar\zeta^2 + 22\left(\zeta+\bar\zeta\right)^8 - 210\left(\zeta+\bar\zeta\right)^7 + 471\left(\zeta+\bar\zeta\right)^6 - 294\left(\zeta+\bar\zeta\right)^5 + 6144\zeta^5\bar\zeta^5 + 13312\zeta^4\bar\zeta^4\Big)$$

$$\begin{aligned} c_4^4(\zeta,\bar\zeta) = \frac{1}{18}\Big(& 193\left(\zeta+\bar\zeta\right)^6 - 1044\left(\zeta+\bar\zeta\right)^5\zeta\bar\zeta + 1044\left(\zeta+\bar\zeta\right)^4\zeta^2\bar\zeta^2 - 1044\left(\zeta+\bar\zeta\right)^5 \\ &+ 9384\left(\zeta+\bar\zeta\right)^4\zeta\bar\zeta - 17352\left(\zeta+\bar\zeta\right)^3\zeta^2\bar\zeta^2 + 8784\left(\zeta+\bar\zeta\right)^2\zeta^3\bar\zeta^3 + 1044\left(\zeta+\bar\zeta\right)^4 \\ &- 17352\left(\zeta+\bar\zeta\right)^3\zeta\bar\zeta + 39648\left(\zeta+\bar\zeta\right)^2\zeta^2\bar\zeta^2 - 24768\left(\zeta+\bar\zeta\right)\zeta^3\bar\zeta^3 + 3600\zeta^4\bar\zeta^4 \\ &+ 8784\left(\zeta+\bar\zeta\right)^2\zeta\bar\zeta - 24768\left(\zeta+\bar\zeta\right)\zeta^2\bar\zeta^2 + 11552\zeta^3\bar\zeta^3 + 3600\zeta^2\bar\zeta^2\Big) \end{aligned}$$

The cross diagram with mixed external dimensions is given by acting with $\mathcal{H}_{12}$, $\mathcal{H}_{13}$ or $\mathcal{H}_{14}$ on the $\Delta = 1$ result. We obtain the following parametric representations

$$\begin{aligned} \mathcal{W}_0^{2211,4-4\epsilon} = & \frac{\pi^{2-2\epsilon}(\zeta\bar\zeta)^2\Gamma(2-2\epsilon)}{4\Gamma(1-4\epsilon)x_{12}^4x_{34}^2} \\ & \times \int_{(\mathbb{RP}^+)^2} \frac{d\alpha_1 d\alpha_2 d\alpha_3 \alpha_1\alpha_2^{-4\epsilon}\alpha_3}{(\alpha_1+\alpha_2+\alpha_3)\Big(\alpha_2\alpha_3(1-\zeta)(1-\bar\zeta)+\alpha_1(\alpha_2+\alpha_3\zeta\bar\zeta)\Big)^{2-2\epsilon}}. \end{aligned}$$

We obtain for the $\mathcal{O}(1)$ terms

$$\frac{2x_{12}^4x_{34}^2}{\pi^2(\zeta\bar\zeta)^2}\mathcal{W}_0^{2211,4} = \frac{(\zeta+\bar\zeta-2)2iD(\zeta,\bar\zeta)}{(\zeta-\bar\zeta)^3} - \frac{\zeta+\bar\zeta-2\zeta\bar\zeta}{2\zeta\bar\zeta(\zeta-\bar\zeta)^2}\log((1-\zeta)(1-\bar\zeta)) - \frac{\log(\zeta\bar\zeta)}{(\zeta-\bar\zeta)^2}. \tag{B.1}$$

B.2 Cross in dimensional regularisation

The cross term for $\Delta = 1$ in $D = 4 - 4\epsilon$ dimensions is given by:

$$\begin{aligned} \mathcal{W}_0^{1,4-4\epsilon} &= \frac{1}{2}\frac{\zeta\bar\zeta}{x_{12}^2x_{34}^2}\int_{\mathbb{R}^{4-4\epsilon}} \frac{\mathrm{d}^{4-4\epsilon}X(u\cdot X)^4}{\|X\|^4\,\|X-u_1\|^{4(1-4\epsilon)}\,\|X-u_\zeta\|^4} \\ &= \frac{1}{2}\frac{\pi^{2-2\epsilon}\zeta\bar\zeta}{x_{12}^2x_{34}^2}\frac{\Gamma(1-2\epsilon)}{\Gamma(1-4\epsilon)}\int_{(\mathbb{RP}^+)^2}\frac{\mathrm{d}\alpha_1\mathrm{d}\alpha_2\mathrm{d}\alpha_3\alpha_2^{-4\epsilon}}{(\alpha_1+\alpha_2+\alpha_3)(\alpha_1\alpha_2+\alpha_1\alpha_3\zeta\bar\zeta+(1-\zeta)(1-\bar\zeta)\alpha_2\alpha_3)^{1-2\epsilon}} \end{aligned} \tag{B.2}$$

Acting on (B.2) with $\mathcal{H}_{1234}$ we obtain the parametric representation of the $\Delta = 2$ case:

$$\begin{aligned} \mathcal{W}_0^{2,4-4\epsilon} &= \frac{1}{2}\frac{(\zeta\bar\zeta)^2}{x_{12}^4x_{34}^4}\int_{\mathbb{R}^{4-4\epsilon}} \frac{\mathrm{d}^{4-4\epsilon}X(u\cdot X)^4}{\|X\|^4\,\|X-u_1\|^{4(1-4\epsilon)}\,\|X-u_\zeta\|^4} \\ &= \frac{2\pi^{2-2\epsilon}}{16}\frac{(\zeta\bar\zeta)^2}{x_{12}^4x_{34}^4}\frac{\Gamma(1-2\epsilon)}{\Gamma(1-4\epsilon)}\times \\ &\int_{(\mathbb{RP}^+)^2}\frac{\mathrm{d}\alpha_1\mathrm{d}\alpha_2\mathrm{d}\alpha_3\alpha_2^{-4\epsilon}(C_1\alpha_1\alpha_2^2\alpha_3+C_2\alpha_1^2\alpha_2\alpha_3+C_3\alpha_2^2\alpha_3^2+C_4\alpha_1\alpha_2\alpha_3^2+C_5\alpha_1^2\alpha_3^2)}{(\alpha_1+\alpha_2+\alpha_3)(\alpha_1\alpha_2+\alpha_1\alpha_3\zeta\bar\zeta+(1-\zeta)(1-\bar\zeta)\alpha_2\alpha_3)^{3-2\epsilon}} \end{aligned} \tag{B.3}$$

The coefficients in the parametric integral (B.3) are given by:

$$\begin{aligned}
C_1 &= (1-6\epsilon)(\zeta+\bar\zeta-\zeta\bar\zeta)+8\epsilon-2\\
C_2 &= -(1-6\epsilon)\zeta\bar\zeta-1+2\epsilon\\
C_3 &= (4\zeta\bar\zeta\epsilon^2-4\epsilon^2(\zeta+\bar\zeta)+8\epsilon^2-4\epsilon+1)(1-\zeta)(1-\bar\zeta)\\
C_4 &= 8\zeta^2\bar\zeta^2\epsilon^2-8\zeta\bar\zeta\epsilon^2(\zeta+\bar\zeta)+\zeta\bar\zeta\left(8\epsilon^2+4\epsilon-2\right)+(1-2\epsilon)(\zeta+\bar\zeta)+2\epsilon-1\\
C_5 &= 4\zeta^2\bar\zeta^2\epsilon^2+\zeta\bar\zeta\left(4\epsilon^2-4\epsilon+1\right)
\end{aligned}$$

The $\mathcal{O}(\epsilon)$ term of the result of equation (B.3) is given by

$$\begin{aligned}
\mathscr{W}^{2,4}_{0,\epsilon} =& \frac{3(\zeta\bar\zeta)^2\left(-\left(\zeta+\bar\zeta\right)^3+2\left(\zeta+\bar\zeta\right)^2\zeta\bar\zeta+2\left(\zeta+\bar\zeta\right)^2-8\zeta\bar\zeta\left(\zeta+\bar\zeta\right)+4\zeta^2\bar\zeta^2+4\zeta\bar\zeta\right)}{2(\zeta-\bar\zeta)^5}f_2\\
&-\frac{4i(\zeta\bar\zeta)^2\left(-3\left(\zeta+\bar\zeta\right)^3+5\left(\zeta+\bar\zeta\right)^2\zeta\bar\zeta+5\left(\zeta+\bar\zeta\right)^2-12\zeta\bar\zeta\left(\zeta+\bar\zeta\right)+4\zeta^2\bar\zeta^2+4\zeta\bar\zeta\right)D(\zeta,\bar\zeta)}{(\zeta-\bar\zeta)^5}\\
&+\frac{3(\zeta\bar\zeta)^2\left(-2\left(\zeta+\bar\zeta\right)^2+3\zeta\bar\zeta\left(\zeta+\bar\zeta\right)+3\zeta+3\bar\zeta-4\zeta\bar\zeta\right)}{2(\zeta-\bar\zeta)^4}\left(\mathrm{Li}_1\left(\zeta\right)\mathrm{Li}_1\left(\bar\zeta\right)+\mathrm{Li}_{1,1}\left(1,\zeta\right)+\mathrm{Li}_{1,1}\left(1,\bar\zeta\right)\right)\\
&-\frac{3\zeta\bar\zeta\left(-\left(\zeta+\bar\zeta\right)^2\zeta\bar\zeta+3\left(\zeta+\bar\zeta\right)\zeta^2\bar\zeta^2-2\zeta^2\bar\zeta^2\right)}{2(\zeta-\bar\zeta)^4}\log(\zeta\bar\zeta)\log((1-\zeta)(1-\bar\zeta))\\
&-\frac{\zeta\bar\zeta\left(\left(\zeta+\bar\zeta\right)^3\zeta\bar\zeta+\left(\zeta+\bar\zeta\right)^3-18\left(\zeta+\bar\zeta\right)^2\zeta\bar\zeta+8\left(\zeta+\bar\zeta\right)\zeta^2\bar\zeta^2+8\zeta\bar\zeta\left(\zeta+\bar\zeta\right)+24\zeta^2\bar\zeta^2\right)}{4(\zeta-\bar\zeta)^4}\log((1-\zeta)(1-\bar\zeta))\\
&+\frac{3(\zeta\bar\zeta)^2\left(-\left(\zeta+\bar\zeta\right)^2+3\zeta\bar\zeta\left(\zeta+\bar\zeta\right)-2\zeta\bar\zeta\right)}{4(\zeta-\bar\zeta)^4}\log^2(\zeta\bar\zeta)+\\
&+\frac{(\zeta\bar\zeta)^2\left(-\left(\zeta+\bar\zeta\right)^4+\left(\zeta+\bar\zeta\right)^3\zeta\bar\zeta+10\left(\zeta+\bar\zeta\right)^3-18\left(\zeta+\bar\zeta\right)^2\zeta\bar\zeta+8\left(\zeta+\bar\zeta\right)\zeta^2\bar\zeta^2-8\left(\zeta+\bar\zeta\right)^2\right)\log(\zeta\bar\zeta)}{4(\zeta-\bar\zeta)^4(1-\zeta)(1-\bar\zeta)}\\
&-\frac{(\zeta\bar\zeta)^2\left(\zeta\bar\zeta\left(\zeta+\bar\zeta\right)+4\zeta^2\bar\zeta^2+2\zeta\bar\zeta\right)\log(\zeta\bar\zeta)}{(\zeta-\bar\zeta)^4(1-\zeta)(1-\bar\zeta)}
\end{aligned}\tag{B.4}$$

B.3 The expansion of the cross diagram

Here we rederive the cross term in general $\Delta \geq 1$ as an expansion in v and Y.

We start from equation (5.3), replace $v = \zeta\bar\zeta$ and $Y = 1-(1-\zeta)(1-\bar\zeta)$ and make the coordinate transformation $\alpha_i \to \alpha_i^{-1}$. Setting $\alpha_1 = 1$ due to the projectivity of the integral and expanding in Y we arrive at

$$\begin{aligned}
I^\Delta_\times &= \sum_{m=0}^{\infty}\frac{Y^m}{m!}\frac{\Gamma(\Delta+m)}{\Gamma(\Delta)}\int_0^\infty \frac{\mathrm{d}\alpha_2\mathrm{d}\alpha_3(\alpha_2\alpha_3)^{\Delta-1}}{(\alpha_2+\alpha_3+\alpha_2\alpha_3)^{\Delta}(1+\alpha_3+\alpha_2 v)^{\Delta+m}}\\
&= \sum_{m=0}^{\infty}\frac{Y^m}{m!}\frac{\Gamma(\Delta+m)^2}{\Gamma(2\Delta+m)}\int_0^\infty \frac{\mathrm{d}\alpha_3\alpha_3^{\Delta-1}}{(1+\alpha_3)^{2\Delta+m}}{}_2F_1\left(\begin{matrix}\Delta,\Delta+m\\2\Delta+m\end{matrix},1-\frac{\alpha_3 v}{(1+\alpha_3)^2}\right)
\end{aligned}$$

For $a, b \in \mathbb{N}$ the hypergeometric function can be expanded as

$$
{}_2F_1\left(\begin{matrix} a, b \\ a+b \end{matrix}, 1-z\right) = -\frac{\Gamma(a+b)}{\Gamma(a)\Gamma(b)} \sum_{n\geq 0} \left(\log(z) + H^{(1)}_{a+n-1} + H^{(1)}_{b+n-1} - 2H^{(1)}_{n}\right) \times \frac{\Gamma(a+n)\Gamma(b+n)}{\Gamma(a)\Gamma(b)} \frac{z^n}{n!^2},
$$

where $H^{(1)}_n = \sum_{r=1}^{n} 1/r$ is the harmonic number. Using that

$$
\int_0^\infty \frac{\alpha_3^{n+\Delta-1}}{(1+\alpha_3)^{2n+m+2\Delta}} \mathrm{d}\alpha_3 = \frac{\Gamma(\Delta+n)\Gamma(\Delta+m+n)}{\Gamma(2\Delta+2n+m)},
$$

and

$$
\int_0^\infty \frac{\alpha_3^{n+\Delta-1}}{(1+\alpha_3)^{2n+m+2\Delta}} \log\left(\frac{\alpha_3}{(1+\alpha_3)^2}\right) \mathrm{d}\alpha_3 = \frac{\Gamma(\Delta+n)\Gamma(\Delta+m+n)}{\Gamma(2\Delta+2n+m)} \times \left(H^{(1)}_{\Delta+n-1} + H^{(1)}_{\Delta+m+n-1} - 2H^{(1)}_{2\Delta+m+2n-1}\right),
$$

the expansion of $I^\Delta_\times$ reads

$$
I^\Delta_\times = -\sum_{n,m\geq 0} \frac{\Gamma(\Delta+n)^2\Gamma(\Delta+m+n)^2}{\Gamma(\Delta)^2\Gamma(2\Delta+m+2n)} \frac{v^n Y^m}{n!^2 m!} \times \left(\log(v) + 2H^{(1)}_{\Delta+n-1} + 2H^{(1)}_{\Delta+m+n-1} - 2H^{(1)}_{n} - 2H^{(1)}_{2\Delta+m+2n-1}\right).
$$

This expression matches the one given in [109].

Appendix C

Evaluation of the one-loop Witten bubble diagram

In this appendix we give the expressions for the evaluation of the one-loop Witten bubble diagram in dimensional regularisation for $\Delta = 1$ and $\Delta = 2$.

C.1 The one-loop diagrams with equal external dimensions

The general integrals to be solved in dimensional regularisation are given by:

$$\begin{aligned}
\mathcal{W}^{\Delta,4-2\epsilon,s}_{1,\text{div}} &= \frac{1}{2}\frac{(\zeta\bar{\zeta})^{\Delta}}{(x_{12}^2x_{34}^2)^{\Delta}}\int_{\mathbb{R}^{2D}}\frac{\mathrm{d}^{4-2\epsilon}X_1\mathrm{d}^{4-2\epsilon}X_2(u\cdot X_1)^{2\Delta-2}(u\cdot X_2)^{2\Delta-2}}{\|X_1\|^{2\Delta}\|X_1-u_\zeta\|^{2\Delta}\|X_2-u_1\|^{2\Delta-4\epsilon}\|X_1-u_1\|^{-4\epsilon}\|X_1-X_2\|^4}\\
\mathcal{W}^{\Delta,4-2\epsilon,t}_{1,\text{div}} &= \frac{1}{2}\frac{(\zeta\bar{\zeta})^{\Delta}}{(x_{12}^2x_{34}^2)^{\Delta}}\int_{\mathbb{R}^{2D}}\frac{\mathrm{d}^{4-2\epsilon}X_1\mathrm{d}^{4-2\epsilon}X_2(u\cdot X_1)^{2\Delta-2}(u\cdot X_2)^{2\Delta-2}}{\|X_1\|^{2\Delta}\|X_2-u_\zeta\|^{2\Delta}\|X_2-u_1\|^{2\Delta-4\epsilon}\|X_1-u_1\|^{-4\epsilon}\|X_1-X_2\|^4}\\
\mathcal{W}^{\Delta,4-2\epsilon,u}_{1,\text{div}} &= \frac{1}{2}\frac{(\zeta\bar{\zeta})^{\Delta}}{(x_{12}^2x_{34}^2)^{\Delta}}\int_{\mathbb{R}^{2D}}\frac{\mathrm{d}^{4-2\epsilon}X_1\mathrm{d}^{4-2\epsilon}X_2(u\cdot X_1)^{2\Delta-2}(u\cdot X_2)^{2\Delta-2}}{\|X_1\|^{2\Delta}\|X_2-u_\zeta\|^{2\Delta}\|X_1-u_1\|^{2\Delta-4\epsilon}\|X_2-u_1\|^{-4\epsilon}\|X_1-X_2\|^4}\\
\mathcal{W}^{\Delta,4,s}_{1,\text{fin}} &= \frac{1}{2}\frac{(\zeta\bar{\zeta})^{\Delta}}{(x_{12}^2x_{34}^2)^{\Delta}}\int_{\mathbb{R}^{8}}\frac{\mathrm{d}^4X_1\mathrm{d}^4X_2(u\cdot X_1)^{2\Delta-3}(u\cdot X_2)^{2\Delta-3}}{\|X_1\|^{2\Delta}\|X_1-u_\zeta\|^{2\Delta}\|X_2-u_1\|^{2\Delta}\|X_1-X_2\|^2}\\
\mathcal{W}^{\Delta,4,t}_{1,\text{fin}} &= \frac{1}{2}\frac{(\zeta\bar{\zeta})^{\Delta}}{(x_{12}^2x_{34}^2)^{\Delta}}\int_{\mathbb{R}^{8}}\frac{\mathrm{d}^4X_1\mathrm{d}^4X_2(u\cdot X_1)^{2\Delta-3}(u\cdot X_2)^{2\Delta-3}}{\|X_1\|^{2\Delta}\|X_2-u_\zeta\|^{2\Delta}\|X_2-u_1\|^{2\Delta}\|X_1-X_2\|^2}\\
\mathcal{W}^{\Delta,4,u}_{1,\text{fin}} &= \frac{1}{2}\frac{(\zeta\bar{\zeta})^{\Delta}}{(x_{12}^2x_{34}^2)^{\Delta}}\int_{\mathbb{R}^{8}}\frac{\mathrm{d}^4X_1\mathrm{d}^4X_2(u\cdot X_1)^{2\Delta-3}(u\cdot X_2)^{2\Delta-3}}{\|X_1\|^{2\Delta}\|X_2-u_\zeta\|^{2\Delta}\|X_1-u_1\|^{2\Delta}\|X_1-X_2\|^2}
\end{aligned} \tag{C.1}$$

The auxiliary integrals used to obtain the parametric representation of the finite integrals for $\Delta = 2$ are given by

$$\begin{aligned}
\tilde{\mathcal{W}}^{2,4,s}_{1,\text{fin}} &= \frac{1}{8}\int_{\mathbb{R}^8}\frac{\mathrm{d}^4X_1\mathrm{d}^4X_2}{\|X_1-\vec{x}_1\|^2\|X_1-\vec{x}_2\|^4\|X_2-\vec{x}_3\|^4\|X_2-\vec{x}_4\|^2\|X_1-X_2\|^2}\\
&= \frac{1}{8}\frac{x_{14}^2}{x_{12}^4x_{34}^4}(\zeta\bar{\zeta})^2\int_{\mathbb{R}^8}\frac{\mathrm{d}^4X_1\mathrm{d}^4X_2}{\|X_1\|^2\|X_1-u_\zeta\|^4\|X_2-u_1\|^2\|X_1-X_2\|^2}\\
\tilde{\mathcal{W}}^{2,4,t}_{1,\text{fin}} &= \frac{1}{8}\int_{\mathbb{R}^8}\frac{\mathrm{d}^4X_1\mathrm{d}^4X_2}{\|X_1-\vec{x}_1\|^2\|X_1-\vec{x}_3\|^4\|X_2-\vec{x}_2\|^2\|X_2-\vec{x}_4\|^4\|X_1-X_2\|^2}
\end{aligned}$$

$$
\begin{aligned}
&= \frac{1}{8}\frac{\zeta\bar{\zeta}}{x_{12}^2 x_{34}^4}\int_{\mathbb{R}^8}\frac{\mathrm{d}^4X_1\mathrm{d}^4X_2}{\|X_1\|^2\|X_2-u_1\|^4\|X_2-u_\zeta\|^2\|X_1-X_2\|^2} \\
\tilde{\mathscr{W}}_{1,\text{fin}}^{2,4,u} &= \frac{1}{8}\int_{\mathbb{R}^8}\frac{\mathrm{d}^4X_1\mathrm{d}^4X_2}{\|X_1-\vec{x}_1\|^2\|X_1-\vec{x}_4\|^4\|X_2-\vec{x}_2\|^2\|X_2-\vec{x}_3\|^4\|X_1-X_2\|^2} \\
&= \frac{1}{8}\frac{\zeta\bar{\zeta}}{x_{12}^2 x_{34}^4}\int_{\mathbb{R}^8}\frac{\mathrm{d}^4X_1\mathrm{d}^4X_2}{\|X_1\|^2\|X_1-u_1\|^4\|X_2-u_\zeta\|^2\|X_1-X_2\|^2}\,.
\end{aligned}
\tag{C.2}
$$

The integrals to be solved in the AdS-invariant regularisation are given by:

$$
\begin{aligned}
\mathscr{W}_1^{\Delta,\delta,s} =& \frac{1}{4}\frac{(\zeta\bar{\zeta})^\Delta}{(x_{12}^2x_{34}^2)^\Delta}\int_{\mathbb{R}^8}\frac{\mathrm{d}^4X_1\mathrm{d}^4X_2 z_1^{2\Delta-4}z_2^{2\Delta-4}}{\|X_1\|^{2\Delta}\|X_1-u_\zeta\|^{2\Delta}\|X_2-u_1\|^{2\Delta}}\left(\frac{K^\delta(\mathbf{X}_1,\mathbf{X}_2)^\Delta}{1-K^\delta(\mathbf{X}_1,\mathbf{X}_2)^2}\right)^2 \\
\mathscr{W}_1^{\Delta,\delta,t} =& \frac{1}{4}\frac{(\zeta\bar{\zeta})^\Delta}{(x_{12}^2x_{34}^2)^\Delta}\int_{\mathbb{R}^8}\frac{\mathrm{d}^4X_1\mathrm{d}^4X_2 z_1^{2\Delta-4}z_2^{2\Delta-4}}{\|X_2\|^{2\Delta}\|X_1-u_\zeta\|^{2\Delta}\|X_1-u_1\|^{2\Delta}}\left(\frac{K^\delta(\mathbf{X}_1,\mathbf{X}_2)^\Delta}{1-K^\delta(\mathbf{X}_1,\mathbf{X}_2)^2}\right)^2 \\
\mathscr{W}_1^{\Delta,\delta,u} =& \frac{1}{4}\frac{(\zeta\bar{\zeta})^\Delta}{(x_{12}^2x_{34}^2)^\Delta}\int_{\mathbb{R}^8}\frac{\mathrm{d}^4X_1\mathrm{d}^4X_2 z_1^{2\Delta-4}z_2^{2\Delta-4}}{\|X_1\|^{2\Delta}\|X_2-u_\zeta\|^{2\Delta}\|X_1-u_1\|^{2\Delta}}\left(\frac{K^\delta(\mathbf{X}_1,\mathbf{X}_2)^\Delta}{1-K^\delta(\mathbf{X}_1,\mathbf{X}_2)^2}\right)^2 .
\end{aligned}
\tag{C.3}
$$

C.1.1 $\Delta = 1$

The finite integrals are the L_0' integrals which are discussed in detail in appendix C.1.4.

The divergent integrals in the parametric representation are given by

• For the s-channel

$$
\mathscr{W}_{1,\text{div}}^{1,4-2\epsilon,s} = \frac{\pi^{4-2\epsilon}\zeta\bar{\zeta}}{\Gamma(-2\epsilon)x_{12}^2x_{34}^2}\int\limits_{(\mathbb{RP}^+)^4}\prod_{i=1}^5\mathrm{d}\alpha_i\frac{\alpha_3^{-1-2\epsilon}\alpha_1^{-2\epsilon}\alpha_5(U^s)^{-1-\epsilon}}{(F^s)^{1-2\epsilon}}
\tag{C.4}
$$

with

$$
\begin{aligned}
U^s &:= (\alpha_2+\alpha_3+\alpha_4)\alpha_5 + (\alpha_2+\alpha_3+\alpha_4+\alpha_5)\alpha_1 \\
F^s &:= \alpha_4(\alpha_3\alpha_5+\alpha_1(\alpha_3+\alpha_5))(1-\zeta)(1-\bar{\zeta}) + \alpha_2\alpha_4(\alpha_1+\alpha_5)\zeta\bar{\zeta} \\
&\quad + \alpha_2(\alpha_3\alpha_5+\alpha_1(\alpha_3+\alpha_5))
\end{aligned}
\tag{C.5}
$$

• For the t-channel

$$
\mathscr{W}_{1,\text{div}}^{1,4-2\epsilon,t} = \frac{\pi^{4-2\epsilon}\zeta\bar{\zeta}}{\Gamma(-2\epsilon)x_{12}^2x_{34}^2}\int\limits_{(\mathbb{RP}^+)^4}\prod_{i=1}^5\mathrm{d}\alpha_i\frac{\alpha_2^{-1-2\epsilon}\alpha_3^{-2\epsilon}\alpha_5(U^t)^{-1-\epsilon}}{(F^t)^{1-2\epsilon}}
$$

with

$$
\begin{aligned}
U^t &:= (\alpha_1+\alpha_2)(\alpha_3+\alpha_4) + (\alpha_1+\alpha_2+\alpha_3+\alpha_4)\alpha_5 \\
F^t &:= \alpha_4((\alpha_1+\alpha_2)\alpha_3+(\alpha_2+\alpha_3)\alpha_5)(1-\zeta)(1-\bar{\zeta}) + \alpha_1\alpha_2(\alpha_3+\alpha_4+\alpha_5) \\
&\quad + \alpha_1\alpha_5(\alpha_3+\alpha_4\zeta\bar{\zeta})
\end{aligned}
\tag{C.6}
$$

- For the u-channel

$$\mathcal{W}_{1,\text{div}}^{1,4-2\epsilon,u} = \frac{\pi^{4-2\epsilon}\zeta\bar{\zeta}}{\Gamma(-2\epsilon)x_{12}^2x_{34}^2}\int\limits_{(\mathbb{RP}^+)^4}\prod_{i=1}^{5}\mathrm{d}\alpha_i\frac{\alpha_1^{-1-2\epsilon}\alpha_4^{-2\epsilon}\alpha_5(U^u)^{-1-\epsilon}}{(F)^{1-2\epsilon}}$$

with

$$\begin{aligned}U^u &:= (\alpha_1+\alpha_2)(\alpha_3+\alpha_4)+(\alpha_1+\alpha_2+\alpha_3+\alpha_4)\alpha_5\\ F^u &:= \alpha_3\alpha_4\alpha_5+\alpha_1\alpha_3(\alpha_4+\alpha_5)+\alpha_2(\alpha_4\alpha_5+\alpha_1(\alpha_3+\alpha_4+\alpha_5))(1-\zeta)(1-\bar{\zeta})\\ &\quad+\alpha_2\alpha_3(\alpha_4+\alpha_5\zeta\bar{\zeta}).\end{aligned} \tag{C.7}$$

The result is given by

$$\mathcal{W}_{1,\text{div}}^{1,4-2\epsilon,i} = -\frac{\pi^2}{\epsilon}\mathcal{W}_0^{1,4-4\epsilon}+\mathcal{W}_{1,\text{finite}}^{1111,i}\quad\text{with} i=s,t,u\,,$$

where $\mathcal{W}_{1,\text{finite}}^{1111,i}$ for each channel is given by

$$\mathcal{W}_{1,\text{finite}}^{1111,i} = \frac{\pi^4 v}{2x_{12}^2x_{34}^2}L_0^{1,i} \tag{C.8}$$

where the integrals $L_0^{1,i}$ for $i\in\{s,t,u\}$ ar given in section C.1.3.

C.1.2 $\Delta = 2$

The finite integrals are given by:

$$\begin{aligned}W_{1,\text{fin}}^{2,4,s} =&\frac{\pi^4}{2}\frac{(\zeta\bar{\zeta})^2}{(x_{12}x_{34})^4}\int\limits_{(\mathbb{RP}^+)^3}\prod_{i=1}^{4}\mathrm{d}\alpha_i\frac{\alpha_1\alpha_2\alpha_3\alpha_4(\alpha_4(\alpha_1+\alpha_2+\alpha_3)+\alpha_3(\alpha_1+\alpha_2))^{-1}}{(\alpha_1\alpha_2(\alpha_3+\alpha_4)\zeta\bar{\zeta}+\alpha_1\alpha_3\alpha_4(1-\zeta)(1-\bar{\zeta})+\alpha_2\alpha_3\alpha_4)^2},\\ W_{1,\text{fin}}^{2,4,t} =&\frac{\pi^4}{2}\frac{(\zeta\bar{\zeta})^2}{(x_{12}x_{34})^4}\int\limits_{(\mathbb{RP}^+)^3}\prod_{i=1}^{4}\mathrm{d}\alpha_i\frac{\alpha_1\alpha_2\alpha_3\alpha_4(\alpha_4(\alpha_1+\alpha_2+\alpha_3)+\alpha_2(\alpha_1+\alpha_3))^{-1}}{(\alpha_1\alpha_3(\alpha_2+\alpha_4)(1-\zeta)(1-\bar{\zeta})+\alpha_1\alpha_2\alpha_4\zeta\bar{\zeta}+\alpha_2\alpha_3\alpha_4)^2},\\ W_{1,\text{fin}}^{2,4,u} =&\frac{\pi^4}{2}\frac{(\zeta\bar{\zeta})^2}{(x_{12}x_{34})^4}\int\limits_{(\mathbb{RP}^+)^3}\prod_{i=1}^{4}\mathrm{d}\alpha_i\frac{\alpha_1\alpha_2\alpha_3\alpha_4(\alpha_1(\alpha_2+\alpha_3+\alpha_4)+\alpha_4(\alpha_2+\alpha_3))^{-1}}{(\alpha_1\alpha_2(\alpha_3+\alpha_4\zeta\bar{\zeta})+\alpha_1\alpha_3\alpha_4(1-\zeta)(1-\bar{\zeta})+\alpha_2\alpha_3\alpha_4)^2}.\end{aligned} \tag{C.9}$$

The solution to the integrals (C.9) is given by

$$\begin{aligned}\mathcal{W}_{1,\text{fin}}^{2,4,s} &= \frac{\pi^4}{8}\frac{(\zeta\bar{\zeta})^2}{(x_{12}x_{34})^4}\left(\frac{(\zeta+\bar{\zeta}-2)8iD(\zeta,\bar{\zeta})}{(\zeta-\bar{\zeta})^3}+\frac{(4\zeta-2)\bar{\zeta}-2\zeta}{\zeta\bar{\zeta}(\zeta-\bar{\zeta})^2}\log((1-\zeta)(1-\bar{\zeta}))-\frac{4\log(\zeta\bar{\zeta})}{(\zeta-\bar{\zeta})^2}\right)\\ \mathcal{W}_{1,\text{fin}}^{2,4,t} &= \frac{\pi^4}{8}\frac{(\zeta\bar{\zeta})^2}{(x_{12}x_{34})^4}\left(-\frac{(\zeta+\bar{\zeta})8iD(\zeta,\bar{\zeta})}{(\zeta-\bar{\zeta})^3}+\frac{(4\zeta-2)\bar{\zeta}-2\zeta}{(1-\zeta)(1-\bar{\zeta})(\zeta-\bar{\zeta})^2}\log(\zeta\bar{\zeta})-\frac{4\log((1-\zeta)(1-\bar{\zeta}))}{(\zeta-\bar{\zeta})^2}\right)\\ \mathcal{W}_{1,\text{fin}}^{2,4,u} &= \frac{\pi^4}{8}\frac{(\zeta\bar{\zeta})^2}{(x_{12}x_{34})^4}\left(-\frac{((4\zeta-2)\bar{\zeta}-2\zeta)4iD(\zeta,\bar{\zeta})}{(\zeta-\bar{\zeta})^3}+\frac{2(\zeta+\bar{\zeta})}{(\zeta-\bar{\zeta})^2}\log(\zeta\bar{\zeta})-\frac{2(\zeta+\bar{\zeta}-2)\log((1-\zeta)(1-\bar{\zeta}))}{(\zeta-\bar{\zeta})^2}\right)\end{aligned} \tag{C.10}$$

The divergent integrals in the parametric representation is given by
• For the s-channel

$$\mathcal{W}_{1,\mathrm{div}}^{2222,4-2\epsilon,s} = \frac{4\pi^{4-2\epsilon}(\zeta\bar{\zeta})^2}{16\Gamma(-2\epsilon)x_{12}^4x_{34}^4}\int_{(\mathbb{RP}^+)^4}\prod_{i=1}^{5}\mathrm{d}\alpha_i\frac{\alpha_3^{-1-2\epsilon}\alpha_1^{-2\epsilon}\alpha_5(U^s)^{-1-\epsilon}}{(F^s)^{3-2\epsilon}} \times F_s(\zeta,\bar{\zeta},\epsilon;\alpha_1,\alpha_2,\alpha_3,\alpha_4,\alpha_5), \quad \text{(C.11)}$$

with U^s and F^s given in (C.6).
• For the t-channel

$$\mathcal{W}_{1,\mathrm{div}}^{2222,4-2\epsilon,t} = \frac{4\pi^{4-2\epsilon}(\zeta\bar{\zeta})^2}{16\Gamma(-2\epsilon)x_{12}^4x_{34}^4}\int_{(\mathbb{RP}^+)^4}\prod_{i=1}^{5}\mathrm{d}\alpha_i\frac{\alpha_2^{-1-2\epsilon}\alpha_3^{-2\epsilon}\alpha_5(U^t)^{-1-\epsilon}}{(F^t)^{3-2\epsilon}} \times F_t(\zeta,\bar{\zeta},\epsilon;\alpha_1,\alpha_2,\alpha_3,\alpha_4,\alpha_5),$$

with U^t and F^t given in (C.6).
• For the u-channel

$$\mathcal{W}_{1,\mathrm{div}}^{2222,4-2\epsilon,u} = \frac{4\pi^{4-2\epsilon}(\zeta\bar{\zeta})^2}{16\Gamma(-2\epsilon)x_{12}^4x_{34}^4}\int_{(\mathbb{RP}^+)^4}\prod_{i=1}^{5}\mathrm{d}\alpha_i\frac{\alpha_1^{-1-2\epsilon}\alpha_4^{-2\epsilon}\alpha_5(U^u)^{-1-\epsilon}}{(F^u)^{3-2\epsilon}} \times F_u(\zeta,\bar{\zeta},\epsilon;\alpha_1,\alpha_2,\alpha_3,\alpha_4,\alpha_5),$$

with U^u and F^u given in (C.7).

The expansion of the prefactors starts at $\mathcal{O}(\epsilon)$ so only integrals that diverge at least with ϵ^{-1} contribute to the final result. When only keeping those terms, the functions F_s, F_t and F_u are given by:

$$\begin{aligned}F_s &= C_1(\alpha_1^2\alpha_2\alpha_4\alpha_5^2 + 2\alpha_1\alpha_2\alpha_3\alpha_4\alpha_5^2 + \alpha_2\alpha_3^2\alpha_4\alpha_5^2)\\ &+ C_2(\alpha_1\alpha_2^2\alpha_4\alpha_5^2 + \alpha_2^2\alpha_3\alpha_4\alpha_5^2 + \alpha_1^2\alpha_2^2\alpha_4\alpha_5) + C_3(\alpha_1^2\alpha_4^2\alpha_5^2 + 2\alpha_1\alpha_3\alpha_4^2\alpha_5^2 + \alpha_3^2\alpha_4^2\alpha_5^2)\\ &+ C_4(\alpha_1^2\alpha_2\alpha_4^2\alpha_5 + \alpha_1\alpha_2\alpha_4^2\alpha_5^2 + \alpha_2\alpha_3\alpha_4^2\alpha_5^2) + C_5(2\alpha_1\alpha_2^2\alpha_4^2\alpha_5 + \alpha_2^2\alpha_4^2\alpha_5^2 + \alpha_1^2\alpha_2^2\alpha_4^2)\\ &\qquad + \alpha_1^2\alpha_2^2\alpha_5^2 + 2\alpha_1\alpha_2^2\alpha_3\alpha_5^2 + \alpha_2^2\alpha_3^2\alpha_5^2\end{aligned}$$

$$\begin{aligned}F_t &= C_1(\alpha_1^2\alpha_3^2\alpha_4\alpha_5+\alpha_1\alpha_2^2\alpha_4\alpha_5^2+2\alpha_1\alpha_2\alpha_3\alpha_4\alpha_5^2+\alpha_1\alpha_3^2\alpha_4\alpha_5^2)+C_2(\alpha_1^2\alpha_2\alpha_4\alpha_5^2+\alpha_1^2\alpha_3\alpha_4\alpha_5^2)\\ &+ C_3(\alpha_2^2\alpha_4^2\alpha_5^2 + 2\alpha_2\alpha_3\alpha_4^2\alpha_5^2 + \alpha_3^2\alpha_4^2\alpha_5^2 + \alpha_1^2\alpha_3^2\alpha_4^2 + 2\alpha_1\alpha_3^2\alpha_4^2\alpha_5)\\ &+ C_4(\alpha_1^2\alpha_3\alpha_4^2\alpha_5 + \alpha_1\alpha_2\alpha_4^2\alpha_5^2 + \alpha_1\alpha_3\alpha_4^2\alpha_5^2) + C_5\alpha_1^2\alpha_4^2\alpha_5^2\\ &\qquad + \alpha_1^2\alpha_2^2\alpha_5^2 + 2\alpha_1^2\alpha_2\alpha_3\alpha_5^2 + \alpha_1^2\alpha_3^2\alpha_5^2\end{aligned}$$

$$\begin{aligned}F_u &= C_1(\alpha_1^2\alpha_2\alpha_3\alpha_5 + 2\alpha_1\alpha_2\alpha_3\alpha_4\alpha_5^2 + \alpha_2^2\alpha_3\alpha_4^2\alpha_5 + \alpha_2\alpha_3\alpha_4^2\alpha_5^2)\\ &+ C_2(\alpha_1\alpha_2\alpha_3^2\alpha_5^2 + \alpha_2^2\alpha_3^2\alpha_4\alpha_5 + \alpha_2\alpha_3^2\alpha_4\alpha_5^2) + C_3(\alpha_1^2\alpha_2^2\alpha_5^2 + 2\alpha_1\alpha_2^2\alpha_4\alpha_5^2 + \alpha_2^2\alpha_4^2\alpha_5^2)\\ &+ C_4(\alpha_1\alpha_2^2\alpha_3\alpha_5^2 + \alpha_2^2\alpha_3\alpha_4\alpha_5^2) + C_5\alpha_2^2\alpha_3^2\alpha_5^2 + \alpha_1^2\alpha_3^2\alpha_5^2 + 2\alpha_1\alpha_3^2\alpha_4\alpha_5^2 + \alpha_2^2\alpha_3^2\alpha_4^2\\ &\qquad + 2\alpha_2\alpha_3^2\alpha_4^2\alpha_5 + \alpha_3^2\alpha_4^2\alpha_5^2\end{aligned}$$

with the coefficients C_i given by

$$
\begin{aligned}
C_1 &= (1-6\epsilon)(\zeta+\bar\zeta-\zeta\bar\zeta)+8\epsilon-2,\\
C_2 &= -(1-6\epsilon)\zeta\bar\zeta-1+2\epsilon,\\
C_3 &= (4\zeta\bar\zeta\epsilon^2-4\epsilon^2(\zeta+\bar\zeta)+8\epsilon^2-4\epsilon+1)(1-\zeta)(1-\bar\zeta),\\
C_4 &= 8\zeta^2\bar\zeta^2\epsilon^2-8\zeta\bar\zeta\epsilon^2(\zeta+\bar\zeta)+\zeta\bar\zeta\left(8\epsilon^2+4\epsilon-2\right)+(1-2\epsilon)(\zeta+\bar\zeta)+2\epsilon-1,\\
C_5 &= 4\zeta^2\bar\zeta^2\epsilon^2+\zeta\bar\zeta\left(4\epsilon^2-4\epsilon+1\right).
\end{aligned}
$$

Integrating over the Feynman parameters we obtain the result for the channels $i=s,t,u$

$$
\mathcal{W}_1^{2222,4-2\epsilon,i} = -\frac{\pi^2}{\epsilon}\mathcal{W}_0^{2222,4-4\epsilon}+3\pi^2\mathcal{W}_0^{2222,4}+\frac{3\pi^4}{8x_{12}^4x_{34}^4}L_0^{2,i}+\frac{1}{2}\mathcal{W}_{\text{fin}}^{2222,i}+\mathcal{O}(\epsilon^2)
$$

After a minimal substraction scheme, i.e. subtracting the term $-\frac{\pi^2}{\epsilon}\mathcal{W}_0^{2,4-4\epsilon}$ the remaining finite piece is given by

$$
\mathcal{W}_{1,\text{finite}}^{2222,i} = 3\pi^2\mathcal{W}_0^{2222,4}+\frac{3\pi^4}{8x_{12}^4x_{34}^4}L_0^{2,i}+\frac{1}{2}\mathcal{W}_{\text{fin}}^{2222,i}. \tag{C.12}
$$

where $\mathcal{W}_0^{2222,4}$ is given in (5.5), the contributions $\mathcal{W}_{\text{fin}}^{2222,i}$ were denoted $\mathcal{W}_{\text{fin}}^{2,4,i}$ in equation (C.10) and $L_0^{2,i}$ is evaluated in section C.1.3.

C.1.3 L_0^Δ integrals

The L_0^Δ pieces appearing in the finite part of the one-loop bubble integrals of $\Delta=1$ and $\Delta=2$ are given by:

$$
L_0^\Delta(\mathbf{x},\mathbf{y},\mathbf{z}) = \int_0^\infty d\sigma\int_0^1 d\varrho\,\frac{(\sigma\varrho(1-\varrho))^{\Delta-1}\log(1+\sigma)}{(1+\sigma)^\Delta\,(\sigma\varrho(1-\varrho)\mathbf{x}+\varrho\mathbf{y}+(1-\varrho)\mathbf{z})^\Delta}
$$

Where the three channels are given by

- s-channel: $\mathbf{x}\to v$, $\mathbf{y}\to 1-Y$, $\mathbf{z}\to 1$
- t-channel: $\mathbf{x}\to 1-Y$, $\mathbf{y}\to v$, $\mathbf{z}\to 1$
- u-channel: $\mathbf{x}\to 1$, $\mathbf{y}\to 1-Y$, $\mathbf{z}\to v$

They are linearly reducible and given by single valued polylogarithms of maximal weight three

For $\Delta = 1$ we have

$$
\begin{aligned}
L_0^{1,s}(\zeta,\bar\zeta) &= \frac{f_1(\zeta,\bar\zeta)-2i\log(\zeta\bar\zeta)D(\zeta,\bar\zeta)}{\zeta-\bar\zeta}\\
L_0^{1,t}(\zeta,\bar\zeta) &= \frac{f_1(\zeta,\bar\zeta)-2i\log((1-\zeta)(1-\bar\zeta))D(\zeta,\bar\zeta)}{\zeta-\bar\zeta}\\
L_0^{1,u}(\zeta,\bar\zeta) &= \frac{f_1(\zeta,\bar\zeta)}{\zeta-\bar\zeta}.
\end{aligned} \tag{C.13}
$$

For $\Delta = 2$ we have

$$L_0^{2,s}(\zeta,\bar\zeta)\cdot(\zeta-\bar\zeta)^5 = \Big(\big(\zeta+\bar\zeta\big)^2 - 3\,\big(\zeta+\bar\zeta\big)\,\zeta\,\bar\zeta + 2\,\zeta\,\bar\zeta\Big)\,f_3(\zeta,\bar\zeta)$$
$$+\Big(-\big(\zeta+\bar\zeta\big)^3 + 2\,\big(\zeta+\bar\zeta\big)^2\zeta\,\bar\zeta + 2\,\big(\zeta+\bar\zeta\big)^2 - 8\,\big(\zeta+\bar\zeta\big)\,\zeta\,\bar\zeta + 4\,\zeta^2\bar\zeta^2 + 4\,\zeta\,\bar\zeta\Big)\,f_1(\zeta,\bar\zeta)$$
$$-2\,i\,\Big(2\,\zeta^3\bar\zeta + 8\,\zeta^2\bar\zeta^2 + 2\,\zeta\,\bar\zeta^3 - \zeta^3 - 11\,\zeta^2\bar\zeta - 11\,\zeta\,\bar\zeta^2 - \bar\zeta^3 + 2\,\zeta^2 + 8\,\zeta\,\bar\zeta + 2\,\bar\zeta^2\Big)\ln\big(\zeta\,\bar\zeta\big)\,D(\zeta,\bar\zeta)$$
$$-4\,i\,\Big(\zeta^3\bar\zeta + 6\,\zeta^2\bar\zeta^2 + \zeta\,\bar\zeta^3 - \zeta^3 - 7\,\zeta^2\bar\zeta - 7\,\zeta\,\bar\zeta^2 - \bar\zeta^3 + 2\,\zeta^2 + 4\,\zeta\,\bar\zeta + 2\,\bar\zeta^2\Big)\,D(\zeta,\bar\zeta)$$
$$-2\,\big(\zeta-\bar\zeta\big)\,\zeta\,\bar\zeta\,\big(\zeta+\bar\zeta-2\big)\ln\big(\zeta\,\bar\zeta\big)$$
$$+\big(2\,\zeta\,\bar\zeta-\zeta-\bar\zeta\big)\big(\zeta-\bar\zeta\big)\big(\zeta+\bar\zeta-2\big)\ln\Big((-1+\zeta)\big(-1+\bar\zeta\big)\Big) + 2\,\big(\zeta-\bar\zeta\big)^3$$

$$L_0^{2,t}(\zeta,\bar\zeta)\cdot(\zeta-\bar\zeta)^5 = \Big((3\,\zeta-2)\,\bar\zeta^2 + \big(3\,\zeta^2 - 8\,\zeta + 3\big)\,\bar\zeta - 2\,\zeta^2 + 3\,\zeta\Big)\,f_4(\zeta,\bar\zeta)$$
$$+\Big((2\,\zeta-1)\,\bar\zeta^3 + \big(8\,\zeta^2 - 11\,\zeta + 2\big)\,\bar\zeta^2 + \big(2\,\zeta^3 - 11\,\zeta^2 + 8\,\zeta\big)\,\bar\zeta - \zeta^3 + 2\,\zeta^2\Big)\,f_1(\zeta,\bar\zeta)$$
$$+2\,i\big((-2\zeta+1)\,\bar\zeta^3 - \big(8\,\zeta^2 - 11\,\zeta + 2\big)\,\bar\zeta^2 - \big(2\,\zeta^3 - 11\,\zeta^2 + 8\,\zeta\big)\,\bar\zeta$$
$$+(-2+\zeta)\,\zeta^2\big)\ln\Big((1-\zeta)\big(1-\bar\zeta\big)\Big)\,D(\zeta,\bar\zeta)$$
$$-4\,i\,\Big(\zeta\,\bar\zeta^3 + \big(6\,\zeta^2 - 8\,\zeta + 1\big)\,\bar\zeta^2 + \zeta\,\big(\zeta^2 - 8\,\zeta + 6\big)\,\bar\zeta + \zeta^2\Big)\,D(\zeta,\bar\zeta)$$
$$-\big(2\,\zeta\,\bar\zeta - \zeta - \bar\zeta\big)\big(\zeta^2 - \bar\zeta^2\big)\ln\big(\zeta\,\bar\zeta\big) + 2\,\big(1-\bar\zeta\big)(1-\zeta)\big(\zeta-\bar\zeta\big)\big(\zeta+\bar\zeta\big)\ln\Big((1-\zeta)\big(1-\bar\zeta\big)\Big)$$
$$+2\,\big(\zeta-\bar\zeta\big)^3 \tag{C.14}$$

$$L_0^{2,u}(\zeta,\bar\zeta)\cdot(\zeta-\bar\zeta)^5 = \Big(\zeta^2 + 4\,\zeta\,\bar\zeta + \bar\zeta^2 - 3\,\zeta - 3\,\bar\zeta\Big)\,f_5(\zeta,\bar\zeta)$$
$$+\Big(2\,\zeta^3\bar\zeta + 8\,\zeta^2\bar\zeta^2 + 2\,\zeta\,\bar\zeta^3 - \zeta^3 - 11\,\zeta^2\bar\zeta - 11\,\zeta\,\bar\zeta^2 - \bar\zeta^3 + 2\,\zeta^2 + 8\,\zeta\,\bar\zeta + 2\,\bar\zeta^2\Big)\,f_1(\zeta,\bar\zeta)$$
$$-4\,i\,\Big(2\,\zeta^3\bar\zeta + 4\,\zeta^2\bar\zeta^2 + 2\,\zeta\,\bar\zeta^3 - \zeta^3 - 7\,\zeta^2\bar\zeta - 7\,\zeta\,\bar\zeta^2 - \bar\zeta^3 + \zeta^2 + 6\,\zeta\,\bar\zeta + \bar\zeta^2\Big)\,D(\zeta,\bar\zeta)$$
$$-\big(2\,\zeta\,\bar\zeta - \zeta - \bar\zeta\big)\big(\zeta-\bar\zeta\big)\big(\zeta+\bar\zeta\big)\ln\big(\zeta\,\bar\zeta\big)$$
$$+\big(2\,\zeta\,\bar\zeta - \zeta - \bar\zeta\big)\big(\zeta-\bar\zeta\big)\big(\zeta+\bar\zeta-2\big)\ln\Big((1-\zeta)\big(1-\bar\zeta\big)\Big) + 2\,\big(\zeta-\bar\zeta\big)^3$$

C.1.4 L_0' integrals

The finite integrals for $\Delta = 1$ are much harder to evaluate since they involve elliptic integrals in the parametric representation. Therefore we were not able to find closed expressions. But as the main goal of this work is to extract anomalous dimensions of the double-trace operators in the dual CFT, we are mainly interested in the coefficients of the $\log(v)^n$ terms. After identifying these terms the rest of the integral is finite and we can expand the integrand in powers of v and Y and integrate over the coefficients.

Let us first note that the integrals involved in the finite piece are all of the form

$$I(v_1, v_2) := \int_{\mathbb{R}^8} \frac{\mathrm{d}^4X\mathrm{d}^4Y}{\|X\|^2\,\|Y-v_1\|^2\,\|Y-v_2\|^2\,\|X-Y\|^2\;u\cdot X\,u\cdot Y}.$$

Comparing with (C.1) we recognise the finite pieces of the different channels as:

$$\begin{aligned}\mathcal{W}^{1,4,s}_{1,\text{fin}} =& \frac{1}{2}\frac{(\zeta\bar{\zeta})^{\Delta}}{(x_{12}^2x_{34}^2)^{\Delta}}I(u_1,u_1-u_\zeta),\\ \mathcal{W}^{1,4,t}_{1,\text{fin}} =& \frac{1}{2}\frac{(\zeta\bar{\zeta})^{\Delta}}{(x_{12}^2x_{34}^2)^{\Delta}}I(u_1,u_\zeta),\\ \mathcal{W}^{1,4,u}_{1,\text{fin}} =& \frac{1}{2}\frac{(\zeta\bar{\zeta})^{\Delta}}{(x_{12}^2x_{34}^2)^{\Delta}}I(u_\zeta,u_\zeta-u_1).\end{aligned}$$

A parametric representation is given by

$$I(v_1,v_2) := \pi^4 \int\limits_{(\mathbb{RP}^+)^4} \frac{d\alpha_0\cdots d\alpha_5}{(\frac{\alpha_1+\alpha_2+\alpha_3}{4}\alpha_4^2+\frac{\alpha_0+\alpha_1}{4}\alpha_5^2+\frac{\alpha_1}{2}\alpha_4\alpha_5+\hat{F})^2},$$

with

$$\hat{F} = -(v_1-v_2)^2(\alpha_0+\alpha_1)\alpha_2\alpha_3 - v_1^2\alpha_0\alpha_1\alpha_2 - v_2^2\alpha_0\alpha_1\alpha_3\,.$$

Changing variables to

$$\frac{\alpha_1+\alpha_2+\alpha_3}{4}\alpha_4^2+\frac{\alpha_0+\alpha_1}{4}\alpha_4^2+\frac{\alpha_1}{2}\alpha_4\alpha_4 = \frac{\alpha_1+\alpha_2+\alpha_3}{4}(\beta_4^2+\beta_5^2),$$

with

$$\beta_4 = \alpha_4 + \frac{\alpha_1\alpha_5}{\alpha_1+\alpha_2+\alpha_3}; \qquad \beta_5 = \frac{\alpha_5\sqrt{\alpha_0(\alpha_1+\alpha_2+\alpha_3)+\alpha_1(\alpha_2+\alpha_3)}}{\alpha_1+\alpha_2+\alpha_3}\,.$$

Setting

$$\beta_4 = \frac{t\beta_5\alpha_1}{\sqrt{\alpha_0(\alpha_1+\alpha_2+\alpha_3)+\alpha_1(\alpha_2+\alpha_3)}},$$

and performing the integration over β_5, and changing variables to $\alpha_i \to 1/\alpha_i$ we get

$$\begin{aligned}I(v_1,v_2;0) := -2\pi^4\int_1^\infty dt\int_0^\infty & \frac{d\alpha_0 d\alpha_1 d\alpha_2 d\alpha_3}{(v_1-v_2)^2(\alpha_0+\alpha_1)+v_1^2\alpha_3+v_2^2\alpha_2}\\ &\times\frac{1}{\alpha_1((\alpha_0+\alpha_1)(\alpha_2+\alpha_3)+\alpha_2\alpha_3)+\alpha_0\alpha_2\alpha_3 t^2}.\end{aligned}$$

Setting $x := (v_1-v_2)^2, y := v_1^2$ and $z := v_2^2$, this defines the $L_0'(x,y,z) := I(v_1,v2;0)/(4\pi^4)$ integral

$$L_0'(x,y,z) = \int_1^\infty d\lambda\int_0^\infty ds\int_0^1 dr\frac{\log(1+\lambda s)}{4\lambda\sqrt{(1+s)(1+\lambda s)}(sr(1-r)x+ry+(1-r)z)}.$$

For the s-channel we have

$$(x,y,z) = (v,1-Y,1),$$

For the t-channel we have

$$(x,y,z) = (1-Y,1,v),$$

For the u-channel we have

$$(x,y,z) = (1,v,1-Y).$$

We first evaluate the integral over λ to get

$$
\begin{aligned}
I(s) &= \int_1^\infty \frac{\log(1+s\lambda)}{\lambda\sqrt{1+\lambda s}} d\lambda \\
&= 2\mathrm{Li}_2\left(\frac{1}{\sqrt{s+1}}\right) - 2\mathrm{Li}_2\left(-\frac{1}{\sqrt{s+1}}\right) - \log(s+1)\log\left(\frac{\sqrt{s+1}-1}{\sqrt{s+1}+1}\right).
\end{aligned}
$$

For computing this integral we evaluated

$$
\begin{aligned}
\int_1^\infty \frac{(1+s\lambda)^{-\frac{1}{2}+\epsilon}}{\lambda} d\lambda &= -\frac{2s^{-\frac{1}{2}+\epsilon}{}_2F_1\left(\frac{1}{2}-\epsilon,\frac{1}{2}-\epsilon;\frac{3}{2}-\epsilon;-\frac{1}{s}\right)}{-1+2\epsilon} \\
&= -\log\left(\frac{\sqrt{s+1}-1}{\sqrt{s+1}+1}\right) + \epsilon\Big(2\mathrm{Li}_2\left(\frac{1}{\sqrt{s+1}}\right) - 2\mathrm{Li}_2\left(-\frac{1}{\sqrt{s+1}}\right) \\
&\quad - \log(s+1)\log\left(\frac{\sqrt{s+1}-1}{\sqrt{s+1}+1}\right)\Big) + O\left(\epsilon^2\right)
\end{aligned}
$$

changing variables by setting $s = 1/\sigma^2 - 1$ we have

$$
I(\sigma) = 2\mathrm{Li}_2(\sigma) - 2\mathrm{Li}_2(-\sigma) + 2\log(\sigma)\left(\log(1-\sigma) - \log(1+\sigma)\right) \tag{C.15}
$$

$$
L_0'(x,y,z) = \frac{1}{4}\int_0^1\int_0^1 \frac{I(\sigma)}{(\sigma^2-1)\,xr^2 + ((-x+y-z)\,\sigma^2+x)\,r + z\,\sigma^2} dr d\sigma \tag{C.16}
$$

The vanishing locus of the denominator of the integral

$$
\left(\sigma^2-1\right)xr^2 + \left((-x+y-z)\,\sigma^2+x\right)r + z\,\sigma^2 = 0 \tag{C.17}
$$

defines an elliptic curve. Therefore the result of the integral is an elliptic polylogarithm. We are not interested in the exact expression but in the degeneration limit of the elliptic curve for small v and Y. Therefore, we only evaluate the integrals in the asymptotic $0 \le v \ll 1$ region.

s-channel We can perform the integration over σ right away. The positive root of equation (C.17) in σ is given by

$$
\sigma(r) := \frac{\sqrt{(1-r)\,rv}}{\sqrt{-r^2v + Yr + rv - 1}}.
$$

Note that the limit $v \to 0$ coincides with $\sigma(r) \to 0$, which means that the integration in σ should provide us with the $\log(v)^2$ and $\log(v)$ divergences of the integral. Indeed, performing the integration over σ leads to

$$
\begin{aligned}
L_0'(v,1-Y,1) &= \frac{1}{4}\int_0^1 \log\left(\frac{1-\sigma(r)}{1+\sigma(r)}\right)\frac{dr}{2\left(-1-r^2v+r\left(v+Y\right)\right)\sigma(r)}\log(v)^2 \\
+&\int_0^1 \left(\mathrm{Li}_2(\sigma(r)) - \mathrm{Li}_2(-\sigma(r)) + i\pi\mathrm{Li}_1(-\sigma(r)) - i\pi\mathrm{Li}_1(\sigma(r))\right)\frac{\log(v)dr}{2\left(-1-r^2v+r\left(v+Y\right)\right)\sigma(r)} \\
&+\int_0^1 \log\left(\frac{-i\sqrt{r(1-r)}}{\sqrt{1-Yr}}\right)\frac{\log(v)dr}{2\left(-1-r^2v+r\left(v+Y\right)\right)\sigma(r)} + O(v^0)
\end{aligned}
$$

One can perform the small v series expansion under the integrals and integrate in r term by term.

t-channel Here the $\log(v)$ divergence can be extracted from the r integral. We notice that equation (C.16) can be written as

$$\begin{aligned} L_0'(1-Y,1,y) &= \frac{1}{4}\int_0^1\int_0^1 \frac{I(\sigma)}{(r-r_+(\sigma))(r-r_-(\sigma))}\frac{1}{(\sigma^2-1)(1-Y)}drd\sigma \\ &= \frac{1}{4}\int_0^1 \frac{I(\sigma)\log\left(\frac{r_+(1-r_-)}{r_-(1-r_+)}\right)}{r_- - r_+}d\sigma \end{aligned}$$

with

$$r_\pm = \frac{1}{2}\frac{\sigma^2(v-Y)-(1-Y)\pm\sqrt{(\sigma^2(v-Y)-(1-Y))^2-4\sigma^2 v(\sigma^2-1)(1-Y)}}{\sqrt{(\sigma^2-1)(1-Y)}}$$

The logarithmic term in the numerator diverges with $\log(v)$ in the limit $v \to 0$. The $\log(v)$ term to the integral is therefore given by

$$L_0'(1-Y,1,v) = -\int_0^1 \frac{(\mathrm{Li}_2(\sigma)-\mathrm{Li}_2(-\sigma)+\log(\sigma)(\log(1-\sigma)-\log(1+\sigma)))\,d\sigma}{\sqrt{(Y^2+2Yv+v^2-4v)\,\sigma^4-2\,(Y-1)\,(v+Y)\,\sigma^2+(Y-1)^2}}\log(v)+O(v^0)$$

The integrand can be expanded for small v and Y and integrated term-by-term using the small σ expansion

$$\mathrm{Li}_2(\sigma)-\mathrm{Li}_2(-\sigma)+\log(\sigma)(\log(1-\sigma)-\log(1+\sigma)) = 2\sum_{n\geq 0}\sigma^{2n}\left(\frac{1}{(2n+1)^2}-\frac{\log(\sigma)}{2n+1}\right)$$

so that

$$\begin{aligned} &\int_0^1 (\mathrm{Li}_2(\sigma)-\mathrm{Li}_2(-\sigma)+\log(\sigma)(\log(1-\sigma)-\log(1+\sigma)))\,\sigma^{2m}d\sigma \\ &\qquad = \frac{\pi^2}{6(1+2m)}+\frac{1}{2(1+2m)}\sum_{n=1}^{m}\frac{1}{n^2}. \end{aligned} \tag{C.18}$$

u-channel Repeating the same steps as for the t channel we arrive at the integral

$$L_0'(1,v,1-Y) = -\int_0^1 \frac{(\mathrm{Li}_2(\sigma)-\mathrm{Li}_2(-\sigma)+\log(\sigma)(\log(1-\sigma)-\log(1+\sigma)))\,d\sigma}{\sqrt{1+(v^2+(2Y-4)\,v+Y^2)\,\sigma^4+(-2Y+2v)\,\sigma^2}}\log(v)+O(v^0)$$

The integrand can be expanded for small v and Y and integrated term by term using (C.18).

C.2 The one-loop diagrams with mixed external dimensions

The subleading terms are given by either acting with $\mathcal{H}_{12}, \mathcal{H}_{13}$ or $\mathcal{H}_{14}$ on the divergent part of the $\Delta = 1$ result. In the parametric representation we obtain

- For the s-channel

$$\mathcal{W}_1^{2211,4-2\epsilon,s} = \frac{\pi^{4-2\epsilon}(\zeta\bar{\zeta})^2(1-2\epsilon)}{4\Gamma(-2\epsilon)x_{12}^4x_{34}^2}\int\limits_{(\mathbb{RP}^+)^4}\prod_{i=1}^4 d\alpha_i\frac{\alpha_2\alpha_4\alpha_5(\alpha_1+\alpha_5)\alpha_1^{-2\epsilon}\alpha_3^{-2\epsilon-1}(U^s)^{-\epsilon-1}}{(F^s)^{-2(\epsilon-1)}}$$

with U^s and F^s given in (C.5).
• For the t-channel

$$\mathcal{W}_1^{2211,4-2\epsilon,t} = \frac{\pi^{4-2\epsilon}(\zeta\bar{\zeta})^2}{4\Gamma(-2\epsilon))x_{12}^4 x_{34}^2} \int\limits_{(\mathbb{RP}^+)^4} \prod_{i=1}^{4} d\alpha_i \frac{\alpha_1 \alpha_2^{-1-2\epsilon}\alpha_4\alpha_5^2 (U^t)^{-1-\epsilon}(1-2\epsilon)}{(F^t)^{-2(\epsilon-1)}}$$

with U^t and F^t given in (C.6).
• For the u-channel

$$\mathcal{W}_1^{2211,4-2\epsilon,u} = \frac{\pi^{4-2\epsilon}(\zeta\bar{\zeta})^2}{4\Gamma(-2\epsilon))x_{12}^4 x_{34}^2} \int\limits_{(\mathbb{RP}^+)^4} \prod_{i=1}^{4} d\alpha_i \frac{\alpha_1^{-1-2\epsilon}\alpha_2\alpha_3\alpha_4^{-2\epsilon}\alpha_5^2 (U)^{-1-\epsilon}(1-2\epsilon)}{(F^u)^{-2(\epsilon-1)}}$$

with U^u and F^u given in (C.7).

Integrating over the Feynman parameters and expanding in ϵ we find the following structure for each diagram

$$\mathcal{W}_1^{2211,4-2\epsilon,i} = -\frac{\pi^2}{\epsilon}\mathcal{W}_0^{2211,4-4\epsilon} + \mathcal{W}_{1,\text{finite}}^{2211,i} + \mathcal{O}(\epsilon^2) \text{ with } i = s,t,u$$

where the finite part $\mathcal{W}_{1,\text{finite}}$ for each diagram is given by

$$\begin{aligned}\frac{4x_{12}^4 x_{34}^2}{\pi^4(\zeta\bar{\zeta})^2}\mathcal{W}_{1,\text{finite}}^{2211,s} = &\frac{\zeta+\bar{\zeta}-2}{(\zeta-\bar{\zeta})^3} f_1 - \frac{(\zeta+\bar{\zeta}-2)\log(\zeta\bar{\zeta})}{(\zeta-\bar{\zeta})^3} 2iD(\zeta,\bar{\zeta}) + \frac{4iD(\zeta,\bar{\zeta})}{\zeta\bar{\zeta}(\zeta-\bar{\zeta})} \\ &- \frac{\log(\zeta\bar{\zeta})(\log((1-\zeta)(1-\bar{\zeta})) - \log(\zeta\bar{\zeta})+4)}{(\zeta-\bar{\zeta})^2} \\ &- \frac{2(\zeta+\bar{\zeta}-2\zeta\bar{\zeta})\log((1-\zeta)(1-\bar{\zeta}))}{\zeta\bar{\zeta}(\zeta-\bar{\zeta})^2}\end{aligned}$$

$$\frac{4x_{12}^4 x_{34}^2}{\pi^4(\zeta\bar{\zeta})^2}\mathcal{W}_{1,\text{finite}}^{2211,t} = \frac{\zeta+\bar{\zeta}-2}{(\zeta-\bar{\zeta})^3}(f_1+2f_6) + \frac{2iD(\zeta,\bar{\zeta})}{\zeta\bar{\zeta}(\zeta-\bar{\zeta})} - \frac{4\log(\zeta\bar{\zeta})}{(\zeta-\bar{\zeta})^2} + \frac{\zeta+\bar{\zeta}-2\zeta\bar{\zeta}}{\zeta\bar{\zeta}(\zeta-\bar{\zeta})^2} f_7$$

$$\begin{aligned}\frac{4x_{12}^4 x_{34}^2}{\pi^4(\zeta\bar{\zeta})^2}\mathcal{W}_{1,\text{finite}}^{2211,u} = &\frac{\zeta+\bar{\zeta}-2}{(\zeta-\bar{\zeta})^3} f_1 + \frac{2iD(\zeta,\bar{\zeta})}{\zeta\bar{\zeta}(\zeta-\bar{\zeta})} + \frac{2(2\zeta\bar{\zeta}-\zeta-\bar{\zeta})}{\zeta\bar{\zeta}(\zeta-\bar{\zeta})^2}\log((1-\zeta)(1-\bar{\zeta})) \\ &- \frac{\zeta+\bar{\zeta}}{\zeta\bar{\zeta}(\zeta-\bar{\zeta})^2}\log(\zeta\bar{\zeta})\log((1-\zeta)(1-\bar{\zeta})) - \frac{4\log(\zeta\bar{\zeta})}{(\zeta-\bar{\zeta})^2}\end{aligned}$$

where $D(\zeta,\bar{\zeta})$, f_1, f_6 and f_7 are given in appendix A.2.

C.3 Expressions from unitarity cuts

The unitarity cut of the cross diagram in $D = 4-4\epsilon$ dimensions up to order ϵ is given by

$$\text{Cut}_{u_\zeta}\mathcal{W}_0^{1,4-4\epsilon} = \frac{(2\pi)^3}{4}\frac{(\pi e^\gamma)^{-2\epsilon}v}{(x_{12}x_{34})^2}\int\limits_{-1}^{+1} \mathrm{d}x \frac{(1-x^2)^{-2\epsilon}(\zeta\bar{\zeta})^{1-4\epsilon}}{(\zeta+\bar{\zeta}-x(\zeta-\bar{\zeta}))(\zeta+\bar{\zeta}-2\zeta\bar{\zeta}-x(\zeta-\bar{\zeta}))^{1-4\epsilon}}$$

which evaluates

$$
\begin{aligned}
\mathrm{Cut}_{u_\zeta}\mathcal{W}_0^{1,4-4\epsilon} &= -\frac{v\pi^3}{(x_{12}x_{34})^2}\frac{1}{(\zeta-\bar{\zeta})}\left[\log\left(\frac{1-\zeta}{1-\bar{\zeta}}\right)\right.\\
&- 2\epsilon\left(\mathrm{Li}_{1,1}\left(\bar{\zeta},\frac{\zeta}{\bar{\zeta}}\right) - \mathrm{Li}_{1,1}\left(\zeta,\frac{\bar{\zeta}}{\zeta}\right) + \mathrm{Li}_1\left(\zeta\right)\mathrm{Li}_1\left(\frac{\bar{\zeta}}{\zeta}\right) - \mathrm{Li}_1\left(\bar{\zeta}\right)\mathrm{Li}_1\left(\frac{\zeta}{\bar{\zeta}}\right)\right.\\
&-(\mathrm{Li}_2\left(\zeta\right) - \mathrm{Li}_2\left(\bar{\zeta}\right)) + \log\left(\frac{1-\zeta}{1-\bar{\zeta}}\right)\log((1-\zeta)(1-\bar{\zeta}))\\
&\left.\left.+ \log(\zeta\bar{\zeta})\log\left(\frac{1-\zeta}{1-\bar{\zeta}}\right)\right) + \mathcal{O}(\epsilon^2)\right]
\end{aligned} \tag{C.20}
$$

The $\mathcal{O}(\epsilon^0)$ term of the cut one-loop s-channel integral is given by

$$
\begin{aligned}
I_{1,\mathrm{div}}^{1,\epsilon} = \frac{1}{2(\zeta-\bar{\zeta})}\Big(&\mathrm{Li}_{1,1}\left(\bar{\zeta},\frac{\zeta}{\bar{\zeta}}\right) - \mathrm{Li}_{1,1}\left(\zeta,\frac{\bar{\zeta}}{\zeta}\right) + \mathrm{Li}_1\left(\zeta\right)\mathrm{Li}_1\left(\frac{\bar{\zeta}}{\zeta}\right) - \mathrm{Li}_1\left(\bar{\zeta}\right)\mathrm{Li}_1\left(\frac{\zeta}{\bar{\zeta}}\right)\\
-(\mathrm{Li}_2\left(\zeta\right) - \mathrm{Li}_2\left(\bar{\zeta}\right)) &+ \log\left(\frac{1-\zeta}{1-\bar{\zeta}}\right)\log((1-\zeta)(1-\bar{\zeta})) - \log(\zeta\bar{\zeta})\log\left(\frac{1-\zeta}{1-\bar{\zeta}}\right)\Big) + \mathcal{O}(\epsilon).
\end{aligned} \tag{C.21}
$$

Appendix D

Conformal blocks and OPE coefficients

The squared OPE coefficients for a canonically normalized double trace operator $[\mathcal{O}_i\mathcal{O}_j]_{n,l}$ in an OPE between $\mathcal{O}_i$ and $\mathcal{O}_j$ for a generalized free field has been calculated in [94] and is given by

$$A^{i,j}_{[\mathcal{O}_i\mathcal{O}_j]_{n,l}} = \frac{(-1)^l \left(\Delta_i - \frac{d}{2}+1\right)_n \left(\Delta_j - \frac{d}{2}+1\right)_n (\Delta_i)_{l+n}(\Delta_j)_{l+n}}{l!n!\left(l+\frac{d}{2}\right)_n (\Delta_i+\Delta_j+n-d+1)_n(\Delta_i+\Delta_j+2n+l-1)_l\left(\Delta_i+\Delta_j+n+l-\frac{d}{2}\right)_n},$$

where $(x)_n := \frac{\Gamma(x+n)}{\Gamma(x)}$ is the Pochhammer symbol. The conformal block for a multiplet of dimension Δ and spin l in a four-point function with external dimensions $\Delta_1, \Delta_2, \Delta_3$ and Δ_4 in $d = 3$ space-time dimensions has been calculated in [111] and is given by

$$G^{a,b}_{\Delta,l}(\tilde{v},\tilde{Y}) = \sum_{k=0}^{\infty} \tilde{v}^{\frac{\Delta-l}{2}+k} \sum_{m=0}^{2k} A^{a,b}_{k,m} f^{a,b}_{k,m}(\tilde{Y}),$$

with

$$f^{a,b}_{k,m}(\tilde{Y}) = \tilde{Y}^{l-m}{}_2F_1\left(\frac{\Delta+l}{2}+k-m-a, \frac{\Delta+l}{2}+k-m+b, \Delta+l+2k-2m; \tilde{Y}\right),$$

and

$$\begin{aligned} A^{a,b}_{k,m}(\Delta) = &\sum_{m_1,m_2=0}^{\lfloor\frac{m}{2}\rfloor} (-1)^{m+m_1+1} 4^{m_1+m_2} \frac{(-l)_m(-\lfloor m/2\rfloor))_{m_1+m_2}(k-\lfloor m/2\rfloor)+1/2)_{m_1}}{m!m_1!m_2!(k-m+m_1)!} \\ &\times \frac{(\Delta-1)_{2k-m}(3/2-\Delta)_{m-k-m_1-m_2}(l-\Delta+2)_{2(\lfloor m/2\rfloor-m_2)-n}}{(\Delta+l-m-1)_{2k-m}(\Delta+l)_{2(k+m1-\lfloor m/2\rfloor)-m}} \\ \times \prod_{\alpha\in\{\pm a,\pm b\}} &\left(\left(\frac{1}{2}(\Delta+l)+\alpha\right)_{k-m+m_1}\left(\frac{1}{2}(\Delta-l-1)+\alpha\right)_{m_2}\right)(1+(4ab-1)(n \bmod 2)). \end{aligned}$$

where $a = \frac{\Delta_1-\Delta_2}{2}$ and $b = \frac{\Delta_3-\Delta_4}{2}$ and the conformal cross ratios are defined in a slightly different way as

$$\tilde{v} = \frac{v}{1-Y}; \qquad 1-\tilde{Y} = \frac{1}{1-Y}.$$

Note that we use a slightly different normalization compared to [111].

Bibliography

[1] A. Einstein, *Kosmologische Betrachtungen zur allgemeinen Relativitätstheorie*, *Sitzungsberichte der Königlich Preußischen Akademie der Wissenschaften (Berlin* (1917) 142.

[2] W. de Sitter, *Einstein's theory of gravitation and its astronomical consequences, Third Paper*, *Mon. Not. Roy. Astron. Soc.* **78** (1917) 3.

[3] A. Friedmann, *Über die Krümmung des Raumes*, *Zeitschrift fur Physik* **10** (1922) 377.

[4] A. Friedmann, *Über die Möglichkeit einer Welt mit konstanter negativer Krümmung des Raumes*, *Zeitschrift fur Physik* **21** (1924) 326.

[5] G. Lemaître, *Un Univers homogène de masse constante et de rayon croissant rendant compte de la vitesse radiale des nébuleuses extra-galactiques*, *Annales de la Société Scientifique de Bruxelles* **47** (1927) 49.

[6] E. Hubble, *A Relation between Distance and Radial Velocity among Extra-Galactic Nebulae*, *Proceedings of the National Academy of Science* **15** (1929) 168.

[7] A.A. Penzias and R.W. Wilson, *A Measurement of Excess Antenna Temperature at 4080 Mc/s.*, *apj* **142** (1965) 419.

[8] A.G. Riess, A.V. Filippenko, P. Challis, A. Clocchiatti, A. Diercks, P.M. Garnavich et al., *Observational Evidence from Supernovae for an Accelerating Universe and a Cosmological Constant*, *AJ* **116** (1998) 1009 [`astro-ph/9805201`].

[9] A.A. Starobinsky, *A New Type of Isotropic Cosmological Models Without Singularity*, *Phys. Lett. B* **91** (1980) 99.

[10] A.H. Guth, *The Inflationary Universe: A Possible Solution to the Horizon and Flatness Problems*, *Phys. Rev. D* **23** (1981) 347.

[11] A.D. Linde, *A New Inflationary Universe Scenario: A Possible Solution of the Horizon, Flatness, Homogeneity, Isotropy and Primordial Monopole Problems*, *Phys. Lett. B* **108** (1982) 389.

[12] A. Albrecht and P.J. Steinhardt, *Cosmology for Grand Unified Theories with Radiatively Induced Symmetry Breaking*, *Phys. Rev. Lett.* **48** (1982) 1220.

[13] V.F. Mukhanov and G.V. Chibisov, *Quantum Fluctuations and a Nonsingular Universe*, *JETP Lett.* **33** (1981) 532.

[14] J.M. Maldacena, *Non-Gaussian features of primordial fluctuations in single field inflationary models*, *JHEP* **05** (2003) 013 [astro-ph/0210603].

[15] S. Weinberg, *Quantum contributions to cosmological correlations*, *Phys. Rev. D* **72** (2005) 043514 [hep-th/0506236].

[16] N. Arkani-Hamed and J. Maldacena, *Cosmological Collider Physics*, 1503.08043.

[17] N. Arkani-Hamed, D. Baumann, H. Lee and G.L. Pimentel, *The Cosmological Bootstrap: Inflationary Correlators from Symmetries and Singularities*, *JHEP* **04** (2020) 105 [1811.00024].

[18] S.J. Avis, C.J. Isham and D. Storey, *Quantum Field Theory in anti-de Sitter Space-Time*, *Phys. Rev.* **D18** (1978) 3565.

[19] J.M. Maldacena, *The large N limit of superconformal field theories and supergravity*, *Adv. Theor. Math. Phys.* **2** (1998) 231 [hep-th/9711200].

[20] S.S. Gubser, I.R. Klebanov and A.M. Polyakov, *Gauge theory correlators from non-critical string theory*, *Phys. Lett.* **B428** (1998) 105 [hep-th/9802109].

[21] D.Z. Freedman, S.D. Mathur, A. Matusis and L. Rastelli, *Correlation functions in the CFT(d) / AdS(d+1) correspondence*, *Nucl.Phys.* **B546** (1999) 96 [hep-th/9804058].

[22] E. Witten, *Anti-de Sitter space and holography*, *Adv. Theor. Math. Phys.* **2** (1998) 253 [hep-th/9802150].

[23] W. Mueck and K.S. Viswanathan, *Conformal field theory correlators from classical scalar field theory on AdS(d+1)*, *Phys. Rev.* **D58** (1998) 041901 [hep-th/9804035].

[24] J. Penedones, *Writing CFT correlation functions as AdS scattering amplitudes*, *JHEP* **03** (2011) 025 [arXiv:1011.1485].

[25] F. Aprile, J.M. Drummond, P. Heslop and H. Paul, *Quantum Gravity from Conformal Field Theory*, *JHEP* **01** (2018) 035 [arXiv:1706.02822].

[26] F. Aprile, J.M. Drummond, P. Heslop and H. Paul, *Loop corrections for Kaluza-Klein AdS amplitudes*, *JHEP* **05** (2018) 056 [1711.03903].

[27] O. Aharony, L.F. Alday, A. Bissi and E. Perlmutter, *Loops in AdS from Conformal Field Theory*, *JHEP* **07** (2017) 036 [arXiv:1612.03891].

[28] S. Giombi, C. Sleight and M. Taronna, *Spinning AdS Loop Diagrams: Two Point Functions*, *JHEP* **06** (2018) 030 [arXiv:1708.08404].

[29] L.F. Alday and A. Bissi, *Loop Corrections to Supergravity on $AdS_5 \times S^5$*, *Phys. Rev. Lett.* **119** (2017) 171601 [arXiv:1706.02388].

[30] L.F. Alday and S. Caron-Huot, *Gravitational S-matrix from CFT dispersion relations*, *JHEP* **12** (2018) 017 [1711.02031].

[31] L.F. Alday, A. Bissi and E. Perlmutter, *Genus-One String Amplitudes from Conformal Field Theory*, arXiv:1809.10670.

[32] L.F. Alday, *On genus-one string amplitudes on $AdS_5 \times S^5$*, *JHEP* **04** (2021) 005 [1812.11783].

[33] L.F. Alday and X. Zhou, *Simplicity of AdS Supergravity at One Loop*, *JHEP* **09** (2020) 008 [1912.02663].

[34] L.F. Alday, A. Bissi and X. Zhou, *One-loop Gluon Amplitudes in AdS*, 2110.09861.

[35] J.M. Drummond and H. Paul, *One-loop string corrections to AdS amplitudes from CFT*, *JHEP* **03** (2021) 038 [1912.07632].

[36] D. Carmi, J. Penedones, J.A. Silva and A. Zhiboedov, *Applications of dispersive sum rules: ϵ-expansion and holography*, *SciPost Phys.* **10** (2021) 145 [2009.13506].

[37] E.Y. Yuan, *Loops in the Bulk*, 1710.01361.

[38] E.Y. Yuan, *Simplicity in AdS Perturbative Dynamics*, arXiv:1801.07283.

[39] S. Albayrak and S. Kharel, *Spinning loop amplitudes in anti–de Sitter space*, *Phys. Rev. D* **103** (2021) 026004 [2006.12540].

[40] K. Ghosh, *Polyakov-Mellin Bootstrap for AdS loops*, *JHEP* **02** (2020) 006 [1811.00504].

[41] F. Aprile, J. Drummond, P. Heslop and H. Paul, *One-loop amplitudes in $AdS_5 \times S^5$ supergravity from $\mathcal{N} = 4$ SYM at strong coupling*, *JHEP* **03** (2020) 190 [1912.01047].

[42] D. Ponomarev, *From bulk loops to boundary large-N expansion*, *JHEP* **01** (2020) 154 [1908.03974].

[43] D. Carmi, L. Di Pietro and S. Komatsu, *A Study of Quantum Field Theories in AdS at Finite Coupling*, *JHEP* **01** (2019) 200 [1810.04185].

[44] D. Carmi, *Loops in AdS: From the Spectral Representation to Position Space*, *JHEP* **06** (2020) 049 [1910.14340].

[45] D. Carmi, *Loops in AdS: from the spectral representation to position space. Part II*, *JHEP* **07** (2021) 186 [2104.10500].

[46] A. Costantino and S. Fichet, *Opacity from Loops in AdS*, *JHEP* **02** (2021) 089 [2011.06603].

[47] S. Fichet, *Field Holography in General Background and Boundary Effective Action from AdS to dS*, 2112.00746.

[48] J. Liu, E. Perlmutter, V. Rosenhaus and D. Simmons-Duffin, *d-dimensional SYK, AdS Loops, and 6j Symbols*, arXiv:1808.00612.

[49] D. Meltzer, E. Perlmutter and A. Sivaramakrishnan, *Unitarity Methods in AdS/CFT*, JHEP **03** (2020) 061 [1912.09521].

[50] D. Meltzer and A. Sivaramakrishnan, *CFT unitarity and the AdS Cutkosky rules*, JHEP **11** (2020) 073 [2008.11730].

[51] D. Meltzer, *AdS/CFT Unitarity at Higher Loops: High-Energy String Scattering*, JHEP **05** (2020) 133 [1912.05580].

[52] D. Meltzer, *Dispersion Formulas in QFTs, CFTs, and Holography*, JHEP **05** (2021) 098 [2103.15839].

[53] A. Herderschee, *A New Framework for Higher Loop Witten Diagrams*, 2112.08226.

[54] L. Eberhardt, S. Komatsu and S. Mizera, *Scattering equations in AdS: scalar correlators in arbitrary dimensions*, JHEP **11** (2020) 158 [2007.06574].

[55] I. Bertan and I. Sachs, *Loops in Anti-de Sitter Space*, Phys. Rev. Lett. **121** (2018) 101601 [arXiv:1804.01880].

[56] I. Bertan, I. Sachs and E.D. Skvortsov, *Quantum ϕ^4 Theory in AdS_4 and its CFT Dual*, JHEP **02** (2019) 099 [arXiv:1810.00907].

[57] T. Heckelbacher, I. Sachs, E. Skvortsov and P. Vanhove, *Analytical evaluation of AdS_4 Witten diagrams as flat space multi-loop Feynman integrals*, 2201.09626.

[58] J.S. Schwinger, *Brownian motion of a quantum oscillator*, J. Math. Phys. **2** (1961) 407.

[59] L.V. Keldysh, *Diagram technique for nonequilibrium processes*, *Zh. Eksp. Teor. Fiz.* **47** (1964) 1515.

[60] M. Fukuma, S. Sugishita and Y. Sakatani, *Propagators in de Sitter space*, Phys. Rev. D **88** (2013) 024041 [1301.7352].

[61] J.B. Hartle and S.W. Hawking, *Wave Function of the Universe*, Phys. Rev. D **28** (1983) 2960.

[62] T. Hertog and J. Hartle, *Holographic No-Boundary Measure*, JHEP **05** (2012) 095 [1111.6090].

[63] D. Harlow and D. Stanford, *Operator Dictionaries and Wave Functions in AdS/CFT and dS/CFT*, 1104.2621.

[64] D. Anninos, T. Anous, D.Z. Freedman and G. Konstantinidis, *Late-time Structure of the Bunch-Davies De Sitter Wavefunction*, JCAP **11** (2015) 048 [1406.5490].

[65] N.A. Chernikov and E.A. Tagirov, *Quantum theory of scalar fields in de Sitter space-time*, *Ann. Inst. H. Poincare Phys. Theor. A* **9** (1968) 109.

[66] C. Schomblond and P. Spindel, *Unicity Conditions of the Scalar Field Propagator Delta(1) (x,y) in de Sitter Universe*, *Ann. Inst. H. Poincare Phys. Theor.* **25** (1976) 67.

[67] T.S. Bunch and P.C.W. Davies, *Quantum Field Theory in de Sitter Space: Renormalization by Point Splitting*, *Proc. Roy. Soc. Lond. A* **360** (1978) 117.

[68] B. Allen, *Vacuum States in de Sitter Space*, *Phys. Rev. D* **32** (1985) 3136.

[69] A. Strominger, *The dS / CFT correspondence*, *JHEP* **10** (2001) 034 [hep-th/0106113].

[70] V. Gorbenko and L. Senatore, *$\lambda\phi^4$ in dS*, 1911.00022.

[71] T. Heckelbacher and I. Sachs, *Loops in dS/CFT*, *JHEP* **02** (2021) 151 [2009.06511].

[72] D. Meltzer, *The inflationary wavefunction from analyticity and factorization*, *JCAP* **12** (2021) 018 [2107.10266].

[73] E. Pajer, D. Stefanyszyn and J. Supeł, *The Boostless Bootstrap: Amplitudes without Lorentz boosts*, *JHEP* **12** (2020) 198 [2007.00027].

[74] H. Goodhew, S. Jazayeri, M.H. Gordon Lee and E. Pajer, *Cutting cosmological correlators*, *JCAP* **08** (2021) 003 [2104.06587].

[75] S. Jazayeri, E. Pajer and D. Stefanyszyn, *From locality and unitarity to cosmological correlators*, *JHEP* **10** (2021) 065 [2103.08649].

[76] H. Goodhew, S. Jazayeri and E. Pajer, *The Cosmological Optical Theorem*, *JCAP* **04** (2021) 021 [2009.02898].

[77] H. Gomez, R.L. Jusinskas and A. Lipstein, *Cosmological Scattering Equations*, *Phys. Rev. Lett.* **127** (2021) 251604 [2106.11903].

[78] H. Gomez, R.L. Jusinskas and A. Lipstein, *Cosmological Scattering Equations at Tree-level and One-loop*, 2112.12695.

[79] N. Arkani-Hamed, P. Benincasa and A. Postnikov, *Cosmological Polytopes and the Wavefunction of the Universe*, 1709.02813.

[80] D. Anninos, T. Hartman and A. Strominger, *Higher Spin Realization of the dS/CFT Correspondence*, *Class. Quant. Grav.* **34** (2017) 015009 [1108.5735].

[81] D. Krotov and A.M. Polyakov, *Infrared Sensitivity of Unstable Vacua*, *Nucl. Phys. B* **849** (2011) 410 [1012.2107].

[82] A.M. Polyakov, *Infrared instability of the de Sitter space*, arXiv:1209.4135.

[83] E.T. Akhmedov, *Lecture notes on interacting quantum fields in de Sitter space*, *Int. J. Mod. Phys. D* **23** (2014) 1430001 [1309.2557].

[84] C. Sleight and M. Taronna, *Bootstrapping Inflationary Correlators in Mellin Space*, *JHEP* **02** (2020) 098 [1907.01143].

[85] C. Sleight and M. Taronna, *From AdS to dS exchanges: Spectral representation, Mellin amplitudes, and crossing*, Phys. Rev. D **104** (2021) L081902 [2007.09993].

[86] C. Sleight and M. Taronna, *From dS to AdS and back*, JHEP **12** (2021) 074 [2109.02725].

[87] L. Di Pietro, V. Gorbenko and S. Komatsu, *Analyticity and Unitarity for Cosmological Correlators*, 2108.01695.

[88] M. Hogervorst, J.a. Penedones and K.S. Vaziri, *Towards the non-perturbative cosmological bootstrap*, 2107.13871.

[89] R. Rattazzi, V.S. Rychkov, E. Tonni and A. Vichi, *Bounding scalar operator dimensions in 4D CFT*, JHEP **12** (2008) 031 [0807.0004].

[90] T. Heckelbacher, I. Sachs, E. Skvortsov and P. Vanhove, *Analytical evaluation of cosmological correlation functions*, 2204.07217.

[91] O.W. Greenberg, *Generalized Free Fields and Models of Local Field Theory*, Annals Phys. **16** (1961) 158.

[92] M.E. Fisher, S.-k. Ma and B.G. Nickel, *Critical Exponents for Long-Range Interactions*, Phys. Rev. Lett. **29** (1972) 917.

[93] I. Heemskerk, J. Penedones, J. Polchinski and J. Sully, *Holography from Conformal Field Theory*, JHEP **10** (2009) 079 [arXiv:0907.0151].

[94] A.L. Fitzpatrick and J. Kaplan, *Unitarity and the Holographic S-Matrix*, JHEP **10** (2012) 032 [arXiv:1112.4845].

[95] A.V. Smirnov and F.S. Chuharev, *FIRE6: Feynman Integral REduction with Modular Arithmetic*, Comput. Phys. Commun. **247** (2020) 106877 [1901.07808].

[96] E. Panzer, *Feynman integrals and hyperlogarithms*, Ph.D. thesis, Humboldt U., 2015. 1506.07243. 10.18452/17157.

[97] P. Vanhove, *Feynman integrals, toric geometry and mirror symmetry*, in *KMPB Conference: Elliptic Integrals, Elliptic Functions and Modular Forms in Quantum Field Theory*, pp. 415–458, 2019, DOI [1807.11466].

[98] C. Bogner, S. Borowka, T. Hahn, G. Heinrich, S.P. Jones, M. Kerner et al., *Loopedia, a Database for Loop Integrals*, J. Phys. Conf. Ser. **1085** (2018) 052003.

[99] K. Bönisch, C. Duhr, F. Fischbach, A. Klemm and C. Nega, *Feynman Integrals in Dimensional Regularization and Extensions of Calabi-Yau Motives*, 2108.05310.

[100] P. Mastrolia and S. Mizera, *Feynman Integrals and Intersection Theory*, JHEP **02** (2019) 139 [1810.03818].

[101] S. Weinzierl, *Feynman Integrals*, 2201.03593.

[102] E. Panzer, *On hyperlogarithms and Feynman integrals with divergences and many scales*, *JHEP* **03** (2014) 071 [1401.4361].

[103] A.B. Goncharov, *Multiple polylogarithms and mixed tate motives*, math/0103059.

[104] S. Rychkov, *EPFL Lectures on Conformal Field Theory in D>= 3 Dimensions*, SpringerBriefs in Physics (2016), 10.1007/978-3-319-43626-5, [arXiv:1601.05000].

[105] D. Simmons-Duffin, *The Conformal Bootstrap*, in *Proceedings, Theoretical Advanced Study Institute in Elementary Particle Physics: New Frontiers in Fields and Strings (TASI 2015): Boulder, CO, USA, June 1-26, 2015*, pp. 1–74, 2017, DOI [arXiv:1602.07982].

[106] M. Schottenloher, *A mathematical introduction to conformal field theory*, *Lect. Notes Phys.* **759** (2008) 1.

[107] A.M. Polyakov, *Conformal symmetry of critical fluctuations*, *JETP Lett.* **12** (1970) 381.

[108] P. Di Francesco, P. Mathieu and D. Senechal, *Conformal Field Theory*, Graduate Texts in Contemporary Physics, Springer-Verlag, New York (1997), 10.1007/978-1-4612-2256-9.

[109] F.A. Dolan and H. Osborn, *Conformal four point functions and the operator product expansion*, *Nucl. Phys.* **B599** (2001) 459 [hep-th/0011040].

[110] F.A. Dolan and H. Osborn, *Conformal Partial Waves: Further Mathematical Results*, 1108.6194.

[111] W. Li, *Lightcone expansions of conformal blocks in closed form*, *JHEP* **06** (2020) 105 [1912.01168].

[112] J.L. Cardy, *Scaling and renormalization in statistical physics* (1996).

[113] O. Aharony, S.S. Gubser, J.M. Maldacena, H. Ooguri and Y. Oz, *Large N field theories, string theory and gravity*, *Phys. Rept.* **323** (2000) 183 [hep-th/9905111].

[114] M.S. Costa, J. Penedones, D. Poland and S. Rychkov, *Spinning Conformal Correlators*, *JHEP* **11** (2011) 071 [arXiv:1107.3554].

[115] A.L. Fitzpatrick, J. Kaplan, J. Penedones, S. Raju and B.C. van Rees, *A Natural Language for AdS/CFT Correlators*, *JHEP* **1111** (2011) 095 [arXiv:1107.1499].

[116] N.D. Birrell and P.C.W. Davies, *Quantum Fields in Curved Space*, Cambridge Monographs on Mathematical Physics, Cambridge Univ. Press, Cambridge, UK (1984), 10.1017/CBO9780511622632.

[117] R.M. Wald, *General Relativity*, Chicago Univ. Pr., Chicago, USA (1984), 10.7208/chicago/9780226870373.001.0001.

[118] S. Weinberg, *Gravitation and Cosmology: Principles and Applications of the General Theory of Relativity*, John Wiley and Sons, New York (1972).

[119] S.M. Carroll, *Spacetime and Geometry*, Cambridge University Press (7, 2019).

[120] S.W. Hawking and G.F.R. Ellis, *The Large Scale Structure of Space-Time*, Cambridge Monographs on Mathematical Physics, Cambridge University Press (2, 2011), 10.1017/CBO9780511524646.

[121] N.P.K. Tho, *Geodesics in the (anti-)de Sitter spacetime*, 1605.05046.

[122] M. Ammon and J. Erdmenger, *Gauge/gravity duality: Foundations and applications*, Cambridge University Press, Cambridge (4, 2015).

[123] V. Mukhanov, *Physical Foundations of Cosmology*, Cambridge University Press, Oxford (2005), 10.1017/CBO9780511790553.

[124] M. Luscher and G. Mack, *Global Conformal Invariance in Quantum Field Theory*, *Commun. Math. Phys.* **41** (1975) 203.

[125] V.K. Dobrev, G. Mack, I.T. Todorov, V.B. Petkova and S.G. Petrova, *On the Clebsch-Gordan Expansion for the Lorentz Group in n Dimensions*, *Rept. Math. Phys.* **9** (1976) 219.

[126] V.K. Dobrev, G. Mack, V.B. Petkova, S.G. Petrova and I.T. Todorov, *Harmonic Analysis on the n-Dimensional Lorentz Group and Its Application to Conformal Quantum Field Theory*, vol. 63 (1977), 10.1007/BFb0009678.

[127] M. Berkooz, A. Sever and A. Shomer, *'Double trace' deformations, boundary conditions and space-time singularities*, *JHEP* **05** (2002) 034 [hep-th/0112264].

[128] M. Spradlin, A. Strominger and A. Volovich, *Les Houches lectures on de Sitter space*, in *Les Houches Summer School: Session 76: Euro Summer School on Unity of Fundamental Physics: Gravity, Gauge Theory and Strings*, pp. 423–453, 10, 2001 [hep-th/0110007].

[129] M.F. Paulos, J. Penedones, J. Toledo, B.C. van Rees and P. Vieira, *The S-matrix bootstrap. Part I: QFT in AdS*, *JHEP* **11** (2017) 133 [1607.06109].

[130] C.D. Palmer and M.E. Carrington, *A General expression for symmetry factors of Feynman diagrams*, *Can. J. Phys.* **80** (2002) 847 [hep-th/0108088].

[131] B. Hatfield, *Quantum field theory of point particles and strings* (1992).

[132] E. Witten, *Quantum gravity in de Sitter space*, in *Strings 2001: International Conference*, 6, 2001 [hep-th/0106109].

[133] J. Zinn-Justin, *Quantum field theory and critical phenomena*, vol. 77 of *International Series of Monographs on Physics*, Oxford University Press (4, 2021).

[134] V.A. Smirnov, *Evaluating Feynman integrals*, *Springer Tracts Mod. Phys.* **211** (2004) 1.

[135] R.N. Lee, *Presenting LiteRed: a tool for the Loop InTEgrals REDuction*, 1212.2685.

[136] C. Itzykson and J.B. Zuber, *Quantum Field Theory*, International Series In Pure and Applied Physics, McGraw-Hill, New York (1980).

[137] E. Panzer, *Algorithms for the symbolic integration of hyperlogarithms with applications to Feynman integrals*, *Comput. Phys. Commun.* **188** (2015) 148 [1403.3385].

[138] G. Passarino and M.J.G. Veltman, *One Loop Corrections for e+ e- Annihilation Into mu+ mu- in the Weinberg Model*, *Nucl. Phys. B* **160** (1979) 151.

[139] F.V. Tkachov, *A Theorem on Analytical Calculability of Four Loop Renormalization Group Functions*, *Phys. Lett. B* **100** (1981) 65.

[140] K.G. Chetyrkin and F.V. Tkachov, *Integration by Parts: The Algorithm to Calculate beta Functions in 4 Loops*, *Nucl. Phys. B* **192** (1981) 159.

[141] R.K. Ellis, Z. Kunszt, K. Melnikov and G. Zanderighi, *One-loop calculations in quantum field theory: from Feynman diagrams to unitarity cuts*, *Phys. Rept.* **518** (2012) 141 [1105.4319].

[142] R.J. Eden, P.V. Landshoff, D.I. Olive and J.C. Polkinghorne, *The analytic S-matrix*, Cambridge Univ. Press, Cambridge (1966).

[143] J.L. Bourjaily, H. Hannesdottir, A.J. McLeod, M.D. Schwartz and C. Vergu, *Sequential Discontinuities of Feynman Integrals and the Monodromy Group*, *JHEP* **01** (2021) 205 [2007.13747].

[144] L.D. Landau, *On analytic properties of vertex parts in quantum field theory*, *Nucl. Phys.* **13** (1959) 181.

[145] R.E. Cutkosky, *Singularities and discontinuities of Feynman amplitudes*, *J. Math. Phys.* **1** (1960) 429.

[146] G. 't Hooft and M.J.G. Veltman, *DIAGRAMMAR*, *NATO Sci. Ser. B* **4** (1974) 177.

[147] S. Abreu, R. Britto, C. Duhr and E. Gardi, *From multiple unitarity cuts to the coproduct of Feynman integrals*, *JHEP* **10** (2014) 125 [1401.3546].

[148] S. Caron-Huot, *Analyticity in Spin in Conformal Theories*, *JHEP* **09** (2017) 078 [1703.00278].

[149] M.S. Costa, V. Goncalves and J. Penedones, *Spinning AdS Propagators*, *JHEP* **09** (2014) 064 [arXiv:1404.5625].

[150] D. Zagier, *The Dilogarithm Function*, in *Les Houches School of Physics: Frontiers in Number Theory, Physics and Geometry*, pp. 3–65, 2007, DOI.

[151] J. Ablinger, J. Blumlein and C. Schneider, *Harmonic Sums and Polylogarithms Generated by Cyclotomic Polynomials*, *J. Math. Phys.* **52** (2011) 102301 [1105.6063].

[152] E. Remiddi and J.A.M. Vermaseren, *Harmonic polylogarithms*, *Int. J. Mod. Phys. A* **15** (2000) 725 [hep-ph/9905237].

[153] B. Basso and G.P. Korchemsky, *Anomalous dimensions of high-spin operators beyond the leading order*, *Nucl. Phys.* **B775** (2007) 1 [hep-th/0612247].

[154] L.F. Alday, A. Bissi and T. Lukowski, *Large spin systematics in CFT*, *JHEP* **11** (2015) 101 [arXiv:1502.07707].

[155] L.F. Alday and A. Zhiboedov, *An Algebraic Approach to the Analytic Bootstrap*, *JHEP* **04** (2017) 157 [arXiv:1510.08091].

[156] J. Maldacena, D. Simmons-Duffin and A. Zhiboedov, *Looking for a bulk point*, *JHEP* **01** (2017) 013 [1509.03612].

[157] V. Didenko and E. Skvortsov, *Elements of Vasiliev theory*, arXiv:1401.2975.

[158] I.R. Klebanov and A.M. Polyakov, *AdS dual of the critical O(N) vector model*, *Phys. Lett.* **B550** (2002) 213 [hep-th/0210114].

[159] S. Mizera, *Scattering Amplitudes from Intersection Theory*, *Phys. Rev. Lett.* **120** (2018) 141602 [1711.00469].

[160] S. Abreu, R. Britto, C. Duhr, E. Gardi and J. Matthew, *Generalized hypergeometric functions and intersection theory for Feynman integrals*, *PoS* (2019) 067 [1912.03205].

[161] D. Baumann, D. Green, A. Joyce, E. Pajer, G.L. Pimentel, C. Sleight et al., *Snowmass White Paper: The Cosmological Bootstrap*, in *2022 Snowmass Summer Study*, 3, 2022 [2203.08121].

[162] A. Strominger, *Inflation and the dS / CFT correspondence*, *JHEP* **11** (2001) 049 [hep-th/0110087].